Morphologies and differentiation dynamics of cerebellar granule cell precursors

Hanzel, Michalina

Awarding institution:
King's College London

Morphologies and differentiation dynamics of cerebellar granule cell precursors

Michalina Hanzel

Department of Developmental Neurobiology

King's College London

Thesis submitted for the degree of Doctor of Philosophy (PhD)

April 2017

Abstract

Cerebellar granule cell precursors (GCPs) are born at the rhombic lip and migrate dorsally across the cerebellar anlagen to form a secondary germinative epithelium, the external germinal layer (EGL). Here, the precursors undergo a period of transit amplification during which they proliferate extensively to produce the most numerous cell type in the brain. The morphological sequence of events that characterizes the differentiation of GCPs in the EGL is well established. However, no research has correlated GCP morphologies with their differentiation status. In this project, I examine the morphological features and transitions of GCPs in the chicken cerebellum. I label a subset of GCPs with a stable genomic expression of green fluorescent transgene and follow their development within the EGL in static images and using time-lapse imaging. I use immunohistochemistry to observe cellular morphologies of proliferating and differentiating GCPs to better understand their differentiation dynamics. Results reveal that mitotic activities of GCPs are more complex and dynamic than currently appreciated. While most GCPs divide in the outer and middle EGL, some are capable of division in the inner EGL. Some GCPs remain mitotically active during neurite extension and tangential migration and retract their processes prior to each cell division. The mitotically active precursors can also express differentiation markers such as TAG1 and NeuroD1. Therefore, I explore the expression of NeuroD1 on a cellular level in GCPs using its conserved non-coding element and conclude that the levels of NeuroD1 expression can differ between neighbouring GCPs. Further, I explore the function of NeuroD1 in cerebellar development by overexpressing the protein at the rhombic lip at different developmental stages. Results suggest that misexpression of NeuroD1 promotes context-dependent differentiation and can alter cellular behaviour. When misexpressed in GCPs, NeuroD1 leads to premature differentiation, defects in migration and reduced cerebellar size and foliation. Overall, this thesis provides the first characterisation of individual morphologies of mitotically active cerebellar GCPs *in ovo* and explores in detail the expression and role of the differentiation factor NeuroD1 on the development of rhombic lip derivatives.

Acknowledgements

Firstly, I would like to thank my supervisor, Richard, for being the most supportive and enthusiastic advisor a PhD student could ever wish for. Thanks to Richard's endless passion and excitement for science, this journey has been a joy of scientific discovery. Thank you, Richard, for helping me to grow both as a scientist, and, most importantly, as a person through the extracurricular activities you allowed me to pursue during my time in the lab. I would not be where I am today without your continuous support and encouragement to pursue science, wherever in the world it may take me!

I am also grateful to all the members of the Wingate lab, past and present. Thanks to the amazing budding science writer and illustrator, Tristan, for going through the whole journey together with me and making it so much fun. Thank you to Vicky, who, even though joining only recently, has proven herself to be beyond helpful and friendly. Thank you to Margaret, who became a dear friend and a great scientist herself. Thank you to Tom for making me a published scientist. Thanks, Leigh, for always bringing a big smile to the lab. Deviana, Ting, Shuo, Marcela, Florent- thank you for being great lab members and making the lab a pleasure to work in. Thank you also to my second supervisor, Albert, as well as all the group leaders in the centre. This is indeed an exceptional place to work and I feel grateful to be have been a part of it.

I would also like to thank Mary Beth Hatten for hosting me in her lab during my first year of PhD and allowing me to continue pursuing science as a postdoctoral researcher as part of her team.

Finally, a huge thank you to my wonderful boyfriend, Chris, and my family, for always being there for me and encouraging me all the way until the end.

Table of Contents

Table of Figures

List of abbreviations

GCP- granule cell precursor

GC- granule cell (of the cerebellum)

EGL- external germinal layer (external granular layer)

IGL- internal granular layer

iEGL- inner EGL

oEGL- outer EGL

mEGL- middle EGL

CN- cerebellar nuclei

PC- Purkinje cell

UBC- unipolar brush cell

RL- rhombic lip

VZ- ventricular zone

SVZ- subventricular zone

RGC- radial glial cells

IN- interneurons

ML- molecular layer

PCL- Purkinje cell layer

RMS- rostral migratory stream

Chapter 1: Introduction

1.1 Neurogenesis during the nervous system development

Nervous system development begins very early in embryogenesis with the establishment of the neural tube through the process of neurulation. The neural tube gives rise to all the central and peripheral nervous system neurons by a series of transformations and divisions of the neural precursor cells. The precise ratios of proliferative and neurogenic divisions are regulated by intricate mechanisms, involving numerous internal and external signals and genetic and epigenetic changes. As the nervous system matures and segregates into discrete areas, different types of precursor cells can be observed at different times and locations. Each type has a unique molecular code and morphology, but they share some general characteristics. Cerebellar granule cell precursors, a focus of this thesis, are a type of neuronal progenitor cells, and are best understood in relation to other neuronal progenitor types in the developing brain, which will be introduced first, followed by a detailed description of granule cell precursor development.

1.1.1 Neuronal precursor cells

One way of classifying neuronal progenitors is through their morphology and polarity (Fietz and Huttner, 2011). In this paradigm, there are three types of neuronal progenitors: bipolar, monopolar and non-polar progenitors. All three types have been extensively studied in the cortex, but each type can also be found in other parts of the developing nervous system. With the increasing understanding of the morphological complexity of precursor types in the cortex (Namba and Huttner, 2017), this system might become obsolete, but is at present a good representation of majority of neuronal precursors in the developing nervous system.

Another way of classifying progenitors is by the location of their cell body at mitosis. This distinguishes between two progenitor types: apical and basal, as discussed below.

1.1.1.1 Apical progenitors (bipolar progenitors)

Apical progenitors (APs), also referred to as bipolar progenitors, represent the stem and progenitor cells that exhibit apico-basal polarity and have a bipolar morphology at M-phase. APs include both the neuroepithelial cells (NECs) and the apical radial glial cells (aRGCs), which arise later in development from symmetric divisions of the NECs. These progenitors extend two processes from their cell body- an apical process that forms adherens junctions at the ventricular side, and a basal process contacting the basal lamina (Götz and Huttner, 2005). Both processes remain attached during mitosis, which takes place at the apical surface. Both NECs and aRGCs express Pax6 and nestin, but differ in that aRGCs initiate expression of astroglial markers that NECs lack (Namba and Huttner, 2017).

APs undergo interkinetic nuclear migration and their cell bodies reside in the ventricular zone throughout the cell cycle (Miyata et al., 2015). Polarity proteins such as Par3, Par6 and aPKC are localised to the apical domain of the APs and are important for RGCs proliferation (Lui et al., 2011) Additionally, the presence of primary cilium and the centrosome at the apical plasma membrane functions in signal detection from the cerebrospinal fluid (Lee and Gleeson, 2011; Valente et al., 2014). The cilium is also essential for regulating RGC proliferation (Paridaen et al., 2014). Depending on the mitotic spindle orientation, the fates of the RGC daughter cells are determined. For example, perpendicular cleavage planes result in symmetric RGCs divisions, whereas horizontal cleavage planes are usually neurogenic (Lancaster and Knoblich, 2012; di Pietro et al., 2016). Bipolar progenitors are found in many developing nervous system areas such as the developing retina, the rhombic lip and the developing spinal cord.

1.1.1.2 Basal progenitors (monopolar and nonpolar progenitors)

Monopolar progenitors have only one process extended either towards the apical or the basal surface. Outer-subventricular-zone (OSVZ) progenitors undergo M-phase more basally than AP and were the first to be characterised as this type of

precursor in the cortex. OSVZ progenitors possess a basal process but usually lack any apical processes (LaMonica et al., 2012).

Since their discovery, this progenitor type has been found to be a subtype of a larger class of progenitors, currently referred to as basal RGCs, which can be both monopolar (in either the basal or the apical direction) as well as bipolar (with incomplete basal and apical processes). The expression profile of these progenitors is similar to aRGCs in that they express Pax6, astoglial markers and a proportion expresses Tbr2. However, their expression profiles are complex and differ between species such as mouse and human (Namba and Huttner, 2017).

Another monopolar progenitor type in the cortex, which used to be called short neural precursors, are the apical intermediate progenitors. These cells divide at the apical side, undergo interkinetic nuclear migration and possess the apical membrane with adherens junctions. They do not however have a fully extended basal process. Most of these intermediate progenitors divide symmetrically and generate two neuronal daughter cells. These would not be considered basal progenitors, but neither are they bipolar RGCs. Similarly to aRGCs, they express Pax6, but lack the expression of the astroglial markers (Namba and Huttner, 2017).

Nonpolar progenitors are a subtype of basal progenitors since their mitoses do not happen at the apical side and they are not integrated into the apical junctional belt. These cells, which do not have a clear apico-basal polarity and do not extend long processes in any direction, are currently called basal intermediate progenitors (bIPs). Within this population, there are proliferative and neurogenic bIPs, depending on their proliferative capacity. In rodents, they express Tbr2 and Neurog2 but not Pax6, whereas in gyrencephalic animals Pax6 expression is sustained in this progenitor population (Numba and Huttner, 2017). Expansion of basal progenitors in the cortex is considered instrumental for the expansion of the cortex of gyrencephalic species such as ferrets and primates. Studies have revealed that the numbers, and the proliferative potential, of basal progenitors in such animals far exceeds those in the lissencephalic species such as the mouse (Florio et al., 2015; Nomura et al., 2016; Nonaka-Kinoshita et al., 2013).

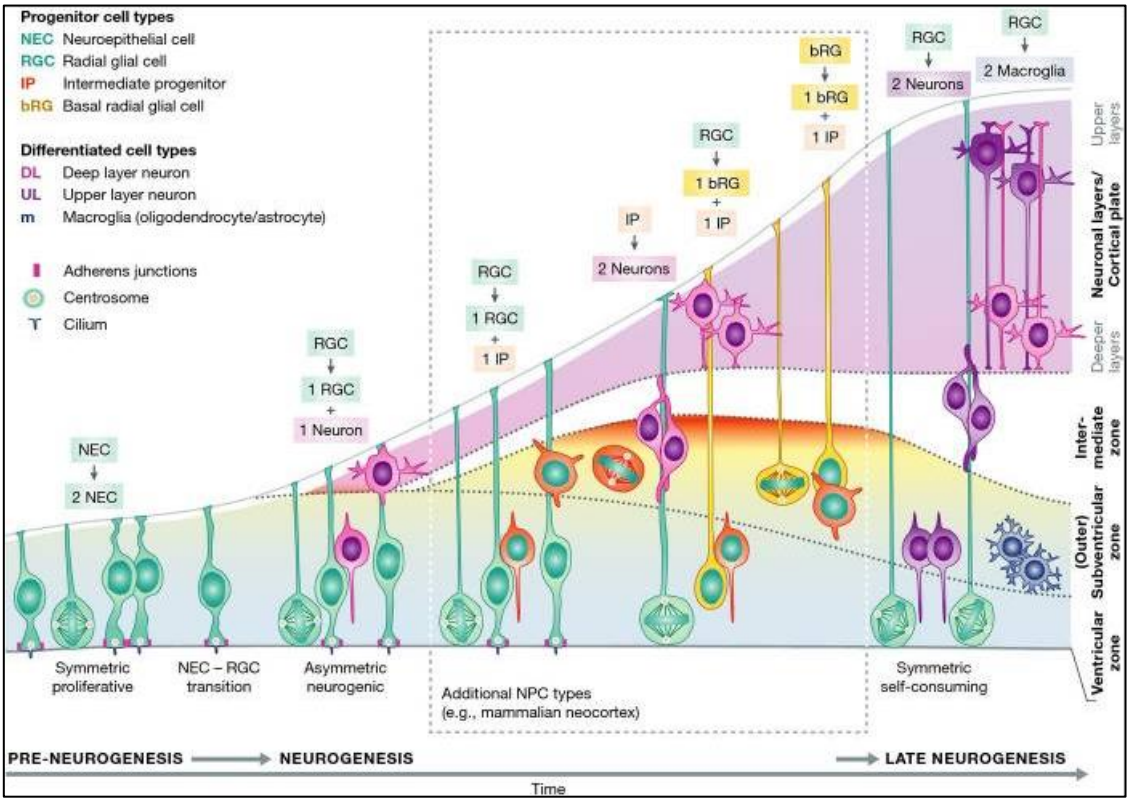

Figure 1-1 Neurogenesis in the developing cortex

A schematic representing different progenitor types and divisions within the developing cortex. Pre-neurogenesis, bipolar neuroepithelial cells divide by proliferative symmetrical divisions at the apical surface to increase in number. As NECs transition into RGCs, they start to preferentially undergo asymmetric neurogenic divisions and produce one RGC daughter cell and one neuron. RGCs can also give rise to monopolar and nonpolar intermediate progenitors that divide in the subventricular zone and have varying polarity. Some RGCs transition into basal RGCs with only a basal attachment. Intermediate progenitors preferentially divide in a terminal symmetric mode, generating two neurons, however they can also give rise to more progenitors, which continue to divide.

(Figure from Paridaen et al., 2014)

Other examples of non-apical neuronal progenitors outside of the cortex include the non-apical progenitors of the zebrafish neural tube (McIntosh et al., 2017), and the delaminated progenitors in the otocyst (Lorenzen et al., 2015).

1.1.2 Neurogenesis and migration of subventricular zone progenitors

Another area of the developing brain where neuronal progenitors have been extensively studied is the subventricular zone of the forebrain, from which the GABAergic granule and periglomerular cell interneurons located in the olfactory bulb derive. These cells are produced throughout the animal's life and represent one of two known populations of cells generated through adult neurogenesis (Pencea et al., 2001; Ponti et al., 2013; Urbán and Guillemot, 2014).

Stem cells located in the SVZ continually undergo mitosis to produce transit amplifying cells, which in turn give rise to migrating neuroblasts. Neuroblasts migrate towards the olfactory bulb within a well-defined pathway called the rostral migratory stream (RMS) and they have been known to be mitotically active throughout their migration (Luskin 1993; Coskun and Luskin 2001), even though they express typically postmitotic protein such as neuron-specific tubulin (recognized by Tuj1 antibody) (Menezes et al., 1995; Zigova et al., 1996) and doublecortin (Gleeson et al., 1999).

In cell culture studies, detailed characterisation of SVZ-derived neuroblasts is possible and have revealed interesting morphological transitions of mitotic neuroblasts during migration (Coskun et al., 2007). Specifically, cultured SVZ progenitors extend leading and trailing processes during migration, as expected from *in vivo* studies, but they were also found to retract all process prior to mitosis and undergo cell division. The daughter cells of these progenitors repeat this extension-retraction sequence generation after generation as they migrate.
The progenitors retract their processes very shortly before cytokinesis, suggesting that the cell had committed to division long before process retraction begins (Coskun et al., 2007).

When neuroblasts reach the olfactory bulb, they switch their cell migration from tangential to radial and integrate within the olfactory bulb laminar structure by differentiating into either granular cells, making dendro-dendritic synapses, or into periglomerular cells, making synapses with mitral cells and olfactory neurons in the glomerular layer. At the stage of differentiation, SVZ-derived neurons express NeuN, a neuronal marker. However, other typical neuronal markers expressed in postmitotic neurons in other neuronal systems can be expressed in the migrating mitotic neuroblasts. In conclusion, marker expression in the different SVZ progenitors is fluid and multiple markers need to be used in combination to properly identify SVZ cell types (Mamber et al., 2013).

1.1.3 Neuronal differentiation programmes

Deciphering how the striking diversity of neuronal subtypes is created during embryonic and postnatal development is a major challenge for developmental neurobiologists. Mechanisms implicated in neurogenesis include extrinsic cues such as secreted polypeptide growth factors, adhesion molecules, extracellular matrix components and neuronal activity (Fietz et al., 2012). However, a wealth of evidence additionally supports the importance of cell intrinsic mechanisms in neuronal development. One of the best characterised mechanisms by which neurons acquire their shape and position, which regulate neuronal development largely independently of cellular environments, are transcription factors and their intracellular cascades.

Transcription factors can govern entire developmental programmes by intrinsically directing differentiation stages, or by altering competency and responses to extrinsic cues and are therefore considered to lie at the interface of extrinsic and intrinsic cellular signals. Over time, cells committed to the neuronal fate become independent of extracellular signals through the expression of neuronal-specific genes, a process catalysed by proneural factors such as basic helix-loop-helix transcription factors.

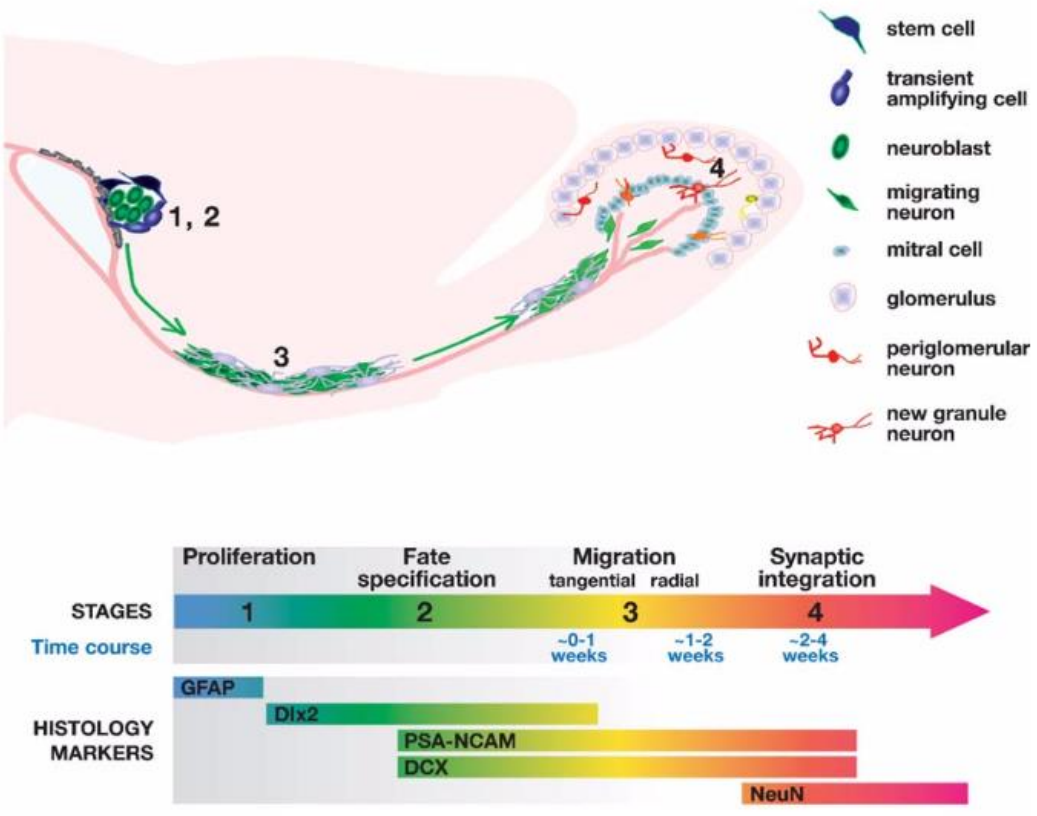

Figure 1-2 Neurogenesis, migration and differentiation of subventricular zone progenitors

Olfactory bulb (OB) neurons are born at the subventricular zone (SVZ) of the forebrain throughout the animal's life. The stem cells (1) give rise to the transient amplifying cells that further divide into neuroblasts (2). Neuroblasts migrate from the SVZ to the OB in the rostral migratory stream (3). During migration, the neuroblasts continue to divide. When they reach the OB, they change their migration mode from tangential to radial. They differentiate terminally into either the periglomerular or granule neurons and integrate into the OB circuitry (4). Throughout differentiation, SVZ derived neuroblasts express numerous markers, including neuronal differentiation genes, while actively proliferating.
(Figure taken from Ming and Song, 2005)

1.1.3.1 Basic helix-loop-helix transcription factors

Basic helix-loop-helix (bHLH) transcription factors (TFs) are proneural genes first identified in *Drosophila melanogaster* based on their ability to confer a neural identity onto naïve ectodermal cells. The first families of proneural genes identified were the members of the *achaete-scute* complex, as well as *atonal, amos* and *cato*. These were then found to be conserved and expanded in vertebrates and include the *Neurogenin* proneural genes, *Neurogenic differentiation* genes such as *NeuroD1*, as well as *Olig* differentiation genes. The proneural bHLH factors are key regulators of neurogenesis, coordinating a neuronal fate and specific subtype identity. They are considered necessary (by loss of function) and sufficient (by gain of function) to activate genetic neuronal differentiation programmes (Farah et al., 2000; Huang et al., 2014; Guillemot, 2007).

Proneural genes encode Class II bHLH transcription factors and are characterised by their tissue- specific expression profiles. Class I bHLH proteins/ E-proteins, in contrast, are more ubiquitously expressed and act as dimerization partners for class II bHLH proteins, forming protein-protein interactions through the HLH domains, comprised of two alpha-helixes connected by a loop (Meredith and Johnson, 2000; Murre et al., 1989). bHLH factors can cross-regulate each other and hence direct different cell fate decisions. The balance between the different expression profiles of each factor determines the differentiation status of the cell (Bertrand et al., 2002).

Proneural bHLH transcription factors include a group of bHLH differentiation genes, that mediate the terminal differentiation of neurons and belong to the NeuroD/Nex family. These genes are E box binding TFs that, when overexpressed, can induce cell cycle arrest and neuronal differentiation in culture (Farah et al., 2000). The genes are expressed in the differentiating neurons in the cortex, however, single and double knockout mice for NeuroD1, NeuroD1 or Nex2 show no abnormal phenotype in cortical differentiation. This suggests a strong redundancy between different members of the family, or existence of another

differentiation TF that regulates cortical neurons terminal differentiation (Ross et al., 2003). However, in the cerebellum and the hippocampus, NeuroD1 has been shown to be essential for normal development of glutamatergic neurons (see Chapter 4).

A lot of research has been conducted into the roles of different proneural bHLH transcription factors in cortical development (reviewed in Ross et al., 2003; Wilkinson et al., 2013). In short, the two most important proneural genes in cortical development are *Neurog1/2* and *Ascl1* which function as a central genetic switch to control a binary choice between cortical and subcortical cell fates in cortical progenitors. Expression and function of these genes are regulated at many levels, including dynamic expression, phosphorylation and target gene selection. Importantly, the same bHLH factors can have more than one function during cortical development and their function depends on the cellular context (Ross et al., 2003; Wilkinson et al., 2013).

1.1.3.2 Atoh1 role during development

In the cerebellum, the two proneural bHLH TFs, Atoh1 and Ptf1a, specify the two neurogenic primordia: the rhombic lip and the ventricular zone, respectively. Atoh1 has diverse roles during development in many parts of the brain. It is required for terminal differentiation of hair cells in the ear but also early specification of neurons in the cerebellum. Additionally, Atoh1 has roles outside of neurogenesis, for example in cell cycle regulation in the intestine. A genome-wide screening for potential targets for Atoh1-mediated gene transcription identified 601 potential genes involved in gene transcription, cell cycle, chromosomal organisation, metabolism, Shh signalling, Notch signalling and other signalling pathways (Klisch et al., 2011). Therefore, overall, the function of Atoh1 is in cell cycle maintenance and differentiation, even though its effects are context-dependent (reviewed in Mulvaney and Dabdoub 2012).

An enhancer of Atoh1 has been identified that directs Atoh1 expression in the cerebellum and the ear (Helms et al., 2000). Several proteins have also been identified that directly interact with this enhancer to upregulate or downregulate Atoh1 expression, including Atoh1 itself in an autoregulation loop. Targets of Atoh1-mediated transcription are tissue-dependent (Lai et al., 2011). Atoh1 activity is additionally modulated at the protein level by competitive binding, restriction of transcriptional activities through heterodimer formation and post-translational mechanisms. Therefore, regulation of Atoh1 has multiple levels of control and the molecular context within which Atoh1 is expressed is crucial to its activity.

In the cerebellum, Atoh1 is transiently expressed in early RL derivatives, and in GCPs during their proliferative developmental stage. Atoh1 knockout mice fail to develop an EGL (Ben-Arie et al., 1997) and therefore no GCs are formed. Similarly, overexpression of Atoh1 leads to granule cell differentiation defects through aberrant expression of early differentiation markers (Helms et al., 2001). Elevated levels of Math1 cause an uncoupling of differentiation events that decrease the probability of a GCP successfully progressing through development to form a mature granule cell. Because NeuroD1 is also a target of Math1, its expression is elevated in the outer EGL following Math1 overexpression. NeuroD1 expression and function is discussed in further detail in Chapter 4.

1.2 The cerebellum: development, anatomy and function

The cerebellum and its beautifully defined, laminar structure has been a fascination of neuroscientists for centuries. The apparent complexity achieved with just two main cell types allows a scientist to ask and explore a huge variety of developmental questions that, in comparison to other brain structures, can be relatively easily investigated. In this thesis, development of one of the two cell types, the cerebellar granule cell, is explored in detail. It is therefore helpful to understand what the cerebellum is, how its development is orchestrated, and where the different cell types are derived from.

1.2.1 The structure and function of the adult cerebellum

The cerebellum is a well-defined structure of the brain responsible for the coordination of movement and sensorimotor functions, as well as regulation of muscle tone and balance (Ito, 2006). Recent evidence suggests that it also plays a role in higher cognitive and emotional functions such as speech, spatial memory (Allen, 2006; Ito, 2008; Rodríguez et al., 2005; Stoodley, 2012; Strick et al., 2009) and most recently, encoding expectation of reward (Wagner et al., 2017). It is the second largest brain structure, located posteriorly and inferiorly in the cranial cavity. It consists of a central area termed the vermis and two cerebellar hemispheres, which are further subdivided into lobes with specific functions.

The cerebellum, like the cerebrum, consists of a cortex where the grey matter is found, and of areas of white matter further subdivided into white matter tracts and cerebellar nuclei. The adult cerebellar cortex is composed of three layers: the molecular layer (ML), Purkinje cell layer (PCL) and the internal granular layer (IGL), depicted in **Figure 1-3C**. The cerebellar cortex connectivity and structure is remarkably simple with only two main types of neurons, the granule cells (GCs) and Purkinje cells (PCs), making the majority of synaptic connections. Additionally, a diverse set of interneurons (INs) modulate the synaptic output of the GABAergic Purkinje cells to the cerebellar nuclei (Roussel and Hatten, 2011). GCs are the main excitatory cell type of the cerebellum and constitute the most numerous neuronal population of the entire brain. GCs, unipolar brush cells (UBCs) and eurydendroid

cells use glutamate for neurotransmission. On the other hand, PCs are the major inhibitory cell type in the cerebellum and, among INs such as basket cells, Golgi and stellate cells, release GABA as their neurotransmitter, with some INs also releasing glycine as a co-transmitter, or on its own (Leto et al., 2015; Sotelo, 2004).

The neurons in the cerebellum receive excitatory input from the neurons of the precerebellar nuclei through two major afferent fibres: the climbing and mossy fibres. The former originate within the inferior olive nuclei and innervate PC dendrites, whereas the latter come from other precerebellar nuclei (e.g. the vestibular nucleus and pontine nuclei) and synapse onto GCs, forming cerebellar glomeruli (Sotelo, 2004). **Figure 1-3C** illustrates this basic synaptic organization.

The organization pattern within the cerebellum is very characteristic and continuous throughout the anterior-posterior length of the structure. In the ML, a region of low cell density but high synaptic incidence, PC dendrites receive inputs form climbing fibres and GC axons whereas in the IGL, which has a very high cellular density, GCs synapse with mossy fibres and Golgi INs. Between these two layers, the PC cell bodies form a distinctive monolayer, and project their axons outside of the cerebellar cortex. This stereotyped three-dimensional geometry has been very useful in determining the functions of all types of cerebellar cells and has facilitated establishment of the cerebellum as a favoured model for studying neurogenesis and circuit connectivity in the brain (Sotelo 2004).

One of the most striking features of the cerebellum of some mammals, birds and fish is its highly complex foliation pattern, as pictured in **Figure 1-3A-B**. The structure of the cerebellum differs throughout the animal kingdom from simple and unfoliated to extremely complex. A unified scheme for naming the lobules in the vermis of birds and mammals has been proposed and is still in use, dividing the cerebellum into ten main lobules, which are further subdivided in some species (Larsell, 1948). The extensive foliation of the cerebellum arises as a consequence of the high proliferation rates of granule cell precursors (GCPs) in the external germinal layer (EGL) during development and, as a consequence, the surface area of the cerebellum increases much more than its volume. This phenomenon has significant evolutionary implications and a deeper understanding of this process is

vital for fuller appreciation of the molecular details of cerebellar development (Butts et al., 2011).

Interestingly, the fact that the cerebellum modulates the function of all areas of the neocortex (Buckner, 2013) suggest that the two brain areas must have co-evolved. This is emphasised in higher mammals where the hemispheres are enriched for the connections to the neocortex. Furthermore, the ratio of the number of neurons in the cerebellum and the neocortex is remarkably constant across the mammalian species, reflecting the close co-evolution of the two regions (Herculano-Houzel et al., 2010).

1.2.2 The early specification of the cerebellum during vertebrate development

During development, the nervous system arises from a homogenous sheet of epithelial cells, which later undergo morphological changes to form the neural tube, which in turn gives rise to the entire central nervous system. The future brain region forms in the anterior portion of the neural tube and from a very early stage the tube is regionalized into vesicles which will become the forebrain, midbrain and the hindbrain. The cerebellum arises from the caudal portion of the mesencephalic vesicle and the rostral portion of the metencephalic vesicle (Martinez and Alvarado-Mallart, 1989), at the level of rhombomere 1 (Eddison et al., 2004), which is located between the expression domains of Hoxa2 posteriorly and Otx2 anteriorly (Wingate and Hatten 1999).

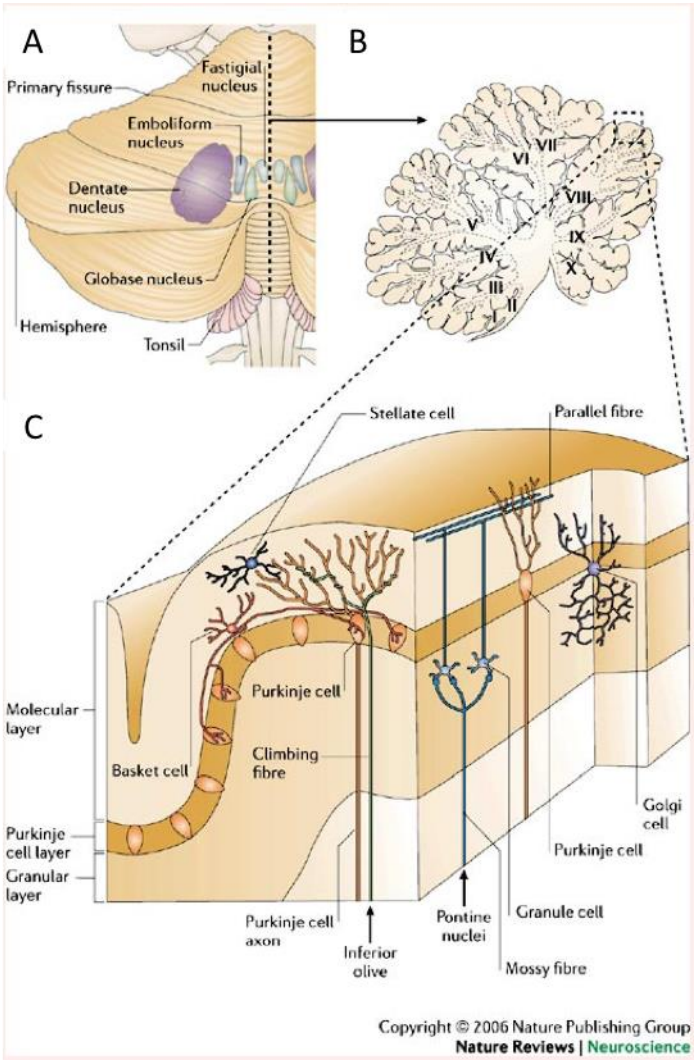

Figure 1-3: The structure of the adult human cerebellum

A) The ventral view of the human cerebellum, depicting the human cerebellar nuclei: the dentate nucleus, the fastigial nucleus, the globase nucleus and the emboliform nucleus. **B)** A midsagittal cross-section through the cerebellum showing the lobular organization. The main lobes are denoted with Roman numerals (I to X). **C)** The neurons and their connections in the human cerebellar cortex. Granule cells (blue) send their T-shaped axons, the parallel fibres, into the molecular layer to synapse onto Purkinje cell dendrites (red), which project their axons outside the cerebellar cortex onto cerebellar nuclei. Mossy fibres from the pontine nuclei synapse onto GC dendrites in the granular layer. Climbing fibres from the inferior olive synapse with Purkinje cell dendrites. Interneurons (stellate cells, basket cells, Golgi cells) are present throughout the cerebellar cortex to modulate the cerebellar output. (*Figure taken from Ramnani, 2006*)

Transplantation studies, among others, have confirmed that the isthmus located at the midbrain-hindbrain boundary has organizing activity for the midbrain and the cerebellum (reviewed in Sotelo 2004). Highly specific expression of two transcription factors is found at the junction where the isthmus is located. The midbrain tissue expresses Otx2, whereas the hindbrain tissue expresses Gbx2 (Joyner et al., 2000). These two proteins inhibit the expression of each other, and thus define a strong border between both territories. Additionally, the fact that Gbx2 represses Otx2 in the metencephalon is instrumental in development of the cerebellum in this region (Millet et al., 1999).

The isthmus organizing activity is achieved by a secreted molecule Fgf8, which, when introduced on a bead onto diencephalon tissue, has the ability to induce ectopic midbrain and cerebellum (Martinez and Alvarado-Mallart, 1989). Fgf8 expression in turn is induced by the action of a number of transcription factors, which cross-regulate each other. Firstly, Otx2 in the midbrain induces the expression of Lmx1b, which prevents the expression of Fgf8 in the nearby cells. However, Lmx1b induces expression of Wnt1 in the midbrain cells, which, when secreted, induces expression of Fgf8 in hindbrain cells. Therefore, the reciprocal interactions between Gbx2 and Otx2 establish the precise location of Fgf8 expression domain (Nakamura and Watanabe, 2005). Strong Fgf8 signalling leads to the formation of a cerebellum whereas weak signalling results in the formation of the tectum (Sato et al., 2001).

1.2.3 The specification of cerebellar cell types during development

In contrast to many other brain regions, the cerebellum consists of two distinct germinal zones. In addition to the ventricular zone (VZ), also known as the primary germinal zone, neural proliferation takes place in a secondary germinal zone known as the external germinal layer. The EGL contains granule cell precursors (GCPs), which have migrated there from the rhombic lip (RL), a specialized germinative epithelium located at the interface between the neural tube and the roof plate of the fourth ventricle (**Fig. 1-4**, Wingate 2001).

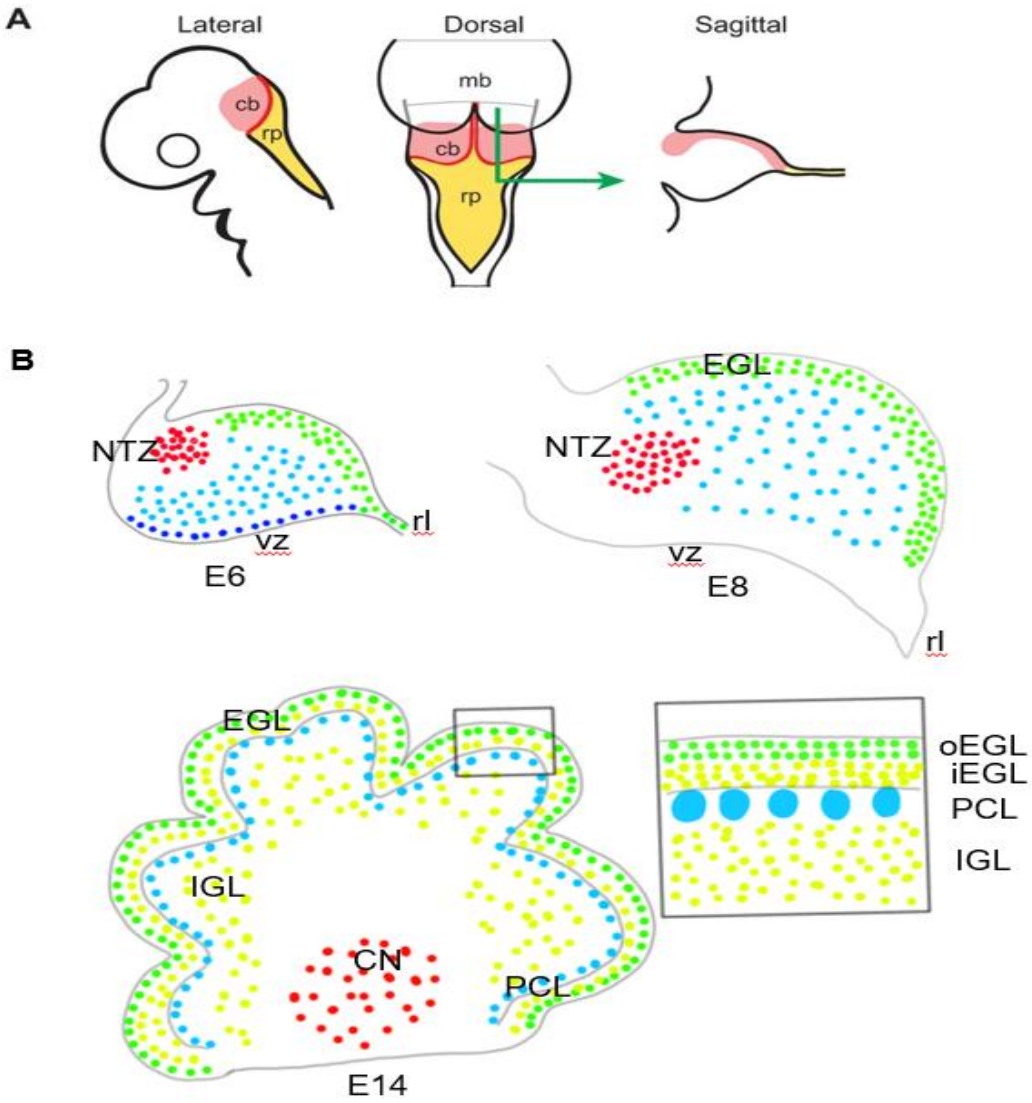

Figure 1-4: Specification and development of the cerebellum

A) The location of the upper rhombic lip (red line) in a chick embryo at E4 at the border between the neural tube and the roof plate of the fourth ventricle. A lateral, dorsal and sagittal views are shown. (*Modified from Butts et al, 2014*) **B)** The location of different types of neurons within the developing chick cerebellum at different developmental stages (E6, E8, E14). The Atoh1^{+ve} rhombic lip gives rise first to NTZ cells(red) and then GCPs (green), which migrate tangentially to populate the dorsal cerebellar anlagen. Purkinje cells (light blue), derived from the ventricular zone progenitors (dark blue) release Shh for GCP proliferation. At E14 the EGL is divided into the outer and the inner layers, where GCPs undergo different phases of development. After transit amplification stage, postmitotic granule cells (yellow) migrate radially into the inner granular layer, passing Purkinje cell bodies and leaving behind the parallel fibres. *NTZ= nuclear transitory zone CN= cerebellar nuclei PCL= Purkinje cell layer rl= rhombic lip vz=ventricular zone rp=roof plate*

Figure 1-4 shows the position of the RL and the formation of the EGL. The RL gives rise to all the glutamatergic neurons of the cerebellum, including the glutamatergic neurons of the cerebellar nuclei (CN) and the granule cells, as well as other ventral populations of extra-cerebellar glutamatergic neurons of the rostral hindbrain (Wingate and Hatten 1999).

The ventral cells, destined for the lateral pontine nucleus and the locus coeruleus begin to proliferate in the mouse embryo by E10, whereas GC proliferation is a much longer-term process, lasting from E12 to P15 in the mouse. The specification of glutamatergic cells at the RL is chiefly controlled by the basic helix-loop-helix transcription factor Atoh1 (Math1 in mouse) (Ben-Arie et al., 1997), expression of which is turned off as the early-born cells leave the RL. However, Atoh1 continues to be expressed in GCPs that migrate tangentially away from the RL and populate the EGL. Atoh1 expression is then turned off in post-mitotic granule cells (Machold and Fishell 2005; Wang et al., 2005). Studies confirm that Atoh1 expressing progenitors of the RL generate all glutamatergic neurons of the cerebellum in a sequence of migratory waves (Machold and Fishell 2005; Carletti and Rossi 2008; Green and Wingate 2014).

As a proof of principle for the role of major developmental regulators of granule cell specification, Salero and Hatten (2007) treated embryonic stem cells with cerebellar organizers (Fgf8, retinoic acid), followed by a treatment with dorsalizing agents (Wnt1, Wnt3a, Gdf7, Bmp6 and Mbp7) and mitogens known to expand the GCP population (Sonic Hedgehog, Jag1). This treatment, along with culturing on medium conditioned with cerebellar glial cells, resulted in ES cell-derived cells expressing a number of granule cells markers, including Math1. Moreover, when injected into the cerebella of living mice, these ES cell-derived cells migrated into the IGL and differentiated as functioning granule cells. This study confirms the role of local signals in normal cerebellar granule cell neuron specification.

The second major cell type of the cerebellum, the Purkinje cells are born from the ventricular zone and are among the first-born neurons of the cerebellum, just slightly later than the cerebellar nuclei (CN) neurons (Morales and Hatten, 2006).

Purkinje cells are generated in a three-day period and migrate immediately underneath the forming EGL, where they establish the future Purkinje cell layer (PCL). Ptf1a gene, a basic helix-loop-helix (bHLH) transcription factor, is required to generate Purkinje cells and all other GABA-ergic interneurons of the cerebellum (Hoshino et al., 2005). Inhibitory INs such as Golgi, basket and stellate cells, first believed to be descendants of EGL precursor cells (Miale and Sidman, 1961), are in fact VZ-derived and born in the cerebellar prospective white matter from $Pax2^{+ve}$ IN progenitors. Postmitotic INs migrate to their respective positions within the cerebellar cortex after birth (Zhang and Goldman 1996; Leto et al., 2010). Activation of the Wnt/ β-Catenin signalling pathway has been proposed to affect the differentiation of cells born at the ventricular zone (Selvadurai and Mason, 2012).

1.2.3.1 Temporal specification of chicken rhombic lip derivatives

The chicken model has been used extensively to examine the specification of cells at the rhombic lip. A series of electroporation experiments have recently revealed the sequence of production of different neuronal cell types from the $Atoh1^{+ve}$ rhombic lip (Green and Wingate 2014). The results reinforced the principle that the dorsoventral position of RL derivatives is correlated with the organisation of discrete neurogenic temporal windows (Machold and Fishell, 2005; Wang et al., 2005; Gilthorpe et al., 2002; Hagan and Zervas 2012). The authors reported that there are four separate populations of neurons born at the RL in the chicken between stages 22-28 (E4-E6) and each population has a distinct window of production and expresses different molecular markers. As **Figure 1-5** summarises, most ventral, extracerebellar $Lhx9^{+ve}$ cells are generated at E4/st22, which are then followed by cells of the lateral cerebellar nucleus ($Lhx9^{-ve}$, $Tbr1^{-ve}$). Next, the $Tbr1^{+ve}$ cells of the medial cerebellar nucleus are generated. The final population of neurons are the $Math1^{+ve}$, $Pax6^{+ve}$ granule cell precursors of the EGL, which are born at E6/st28. All of these cell populations have different axonal projections and can be distinguished by their morphology, position and molecular markers. Other studies also showed that unipolar brush cells (UBCs) are generated at the RL alongside the GCPs, but they follow a different migratory route, through the forming cerebellar white matter instead of dorsally, under the pial surface like all the other $Atoh1^{+ve}$ RL derivatives (Englund et al., 2006).

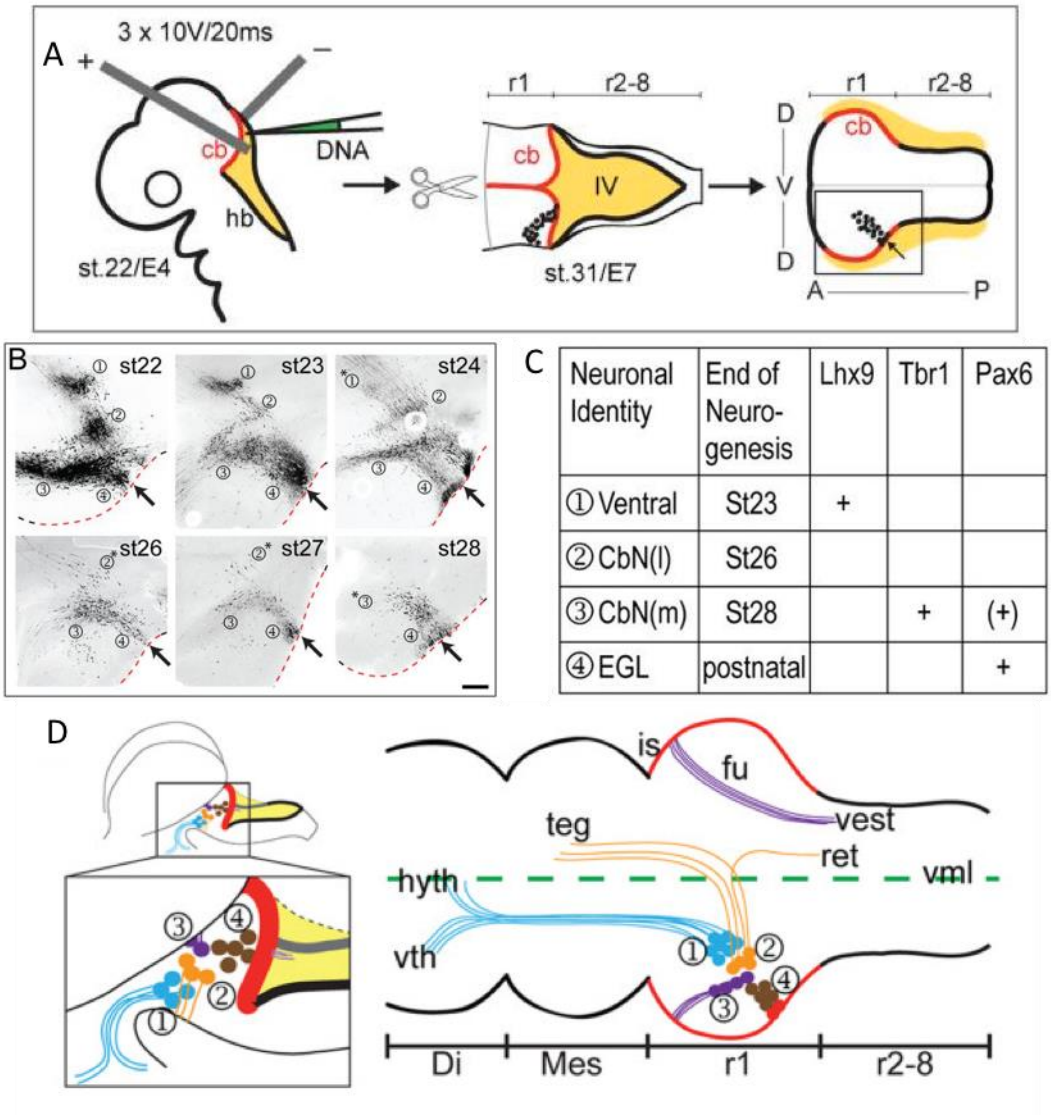

Neuronal Identity	End of Neuro-genesis	Lhx9	Tbr1	Pax6
① Ventral	St23	+		
② CbN(l)	St26			
③ CbN(m)	St28		+	(+)
④ EGL	postnatal			+

Figure 1-5 The temporal specification of chicken rhombic lip derivatives

A) Electroporation of chicken embryos. DNA (Atoh1 enhancer sequence driving cre -recombinase along with lox-stop-lox-GFP plasmid to distinctly label Atoh1^{+ve} rhombic lip cells) is injected into the fourth ventricle underneath the rhombic lip. Positive and negative electrodes are positioned to electroporate the cerebellar RL only. The hindbrain is dissected and flat-mounted. **B)** Electroporation of Atoh1-cre and stop-GFP constructs at different stages (st22-st28) results in the presence of distinct neuronal rhombic lip (Atoh1^{+ve}) derived populations at E7, identified based on their migration patterns. **C)** Summary of the four populations of cells electroporated at the chicken RL and their molecular characterisation. **D)** Summary of the neuronal positioning and axonal projections of the four neuronal RL-derived populations.

(*Figure modified from Green and Wingate, 2014*)

1.3 Development of the cerebellar granule cells

Granule cells of the cerebellum are the most numerous neuronal subtype in the brain. Their development has been extensively studied to better understand neuronal proliferation, differentiation, migration and circuit formation. Due to the prevalence of childhood cerebellar cancer, medulloblastoma, deciphering the molecular programmes for GC neurogenesis has immense clinical relevance. Additionally, during development, GCs undergo remarkable migratory behaviours, including both tangential and radial modes of migration. This makes granule cells especially valuable in studying all neuronal differentiation processes and has therefore attracted a great interest from neurobiologists.

1.3.1 Neurogenesis within the external germinal layer

GCPs are born at the RL at E12.5 in the mouse (E6 in the chicken) and spread across the dorsal side of the cerebellar anlagen by tangential migration between E13 and E16 to form the secondary proliferative zone interchangeably called external germinal layer (EGL) and external granular layer (Alder et al., 1996). Preference is given to the former as it implies the transience of this developmental structure. Excluding the recently discovered nestin-expressing GCPs in the EGL, (Li et al., 2013), the RL has been confirmed as the only source of GC neurons in the cerebellum (reviewed in Wullimann et al., 2011), as demonstrated by a number of detailed studies, including chick-quail chimeras, genetic fate mapping in the mouse and retroviral labelling in the rat (Hallonet et al., 1990; Martinez and Alvarado-Mallart 1989; Machold and Fishell 2005; Wang et al., 2005; Zhang and Goldman 1996; Sgaier et al., 2005). GCPs reside in the EGL for an extended period of time and divide predominantly by proliferative symmetric divisions to increase their population size and then the individual clones derived from the early GCPs differentiate en masse by terminal symmetric divisions (Espinosa and Luo 2008; Nakashima et al., 2015). Interestingly, a novel population of nestin-expressing GCPs has recently been found in the EGL. These cells are committed to the GC lineage but show differences to the classical GCPs in that they reside in the deep parts of the EGL and are mostly quiescent. However, they are more susceptible to forming tumours due to their increased genomic instability (Li et al., 2013).

The EGL is one cell in thickness at the start of formation and in time becomes up to eight cells thick due to precursor proliferation (Hatten et al., 1997). Studies suggest that one GCP divides to give rise to around 250 neurons on average (Espinosa and Luo 2008). This means that each precursor cell derived from the RL can undergo eight symmetric proliferative divisions and a terminal symmetric division generating two neurons. Asymmetric divisions (which produce one GCP and one GC neuron) have also been observed, but represent only around 10% of cell divisions in the EGL (Nakashima et al., 2015; Yang et al., 2015). Recent papers have revealed that oriented cell divisions of GCPs underlie the antero-posterior (A-P) growth of the cerebellum and GC clone geometry (Legué et al., 2015). Furthermore, the same authors found that GCP production is differentially regulated in each zone of the cerebellar vermis. For example, the central lobules have a delayed timing of GC production. These analyses indicate that the dynamics of GCP production play a role in determining the 3D structure of the cerebellum (Legué et al., 2016). Moreover, other studies have reported regional differences in gene expression along the A-P axis of the EGL, suggesting a mechanism for different rates of precursor proliferation (Corrales, 2004; Marino et al., 2003; Yaguchi et al., 2009).

Although cell culture of GCPs results in normal morphological and molecular transitions into T-shaped GCs, suggesting that instructions for GC differentiation are cell-intrinsic (Yacubova and Komuro 2002; Kumada et al., 2009), GC differentiation *in vivo* relies on many extrinsic signals. This conclusion was first reached after studies were performed on naturally occurring mutant mice, most notably the *staggerer* (Sonmez and Herrup, 1984) and *reeler* (D'Arcangelo et al., 1995) mutants. These mice show neurological abnormalities due to problems within the Purkinje cell layer, yet they additionally display a reduction in the number of GCs. Further studies using knockout mice and utilizing Purkinje cell ablation method confirmed that GCP proliferation depends on Purkinje cells (Smeyne et al., 1995). Investigation into the identity of the molecule secreted by Purkinje cells implicated the mitogen, Sonic Hedgehog (Shh) (Wechsler-Reya and Scott, 1999; Dahmane and Ruiz i Altaba, 1999; Wallace, 1999; Lewis et al., 2004). Shh starts to be expressed in Purkinje cells at E16.5 and its expression continues

until adulthood (Lewis et al., 2004). Experiments with anti-Shh antibody injections into the EGL resulted in a thinner EGL and a reduction in GC proliferation whereas addition of Shh to *in vitro* cerebellar cultures results in higher cell proliferation (Wallace, 1999). More sophisticated experiments, using Cre-medited knockout of Shh expression specifically in Purkinje cells leads to complete absence of the EGL and consequently the IGL (Lewis et al., 2004), confirming Purkinje cells as the source of the Shh signal. *Gli2* is thought to be the main mediator of the Shh signal and the resultant proliferation of GCPs (Behesti and Marino, 2009). Elegant genetic manipulations involving removing the activators (Gli1 and Gli2) and the receptor of Shh (Smoothened) demonstrate the importance for Shh in cerebellar histogenesis, as different levels of Shh signalling change the complexity of the cerebellar foliation pattern (Corrales et al., 2006). Deregulation of Shh signalling is also observed in human medulloblastoma cases (Hatten and Roussel, 2011).

Although Shh signalling has been repeatedly shown to affect the proliferation and differentiation of GCPs in the EGL, there are many other important downstream targets of, or factors working alongside, Shh. For example, *N-myc* is essential for the rapid expansion of GCPs (Hatton et al., 2006; Knoepfler et al., 2002; Kenney et al., 2003) and a member of the polycomb group, *Bmi1*, is also crucial for the clonal expansion and implicated in human medulloblastoma cases (Leung et al., 2004). The components of the Notch and Wnt pathways also play a role in GCP proliferation and differentiation decisions (Behesti and Marino, 2009). Additionally, Notch2 signalling inhibits differentiation of GCPs (Solecki et al., 2001), possibly through upregulation of Atoh1 expression as a consequence of antagonizing BMP signalling (Zhao et al., 2008; Machold et al., 2007).

More recent studies have added many other genes and proteins to the list of factors affecting GC development in the EGL: Wnt signalling (Anne et al., 2013), neurotrophins (Katoh-Semba et al., 2000; Zanin et al., 2016), cell-cycle regulators (Miyazawa et al., 2000), microRNAs (Constantin et al., 2016) various transcription factors (Lee et al., 2012; Rossman et al., 2014; Barthelery and Manfredi 2016; de la Torre-Ubieta and Bonni 2011), growth factors (Elvers et al., 2005; Fernandez et al., 2010; Ye et al., 1996), integrin signalling (Blaess et al., 2004; Mills et al., 2006), apical complex proteins (Park et al., 2016), among others. Therefore, GCP

proliferation and differentiation is a complex process, regulated by a large number of factors and signalling pathways. This complexity and the many interactions between the different signals are not yet fully understood.

After completing their rounds of divisions and becoming post-mitotic, GCs start to leave the EGL around the animal's time of birth, resulting in a gradual loss of the EGL and the formation of the internal granular layer (IGL). The formation of the IGL continues until P20 when it is considered complete.

1.3.2 Migration of granule cells within the external germinal layer

Accumulating evidence suggests that neuronal migration requires orchestration of multiple molecular events. Pathway selection, formation of adhesive interaction and activation of specific ion channels, receptors and cytoskeletal elements are a just some aspects of successful migration (Singh and Solecki, 2015; Compagnucci et al., 2016; Komuro and Yacubova, 2003; Ayala et al., 2007). The developing cerebellum has long provided a preferred assay system for studying basic mechanisms for neuronal migration and differentiation. A wealth of information has been obtained by studying GC migration in dissociated cultures (Rivas and Hatten, 1995; Yacubova and Komuro, 2002; Kawaji et al., 2004; Kumada et al., 2009) as well as in brain slices (Komuro and Rakic 1995; 1998; Komuro et al., 2001; Nakashima et al., 2015). Observations of GCP cell movement in slices have revealed that their migration is a very dynamic process and changes in shape, direction and rate of migration can be detected.

Cajal offered his initial insight into GCP migration in 1911 using Golgi staining preparations (Cajal, 1911) and his proposed sequence of cellular behaviour still remains largely accepted today with few adjustments (**Figure 1.6A**). Cajal first observed that as GCPs enter the EGL after migration from the RL they become round, retract their tangential processes but are attached to the pia, and begin to divide extensively. Later, as they become postmitotic, they begin to migrate tangentially in the EGL in the mediolateral directions, descending into the inner EGL. Recent studies, mostly performed by Komuro et al in late 1990s and beyond,

have provided a detailed analysis of GCs migration within the developing cerebellum.

Arguably, researchers have concentrated most efforts on elucidating the mechanisms for radial migration of granule cells from the EGL to the IGL. However, it has been correctly recognized that tangential movement within the EGL is critical to our understanding of the formation of cerebellar compartments. Clonally related cells are allocated in specific areas of the developing cerebellar hemispheres as a consequence of their tangential migration in the EGL (Espinoza and Luo, 2008, Legue et al., 2015). Thus, studying this phase of granule cell development in detail is essential to our understanding of cerebellar compartmentalisation.

Starting with the proliferating precursors in the outer EGL, Komuro et al (2001) followed cells in cerebellar slices as they descend into the IGL. The authors confirmed that the EGL is divided into layers with proliferating precursors located in the top layers, whereas postmitotic granule cells (showing no BrdU labelling) located underneath the precursors in the lower EGL. After the last symmetric division of GCP the cells remain in the EGL for 1 to 2 days, and, when in the middle layer of the EGL, become oriented in the transverse plane and extend two horizontal processes. These two processes are nearly always of a different size. The longer, thicker process is similar to a leading process with a large filopodium at the tip, whilst the shorter, thinner one, looks like an axon. However, when at the bottom of the EGL, both processes become long and of uniform thickness as they transition into the parallel fibre (Komuro et al., 2001).

GCPs undergo substantial tangential migration within the EGL with systematic changes in their tempo, mode and shape depending on their position within the EGL. For example, the rate of cell movement is the highest within the middle part of the EGL when, at the same time, the length of the leading process is the shortest. A saltatory mode of migration is observed at this stage with cells fluctuating between rapid advancement and complete immobility. When reaching the bottom of the EGL, immature GCs slow down their migration and extend longer processes. The cell soma also changes shape, becoming more round when movement is the

slowest and adopting a spindle-shape when migrating at a faster rate. The migration is generally quite fast, averaging a rate of approx. 14.8um/h in the middle of the EGL. The average distance that each GC travels within the EGL is over 220um, however some cells can travel significantly longer distances (Komuro et al., 2001).

Upon reaching the EGL/ ML boundary, the cells extend a third, vertical, process, that they will use to descend radially into the IGL. It is of great interest to understand how the granule cell makes the decision to cease its tangential migration and start descending into the IGL. Komuro et al (2001) have observed that the sign of ending tangential migration is a reduction in cell body movement and an extension of a new vertical process, which actively searches for potential guidance cues using lamellopodia and filopodia. The cell nucleus then translocates into the newly formed vertical process and starts to quickly descend toward the bottom of the ML. The cell leaves behind a thin trailing process which becomes the parallel fibre. Kawaji et al (2004) concluded that tangentially migrating GCs are guided by axonal leading processes: they have a large growth cone and elongate rapidly to form parallel fibre axons expressing $Ankyrin_B$. Interestingly however, there is another mechanism of parallel fibre formation whereby one parallel fibre originates from the leading process, and the other develops later in a separate manner (Komuro et al., 2001). However, the transition from a leading process into an axon, and at which point in development of GCs the horizontal processes represent one or the other, is not precisely defined.

1.3.3 Radial migration of granule cells

After leaving the EGL the maturing GCs start to migrate radially towards the IGL where they will reside in the mature cerebellum. Semaphorin6A has been implicated in the switch from tangential to radial migration by binding to Plexin A2 (Kerjan et al., 2005; Renaud et al., 2008). During the migration through the ML the cell body elongates vertically, forms an extensive adhesion junction between the cell's surface and the glia through the ASTN1 adhesion protein (Fishell and Hatten, 1991), and extends a voluminous leading process, as well as a thinner trailing process. The leading process is considered dendritic, whereas the trailing process

develops into the parallel fibre (Kawaji et al., 2004). Electron microscopy studies (Rakic, 1971) have indicated that the soma of GCs is closely apposed to the Bergmann glial fibres, which suggests that, analogous to new-born cortical neurons that use radial glial cells for migration, GC neurons use Bergmann glia for guiding their migration to the IGL.

Interestingly, the rates of migration within the ML vary depending on the age of the cerebellum, continually increasing as the cerebellum matures. Therefore, even though the width of the molecular layer and the IGL increases as more and more neurons differentiate, it takes roughly the same time for GCs to reach their final position in the IGL throughout development (Komuro and Rakic 1995). The time depends not only on the simple speed of migration but also on the proportion of time when cells are stationary or move in the backwards direction. Forward movement of the cell soma is coordinated by the PAR6 polarity complex, which localises to the centrosome and the soma and activates the actomyosin contractile motors in the proximal region of the leading process (Solecki et al., 2004; 2009).

Upon leaving the ML and entering the Purkinje cell layer, the cell soma of GCs transforms its shape to a sphere and slows down its movement, ultimately becoming stationary for an average of 115 min (Komuro and Rakic, 1998). At this stage, the migrating GCs lose their attachment to the Bergmann glia and require new guidance cues to complete their migration. The observation that the distal portion of the leading process develops a high number of lamellopodia and filopodia suggests that active search for such cues is taking place at this stage in differentiation. Studies in cell culture have shown that both cytology and migratory behaviour of GCs changes depending on the substrate on which they are plated (Yacubova and Komuro, 2003).

When the cell makes the decision to continue its migration, it accelerates the rate of movement just before reaching the IGL. Although no Bergmann glia are present in the IGL, GCs are able to maintain similar speed of migration in this layer. It is not yet clarified how GCs restart their migration and find their way into their position in the IGL, however several extracellular matrix molecules have been proposed. Alternatively, the ascending axons of earlier- generated GCs might guide the cells

that arrive later (Yacubova and Komuro, 2003). Either way, cells arrive to their position in the IGL and cease migration at the IGL-white matter border where they become round and stationary again. They will then differentiate, develop dendrites and establish synapses with mossy fibres in the IGL, where they reside in the mature cerebellum.

1.3.4 Insights into granule cell development from tissue and cell culture studies

Substantial amounts of data have been gathered on GC differentiation in brain slices and this represents an important part of research on GC behaviour, reflective of their *in vivo* environment. Many studies demonstrate that contact with neighbouring cells and numerous external guidance cues such as attractive and repulsive molecules as well as extracellular matrix and adhesion molecules control GC migration (e.g. Alcántara et al., 2000; Yacubova and Komuro 2002). However, studies of GC cultures *in vitro* reveal interesting aspects of GC development that are difficult to study *in vivo*, such as their intrinsic program of differentiation or the existence of an internal clock.

Studies have reported that isolated, dissociated GCs go through a characteristic sequence of differentiation without the need for cell-to-cell contact (Yacubova and Komuro, 2002; Kumada, 2008). Three migratory phases were observed in GC cell cultures (Yacubova and Komuro, 2002). First, within the first 20hrs in vitro, GCs initiate their migration by extending a single leading process and following the process with their somata. During this stage, they show the highest rate of turning, extend multiple short processes and maintain the shortest movement cycles. Secondly, the cells bifurcate their leading process, which becomes much longer and thicker, and the nucleus and the surrounding cytoplasm enter one of the branches. Movement speed, as well as time spent moving is highest during this stage. Lastly, the cells slow down their movement, show high frequency of turning and move for extended amount of time until they become stationary, extend a lamellopodium and emit several thin processes. The speed, turning behaviour and movement cycles of GC change throughout observation time in a stage-dependent manner.

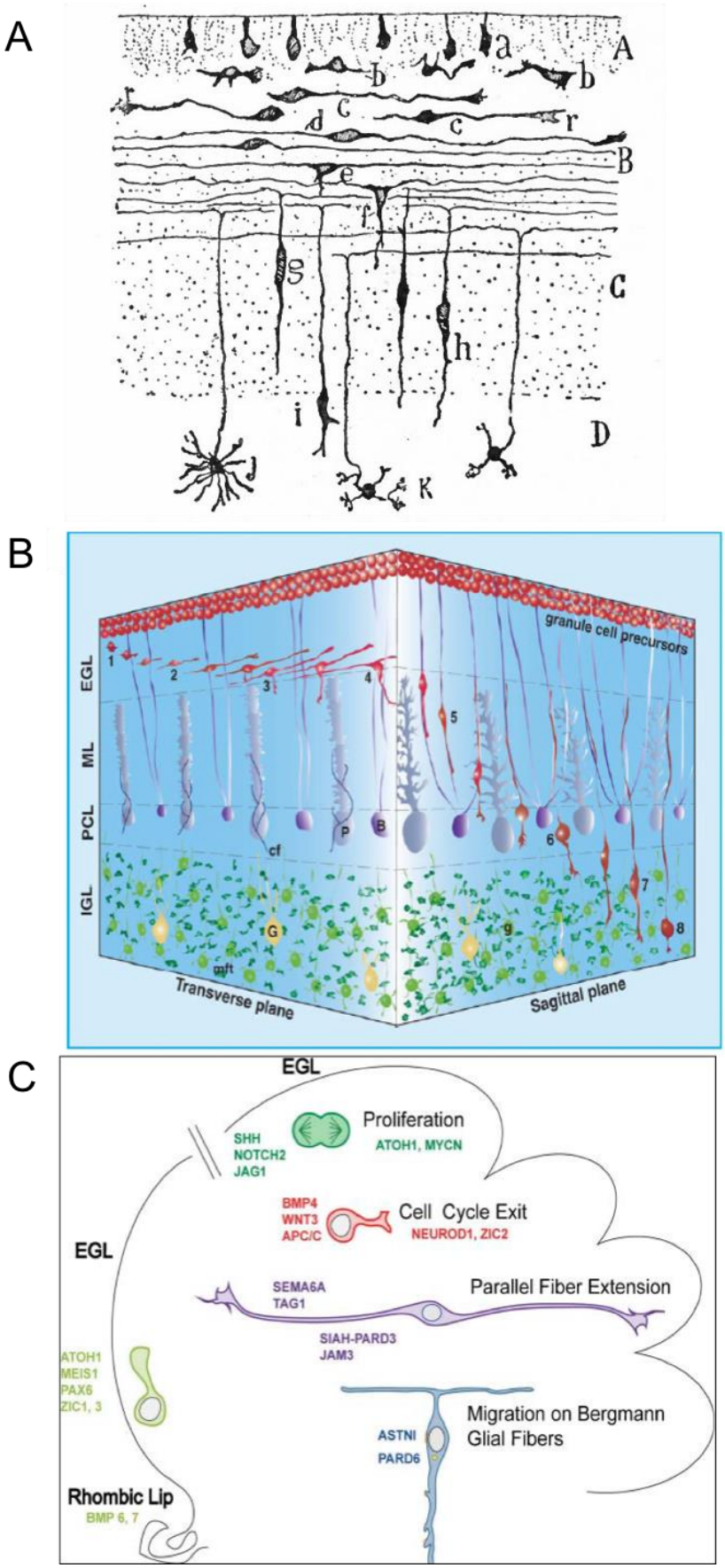

Figure 1-6 Migration and neurogenesis of granule cells during development

(next page)

Previous page:

Figure 1-6 Migration and neurogenesis of GCs during development

A) A drawing of granule cell morphological development by Cajal (1911). A, Layer of undifferentiated cells; B, layer of cells in horizontal bipolar stage; C, partly formed molecular (plexiform) layer; D, granular layer; b, beginning differentiation of granule cells; c, cells in monopolar stage; d, cells in bipolar stage; e,f, beginning of descending dendrite and of unipolarisation of cell; g,h, i, different stages of unipolarisation or formation of single process connecting with the original two processes; j, cell showing differentiating and completed dendrites; k, fully formed granule cell (caption from Bailey and Miller, 1921).

B) A three-dimensional representation of granule cell migration from the EGL to the IGL in early postnatal mouse cerebellum. First, the post-mitotic GC extends two uneven horizontal processes (1) and migrates tangentially in the direction of the longer process (2). At the border between the EGL and ML a vertical process is extended (3) and radial migration is initiated (4). Granule cells migrate in close association with Bergmann glia (5). When they reach the PCL, granule cells undergo a stationary phase (6) and resume glia-independent migration in the IGL (7). They complete their migration in the bottom of the IGL (8). *Abbreviations: P, Purkinje cell; B, Bergmann glia; G, Golgi cell; g, postmigratory granule cell; cf, climbing fiber; mft, mossy fiber terminal.*

C) The phases of granule cell differentiation and the key molecules involved. As the GCP migrates from the RL to the EGL, it expresses Atoh1, Meis1, Pax6 and Zic1 and Zic3. During the transit amplification stage in the EGL, proliferation is governed by Shh signalling and Notch signalling. The cells continue to express Atoh1, along with MycN. As the cell exits the cell- cycle, it responds to BMP and Wnt signalling. The APC/C system is involved in downregulation of Atoh1, as is expression of NeuroD1 and Zic2. As the cells begin to extend horizontal processes, they express early axonal markers such as TAG1 and their germinal zone exit is guided by semaphorins and polarity proteins. Further, their radial migration is guided by Pard6 and dependent on Astrotactin signalling. Radial migration is guided by the Bergmann glial fibres.

(Figures from Komuro and Yacubova, 2003 and Leto et al., 2015).

More recent analysis of GC turning behaviour *in vitro* revealed clearly that the cells turn autonomously and this is regulated by intrinsic programs, which are modulated by extrinsic signals (Kumada et al., 2009).

Interestingly, the aforementioned *in vitro* studies only investigated migration of granule cells and have not reported on any mitotic activity of GCs in their culture experiments. Only one study reported mitotic behaviour in dissociated GCPs culture (Wolf et al., 1997), and revealed interesting morphological characteristics of mitotic GCPs. The authors found that GCPs can elaborate neurites before mitosis, which remain extended for the duration of mitosis. Additionally, some cells exhibited an inheritance of neuritic morphology i.e. the shape, length, width and orientation of neurites were the same before and after mitosis. The divisions were asymmetric, in that only one daughter cell inherited the process. However, some processes were remodelled or regressed completely during mitosis. Overall, the authors' observations indicate that neuronal precursors have the capacity to simultaneously divide and elaborate neurites and hence the presence of neuritic cytoskeleton does not prevent cell mitosis. Unfortunately, no other studies about this process have since been performed on GCPs *in vitro* or *in vivo* and nothing is known about the mechanisms behind this morphological behaviour.

1.4 Re-examining granule cell precursor morphological transitions and mechanisms of differentiation

Taking all the literature on granule cell precursors development into account, there seems to be a disconnect between some recent findings and the established model of GCP morphological changes. Especially perplexing is the existence of the so-called intermediate precursors in the EGL i.e. the cells at the juxtaposition of proliferating and differentiating cells in the middle of the EGL, that co-express both types of markers (Xenaki et al., 2011, Miyazawa et al., 2000). Little is known about this population of GCPs and their morphology *in vivo* has not been previously explored. Nothing is known about the behaviour of those cells in terms of migration, process extension and retraction or division mode. The chicken embryo is an excellent model system in which to study the behaviour of cerebellar GCPs *in*

ovo in order to shed some light on some of the outstanding details of their development.

1.4.1 Chick embryo as a model system in cerebellar research

Much work on the development of the cerebellum has been performed in chicken embryos (Green and Wingate, 2014; Gilthorpe et al., 2002; Green et al., 2014; Eddison et al., 2004; Wingate and Hatten, 1999; Wingate, 2001; Wilson and Wingate, 2006; Wilson et al., 2007) as they offer many advantages over other model organisms. Firstly, the chicken embryo can be easily manipulated in the egg, until embryonic day 6, without affecting its normal development. The preferred technique for genetic manipulation is electroporation (**Fig1-5A**) (Momose et al., 1999; Price, 2007; Swartz et al., 2001), however pharmacological and transplantation studies can also be performed. By using electroporation, gain-of-function studies by spatially and temporally controlled expression of a target gene are possible. Using RNAi additionally allows studying loss-of-function phenotypes.

Secondly, the chicken cerebellum cellular and molecular structure and basic developmental transitions are very similar to the mouse, the preferred model for cerebellum development studies. The chick cerebellum develops from rhombomere 1 and is divided into two neurogenic zones that produce glutamatergic (at the RL) and GABA-ergic (at the VZ) neurons in similar sequence and localisation to the mouse. The layers of the adult cerebellar cortex are the same in the two species. There are some differences in the cerebellar connectivity and number of cerebellar nuclei between chick and mouse (Green and Wingate, 2014), but these differences should not influence the basic biological behaviour of GCPs at the RL and in the EGL.

Thirdly, certain genetic experiments that would be very complicated and costly in the mouse system, are comparatively straightforward in the chick. In this project, labelling of a subset of RL-derived neurons allows them to be traced and observed long-term, as well as easily manipulated genetically by electroporating plasmids encoding various genetic constructs into the rhombic lip.

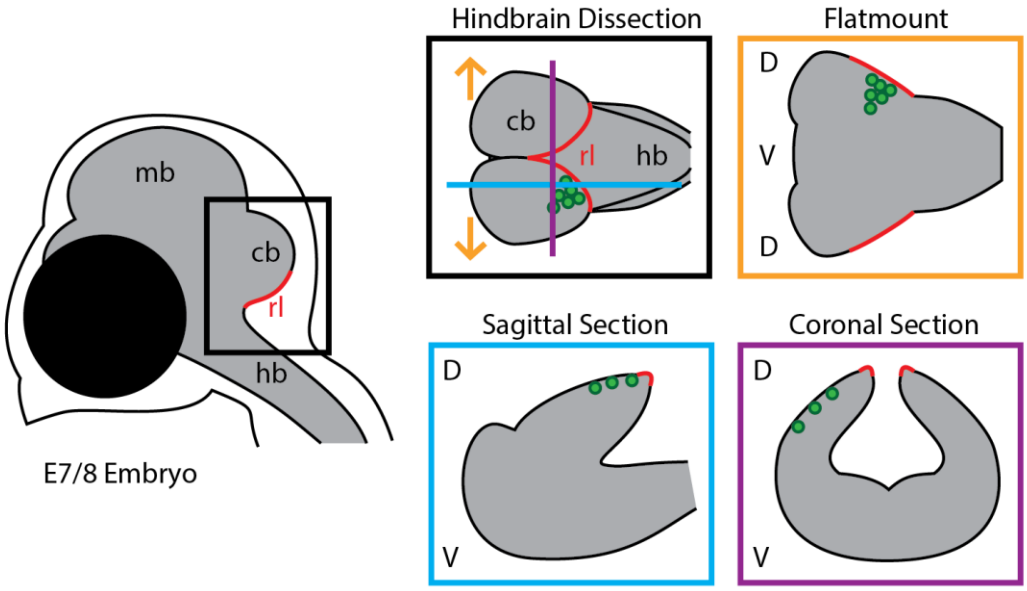

Figure 1-7 Chicken system is an excellent model for studying rhombic lip derivatives development

After chicken embryos are electroporated at E4-E6 at the level of the rhombic lip (red), they can be harvested at E7/E8 (up until E14). At E7/8 the hindbrain can be dissected out of the embryo with the developing cerebellum on the dorsal side. The cerebellum can be flatmouted to examine the pattern of migration of rhombic lip derivatives (green dots). To observe the dorso-ventral distribution of cells, the emrbyos can be cut in a sagittal or coronal orientation.

Throughout the thesis these symbols are used to denote the different mounting and sectioning methods:

 **flatmount**

 **sagittal**

 **coronal**

1.4.2 Aims of the project

This thesis has two main parts that focus on the morphological changes and differentiation of GCPs of the cerebellum. In the first part, I re-examine the morphological transitions of GCPs during the development of the chicken cerebellum. I use *in ovo* electroporation to individually label GCPs at the rhombic lip and observe their morphologies in the established EGL. Immunohistochemistry using proliferation and differentiation markers allows me to examine specifically the morphologies of mitotic and differentiating cells in different layers of the EGL. Additionally, I use time-lapse microscopy to observe the morphological transition of dividing GCPs in the EGL in *ex vivo* cerebellar slices.

In the second part of the thesis, I investigate one known molecular factor implicated in cerebellar development, a basic helix-loop-helix transcription factor, NeuroD1. I investigate its function in GCP development by studying its expression at the cellular level and by misexpressing the gene at the RL. Additionally, the effects of NeuroD1 overexpression on other RL derivatives are examined, for a more complete understanding of NeuroD1 function in cerebellar development.

Chapter 2: Morphological characterisation of chick cerebellar granule cell precursors

2.1 Background

Development of granule cells of the cerebellum has been studied at least since the time Ramon y Cajal (1911) had drawn his first pictures of the remarkable morphological changes these cells undergo as they migrate all the way from the rhombic lip to their final destination in the inner granular layer. Subsequently, a great deal of work has gone into understanding the migration of granule cells, leading to a number of important discoveries about general control of neuronal migration during development. Relatively little work has been done, however, to understand the precise changes that granule cell precursors (GCPs) undergo as they make their decision to stop proliferating and start differentiation. To answer such questions, an in depth understanding of GCPs development is required, including their complete morphological characterisation. In this chapter, I attempt a detailed characterisation of the morphological features of GCPs in the chick cerebellum by sparse labelling of the EGL cells followed by immunohistochemistry for proliferation and differentiation markers. This simple approach combined with high resolution imaging is a surprisingly powerful method to study GCPs in detail not previously described in the available literature.

2.1.1 Morphological changes of granule cell precursors during development- historical to current perspective

Neuronal morphology tracing has been a fascination since neuroscientists had been able to label individual cells in the brain. The methods used in the XIX and XX centuries used silver-impregnation techniques and electron microscopy or autoradiography (Ramon y Cajal, 1892, Hausmann and Sievers, 1985, Fujita, 1967). However, these methods were difficult to implement and very harsh, especially on embryonic material. Therefore, the first morphological analysis of granule cells in the cerebellum was performed on older specimens, at advanced stages of

development. However, already in 1892 Ramon y Cajal (1892) was able to observe, for the first time, the differentiation sequences of granule cell precursors as they leave the EGL and migrate towards the IGL. The findings were then advanced by the studies of Lugaro (1894). Both authors suggested that, in the chicken, granule cell precursors are proliferative between 11th and 13th day of incubation. This result did not however take into account a massive proliferation period that extend all the way until embryonic day 20, with the peak of proliferation on day 15. This insight was only possible with the use of tritiated thymidine, first done by Miale and Sidman (1961) and later by Hanaway (1967). Morphological studies of granule cells in the chicken were since then only undertaken in 1983 by Quesada and Genis-Galvez (1983) who used a modified Golgi staining technique to label the granule cells. After this Golgi study was performed no further research was published on the proliferation and differentiation sequence of granule cell precursors in the chicken embryo.

Studies in the mouse and other species have also been sparse and no study has attempted to correlate morphologies of cells labelled in the EGL with their individual differentiation status. Most studies that labelled cells *in vivo* made assumptions about cellular differentiation based on cellular morphology. For example, Komuro (et al., 2001) labelled P10 mouse cerebellar slices with a lipophilic dye and observed morphologies of granule cells in order to study tangential migration. Notably, they reported the morphologies of GCPs to have 'a round soma without any long processes'. In contrast, they state that 'postmitotic granule cells had spindle-shaped cell bodies […] with two horizontal processes". A similar sentiment can be seen in many publications that seem to derive their conclusions from the original Golgi studies that never attempted to correlate morphology with differentiation status of the cell. However, a number of recent studies have identified a population of 'intermediate progenitors' in the EGL, which are cells that express both postmitotic and proliferative markers at the same time (Xenaki et al., 2011, Miyazawa et al., 2000). However, those authors did not address the issue of morphological features of such cells and what transitions they could undergo to become an intermediate progenitor. Many questions therefore remain about the correlation between morphology and differentiation of granule cells in the cerebellum.

To better understand the historical and current view on granule cells development, a survey of important papers looking at the morphologies of granule cells in the cerebellum was performed. The results are summarised in Table 1.

Paper reference	Species, stage	Summary picture	Representative quote
Cajal, 1911	Rat, post-natal	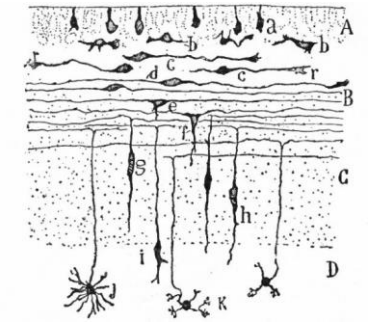	Schematics of camera lucida drawings of Golgi stained granule cells at various developmental stages
Fujita 1967	Mouse, P10-11	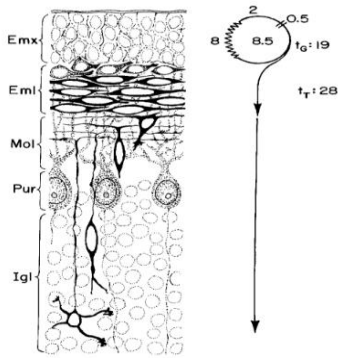	Morphologies drawn after Cajal
Rakic and Sidman 1970	Human, many foetal, neonatal and adult stages	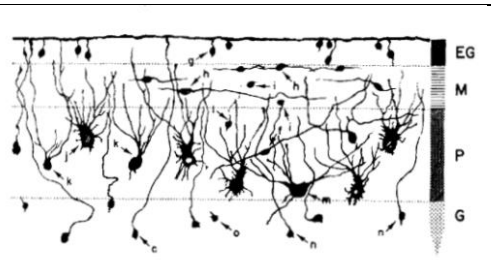	"At 16 weeks the superficial part of the external granular layer contains cells with round or oval somas and short vertically-oriented processes (g in fig. 8B)."
Altman 1972	Rat	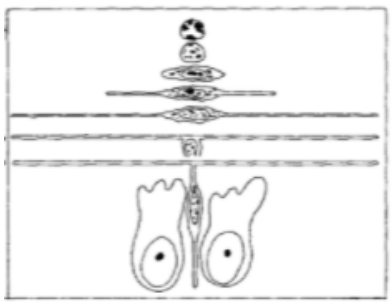	"Illustration of the proliferative round cells into spindle-shaped premigratory, differentiating cells, which first produce by extrusion of horizontal portion, then the vertical portion of the parallel fibres."

Table 2-1 Literature review of granule cell morphological development

Quesada, Genis-Galves, 1983	Chick E8-E15	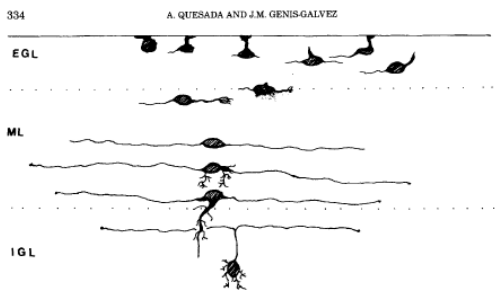	"In the cerebellum of the chick embryo at 8 to 15 days of incubation, small polyhedral or spheroidal germinal cells can be seen always […] in the outermost part of EGL in contact with pial surface"
Husmann and Sievers, 1985	Rat, E15-P20	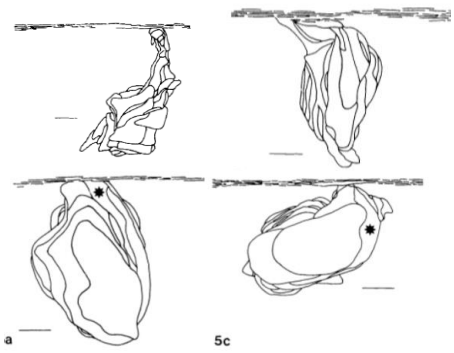	"Persistent contact with the basal lamina may mediate stimuli maintaining external granule cells in a proliferative state"
Gao and Hatten 1993	Mouse, early post-natal	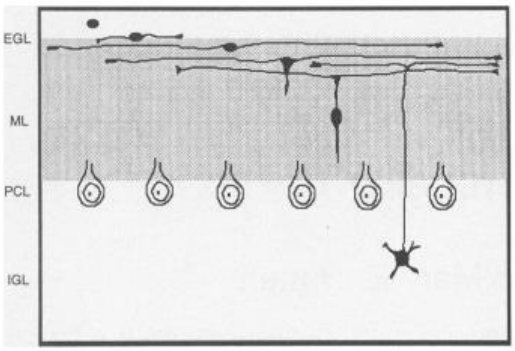	"Spacio-temporal pattern of granule cell differentiation and migration in vivo. GCPs proliferate in the superficial aspect of the EGL, then postmitotic cells descend into the deeper aspect of the EGL where they extend two long processes…"
Ryder and Cepko 1994	Chicken E8- E18	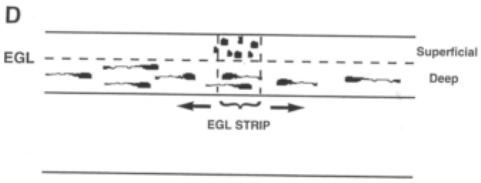	"After proliferating in the superficial EGL, cells extend leading processes in deep EGL and migrate long distances medial and lateral"
Nagata and Nakatsuji 1994	Mouse, P5-P7, cell culture	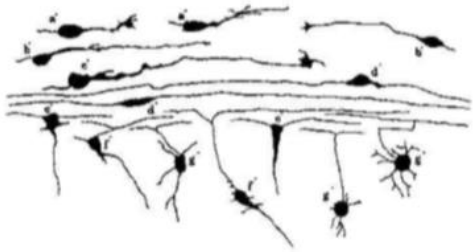	" Schematic drawing of the time-dependent morphological change of labeled granule cell neurons organotypic culture, traced from fluorescent microscopy"

Table 2-1 Literature review of granule cell morphological development

Komuro et al., 2001	Mouse, P10	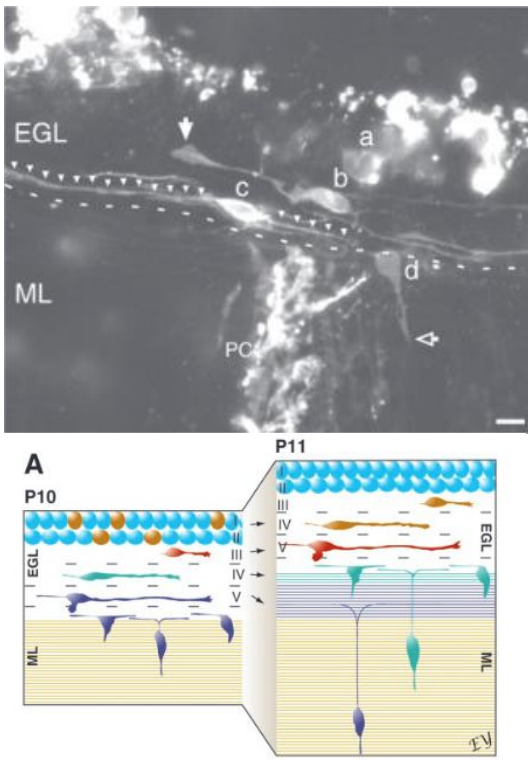	"The granule cell precursor (*a*) has a round soma without any long processes. Postmitotic granule cells (*b,c*) had spindle-shaped cell bodies [...] with two horizontal processes" "At P10, the granule cell precursors proliferate within [...] levels I and II. After their final division, tangentially migrating granule cells [...] start to leave the EGL
Manzini et al., 2006	P5 mouse, cell culture	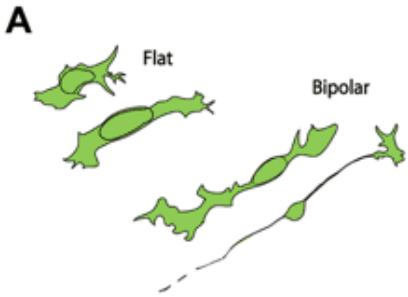	"Tracings of the two morphologies observed in cultured granule cells: flat, amoeboid cells with a large nucleus and no processes; and bipolar cells.[...] Flat cells are immature, proliferating neuron progenitors."
Govek et al., 2011 (review)	N/A	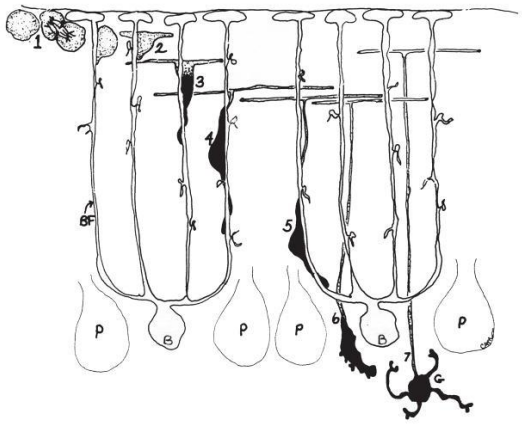	"During postnatal cerebellar development, granule cell progenitors (GCPs) proliferate in the outer region of the external granule layer (EGL) (1). After exiting the cell cycle, GCPs move into the lower aspect of the EGL and commence differentiation, extending bipolar axons, the parallel fibers"

Table 2-1 Literature review of granule cell morphological development

A collection of papers that specifically look at morphological changes during the development of granule cells. The reference, species and age are noted. A picture and a quote best representing the authors' conclusions are included.

In summary, the current understanding of the morphological changes of granule cells during development (e.g. Komuro et al., 2001, Manzini et al., 2006, Govek et al., 2011) has not changed substantially from the first characterisations performed by Cajal (1911). The consensus in the field seems to be that granule cell precursors are “round” or “polyhedral” or “polymorphous” cells without any long processes and reside in the outer EGL, possibly in contact with the pial membranes with a basal process (Hager et al., 1995; Hausmann and Sievers, 1985). The processes extended from the cells for tangential migration are assumed to extend only in postmitotic cells and represent leading and trailing processes that slowly transform into developing axons. Interestingly, some early authors (Altman, 1972) disputed the notion of tangential migration in the inner EGL, which has now been proven to take place. Once in the inner EGL, the cells are fully postmitotic and extend a third, radial process that leads to their radial migration towards the IGL. None of the published papers mention the possibility of a postmitotic-looking granule cell (long processes, spindle-shaped cell body) reverting to a less differentiated morphology, for example, by retracting processes and dividing.

A substantial number of papers that study the differentiation of granule cells do not specifically look at them as individual cells but rather at the population level in terms of expression of genes and tissue behaviour (see section 1.2.1). Various mutations have been studied that affect proliferation and differentiation of granule cells during development (e.g. Sonmez and Herrup 1984, D’Arcangelo et al. 1995), however those phenotypes are always observed on whole organ and tissue level and little effort has been performed to understand the effects of such manipulations on individual morphologies and the intricate cellular behaviour of granule cells.

2.1.2 Markers of proliferation and differentiation

There are a number of methods that have been used to study proliferation and differentiation dynamics in the developing cerebellum. They all have their advantages and drawbacks and I will discuss them all in turn and justify my choice of methods to use in my experiments.

Proliferation can be studied by antibodies to proteins expressed in cycling cells or by incorporation of synthetic nucleosides. The antibodies used to study proliferation in the cerebellum include anti-phospho-histone H3 (PH3), anti-PCNA and anti-Ki67. Anti-PH3 antibody is used to detect cells that are undergoing mitosis, specifically marking the M-phase of the cell cycle. Because mitosis is a short phase of the cell cycle, only a small percentage of cells are labelled with PH3 at any one time in a tissue. Depending on the pattern of PH3 localisation during mitosis, it is possible to distinguish between the different phases of mitosis (see Figure 2-1).

PCNA, proliferating cell nuclear antigen, is important in both the repair and the replication of DNA. The expression of PCNA is increased during the G1 and S phases and decreased upon the cell converting into G2 and M phases. Nevertheless, this marker can also be detected in the early G0 phase, which is caused by the long half-life period of the protein of eight to twenty hours. Therefore, it is likely to be expressed in some postmitotic cells in the inner EGL.

Ki67 is a nuclear protein, which can be used as a marker for dividing cells. It can be found in all time-courses of cell cycle except G0 and early G1 phases and in the quiescent cells. Both PCNA and Ki-67 can be used to label dividing cells, but PCNA is broader than Ki67, which are both broader than PH3. The use of PCNA as a proliferation marker has been questioned in recent literature (e.g. Zacchetti et al., 2003). Even though Ki67 was the most promising candidate to study granule cell proliferation, the use of Ki67 has never been reported in chicken tissue and no antibody was easily available at this time.

BrdU incorporation assays are a gold standard in studying proliferation. Detection of new-born granule cells is mainly based on the fact that BrdU is incorporated at S-phase-into the DNA in the nucleus and thus defines the S-phase effectively. However, application of BrdU through intravenous injection make it an inconvenient method for studying E14 chicken tissue. The method also detects new-born neurons and hence morphologies of labelled cells might not correspond to proliferating cells only.

Therefore, for the high specificity as a proliferation marker, availability and convenience, anti-PH3 antibodies are used in this project to examine proliferation.
A small arsenal of available markers exists to study differentiation of granule cell. The most commonly used antibodies for studying differentiation of GCPs include Tuj1, p27, NeuroD1, NeuN, and Axonin-1.
Tuj1, also known as β-tubulin III, has been found to label newly generated immature postmitotic neurons (Lee et al., 1990). It is expressed in early postmitotic and differentiated neurons and in some mitotically active neuronal precursors (Xenaki et al., 2011).
P27 is a cyclin-dependent kinase inhibitor expressed in differentiating GCs.
It is expressed in a small number of mitotically active GCPs as well (Miyazawa et al., 2000).
NeuroD1 has been used as a differentiation marker of granule cells in many papers (see **Table 4-1**).
NeuN is a soluble nuclear protein (Mullen et al., 1992) that is localized to the cell nucleus and in the cytoplasm of postmitotic neurons (Lind et al., 2005). It is not known to be expressed in mitotic cells making it a good marker of postmitotic neurons.

Axonin 1 (or TAG1 in mouse) is a member of the contactin family of adhesion molecules belonging to the immunoglobulin superfamily. It is expressed in specific neurons transiently on the axonal surface during the fetal period. In postnatal stages, TAG-1 is expressed in cerebellar granule cells, hippocampal pyramidal cells, and the juxtaparanodal regions of myelinated nerve fibres in the embryonic nervous system (Masuda, 2017). TAG-1 plays important roles in axonal elongation, axonal guidance, and cellular migration. In the postnatal nervous system, it also plays an essential role in the formation of myelinated nerve fibres. Axonin-1 is expressed on differentiating GCs in the inner EGL and sporadically co-labels with proliferation markers (Xenaki et al., 2011).

In this project three of these antibodies have been tried: Axonin-1, Tuj1 and NeuN and only Axonin-1 produced useful results. Therefore, Axonin-1 is used here as a marker of differentiating GCs in the chick cerebellum.

2.1.3 Aims of the study

In this chapter I will selectively label granule cell precursors *in ovo* in the chicken cerebellum and examine the morphology of proliferative cells in the EGL. I will use differentiation markers to further study granule cell precursors to understand how their morphologies correlate with their differentiation status. I will also present a new technique that can be used to further study granule cell precursors *ex ovo* by electroporation and culture of cerebellar slices.

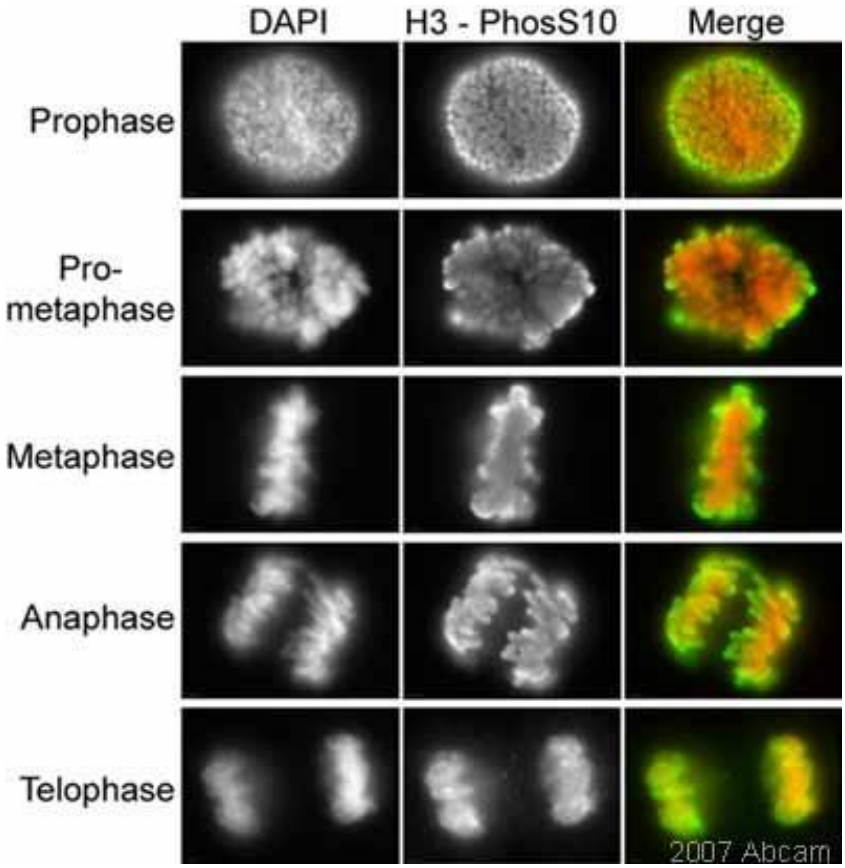

Figure 2-1 Pattern of expression of PH3 at different mitotic stages
Anti- Histone H3 (phosphoS10) in asynchronous HeLa cells, in conjunction with a goat anti-rabbit secondary antibody conjugated to Cy3. Cells were also counterstained with DAPI in order to highlight the nucleus. This image is courtesy of an Abreview submitted by Dr Kirk McManus (abcam.com website)

2.2 Results

2.2.1 Granule cell precursors can be observed at late stages of cerebellum development by using stable genomic integration of transgenes

Electroporation of the rhombic lip is a convenient method of observing and studying the behaviour of rhombic lip derivatives, including granule cells. The first GCPs are born at E6 in the chick and an electroporation at either E4, E5 or E6 labels individual cells in this cell population, which can be observed when embryos are sacrificed after E6 (Green and Wingate, 2014a). To study the early formation of the EGL, the rhombic lip was electroporated with the control CAAGS-GFP plasmid at E5 and the embryos were fixed at E8 and then stained for the proliferation marker PH3.

As shown in **Figure 2-2A-C**, at the site of electroporation in most embryos (**A**, GFP signal) a reduced PH3 labelling (**B**, red signal) was observed. After this observation, effort was made to reduce the negative impact of the procedure by lowering the voltage of the electroporator (20V to 10V) and by taking care to reduce contact between the embryo and the electrodes. However, still fewer cells than expected labelled with PH3 at this stage of development. Some cells that did stain for PH3 at E8 following an E5 electroporation are shown in **Figure 2-2D-H**. Most of them have round morphologies with no processes, but some show long processes while undergoing mitosis. However, analysis of proliferative cells at E8 was very inefficient due to the low numbers of electroporated cells that co-expressed PH3 and therefore, a preference was given to study proliferative granule cells at a later stage of development, at E14.

Consequently, in this project morphologies of GCPs were examined in an established EGL at E14, close to the peak of proliferation of GCPs in the chick. To investigate which cellular morphologies of cells in the EGL correspond to proliferative GCPs, chick embryos were electroporated at E4 with the combination of p2TK-CAGGS-GFP and pCAGGS-T2TP constructs (referred to collectively as Tol2:GFP) and the embryos were allowed to develop until E14.

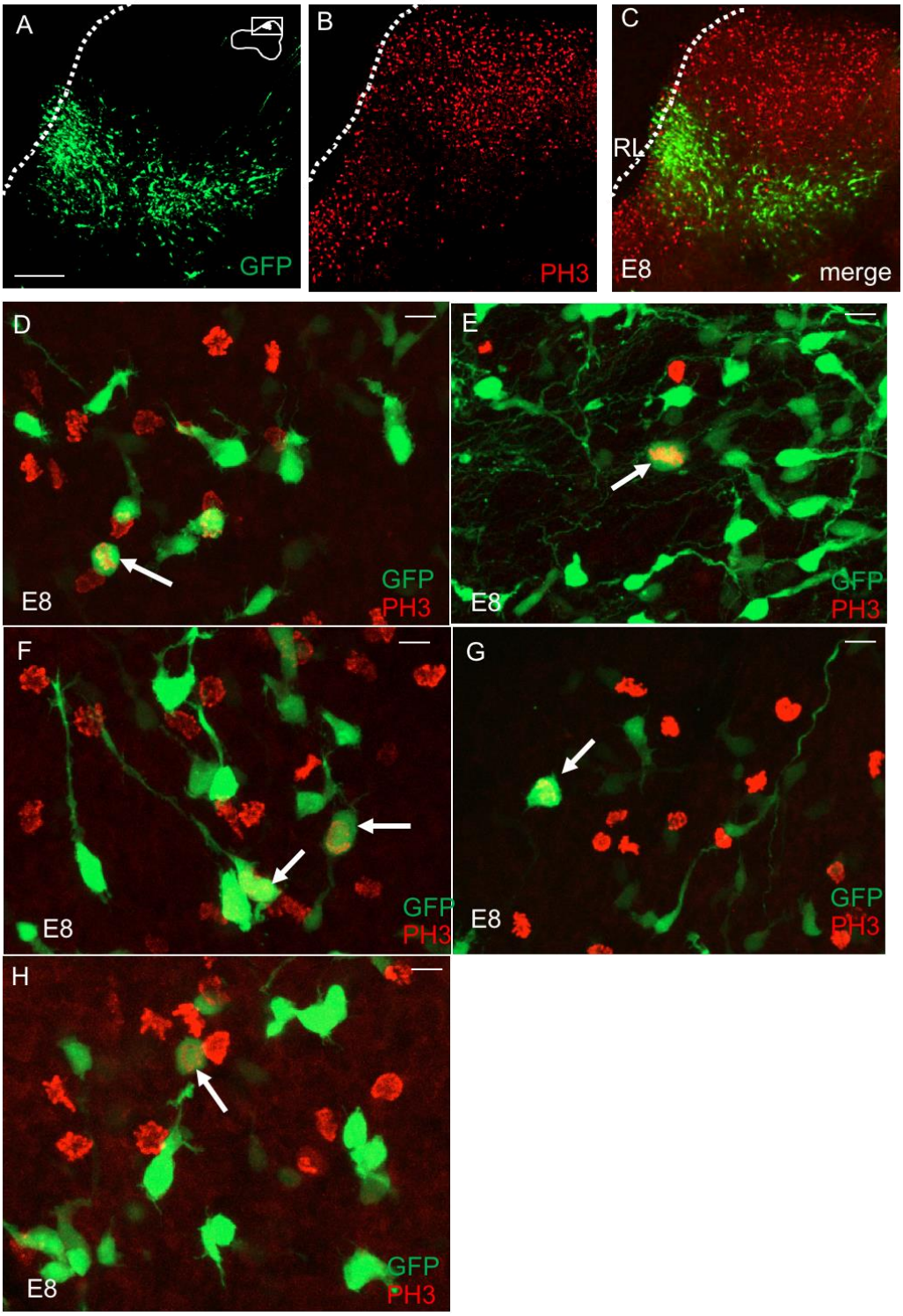

Figure 2-2 Electroporation of the rhombic lip reduces proliferation of electroporated cells

A-C) Embryos were electroporated with CAGGS-GFP at E5 and fixed at E8. Tissue was stained with anti-PH3 antibody. The electroporated area has a decreased level of PH3 signal. **D-H)** Examples of electroporated cells that stain for the proliferation marker PH3 at E8. Most cells have round morphologies with no processes, but some show long processes (e.g. cell in F). Scale bar= 200μm (A-C), 10μm (D-H)

Tol2 genomic integration method (depicted in **Figure 2-3A**) had to be employed due to plasmid dilution effect observed when non-integrating plasmids such as CAGGS-GFP are used to observe highly proliferating cells like granule cell precursors (Sato et al., 2007). Tol2 system, on the other hand, allows for integration of a gene of interest (in this case GFP) into the genome of the animal by the action of Tol2 transposase. This results in a stable expression of the gene throughout the lifespan of the animal and allows for visualisation of cells electroporated at E4 much later in development, at E14. **Figure 2-3B** illustrates that due to the extensive proliferation of GCPs, the cells that express CAGGS-GFP at E8, lose that fluorescence during development and there is no GFP signal seen at E14 (bottom panel). In contrast, following an electroporation with Tol2:GFP constructs, the embryos sacrificed at E14 had a high frequency of fluorescent cells in their cerebella (top panel).

The fluorescent cerebella were fixed and sectioned in a coronal orientation into 50μm sections with a cryostat. Coronal orientation, as exemplified in **Fig 2-3 C**, is preferred due to parallel fibres extension in the medio-lateral direction. A sagittal section would cut across these processes and would not accurately reflect the morphologies of developing GCPs. The sections were stained with the proliferation markers PH3 and the differentiation marker Axonin-1 to examine cellular morphologies shown by proliferating and differentiating cells.

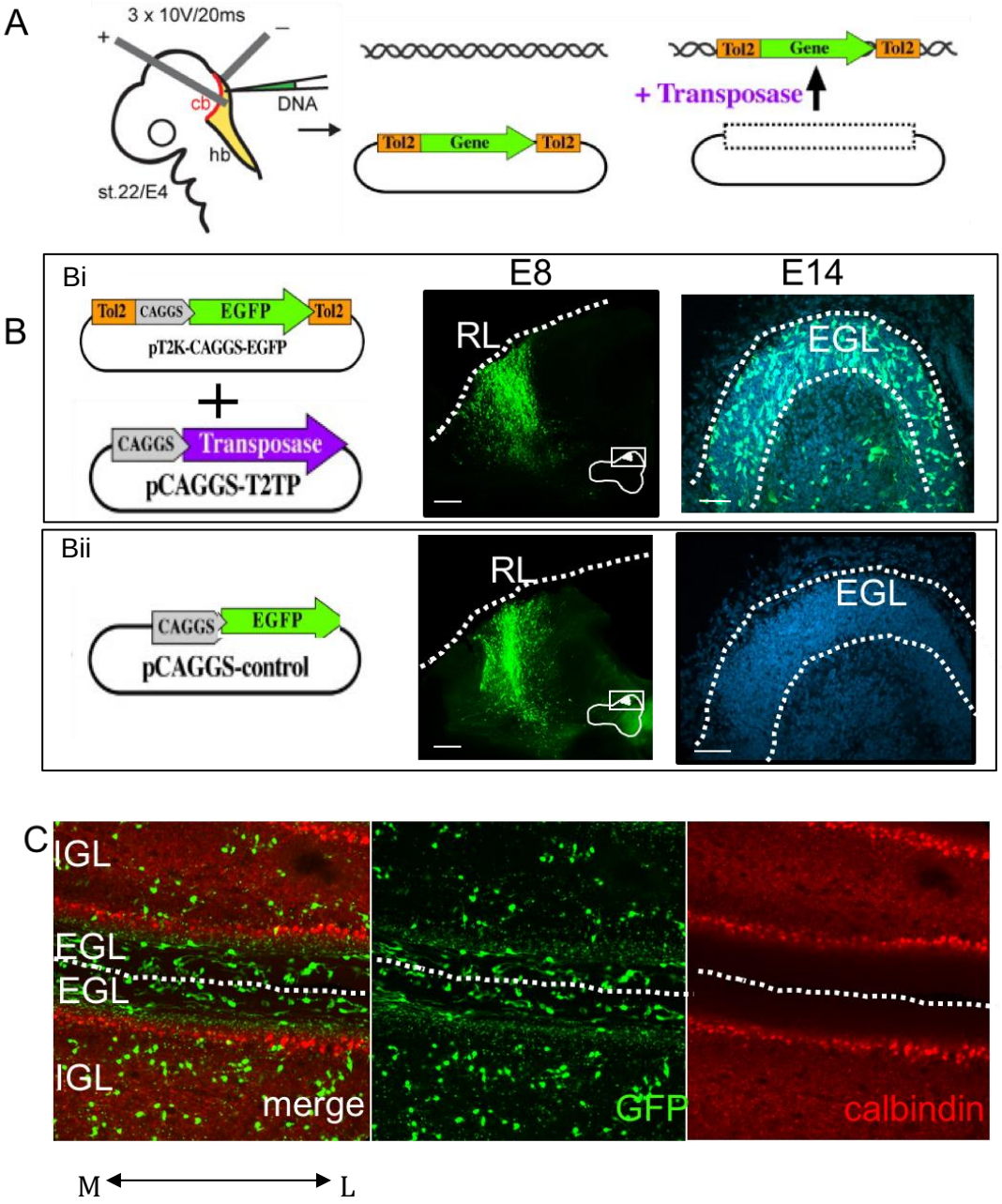

Figure 2-3 Electroporation of constructs using Tol2 transposase results in stable integration of genes of interest into the genome *(next page)*

Previous page:

Figure 2-3 Electroporation of constructs using Tol2 transposase results in stable integration of genes of interest into the genome

A) A schematic representing the electroporation protocol and explaining the Tol2 system. GFP gene ("Gene") is flanked by the Tol2 sites on both sides on one plasmid. A second plasmid encodes the Transposase, which, when translated, will integrate the GFP gene into the genome of the host embryo. **B)** Comparison between the Tol2 stable integration method (Bi) and the electroporation of CAGGS-GFP control plasmid (Bii) into the rhombic lip of an E5 embryo. At E8, both combinations result in strong fluorescence signal in the cells migrating from the rhombic lip. At E14, however, CAGGS-GFP fluorescence is no longer visible due to plasmid dilution, whereas GFP integration into the genome with Tol2 transposase results in high number of highly fluorescent cells throughout the cerebellum. *(Diagrams modified from Green et al., 2014 and Sato et al., 2007)* **C)** The E14 cerebella electroporated with Tol2:GFP were sectioned in a coronal orientation to preserve morphology of extending parallel fibres in the inner EGL and best reflect the morphologies of GCPs throughout the EGL. Anti-calbindin stain was used to visualise the Purkinje cells and cerebellar layers. Granule cells (GFP) were found in the EGL and the IGL. The orientation is medio-lateral (M-L).
Scale bar= 200μm (B at E8) 20μm (B at E14; C)

2.2.2 The mitotic index of electroporated GCPs is unaltered at E14

Staining the cerebellar slices with anti-PH3 antibodies established that only a small proportion of GFP-positive granule cells were in M-phase at the time of tissue fixation. To investigate whether a smaller proportion was labelled than expected, the mitotic index i.e. the number of $PH3^{+ve}$ cells as a proportion of all cells in the EGL (stained by DAPI) was calculated and then compared to the mitotic index of the GFP^{+ve} cells.

Mitosis only takes around 5-6% of the cell cycle length, depending on the tissue, and therefore I would expect around 6% of cells in the outer EGL to be expressing PH3 if all the EGL cells were actively in the cell cycle. As shown in **Figure 2-4E**, 2.35% of all cells in the EGL were found to express PH3 (representing an average mitotic index of 2.66), which is in good agreement with previous studies on granule cells mitosis (Miyazawa et al., 2000; Sudarov and Joyner 2007; Smeyne and Goldowitz 1989; Migheli et al., 1999; Fujita 1967). This is less than 6% due to the fact that the inner half of the EGL contains mostly postmitotic cells. If only the upper half of the EGL was considered, the proportion of $PH3^{+ve}$ cells would be higher, and would approach around 6%. Ideally, to characterise the mitotic index of GCPs, only the cycling cells should have been included in the analysis (e.g. by labelling with PCNA) instead of all EGL cells.

Similarly, when the number of GFP^{+ve} cells that co-express PH3 were counted, the results, seen in **Figure 2-4F**, showed that the number of cells that were co-expressing GFP and PH3 had an average mitotic index of 2.24 and the difference between the two results was not statistically significant (**Figure 2-3G**). This suggests that the mitotic activity of the electroporated cells in the EGL were not affected by, or recovered from, the electroporation method and the cells have resumed normal proliferative behaviour after migrating from the rhombic lip and reaching the EGL.

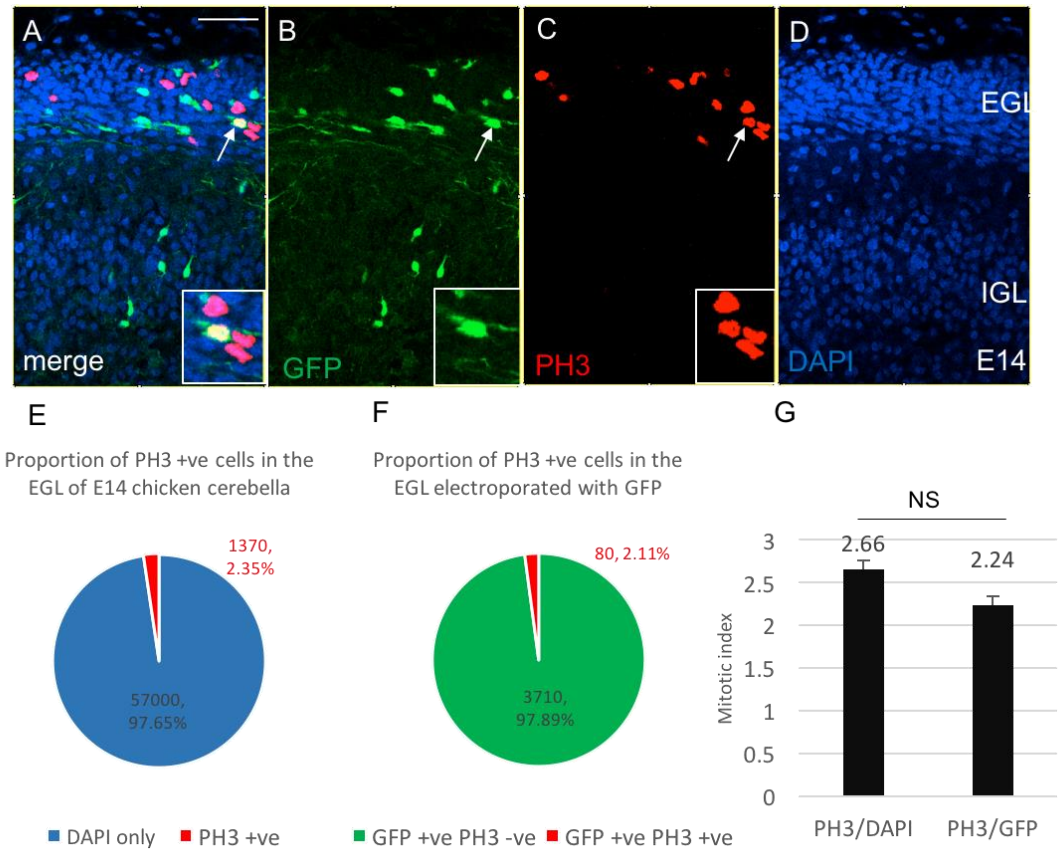

Figure 2-4: Electroporated GCPs are as likely to express PH3 as unelectroporated cells in the EGL at E14

Embryos were electroporated with Tol2:GFP at E4 and sacrificed at E14. Cerebella were sectioned in a coronal orientation and stained with anti-PH3 antibody. **A-D)** show an example of the cerebellar tissue where (**B**) GFP electroporated cells can be seen in the EGL. (**C**) PH3 expressing cells are shown in red. (**D**) DAPI staining shows all cells in the tissue. Some electroporated cells co-express PH3 (insert). **E)** DAPI stained cells in the EGL were counted in 15 slices from 3 different cerebella and $PH3^{+ve}$ cells were quantified. 2.35% of all EGL cells express PH3. **F)** All electroporated cells (GFP expressing) were counted in the same tissues and the number co-expressing PH3 was quantified. 2.11% of cells co-expressed GFP and PH3. **G)** The differences between the mitotic index of all granule cell in the EGL and electroporated granule cells were not statistically significant (p=0.3104 with paired Student's T-test). Scale bar= 100µm

2.2.3 Most dividing GCPs reside in the outer and middle EGL but some are found in the inner EGL

Based on previous literature (Table 2-1), it can be assumed that proliferating GCPs are located in the outermost EGL and become postmitotic at the stage of initiation of tangential migration. However, it became apparent from the obtained results, that $PH3^{+ve}$ cells reside in all regions of the EGL and, contrary to expectations, are not confined to the outer EGL (**Figure 2-5A-C**). In fact, $PH3^{+ve}$ cells could be seen intermingled with cells in the inner EGL where the postmitotic GCs reside and extend their forming parallel fibres (**Figure 2-5D**).

To quantify the numbers of proliferating cells in the EGL, it was divided into three layers: the outer, middle and inner layer, based on the previous studies that identified these three layers as separate (Xenaki et al., 2011). This division was done based on the number of cell layers found in the EGL in each slice and then divided evenly into three equal layers. For example, if the EGL in the tissue was 12 cells thick, the outer EGL was defined as the first four cell layers, the middle EGL as cell layer 5-8 and the inner EGL as cell layer 9-12 (see **Figure 2-5E**). As **Figure 2-5F** displays, the results show that the highest number of proliferating GCPs is found in the outer and middle EGL, however some are still present in the inner EGL. Most $PH3^{+ve}$ cells were indeed located in the outer EGL (49%), with 44% found in the middle EGL. Only 7% of $PH3^{+ve}$ cells were found in the inner EGL (**Figure 2-5G**). It was clear from these results that GCPs can be found throughout the EGL and hence it was unlikely that they are morphologically uniform.

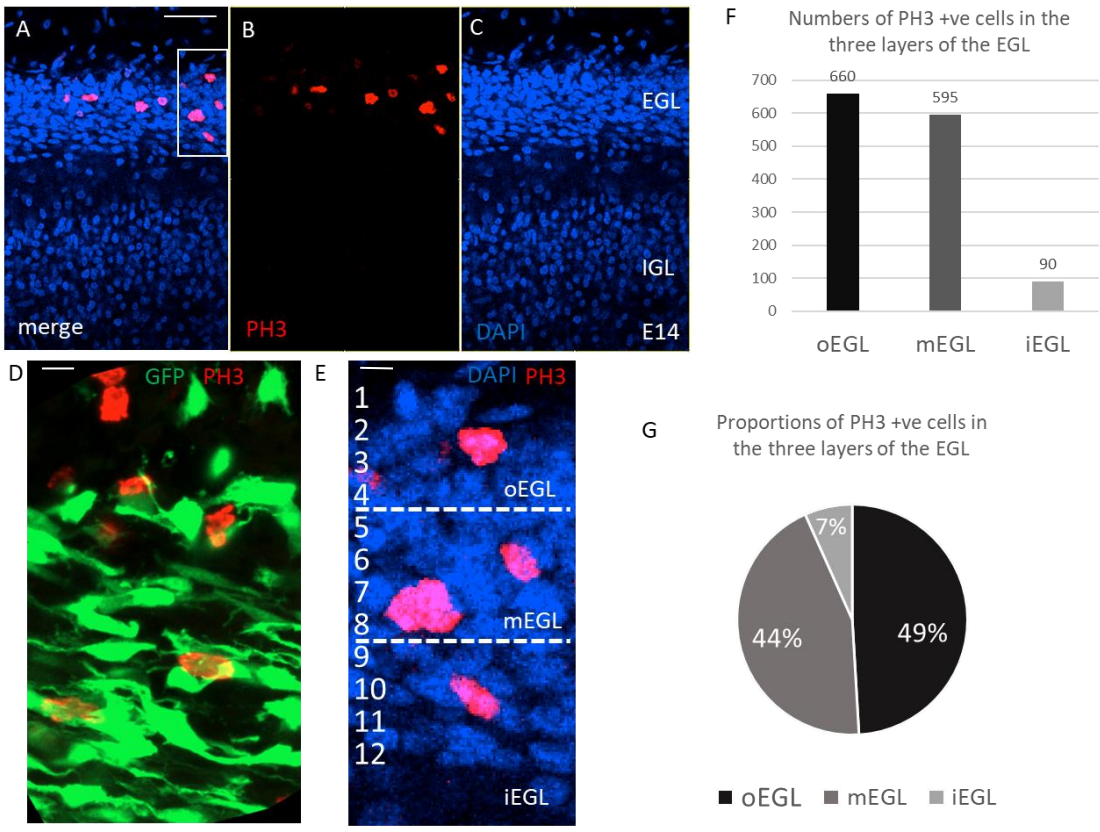

Figure 2-5: PH3 expressing cells are located in all layers of the EGL

EGL of E14 embryos was divided into three equal layers and the numbers of PH3^{+ve} cells in each layer was quantified. **A-C)** shows an example of the PH3 stained tissue. PH3 staining is visible in the EGL and very little is seen in the IGL. PH3 is distributed in all layers of the EGL **D)** A tissue electroporated with Tol2:GFP at E4 and fixed at E14 shows the morphologies of cells in the different layers of the EGL. Even in the inner layers where cells have differentiated morphologies and long processes, there are PH3^{+ve} cells present among the cells. **E)** An example of how the EGL was divided into layers. The EGL was 12 cells thick and therefore cells in layers 1-4 were considered to be outer EGL, cells in layers 5-8 were considered middle EGL and cells in layers 9-12 were inner EGL. **F)** Numbers of PH3^{+ve} cells were quantified in the three layers of the EGL in 15 slices from 3 cerebella. Most cells were present in the outer EGL (660), but nearly equally many were present in the middle EGL (595). Considerably fewer cells were present in the inner EGL (90). **G)** The proportions of PH3^{+ve} cells in the outer EGL (49%), middle EGL (44%) and inner EGL (7%). Scale bar= 100µm(A-C), 10µm (D-E).

2.2.4 Dividing GCPs display different morphologies depending on their position within the EGL

To investigate the morphologies of proliferating GCPs, the GFP expressing $PH3^{+ve}$ cells were imaged at high resolution and analysed according to the layer of the EGL they reside in. For this project, 154 cells from 3 different cerebella were examined in detail and some of the cell morphologies are presented in Figures 2-6 to 2-9. **Figure 2-6** shows the morphologies of cells in the outer EGL. **Figures 2-7 and 2-8** show morphologies of cells in the middle EGL, with Figure 2-7 collecting cells with less elaborate morphologies, and Figure 2-8 showing the cells with processes. **Figure 2-9** collects examples of cells found within the inner EGL.

Most cells found in the outer EGL had a round soma and very small or non-existent processes (**Fig 2-6A, B, C, E**). Some cells had a pial process that extended towards the pial surface (**Fig 2-6D, G, M**). Other oEGL cells had short processes extending tangentially (**Fig 2-6J, L, N**). Cells with processes were more likely to be in the early stages of mitosis such as prophase (**Fig 2-6G, J, L**) or pro-metaphase (**Fig 2-6I, M, N**). When the cells had a round morphology and very short or no processes, they were mostly in the more advanced stages of mitosis, such a metaphase (**Fig 2-6A, B, C, E, K**).

Cells in the middle EGL displayed a wide variety of morphologies. Most cells looked similar to the oEGL cells in that they had a round soma and short or no processes, especially at the time of metaphase (e.g. **Fig 2-7A, B, C, D, E, F, H**). However, many cells showed more elaborate morphologies, with some extending long process of varying thickness, reminiscent of either leading processes (**Fig 2-8C, D, E, J**) or even forming parallel fibres (**Fig 2-8G, K**). Some mEGL cells have processes extended towards the pial surface, even though they were not long enough to reach the pial surface (e.g. **Fig 2-8 B, I**). All of the mEGL cells with extended processes were in the early mitosis stages, mostly prophase (e.g. **Fig 2-8C, E, F, G, I**) or pro-metaphase (**Fig 2-8H, K**). Additionally, some of their cell bodies were elongated and spindle-shaped, as can be seen by the shape of PH3 signal (e.g. **Fig 2-8E, G, H, I**). Few cells were observed in anaphase or telophase but the ones that were never had any processes and were completely round (e.g. **Fig 2-7O, P**).

The $PH3^{+ve}$ cells in the inner EGL were most likely to have an elaborate morphology and long processes. Most cells were found in the prophase stage of mitosis and extended long processes (**Fig 2-9D, E, F, H**). Cells that were in metaphase had round morphologies and appear to be actively retracting their processes (**Fig 2-9C**), or already have retracted them (**Fig 2-9A, B**). Interestingly, some cells could be seen extending two long processes in the same direction, as if the processes have bifurcated (e.g. **Fig 2-9C, D,G**). Some of the elaborate cells extended processes in both directions (**Fig 2-8 D,E,** and **Fig 2-9 C,D,F**) whereas others had only a single long process (**Fig 2-8C, G** and **Fig 2-9G**).

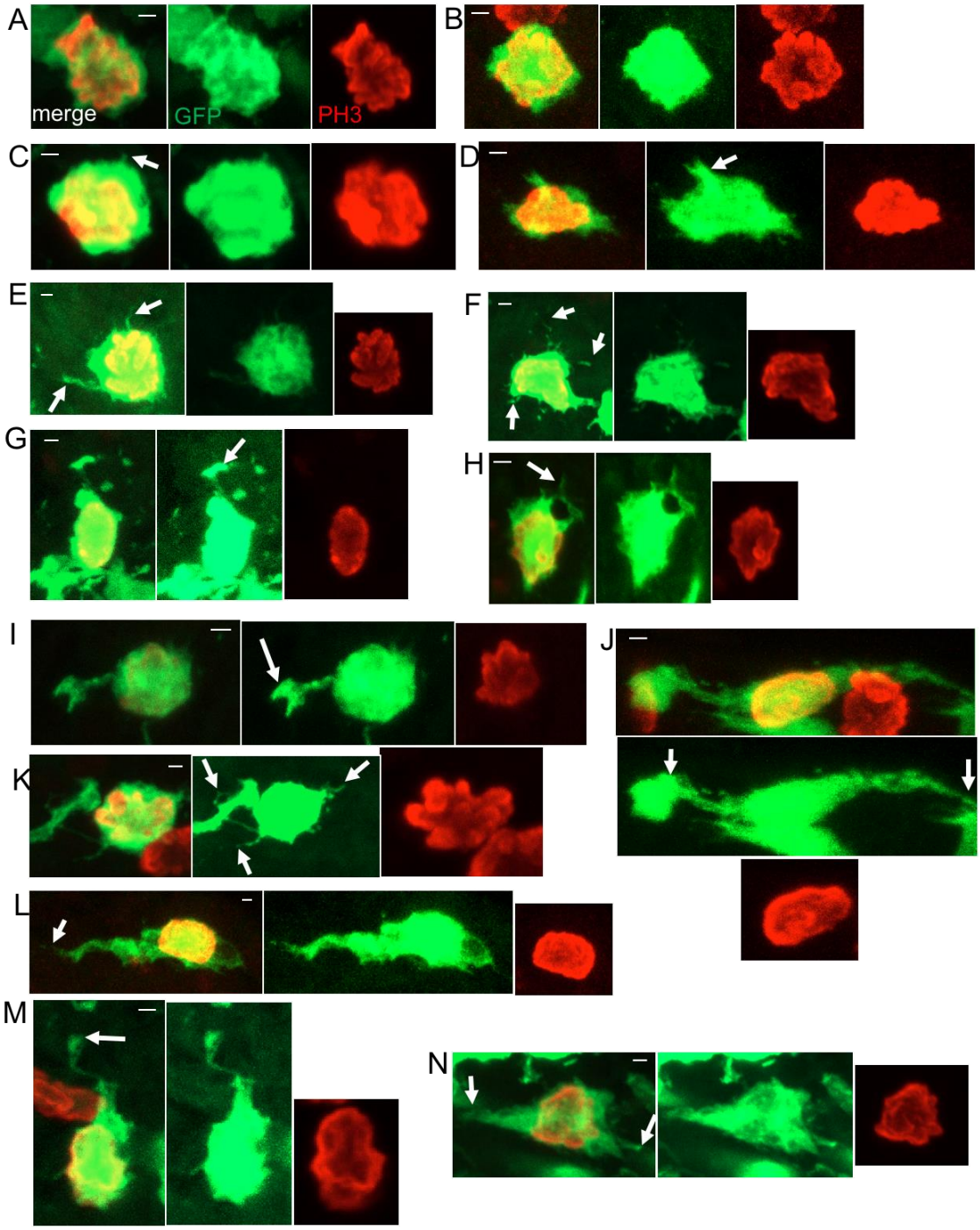

Figure 2-6: Morphologies of electroporated cells expressing PH3 in the outer EGL

A collection of Tol2:GFP electroporated cells located in the outer EGL that stained for the proliferation marker, PH3. For each cell the GFP signal, the PH3 signal and a merged image is shown. The GFP signal is enhanced in some images to enrich small processes. Arrows point to interesting morphological features, such as extended processes. Scale bar= 2µm

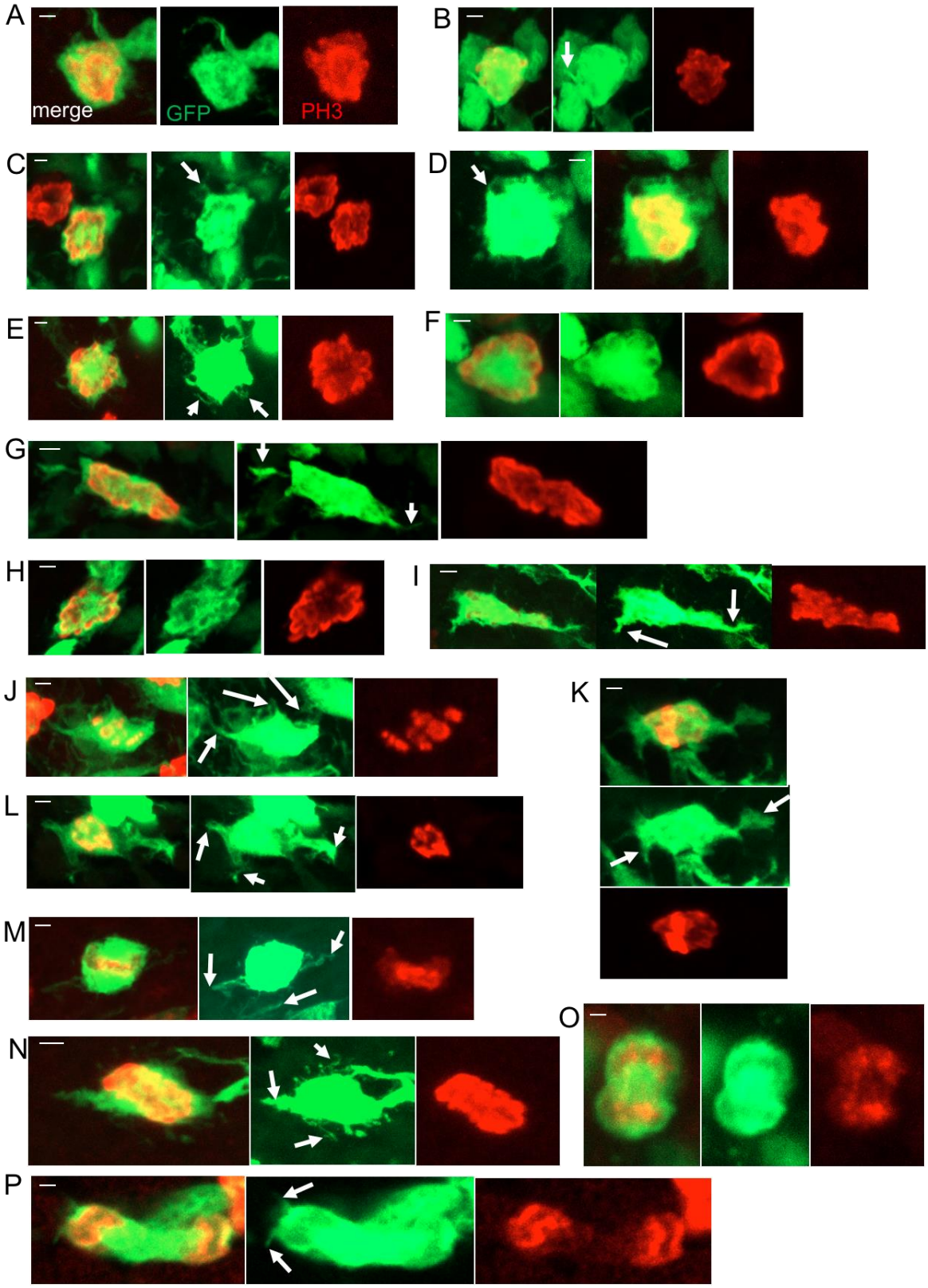

Figure 2-7: Morphologies of electroporated cells expressing PH3 in the middle EGL- part 1 *(next page)*

Previous page:

Figure 2-7: Morphologies of electroporated cells expressing PH3 in the middle EGL- part 1

A collection of Tol2:GFP electroporated cells located in the middle EGL that stained for the proliferation marker, PH3. For each cell the GFP signal, the PH3 signal and a merged image is shown. The GFP signal is enhanced in some images so that smaller processes can be seen. Arrows point to interesting morphological features, such as extended processes. Scale bar= 2μm

Next page:

Figure 2-8: Morphologies of electroporated cells expressing PH3 in the middle EGL- part 2

A collection of Tol2:GFP electroporated cells located in the middle EGL that stained for the proliferation marker, PH3. For each cell the GFP signal, the PH3 signal and a merged image is shown. The GFP signal is enhanced in some images so that smaller processes can be seen. Arrows point to interesting morphological features, such as extended processes. Scale bar= 2μm

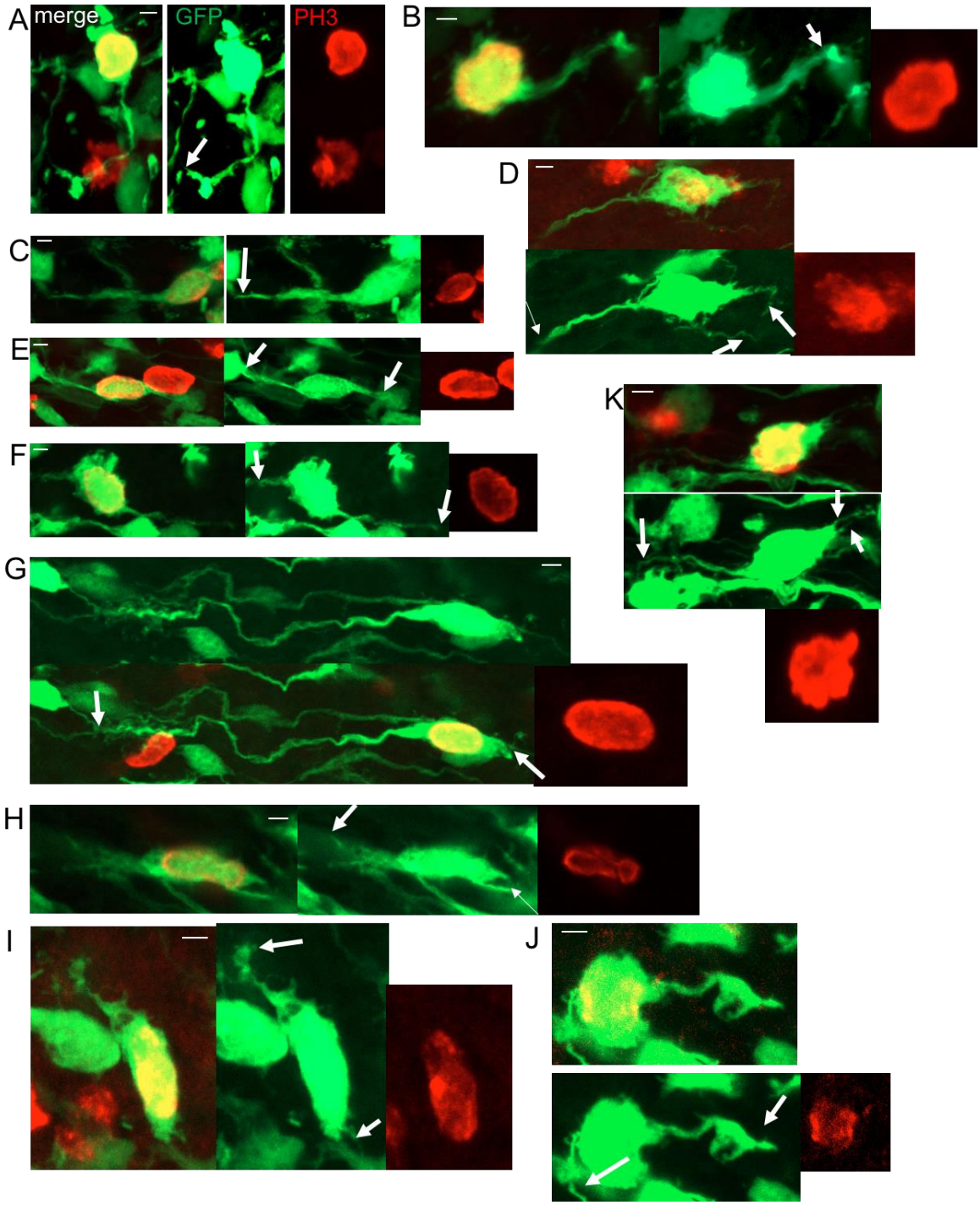

Figure 2-8: Morphologies of electroporated cells expressing PH3 in the middle EGL- part 2 *(previous page)*

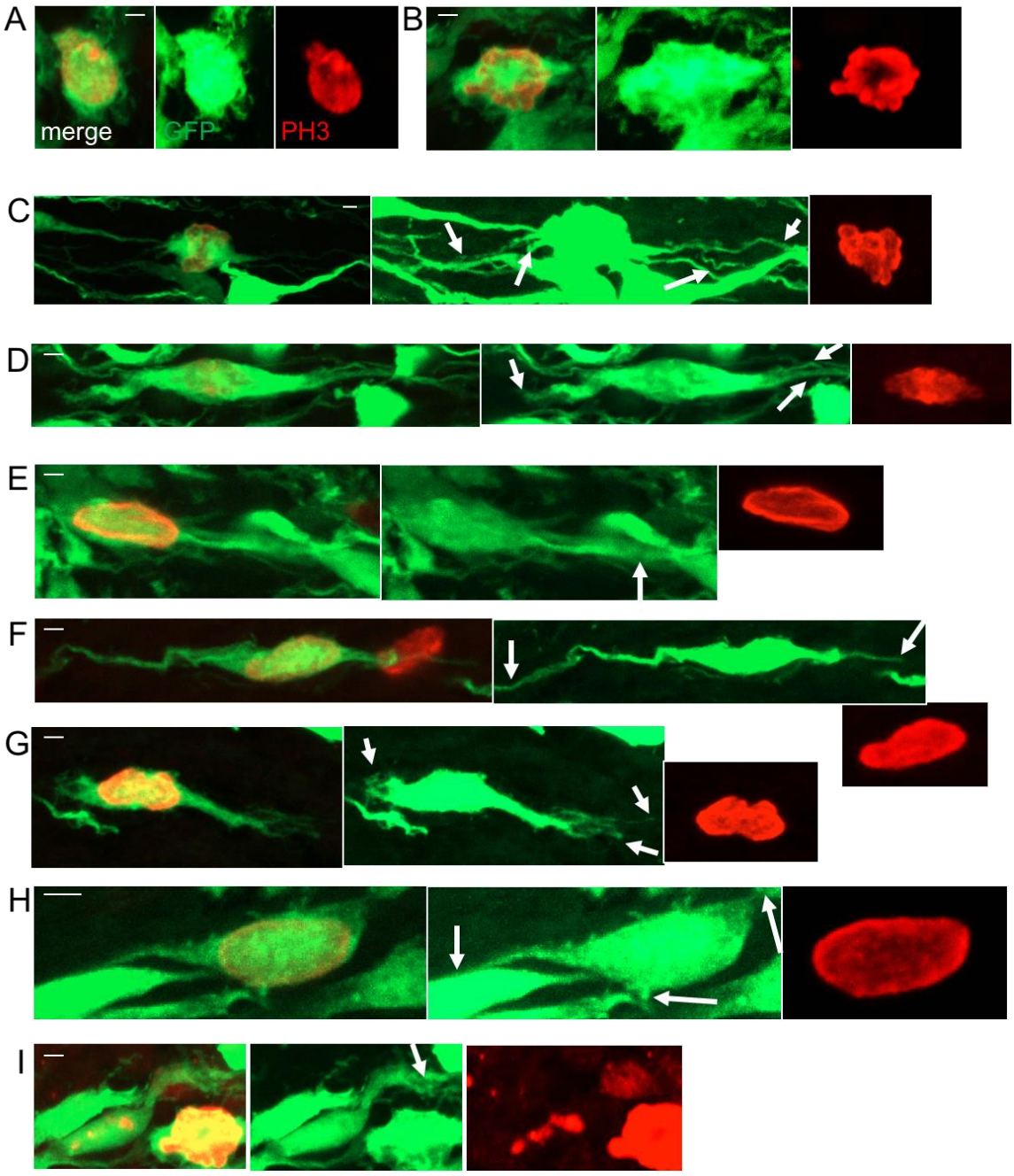

Figure 2-9: Morphologies of electroporated cells expressing PH3 in the inner EGL

A collection of Tol2:GFP electroporated cells located in the inner EGL that stained for the proliferation marker, PH3. For each cell the GFP signal, the PH3 signal and a merged image is shown. The GFP signal is enhanced in some images so that smaller processes can be seen. Arrows point to interesting morphological features, such as extended processes. Scale bar= 2µm

2.2.5 Granule cell precursors can proliferate within the Axonin-1 expressing inner EGL

To confirm whether GCPs proliferating within the inner EGL expressed differentiation markers, the cerebella were stained with anti-Axonin-1 antibody, along with the anti-PH3 antibody. As **Figure 2-10A-B** shows, some PH3^{+ve} cells were found within the Axonin-1^{+ve} inner EGL. As reported above, only 7% of PH3^{+ve} cells are found within the inner EGL, and all those cells would be located within the Axonin-1^{+ve} area, as Axonin-1 is expressed in a broad strip in the inner half of the EGL (**Fig 2-10E**). Axonin-1 expression domain corresponds to the location of cells with a differentiated morphology, such as extended long parallel processes (**Fig 2-10D**) and spindle-shaped cell bodies (**Fig 2-10G**). **Figure 2-10H-K** shows three examples of GFP^{+ve} cells that can be seen in the Axonin-1^{+ve} area. Two of the cells (arrows) are in prophase and extend thick, but relatively short, processes from their cell bodies, whereas one cell (arrowhead) does not have any processes and is in metaphase.

Figure 2-10: PH3 expressing cells can be located in Axonin-1^{+ve} inner EGL
Cerebellar tissue from chick embryos electroporated with Tol2:GFP at E4 and fixed at E14 was stained for PH3 (red) and Axonin-1 (magenta). **A)** An example of cerebellar tissue showing GFP expressing cells, PH3 staining cells, Axonin-1 expression and DAPI stain. **B)** A magnified view of the area in A showing PH3 and Axonin-1 expression only. Notice the PH3^{+ve} cells in the Axonin-1^{+ve} area (arrows). **C)** A magnified view of the boxed area in A showing GFP expressing cells labelled with PH3. The cell is surrounded by differentiated cells with long processes and is located in Axonin-1^{+ve} area. **D-G)** Individual channels from A. **D** shows GFP, **E** shows Axonin-1, **F** shows PH3 and **G** shows DAPI staining. **H and I)** Examples of cells electroporated with GFP and stained for PH3 located within the Axonin-1^{+ve} area. **J)** A magnified view from H. The cell outline is shown with dotted white line. The cell has one process extended tangentially and is in prophase. **K)** A magnified view from I. Two electroporated cells are PH3^{+ve}. One (arrow) looks similar to the cell in J in that it has quite thick processes extended tangentially and is in prophase. The other cell (arrowhead) is in metaphase and does not have any processes extended from the cell body. Scale bar= 20μm

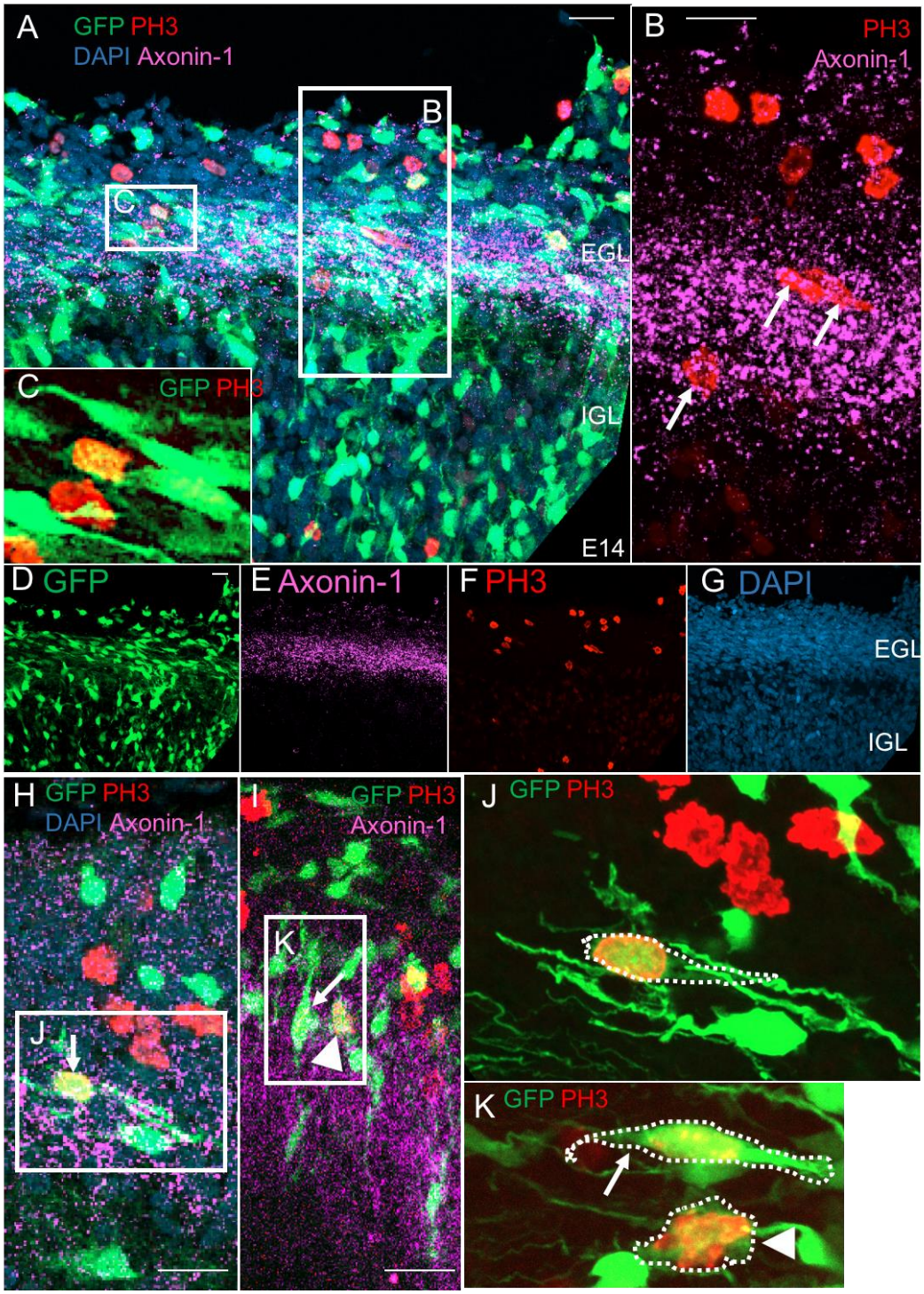

Figure 2-10: PH3 expressing cells can be located in Axonin-1+ve inner EGL

(previous page)

2.2.6 Granule cell precursors have different morphologies depending on their mitotic stage

Depending on the pattern of PH3 staining, it is possible to distinguish between the different stages of mitosis (see **Fig 2-1**). During the detailed imaging of the 154 different $PH3^{+ve}$ cells in the EGL, a clear pattern of their morphologies appeared. Cells at different stages of mitosis, presented different morphological features, which are summarised in **Figure 2-11**. For example, many cells in prophase were found to have extended processes whereas most cells in metaphase had no processes at all, or very short processes. Similarly, none of the cells in anaphase and telophase were seen with extended processes. Moreover, cells in pro-metaphase typically had shorter processes than the cells in prophase and the processes appeared to be in the process of retraction. **Figure 2-11** shows examples of a cell that represents a typical morphology of cells at different mitosis stages. From the 154 cells observed during the project, the numbers of cells at each stage with or without processes were quantified (**Fig 2-11F**). The trends suggest that proliferating GCPs can extend elaborate processes, but these are then retracted prior to cell division.

Next page:

Figure 2-11: Typical granule cell precursors morphologies at different mitotic stages

Examples of typical cellular morphologies of GCPs at different stages of mitosis. GFP signal (green), PH3 label (red) and a merged image are presented. White dots delineate the cell morphology. **A)** A cell in prophase with an extended process. **B)** A cell in pro-metaphase with processes that appear to be retracting. **C)** A cell in metaphase with very short processes. **D)** A cell in anaphase with no processes visible. **E)** A cell in late telophase. There are no processes extended at this point. **F)** Numbers of cells that extended processes at different stages of mitosis. As the mitotic cell reaches cytokinesis, it is increasingly less likely to be extending a process. Scale bar= 2μm

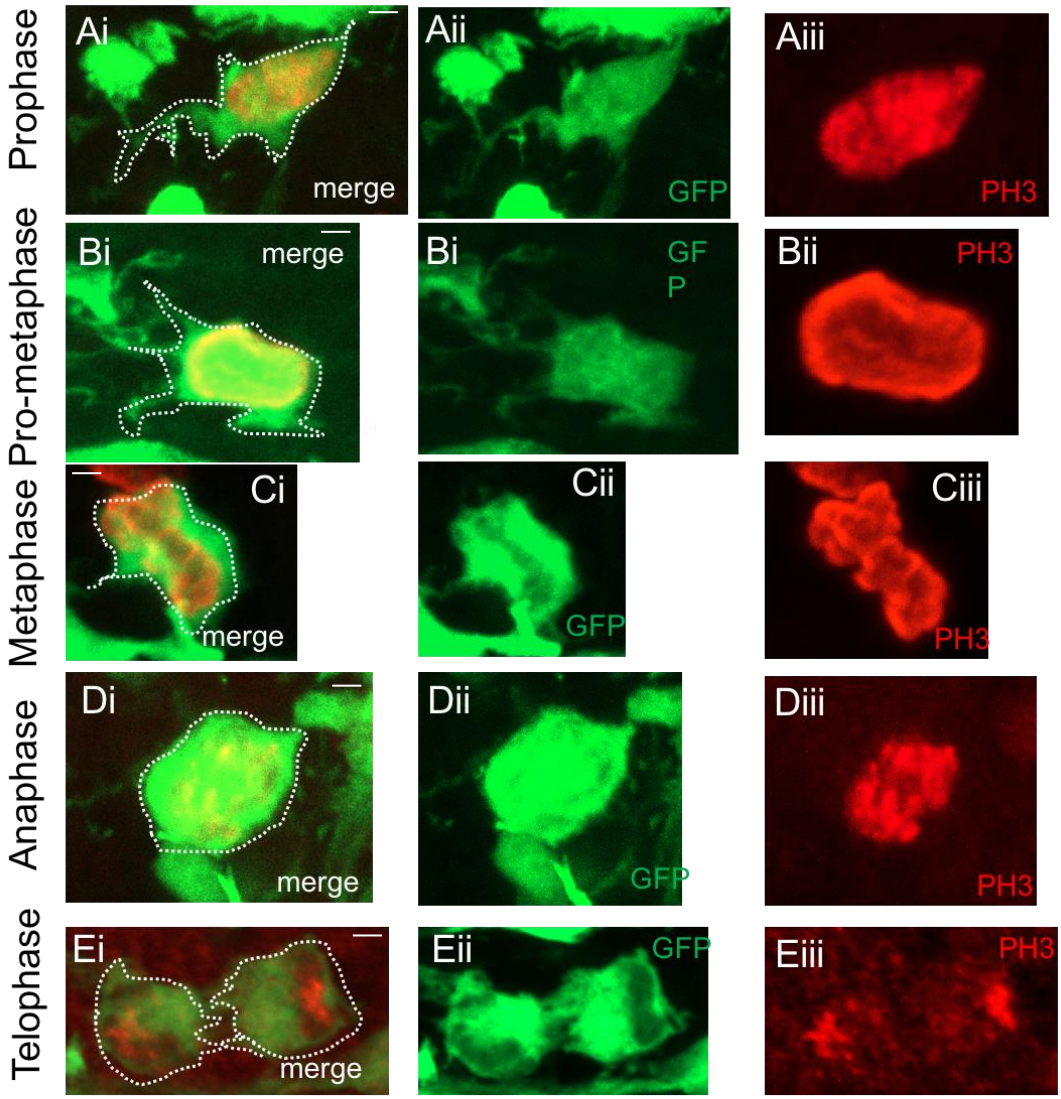

F

Mitosis stage	Cells with a process	Cells without a process
Prophase	16 (94%)	1 (6%)
Prometaphase	18 (66%)	9 (33%)
Metaphase	21 (23%)	69 (77%)
Anaphase	0	2 (100%)
Telophase	0	6 (100%)

Figure 2-11: Typical granule cell precursors morphologies at different mitotic stages *(previous page)*

2.2.7 Granule cell precursors can extend thin and long processes reminiscent of cytonemes

While collecting the different morphologies of $PH3^{+ve}$ GCPs, an interesting morphological feature emerged. Many cells, especially in metaphase, when they appeared round or polyhedral in low magnification imaging, would in fact be seen extending very thin and sometimes quite long filopodia. These processes were only observed when the images were highly overexposed due to their fineness and low fluorescence levels. Some cells had many processes, and some only had one or two and their length differed. Examples of cells with such processes can be found in **Figures 2-6 to 2-9** (e.g. **Fig 2-6B,E,F,K**, **Fig 2-7C,E,M,N**), but **Figure 2-12** shows three representative examples. In **2-12A**, a round cell in metaphase can be seen extending a thin and long process in a tangential direction from one side of the cell body. The cell in **2-12B** has one long and thicker process extended tangentially, and a thinner and shorter process from the other side, among numerous smaller protrusions. The cell in **2-12C** projects many such thin processes, some longer than others. There is a great variability in the number, length and direction of the thin processes in the cells collected during the project, but also the neighbouring cells that did not stain for PH3 which were observed in the outer EGL and are probable GCPs at a different cell cycle stage (two such cells can be seen in **Fig 2-12A,C**). These processes are reminiscent of cytonemes found in other systems that use intercellular signalling.

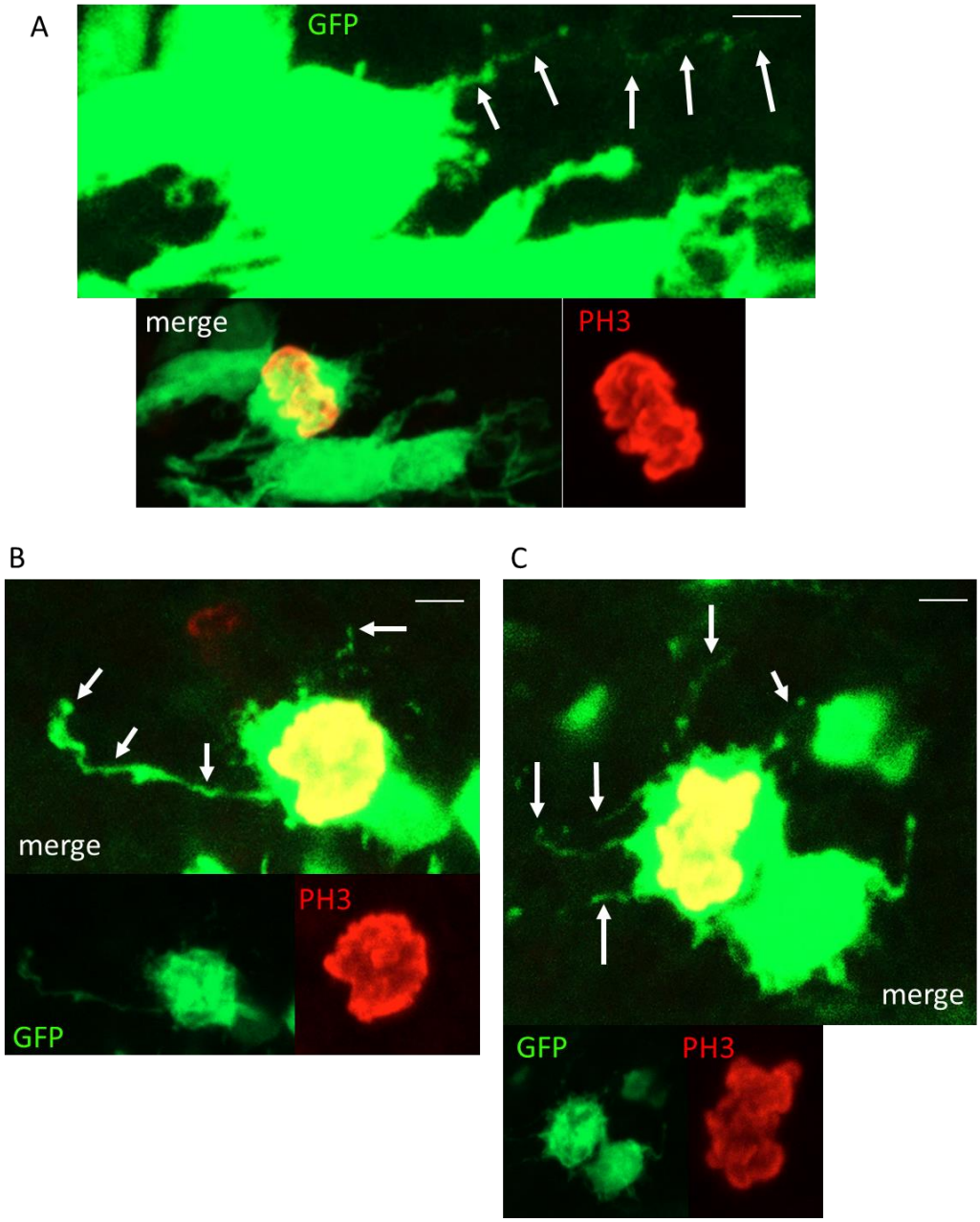

Figure 2-12: Some granule cell precursors extend very thin and long processes

Examples of EGL cells electroporated with Tol2:GFP (green) and labelled with anti-PH3 antibody (red). The GFP signal is overexposed to highlight the existence of very thin and sometimes long processes extending from the cell bodies in multiple directions. Cell in A and C are in metaphase, cell in B is in pro-metaphase. Scale bar= 2µm

2.2.8 Granule cell precursors can be electroporated *ex ovo* to study granule cell development

Numerous genetic tools are available to study various developmental and cellular processes. However, many of those tools are encoded in constructs that are not inducible and therefore difficult to express in the chicken at later stages of cerebellar development, without laborious re-cloning efforts. Establishing an *ex ovo* electroporation protocol of cerebellar tissue was therefore important to allow the use of many invaluable genetic tools in future experiments. The results presented in this chapter so far lead to an interesting developmental question of what is the purpose of the various types of processes that GCPs extend at different times in their developmental programme? Importantly, at what point do these processes become axons? These kinds of questions are difficult to answer using early *in ovo* electroporation and therefore, an *ex ovo* electroporation protocol was designed during the project. The details of the protocol can be found in the Methods (section 6.5) and in Hanzel et al (2015).

As **Figure 2-13** shows, electroporation of cerebellar slices prepared from E14 embryos is possible and results in many cells in the EGL expressing the electroporated constructs. **Fig 2-13A** shows a liberally electroporated slice where many areas of the cerebellar slice express a control RFP construct, whereas in **B**, a focal electroporation of one folia only was achieved. Granule cells electroporated in this protocol could be followed and their behaviour appeared normal, in that many cells started migrating towards the inner EGL after 3 div (**Fig 2-13C**) and their individual morphologies could be traced (**Fig 2-13H**). The integrity of the tissue in culture was examined by calbindin staining and Purkinje cells development was not grossly affected (**Fig 2-13D-E**). An *in situ* hybridisation for Math1 was performed to observe whether expression of this important transcription factor is sustained in culture. The results (**Fig 2-13I-K**) show that for at least 2 div Atoh1 expression is found in the EGL of the cerebellar slice, but there is a pronounced fragmentation of the EGL. The outer EGL seems to separate into two separate bands. The level of Atoh1 expression also decreases consistently as time progresses. At 2 div there is some high expression left in the creases of the cerebellar folia, but little expression at the tips of the folia. Additionally,

proliferation in the slice is abnormal in that a very high number of $PH3^{+ve}$ cells is found in the IGL and the white matter areas, possibility due to enhanced gliogenesis (**Fig 2-13G**). Overall, the technique of cerebellar slice electroporation is a promising method of observing and manipulating the late stage GCPs, with important limitations.

2.2.9 Various genetic tools can be electroporated into cerebellar slices to study granule cell development

During the project, several genetic tools were tested in the cerebellar slices, with varying degrees of success.

2.2.9.1 GAL4-UAS system

Firstly, the utility of GAL4-UAS system in expressing proteins in the chick model was examined. A Math1-GAL4 construct was cloned to drive expression of UAS-driven proteins in Math1-expressing cells only. To check whether the GAL4-UAS system works in the chicken cerebellum, slices were electroporated with Math1-GAL4 and UAS-GFP (data not shown). GFP was successfully expressed in GCPs in the cerebellar slices, proving that in principle, this system can be used to drive proteins encoded in the many available UAS-driven constructs. Two such constructs were tried in the project: axonal (synaptophysin) and dendritic (psd-95) proteins. The rationale behind this experiment was that granule cell precursors might already have axonal polarity in the EGL, before their horizontal processes transform into established axons. Synaptophysin and psd95 are synaptic proteins and synapses are not yet established in GCPs. However, the transport mechanisms that would transport synaptophysin into the axonal pre-synaptic regions could already be active before synapses form. On the other hand, psd-95 is a post-synaptic protein and should therefore only be present in dendrites.

When electroporated into E14 cerebellar slices, synaptophysin was found localised to all cell types with various morphologies, including cells with very short processes, as well as those with long parallel fibres (**Figure 2-14A-B**). Psd-95, in contrast, was always localised to the cell body and never found in the developing processes (**Figure 2-14A,C**). Many combinations of these constructs were tested

(data not shown), including combining them with other constructs such as Atoh1-cre and stop-GFP. Overall, synaptophysin-GFP was not found to be a useful indicator of axon establishment as it was localised to all types of GCP processes In contrast, and somewhat reassuringly, psd95 in all combinations did not leave the cell body of the electroporated cells. Slices were not cultured long enough to determine whether it later localised to developing dendrites of mature granule cells.

2.2.9.2 Fucci cell cycle indicators

Another genetic tool tested in the cerebellar slices was the Fucci (Fluorescent Ubiquitination-based Cell Cycle Indicator) system, which allows study of the cell cycle progression in electroporated cells, through the change of the fluorescent protein expression, depending on the phase of the cell cycle (Méchali and Lutzmann, 2008; Sakaue-Sawano et al., 2008; Zielke and Edgar, 2015). When Geminin-GFP was electroporated on its own into cerebellar slices (to mark cells in S/G2/M phase, **Fig 2-14D**) it was expressed in many cells after 2div. Most cells were found in the EGL and expression was higher at the tips of the folia (**Fig 2-14E**), suggesting higher proliferation rate (also shown by PH3 staining to be the case, T. Varela, pers comm). Similarly, when cdt1-RFP, a marker of the G1 phase, was expressed in the cerebellar tissue, it was expressed in a broad pattern in the EGL and the IGL. Interestingly, more expression seemed to be found in the troughs of the folia than the tips, suggesting higher differentiation rate (**Figure 2-14F**). Unfortunately, when electroporating both constructs into cerebellar tissue, both appeared to be co-expressed in all electroporated cells (data not shown). Therefore, optimisation of both constructs is required before further use.

An additional Fucci construct that labels cell membranes with green fluorescent protein and cells in S-G2-M phase with a red nuclear fluorophore (Myr AG1-KO2-Geminin) has been tested. Unfortunately, contrary to expectations, KO2-Geminin (red) is expressed in some highly differentiated neurons (**Figure 2-14G-H**), suggesting that its expression is not limited to cells in the S-G2-M phase. Similarly, optimisation of this construct needs to be performed in future experiments to check whether lower concentrations can better recapitulate normal expression of the proteins.

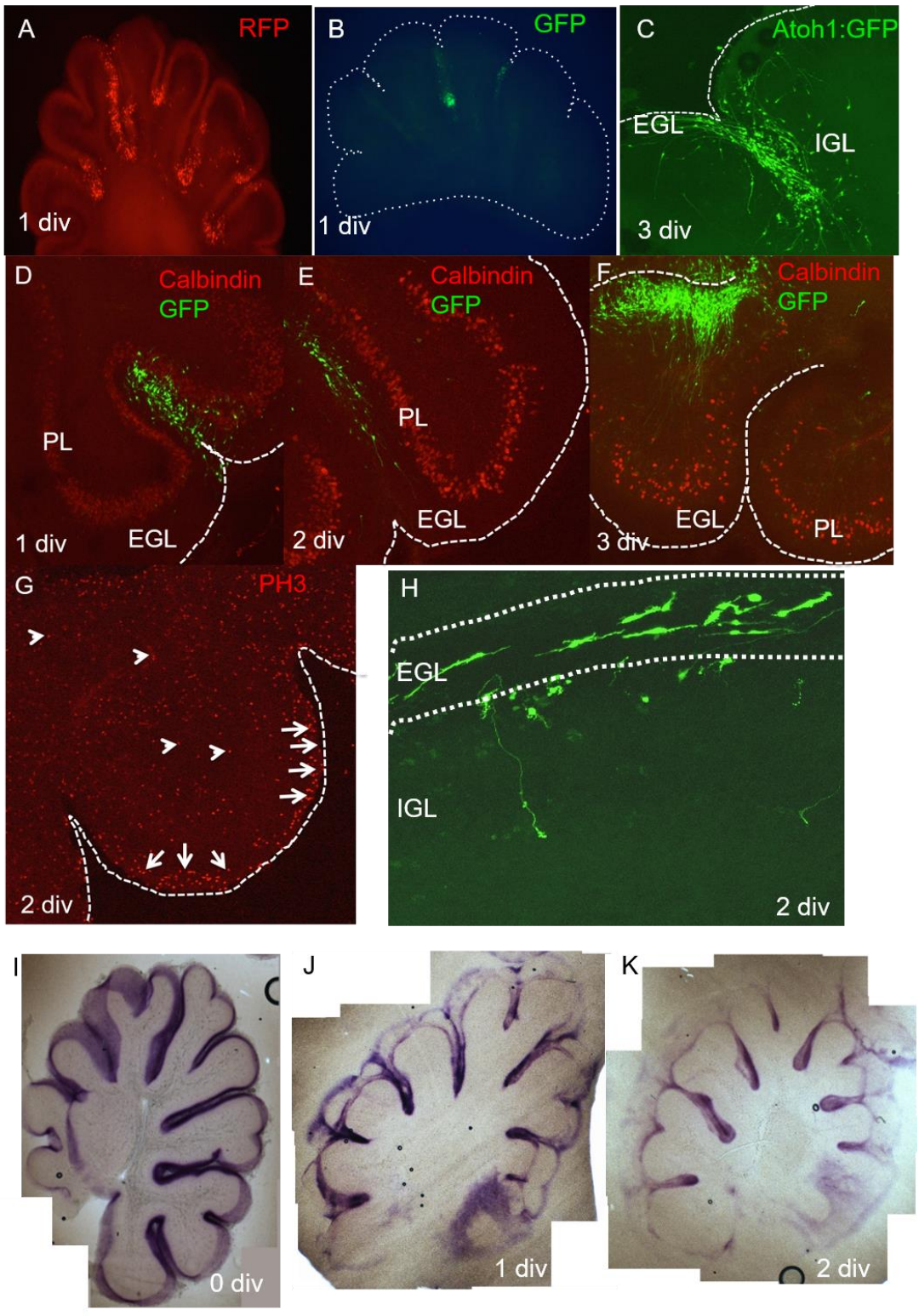

Figure 2-13: Cerebellar slices can be electroporated ex ovo to study granule cell development *(next page)*

Previous page:

Figure 2-13: Cerebellar slices can be electroporated *ex ovo* to study granule cell development

A) E14 cerebellar slice electroporated with CAGGS-RFP plasmid, cultured for 1 div**. B)** E14 cerebellar slice electroporated with CAGGS-GFP plasmid, cultured for 1 div. In this electroporation only one folium was targeted. **C)** Granule cell precursors can be electroporated with Atoh1-cre and stop-GFP plasmids. GFP is only expressed in GCPs, which are the only Atoh1^{+ve} cells in the cerebellum at this stage. Notice many cells migrating towards the IGL after 3 div**. D-F)** E14 cerebellar slices electroporated with CAGGS-GFP plasmid and cultured for 1-3 div. After culture slices were stained for calbindin to assess Purkinje cell health and hence tissue integrity. **G)** A slice of E14 cerebellar tissue cultured for 2 div and stained for the proliferation marker, PH3. Many cells are proliferative in the EGL (arrows) but many are also seen in the IGL and the white matter of the cerebellum (arrowheads). **H)** A magnified view on granule cells developing in the electroporated slice culture. They extend parallel processes and migrate towards the IGL. **I-K)** Atoh1 *in situ* hybridisation in E14 slices, either fixed straight after sectioning with tissue chopper or cultured for 1-2 div. Fragmentation of the EGL is observed in culture.

EGL: External Germinal Layer; IGL: internal granular layer, PL: Purkinje cell layer

Next page:

Figure 2-14 Trials of GAL4-UAS and Fucci genetic tools in cerebellar slices

A) Electroporation of Math1-GAL4 and UAS-synaptophysin-GFP and UAS-psd95-TdTomato into E14 cerebellar slices, cultured for 3 div. **B)** Synaptophysin-GFP is localised to all cellular processes. **C)** psd-95-TdTomato is localised to cell bodies only and is never seen in cell processes. **D)** An illustration of when Geminin and Cdt1 are expressed in cell cycle. **E)** Expression of Geminin-GFP in E14 electroporated tissue after 2div. **F)** Expression of Cdt1-RFP in E14 electroporated tissue after 2 div. **G)** Expression of KO2-Geminin-MyrAG1 in E14 cerebellar tissue after 3 div **H)** Magnification from G. KO2-Geminin expression is found in cells with highly differentiated morphologies (arrows).

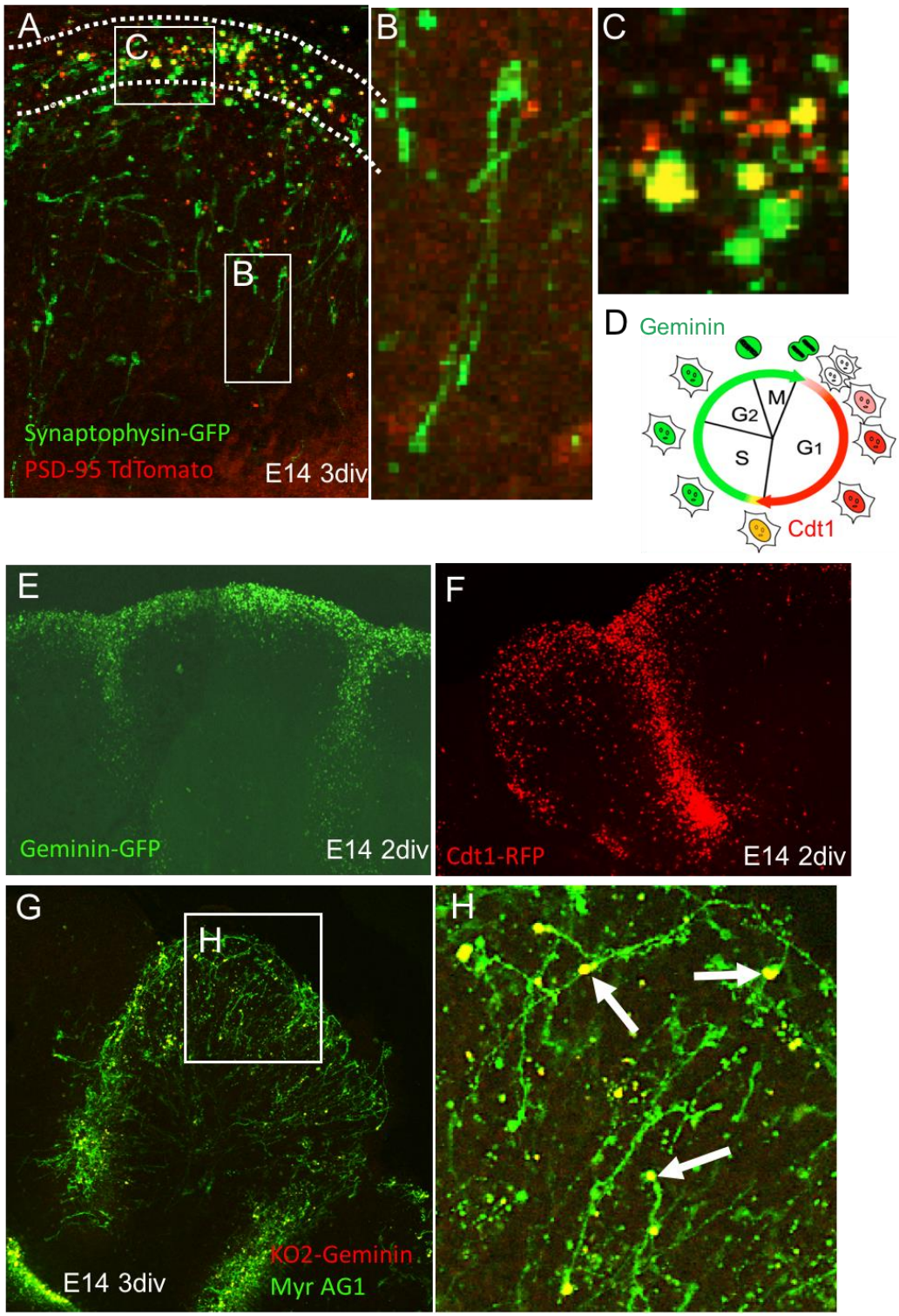

Figure 2-14 Trials of GAL4-UAS and Fucci genetic tools in cerebellar slices

(previous page)

2.3 Discussion

In this chapter I examined in detail the morphologies of cerebellar granule cell precursors in the chicken cerebellum and present evidence for their elaborate morphologies. I observed individually-labelled cells located in the EGL using a genomic integration method through Tol2 transposon- directed integration of the GFP transgene. Using anti-phospho-histone H3 antibody as a marker of mitosis, cells that co-label PH3 and GFP are characterised. Results show that proliferating GCPs are present throughout the EGL, mostly in the outer and middle EGL, but a small proportion is also found in the inner EGL. Mitotic GCPs can have long and elaborate processes reminiscent of leading processes and even of emerging parallel fibres. Some mitotically active cells, mostly in metaphase, also extend very thin processes reminiscent of cytonemes found in other developing systems. Additionally, proliferating cells are found located in the Axonin-1^{+ve} area, suggesting that the current understanding of GCPs is incomplete and their mitotic activity is more complex than anticipated. Further, I develop a way of targeting those cells *ex ovo* to study their development with various available genetic tools that would be difficult to use *in ovo*. Overall, this project provides further insight into the development of GCPs and exposes many gaps in the current understanding of granule cell biology.

2.3.1 Limitations of the experimental approach

A technical difficulty encountered when attempting to explore proliferation of early-born GCPs at early stages of cerebellar development (E8) was that many electroporated embryos at this stage has a decreased proliferation rate observed at the site of electroporation compared to the neighbouring, non-electroporated, areas (**Fig 2-2A-C**). Hence, even though, initially, an examination of early GCPs was planned, this technical issue prevented this part of the project. Interestingly, however, proliferation of GFP-expressing cells in the EGL at E14 appears normal, suggesting that at least a subset of the electroporated cells ultimately regain their proliferative capacity and undergo many rounds of divisions in the EGL.

To study the morphologies of the early-born GCPs, this technical issue will have to be addressed in the future, possibly through lowering the electroporation intensity, duration or number of shocks.

Another possible issue with the approach used in this project to observe GCP morphology is that the GFP constructs used to label GCPs was driven by the activated CAGGS promoter. This means that many cell types other than Math1-expressing RL derivatives could have been labelled at the time of electroporation. Indeed, when examining the slices, I observed a number of cell types labelled with GFP that did not resemble GCs. They were however all located outside of the EGL. The cells were most likely Bergmann glial cells and possibly other types of cerebellar interneurons labelled from the ventricular zone bordering the RL. The working assumption during the project was that no other cell type is known to proliferate within the EGL but GCPs, therefore any $PH3^{+ve}$ cell that was observed in the EGL, was presumed to be a GCP. Because the morphologies of the $PH3^{+ve}$ cells could be observed, this provided additional confirmation for the fact that no $PH3^{+ve}$ cells found within the EGL morphologically resembled any other cell type. Nevertheless, one improvement to the protocol would be to use Math1-Tol2 constructs that would allow more confidence that the cells labelled are RL derivatives only. However, this approach would still not be completely specific for GCs as many other cell types are generated from the $Math1^{+ve}$ RL during development.

The biggest technical issue encountered during the project had been the difficulty in reliably assigning the layers of the cerebellum (outer, middle and inner) due to the coronal sectioning of the tissue. During coronal sectioning, the EGL can be sectioned at different levels and only some sections perfectly represent the layering of the cerebellar cortex normally seen in sagittal sections. Therefore, when assigning the cells to layers many aspects were taken into consideration, including the morphologies of the cells, expression of Axonin-1 and the shape of the nuclei of cells (round in the outer layers, spindle-shaped in the inner layers). Nevertheless, due to this technical issue, some of the quantifications (e.g. numbers of $PH3^{+ve}$ cells in different layers) would ideally need to be re-counted in sagittal sections for confirmation. The reason that tissue was cut coronally was that in

sagittal sections not all types of morphologies of GCPs can be observed. Parallel fibres develop in the medio-lateral direction and sectioning the tissue sagitally would potentially cut through these developing processes, preventing detailed morphological analysis. Reassuringly, however, other authors have reported a similar distribution of $PH3^{+ve}$ cells in the cerebellum, with many located in the deeper layers of the EGL (e.g. Haldipur et al., 2015, Fig1A). Therefore, I am confident that these results broadly represent the actual distribution of proliferative cells in the cerebellum.

Anti- Axonin-1 antibody was used as a differentiation marker of GCs in the above experiments. However, the staining was not clearly defined to individual cells and it was often not possible to decide with certainty whether a cell expressed Axonin-1. The protein was broadly expressed in the inner half of the EGL and its expression was strongest in a defined but broad layer. However, it is possible that individual cells within this broad layer, especially the ones expressing PH3, did not co-express Axonin-1. One possibility to check whether the $PH3^{+ve}$ cells located in the middle and inner EGL express differentiation markers such as Axonin-1, would be to stain them for other known EGL postmitotic markers, preferably with nuclear expression such as NeuN, or Tuj1. Immunohistochemistry for NeuN and Tuj1 was in fact attempted during the project, but the results of the staining were unsatisfactory, even after numerous modifications, and are therefore not presented here. Nevertheless, optimising these antibodies or using another antibody to label the postmitotic EGL cells would aid our understanding of the complexity of the mitotic GCPs. It is known from other studies that some GCPs, termed 'intermediate progenitors', can in fact co-express Axonin-1 and a proliferation marker (Xenaki et al., 2011). Therefore, I am confident that the reported co-expression of Axonin-1 and PH3 in some cells is a true representation of the cellular behaviour *in vivo*.

There are numerous technical considerations regarding the cerebellar slice electroporation protocol developed during the project. Firstly, the robustness of slices to survive in culture without on the one hand undergoing extensive cell death or on the other losing structural integrity limits the thickness of slice to 300μm. A second important consideration is the viscosity of the DNA solution,

which ensures electroporation of DNA at concentrations that are high enough to induce visible or relevant levels of genetic modification. In *in ovo* electroporation of DNA solutions injected into the early embryonic hindbrain, concentrations of fast green dye of approximately 1% are typical. However, in this protocol, concentrations of fast green of 20% are typically used. This ensures a sufficiently viscous DNA solution to prevent dispersal of the DNA following pipetting but before electroporation, but a sufficiently dilute one to mediate efficient electrical conduction. Importantly, even though the Purkinje cell label looks relatively normal even after 3 div, it is clear the integrity of the tissue is compromised based on Atoh1 *in situ* hybridization results that clearly show the fragmentation of the EGL. The situation is not as severe in the creases of the folia and any further research should preferably look at GC behaviour in those areas. Proliferation in the slices is also increased throughout, suggesting a reaction to the sectioning trauma, possibly by increased gliogenesis. PH3 is still visible in the EGL, however, suggesting that normal proliferation of GCPs still occurs and should not be disturbed by changes in proliferation elsewhere in the tissue.

The genetic tools tried during the project will need optimization before they can be used to tackle the remaining questions about GC development. UAS driven proteins are essentially overexpressed in the electroporated cells so their concentration has to be optimized so that protein localization can be determined but adverse effects on cellular development are not triggered. Similarly, Fucci constructs have been shown to be effective in other organs in the chick (Esteves de Lima et al., 2014). Optimising the concentrations of the electroporated constructs, electroporating *in ovo*, and possibly live imaging of the electroporated tissue for signs of cell division should clarify whether these constructs work in cerebellar slices as well.

2.3.2 Dividing granule cell precursors can reside in the inner EGL and possess elaborate processes

The main conclusion from the experiments performed in this project is that the morphological diversity of $PH3^{+ve}$ cells in the EGL is more complex than anticipated. No other cell type except GCPs are known to proliferate within the EGL and therefore the $PH3^{+ve}$ cells are presumed to represent GCPs. Contrary to

previous reports on GCP development (summarised in **Table 2-1**), I observed GCPs with long processes resembling both leading processes found in tangentially migrating cells, as well as thinner, longer processes reminiscent of forming parallel fibres. This is a surprising finding because cells of this morphology were always assumed to represent postmitotic granule cells. The fact that progenitor cells capable of dividing can simultaneously extend elaborate processes raises a large number of questions and calls for revisions to the current understanding of GCPs.

Interestingly, cells observed during this project were morphologically very diverse and their processes differed from one another. In addition to the cells with shorter and thicker processes with growth cones, resembling leading processes, and cells with thin long processes reminiscent of forming parallel fibres, another type of processes was observed. Namely, very thin and sometimes quite long processes extended from the cell bodies of cells mostly in metaphase. Those processes resemble cytonemes seen in other systems where cell to cell signalling is required. Cytonemes are thin filopodia-like processes that are instrumental in morphogen signal exchange between producing and receiving cells (Bischoff et al., 2013; Kornberg, 2014, 2017). For example, cytonemes have been shown to mediate Shh signalling in the chick limb bud (Sanders et al., 2013). In zebrafish, cytonemes have been shown to transport Wnt signalling during neural tube patterning (Stanganello et al., 2015). However, at this stage it is not possible to claim that GCPs indeed extend cytonemes and use them for intercellular signalling in the cerebellum. The processes might represent retraction fibres instead (Fink et al., 2011) and this result requires further investigation.

2.3.3 Dividing granule cell precursors retract their processes prior to cell division

Results presented in this study show that GCPs can be proliferative and exhibit a large number of morphological features, many of which were previously only advocated for postmitotic cells. Interestingly, by using PH3 staining, it was possible to observe the different cell cycle stages and hence the equivalent morphologies of GCPs at each stage. PH3 only marks cells in mitosis, however, mitosis itself has a number of stages that can be followed based on the pattern of PH3 staining (**Fig 2-**

1). During my examination of the PH3 $^{+ve}$ cells, it became apparent that cells undergoing metaphase almost never have any long processes, and mostly resemble polyhedral cells with some thin, cytoneme-like processes only. In contrast, many cells that extended long processes were in the first mitotic stage, prophase.

These results strongly suggest that dividing cells retract their processes during mitosis and a cell never divides while extending long processes. In fact, no cell was observed in metaphase bearing long processes extended from its cell body. Many cells in pro-metaphase, in fact, had a characteristic morphology of retracting their processes, as thin remains of such processes could be seen at high exposure. Therefore, the results suggest that even though GCPs are present in the middle and inner layers of the EGL and have a postmitotic-like morphology, they are still capable of dividing, by morphologically de-differentiating to outer EGL-like morphology of rounding up and retracting all processes. This result presents an interesting new mechanisms for cell differentiation that does not resemble the proliferation of any of the known cortical progenitors. Apical progenitors in the cortex do not retract their processes during division and basal progenitors do not migrate while mitotically active.

2.3.4 Granule cell precursors do not require an attachment to the pia with a basal process to proliferate

A common view held in the field of cerebellar granule cell development is that granule cells are proliferative as long as they retain their attachment to the pial surface. This view had been described first in the Hausmann and Sievers (1985) study where electron microscopy observations revealed that a large number of granule cells have a clear attachment to the basal lamina. However, the study at the time made no effort to ascertain whether those cells were in fact actively proliferating and therefore presented no evidence for this assertion. Nevertheless, other studies made similar suggestions (Koirala et al., 2009; Butts et al., 2014; Chan et al., 2009). In the current study, I have demonstrated that GCPs can be proliferative without any attachment to the basal lamina. This is especially clear when looking at the cells located deep within the EGL, in the middle or even inner

EGL. Those cells have elaborate morphologies, as discussed above, however, very few of them retain any visible process linking them to the basal lamina. There are many cells in the outer EGL that do indeed have an attachment to the basal lamina, however, interestingly, few of them stain for PH3. In fact, out of the 154 $PH3^{+ve}$ cells observed in the study, only 3 cells were observed having a basal process, presumably attaching them to the pia. This might be because PH3 labels cells in mitosis only and GCPs might have a different morphology before their decision to enter mitosis. For example, GCPs might have an attachment to the pia during G1/S phase and lose that attachment prior to entering mitosis. High resolution live imaging of the oEGL cells could shed some light on this possibility in future experiments.

2.3.5 Outstanding questions and proposed further research

Clearly, GCPs located in the EGL are a heterogeneous population of cells, at different stages of their differentiation in different layers. The fact that GCPs express differentiation markers like Axonin-1 (and p27 (Miyazawa et al., 2000) and Tuj1 (Xenaki et al., 2011)) but still are proliferative raises many interesting questions.

For example, at what point are GCPs committed to becoming a differentiated GC? Most literature on granule cells development suggest that they are born by terminal symmetric divisions of GCPs (Espinosa and Luo 2008; Nakashima et al., 2015; Yang et al., 2015) and that asymmetric divisions of GCPs are rare. What is the molecular mechanism dictating those choices and can cellular morphology prior to division be a reliable indicator for subsequent cell fate? Long term live imaging is the best way to answer those questions in future experiments.

Further, what is the significance of the various processes extended by GCPs during development? Is basal attachment a predictor of Math1 expression? Math1 expression is limited to the outermost layer of cells in the EGL (Xenaki et al., 2011), making the correlation plausible. If this is the case, what is the role of Math1 in proliferation of GCPs? Surprisingly, a small number of cells with a pial attachment

expressed PH3. What does this finding mean in terms of GCP proliferative capabilities?

Many GCPs were found extending long processes that are usually associated with postmitotic granule cells. If tangentially migrating GCs can revert to division, what exactly are the different processes they extend at different stages of differentiation and what are the mechanisms that allow morphological de-differentiation?

To answer many of these questions a very careful set of experiments is needed, preferably in an environment as close to the *in vivo* conditions as possible. It would be interesting to see how these questions could be attempted using electroporation of cerebellar slices. Live imaging of cells would also be required to follow cell fate following divisions and cellular behaviour in terms of migration and process retraction.

Chapter 3: Live imaging of dividing granule cell precursors in *ex ovo* cerebellar slices

3.1 Background

In chapter 2 I have explored the morphological features of granule cell precursors in fixed chicken cerebellar tissue. I used immunohistochemistry to label proliferating and differentiating granule cells and correlated cellular morphologies with the differentiation status. I gained novel insights into GCP mitotic behaviour. However, by imaging fixed tissue, I was unable to observe the progressions through which GCPs acquire their morphologies and whether pattern of differentiation is shared by all precursors. To further investigate the proliferative dynamics of GCPs in the EGL, and to provide additional evidence for elaborate morphologies of dividing GCPs seen in static images, I established a live imaging protocol to observe GCPs in cerebellar slices. This *ex vivo* set up allowed me to directly observe GCPs before they divide, at the time of their division, and the behaviour of their daughter cells.

3.1.1 Time-lapse imaging of live tissue as a powerful technique to observe the behaviour of neuronal precursors

Time-lapse imaging of living tissues and cells has become a common and powerful tool in the life sciences to investigate and gain insight into cellular dynamics and functions that were impossible to achieve from studies of fixed specimens. As a technique, it is well established and has become very advanced with two photon microscopy and super-resolution microscopy, for example. The techniques allow the researcher to study complex biological processes in unprecedented detail.

Live imaging has been used in numerous systems to gain profound insights into the behaviour of neuronal precursor cells and their fate acquisition after division. For example, by using live imaging in the zebrafish embryos, Alexandre et al., (2010), were able to observe, for the first time, apical neural progenitors in the zebrafish neural tube undergo asymmetric division. Contrary to all expectations, they observed that the daughter cell destined to become a neuron was derived from the more apical of the two daughters. The more basal daughter inherited the basal process and maintained its proliferative capacity, continuing dividing asymmetrically. This insight would not have been possible without live imaging because the fate of the two daughter cells cannot easily be deduced from static images and the very dynamic nature of process inheritance is easy to misinterpret from static images of fixed specimen.

In the mouse cortex, the proliferative behaviour of the main neuronal progenitors, the radial glial cells, have been investigated using time-lapse imaging since at least 2001 when Noctor et al., (2001) showed, for the first time, that RGCs generate cortical neurons. Since then, time-lapse imaging was used in numerous studies of cortical neural progenitors, for example, in investigating the role of the mitotic spindle in cell fate acquisition (Haydar et al., 2003), the roles of various signalling molecules such as Notch and Delta (Nelson et al., 2013) and the role of the cell cycle length and its effect on cell fate (Pilaz et al., 2016) among many other applications.

Live imaging of neuronal progenitors in the spinal cord has also recently been used to yield interesting new findings about progenitor cells and neuronal behaviour. For example, Das and Storey (2014) have observed a new mechanism for neuronal detachment from the ventricular surface called apical abscission. Insights of this originality and importance would not have been possible without live-imaging techniques and hence I also intended to use this powerful technique to answer previously unaddressed questions about the behaviour of GCPs in the cerebellum.

The main advantage of imaging cellular behaviour in cerebellar slices as opposed to in cell culture is that the environment in which GCPs reside is closest to their *in vivo* environment. Many studies have looked at the behaviour of granule cells in

cell culture (section 1.2.4), however, this system does not allow for observing granule cell behaviour in cerebellar tissue with intact structural and cellular interactions, including the various extracellular signals known to direct GCP development. Therefore, live imaging of cerebellar slices in this project was an attempt to best recapitulate GCPs endogenous environment and analyse GCP behaviour in the context of the tissue, revealing how GCPs behave relative to the neighbouring cells and structures. Other advantages of the time-lapse analysis technique over fixed tissue analysis includes generation of considerably more data points that can be analysed flexibly (Pilaz and Silver, 2014). Cellular behaviour can be tracked in time and space and analysed from multiple perspectives.

3.1.2 Previous attempts at live-imaging of granule cell precursors

Given the great strengths provided by time-lapse imaging, surprisingly few studies have imaged proliferating GCPs in live cerebellar tissue. None have attempted to look at GCP morphologies around the time of cell division. Two recent studies used live imaging in organotypic cerebellar tissue to investigate different division modes of GCPs in the EGL but have not investigated their morphological characteristics or transitions.

The study by Yang et al (2015) used rhombic lip neuronal progenitor specific (Math1-GFP) and differentiated neuron-specific (Dcx-DsRed) mouse reporter lines to study GCP division modes in both cerebellar dissociated cultures, as well as in live cerebellar tissue. The authors report that GCPs undergo non-terminal symmetric, asymmetric and terminal symmetric divisions *ex vivo*. However, their time-lapse movies of those divisions are very short (up to 2 hours) and hence they do not concentrate on any morphological changes that these cells undergo prior to, or after, division. Additionally, because all granule cells are labelled in the Math1-GFP reporter mouse it is very difficult to distinguish individual morphologies of cells. The movies provided by the authors as illustrations of the three modes of division are unfortunately mostly unconvincing to a skilled observer. The authors' interpretation of which cells become the daughter cells after division could easily be disputed and the frame rate in the movie is not sufficient to resolve such disputes. Especially the frames illustrating the asymmetric cell division mode

make it hard to see how one daughter cell could have moved so far away from the other daughter cell in 8 minutes. Leaving such problems aside, the paper did not attempt to look at GCP morphologies and hence does not contribute to answering the specific question of this project. It does, however, demonstrate that imaging dividing GCPs in cerebellar tissue is technically possible.

Another study published in the same year, by Nakashima et al (2015), also observed dividing GCPs in mouse cerebellar dissociated cultures and in cerebellar tissue. The authors used a nuclear marker (Histone2b tagged with EGFP under a CAG promoter) to visualise all electroporated cells and a reporter construct that specifically labels differentiated neurons. Similarly to Yang et al (2015), the construct encoded a doublecortin enhancer element driving DsRed expression. Both papers drew similar conclusions about the frequencies of the three GCP division modes and the fact that granule cells are predominantly generated by terminal symmetric divisions in the cerebellar tissue. However, because this paper used a nuclear marker to visualise GCPs division, the authors missed the opportunity to visualise any changes in morphologies of these GCPs before, during, and after division.

The protocol used by Nakashima et al (2015) would have been an excellent system in which to observe morphological and fate transitions because of the long (up to 24hrs) live imaging sessions in live tissue, which allowed the authors to trace at least two rounds of divisions of individually labelled GCPs in mouse cerebellar slices. The data presented by the authors suggests that GCPs are able to undergo short migratory movements before division because, according to the authors, the cells 'had round nuclei and moved in a random orientation for a short distance'. The authors did not discuss the possibility of GCPs possessing any processes at this stage of their development or how such short migratory movements might occur. In conclusion, at present, no study has been published where the morphological changes of GCPs were observed or reported on. In this chapter, I try to address this omission.

3.1.3 Aims of the study

In this chapter, I use time-lapse imaging technique in live chicken cerebellar tissue to address questions that could not be answered in the previous chapter where only fixed tissue and immunohistochemistry were used to look at a very dynamic process of morphological transitions of cells during development. Observing individually labelled, living, proliferating cells in organotypic slices will allow me to tackle many unanswered questions about GC development. For example, I will be able to observe the dynamic morphological transitions of dividing GCPs and can examine the requirement for the basal attachment to the pial membranes for division. Additionally, I will be able to examine what happens to the horizontal processes extended by the mitotic cells. I could gain insight into the different types of cell division that GCPs undergo and whether all cell division share a stereotyped morphological transition.

3.2 Results

3.2.1 Individually labelled proliferative granule cell precursors can be observed dividing in chicken *ex ovo* cerebellar slices

Electroporation of chicken embryos with Tol2:GFP at E4 and sacrificing the embryos at E12-E14 allowed for a relatively sparse labelling of GCPs to observe individual cellular morphologies. The numbers of dividing GCPs as a proportion of all labelled cells were very low with a maximum of 6% of labelled GCPs dividing during the imaging time. During my project, less than 20 dividing cells were seen in around 25 imaging sessions. Nevertheless, the insights into GCP behaviour gained from the time-lapse movies complement my findings from static images and also establish a proof-of-principle protocol for studying proliferative GCPs in cerebellar slices in the future.

During my project, 14 dividing granule cell precursors derived from 4 different cerebella were observed diving clearly enough for analysis. Even though the same protocol was used on all imaging days, some cerebellar tissue showed a relatively large number of dividing cells (maximum of at least eight dividing GCPs were observed in one tissue) while others contained only one dividing GCP during the time of imaging. Undoubtedly, the larger the number of labelled cells in a tissue, the higher the probability of observing dividing GCPs. However, some dividing GCPs were difficult to observe and characterise due to being in a fluorescent cell-dense area and hence their morphological transitions were obstructed by the neighbouring cells.

Here, details of cells chosen for their relative morphological clarity and interesting behaviour are presented and details of their morphological transitions are discussed. In some of the quantifications and analyses other dividing cells, that were not analysed in detail due to obstructions, will be included.

Table 3-1 collects all the cells that will be discussed in at least some detail in this report. The cells are named according to which tissue they were acquired from (Tx) and the number assigned to each dividing cell (DCx).

Selected cells are analysed in detail in individual figures (**Fig 3-4 to 3-10**). Each figure represents a selection of time frames from all time points acquired during the time-lapse movie. The frames chosen exemplify an interesting transition of the cell and are discussed in detail in the figure legends. All time points for each cell and the reconstructed movies can be found on the DVD supplied. After analysing the cells separately, it was clear that they shared many similarities and showed some differences. Below, I discuss some of the interesting features of dividing GCPs that I observed during filming and analysis.

Cell	Figure reference
T1DC1	Figure 3-4
T1DC2	Figure 3-5
T2DC1	Figure 3-6
T2DC2	Figure 3-6
T2DC3	Figure 3-7
T2DC4	Figure 3-7
T2DC7	Figure 3-8
T3DC1	Figure 3-9
T4DC1	Figure 3-10

Table 3-1 The figure reference for each analysed GCPs from the time lapse movies

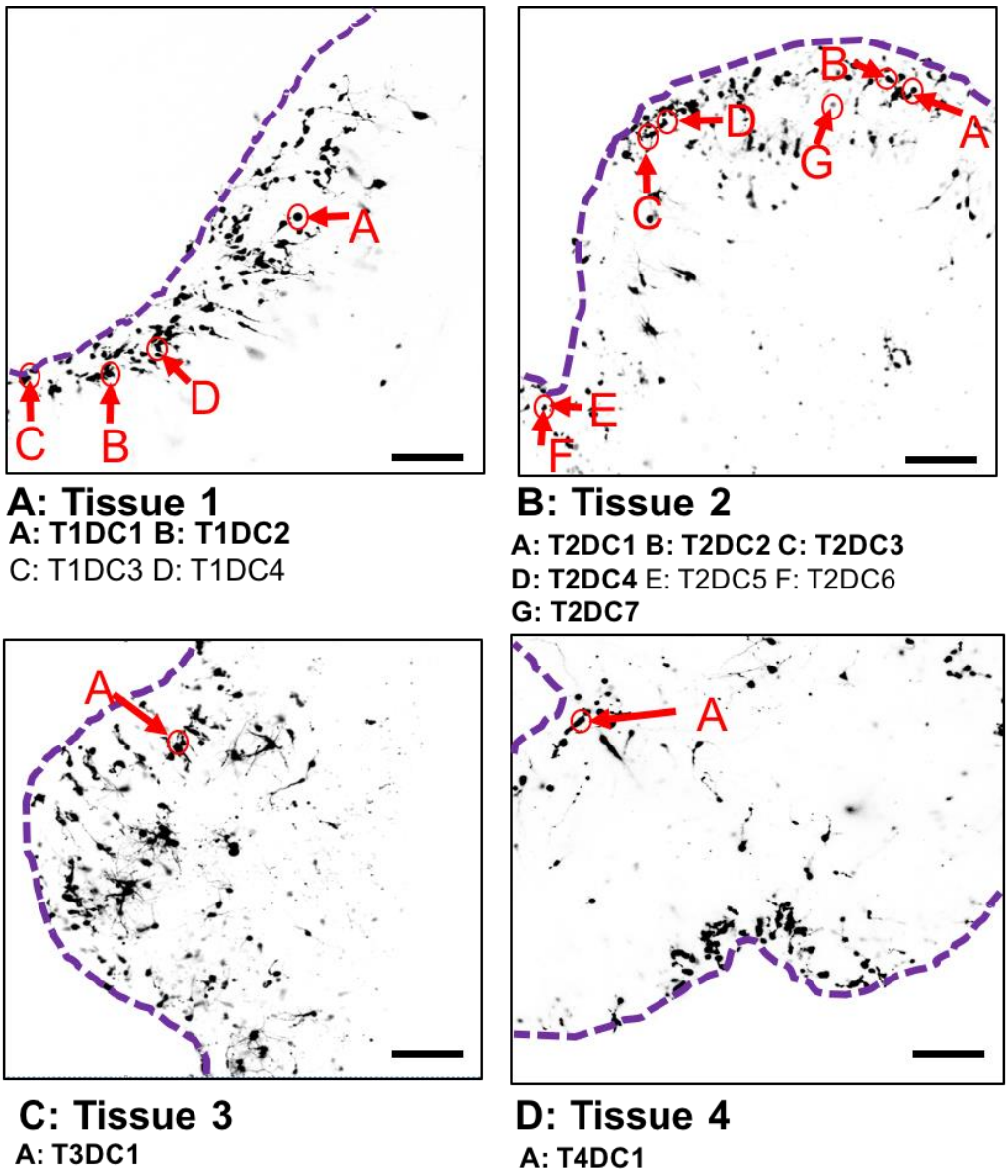

Figure 3-1 Summary of the cerebellar tissues used for live imaging and the positions of all observed cells

Four cerebellar slices from four different electroporated chicken cerebella showed at least one dividing GCP with a clear and interesting morphology. The figure collects a Z projection through one time-point taken of each tissue and shows the positions of the dividing GCPs. Tissue 1 showed at least 4 dividing cells with relatively unobstructed morphologies. Two of these cells, T1DC1 and T1DC2 are analysed in detail in separate figures. Tissue 2 showed at least 8 dividing GCPs and because they are in pairs, they are analysed as pairs in separate figures. From tissue 2 the following cells are analysed in detail: cells T2DC1 and T2DC2; cells T2DC3 and T2DC4 and cell T2DC7. Tissue 3 and tissue 4 show one dividing GCP each and both of these cells are analysed in separate figures. Scale bar = 100µm

3.2.2 The majority of granule cell precursor proliferative divisions occur in the outer and middle EGL, with a few also occurring in the inner EGL

After the imaging of the cerebellar tissue was complete, the tissue was fixed and immunohistochemistry was performed for calbindin (Purkinje cell marker) and labelled with DAPI. Calbindin stain was used as an indicator of the extent of the EGL (as the Purkinje cell layer delineates the inner extent of the EGL). DAPI was used to label cell nuclei and enabled the number of EGL cells to be counted in order to deduce the layer of the EGL (outer, middle, inner) where the labelled proliferating cells were located at the time of division.

Most granule cells seen dividing during the time-lapse experiments were located either in the outer EGL or in the middle EGL. Only one cell (T2DC7) was seen to be dividing in the inner EGL. This cell, however, expresses lower than average levels of fluorescence and therefore it was more difficult to ascertain its morphological transitions. Nevertheless, as **Figure 3-6** quite clearly demonstrates, cell T2DC7 seems to divide perpendicular to the pial surface in the inner EGL, producing two daughter cells, which separate quite clearly from one another. This presents quite a strong evidence that granule cell precursors can undergo divisions within the inner EGL, however those events are rare compared to divisions in the upper two layers. Owing to the relatively low numbers of dividing cells observed in this study it is not possible to estimate precisely the relative numbers of GCPs dividing in the inner EGL, however it can be assumed that these numbers are relatively low. This result complements my experiments carried out in fixed tissue, where I saw a low percentage of dividing GCP is the inner EGL, as well as experiments of others who observe highest rate of division in the outer and middle EGL.

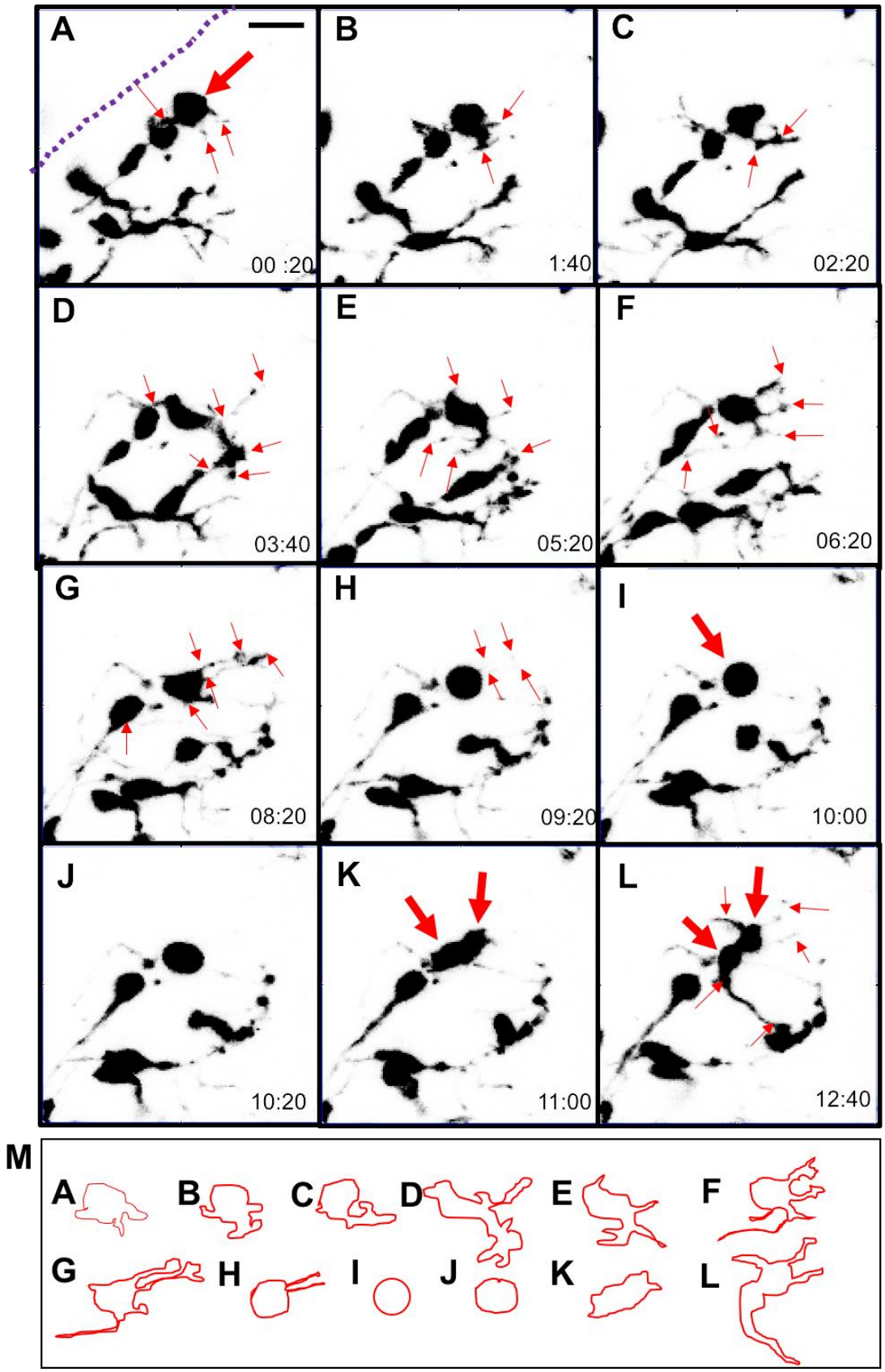

Figure 3-2 Characterization of the dividing granule cell precursor T1DC1

(next page)

Previous page:

Figure 3-2 Characterization of the dividing granule cell precursor T1DC1

A selection of time-frames from the time-lapse movie of T1DC1. Small red arrows point to processes that extend from the cell body. Thick arrows point to the cell of interest and its two daughter cells after division. The purple dotted line shows the position of the pial surface. The panel **M** shows a traced surface of each cell to aid visualisation.

A) At the beginning of the time-lapse a round cell with three small processes can be seen in close proximity to the pial surface. **B**) One of the processes pointing radially can be seen thickening and starting to bifurcate in M-L directions. **C**) One of the branches extends further and bifurcates into two small branches of variable length and thickness. **D**) The horizontal branch becomes thinner as time progresses and appears to be retracted, after which it extends again, this time showing a broad growth cone. After around three hours, the process starts to retract again until it is no longer visible at the time of division. The vertical branch of the process seems very exploratory. The cell body in D appears to begin slight movement away from the pial surface, but stabilises and becomes more rounded by F. **E**) The thick process retracts and instead changes direction to extend a thin long process in the M-L direction. **F**) At this point the cell has five district processes of varying length and thickness in numerous directions. **G**) Most processes extend even further and show distinctive growth cone like protrusions at the tips of the processes which all retract within an hour. **H**) Two of the processes leave faint thin processes behind. **I**) At the time of division even those processes disappear and the cell appears to be completely round, without any processes. J and K) Within an hour the cell divides into two GCs that both extend processes in opposite directions to each other. **L**) The cell on the right seems to extend two processes in a similar place as the precursor cell. Interestingly, it also extends a process towards the pial surface. The cell on the left extends a pronounced thick process towards the inner EGL. Scale bar = 20µm

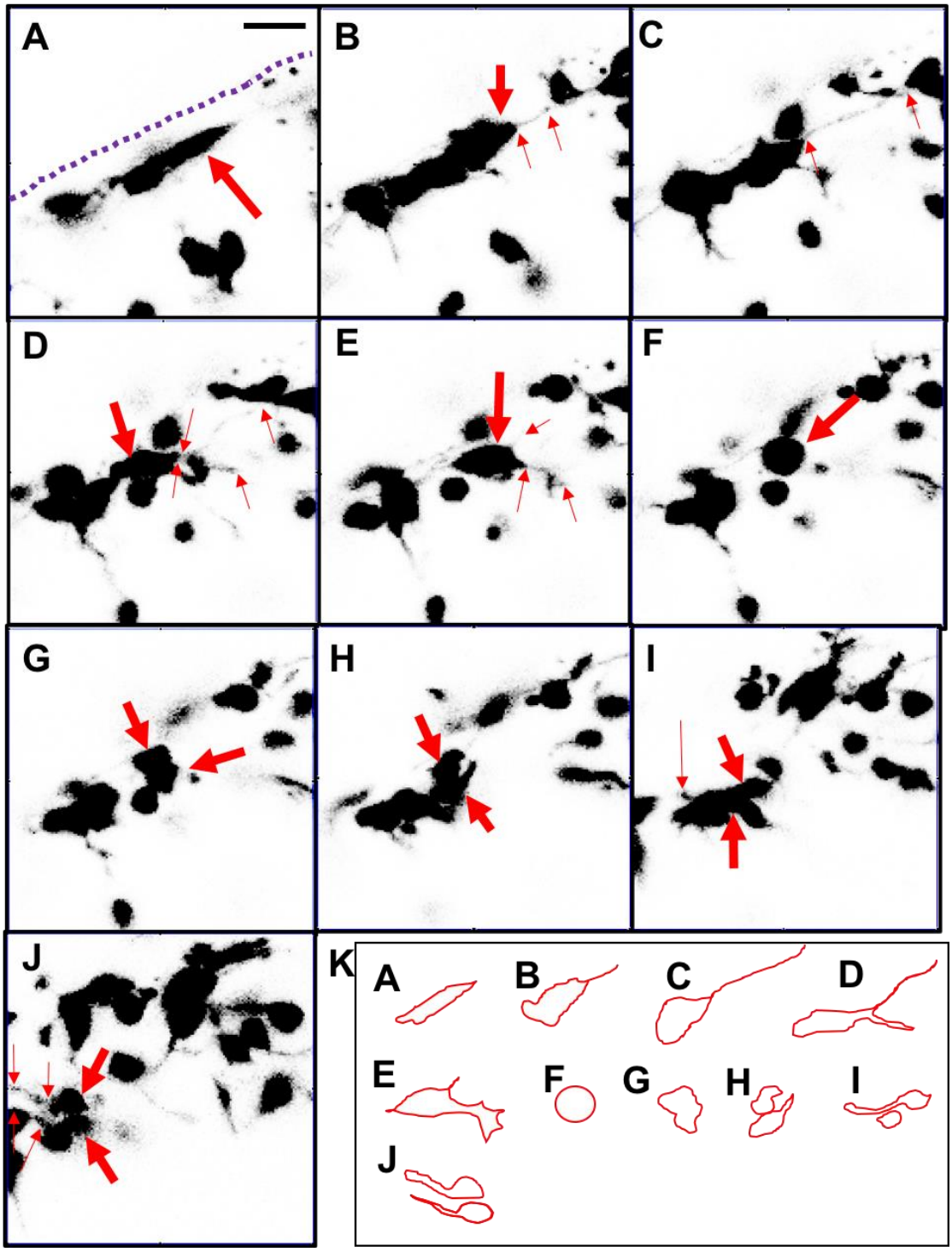

Figure 3-3 Characterization of the dividing granule cell precursor T1DC2

(next page)

Previous page:

Figure 3-3 Characterization of the dividing granule cell precursor T1DC2

A selection of time-frames from the time-lapse movie of T1DC2. Small red arrows point to processes that extend from the cell body. Thick arrows point to the cell of interest and its two daughter cells after division. The purple dotted line shows the position of the pial surface. The panel **K**) shows a traced surface of each cell for visualisation.

A) At the beginning of the time-lapse movie, the cell appears to have an elongated cell body and is positioned close to the pial surface. **B**) The cell body then moves slightly to the left, leaving behind a short thin process and rounding up slightly. **C**) The process elongates and **D**) the cell extends a second, slightly thicker process in a similar direction as the first. **E**) The cell body makes a small migration movement in the direction of the second process, which is the opposite direction to its previous migratory movement, but soon after **F**) retracts both its processes and rounds up ready for cell division. **G**) The cell divides, presumably in a perpendicular plane of division. **H**) The daughter cells migrate away from the site of division by diving deeper into the tissue and migrating tangentially. **J**) At the end of the time-lapse both cells seem to migrate in a similar direction with extended leading processes. Scale bar = 20μm

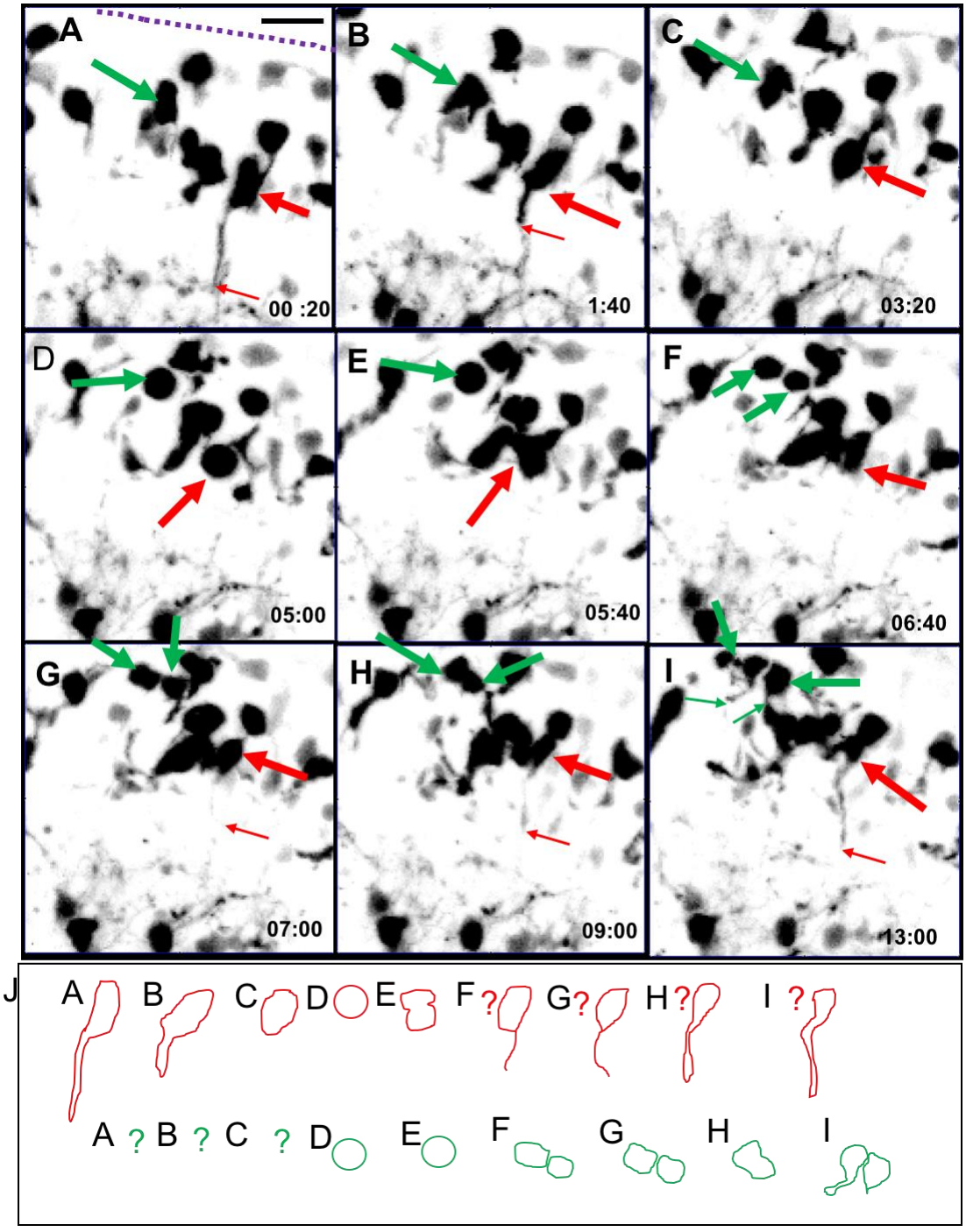

Figure 3-4 Characterization of the dividing granule cell precursor T2DC1 and T2DC2 *(next page)*

Previous page:

Figure 3-4 Characterization of the dividing granule cell precursor T2DC1 and T2DC2

A selection of time-frames from the time-lapse movie of T1DC1 and T1DC2. Thick red arrows point to the cell T2DC1 and its daughter cells and the thick green arrows point to the cell T2DC2 and its daughter cells. The pial surface is delineated with a purple dotted line. Small red and green arrows point to the corresponding cell's processes. The panel **J**) shows a traced surface of each cell for visualisation. I placed a question mark where I could not trace the morphology of the cell due to it being obstructed by other cells. Scale bar = 20μm

<u>Cell T2DC1 (Red arrows):</u>

A) The cell extends a long thick process towards the inner EGL, presumably touching Purkinje cell dendrites with its tip. **B)** The cell then retracts its process and **C and D)** rounds up for cell division. After around 2 hours after rounding up, the cell divides in a perpendicular manner. After that, one of the daughter cells is untraceable within the group of labelled cells, however the other daughter cell **G**) can be seen extending a thin process, which **H and I**) becomes longer and thicker as time progresses. At the end of the time-lapse the cell has not yet reached as far with the process as the mother GCP had at the beginning of the time-lapse.

<u>Cell T2DC2 (Green arrows):</u>

A to C) It is difficult to trace the morphology of this cell before division because it is closely associated with another cell. **D)** The cell can be seen rounding up and **F)** within two hours divides in a parallel orientation. The daughter cells can be seen extending very small processes in multiple directions for the next few hours. At the end of the time-lapse, **I)** One daughter cell extends a longer process towards the inner EGL, and the other can be seen starting to extend a similar process as well.

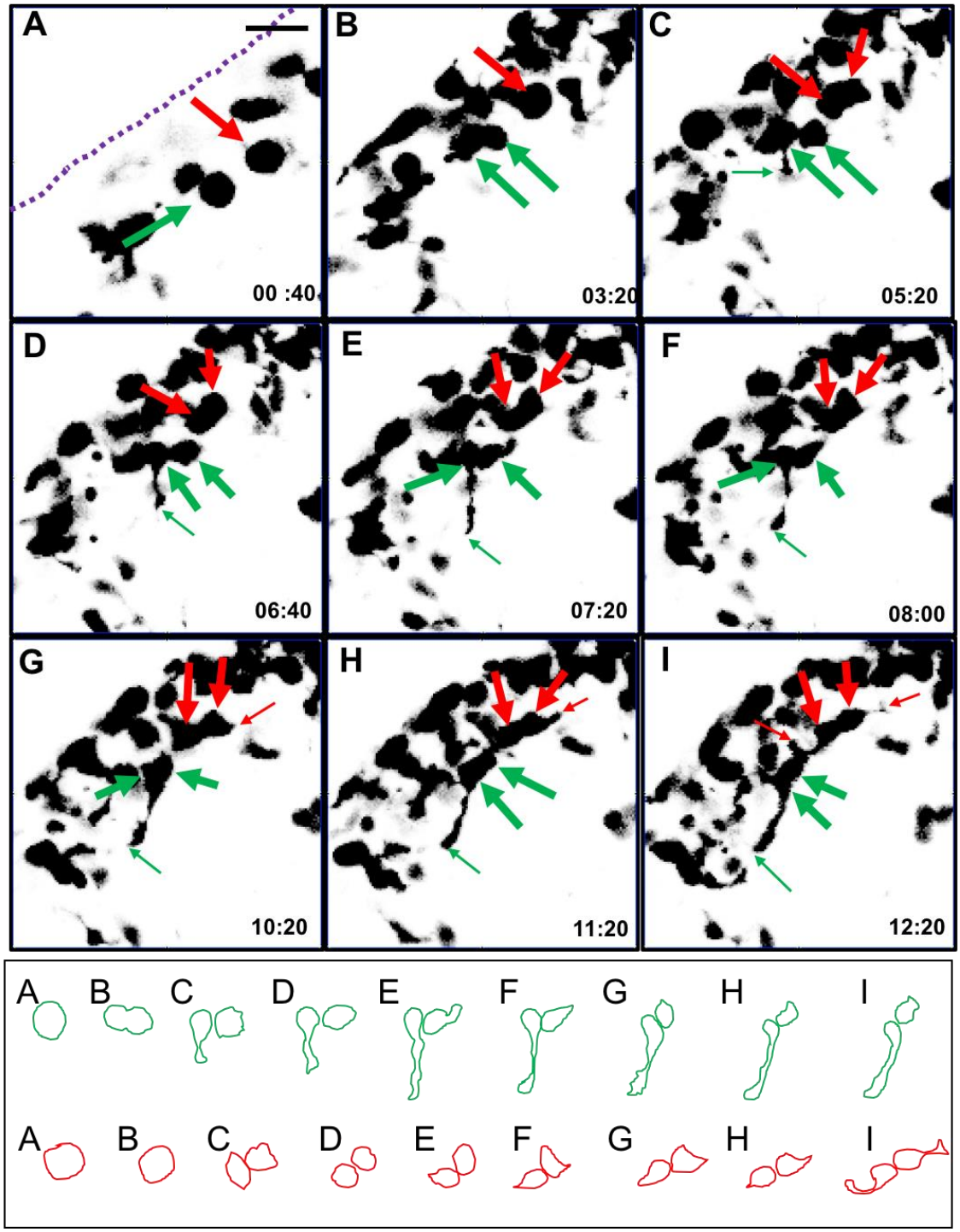

Figure 3-5 Characterization of the dividing granule cell precursor T2DC3 and T2DC4 *(next page)*

Previous page:

Figure 3-5 Characterization of the dividing granule cell precursor T2DC3 and T2DC4

A selection of time-frames from the time-lapse movie of T1DC3 and T1DC4. Thick green arrows point to the cell T2DC3 and its daughter cells and the thick red arrows point to the cell T2DC4 and its daughter cells. The pial surface is delineated with a purple dotted line. Small red and green arrows point to the corresponding cell's processes. The panel **J**) shows a traced surface of each cell for visualisation.

Cell T2DC3 (Green arrows):

A) At the beginning of the time-lapse the cell is already rounded-up, therefore its transitions before division could not be observed. **B**) The cell divides parallel to the pial surface and **C**) one of the daughter cells can be seen extending a thick short processes towards the inner EGL in a radial fashion. **D-F**) The daughter cell continuously extends longer processes whereas the other daughter cell is seen extending a short protrusion briefly in the other direction, before retracting it and remaining process-less until the end of time-lapse. **G-H**) The cell with the process extends its process in a more tangential rather than radial direction, however movement of its cell body is not observed throughout the duration of the time-lapse.

Cell T2DC4 (Red arrows):

A) similarly to T2DC3, this GCP can also be seen rounded up at the beginning of the time-lapse. **C**) It divides two hours after cell T2DC3, also parallel to the pial surface. **D-H**) Throughout the time-lapse imaging, both daughter cells remain close to each other and can be seen extending very short processes in multiple directions, however none of these processes extend far or develop identifiable growth cones. **I**) Towards the end of the time-lapse, the daughter cells extend longer processes in the opposite directions.

Scale bar = 20μm

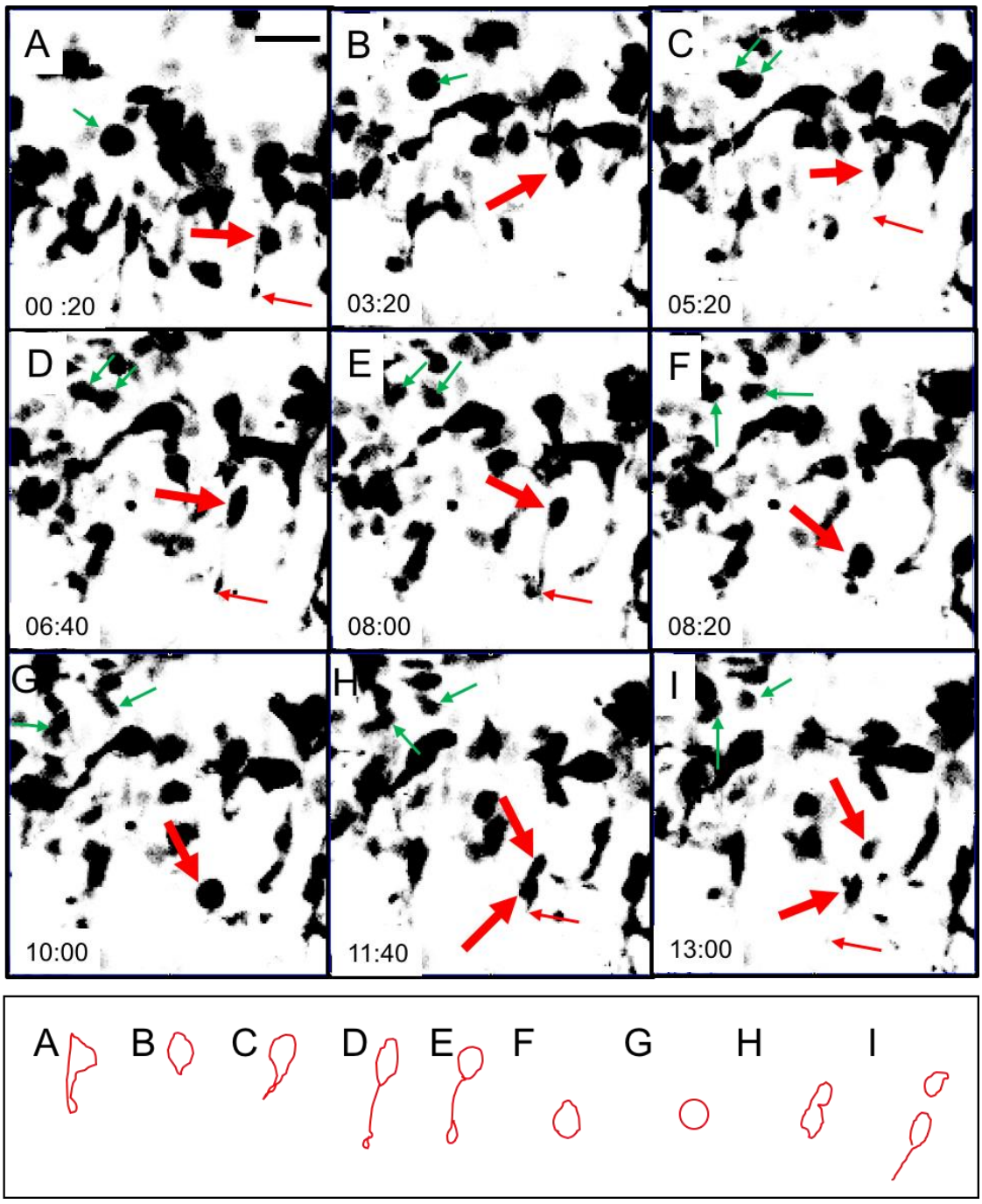

Figure 3-6 Characterization of the dividing granule cell precursor T1DC7

(next page)

Previous page:

Figure 3-6 Characterization of the dividing granule cell precursor T1DC7

A selection of time-frames from the time-lapse movie of T1DC7. Small red arrows point to processes that extend from the cell body. Thick arrows point to the cell of interest and its two daughter cells after division. The purple dotted line shows the position of the pial surface (out of frame for this cell). The green arrows point to a cell presumably from the same clone that divides during the time-lapse. The images are altered to be overexposed as the cells analysed had low fluorescence levels. The panel **J**) shows a traced surface of each cell for visualisation.

A) The cell is located in the inner EGL and has a short, thick process extending towards the IGL. **B**) This process seems to be retracted and **C**) a thinner, shorter process is extended in its place. **D and E**) The process extends further towards the IGL and the cell body elongates. **F**) Within 20min the cell body migrates the length of the process. **G**) Within two hours the cell body rounds up and **H**) seems to divide 1.5hrs afterwards in a perpendicular plane of division. **I**) One of the daughter cells moves slightly towards the direction of the oEGL whilst the other extends a small process further into the IGL.

Scale bar = 20μm

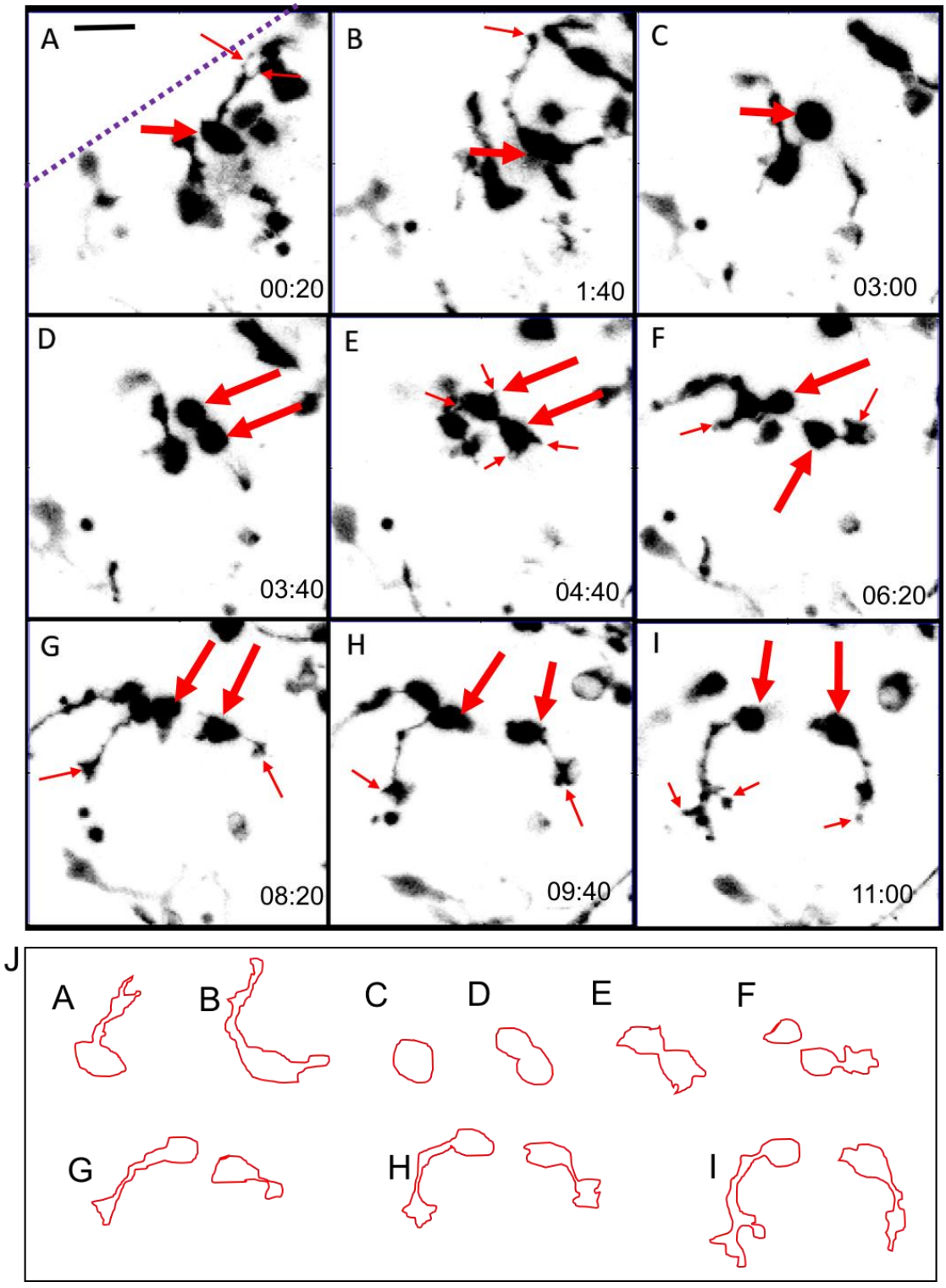

Figure 3-7 Characterization of the dividing granule cell precursor T3DC1

(next page)

Previous page:

Figure 3-7 Characterization of the dividing granule cell precursor T3DC1

A selection of time-frames from the time-lapse movie of T3DC1. Small red arrows point to processes that extend from the cell body. Thick arrows point to the cell of interest and its two daughter cells after division. The purple dotted line shows the position of the pial surface. The panel **J**) shows a traced surface of each cell for visualisation.

A) At the beginning of the time-lapse the cell can be seen extending a thick long process towards the pia that bifurcates at the tip into two short thin processes. **B**) The cell body is seen moving slightly inwards, toward the inner EGL, before the cell body returns to the starting position and **C**) retracts is processes. **D**) the cell divides perpendicularly to the pial surface and **E-G**) the two daughter cells migrate away from each other before **H-I**) both facing the inner EGL direction. The daughter cells extend thick and long leading processes with pronounced structures at the tips that resemble growth cones.

Scale bar = 20μm

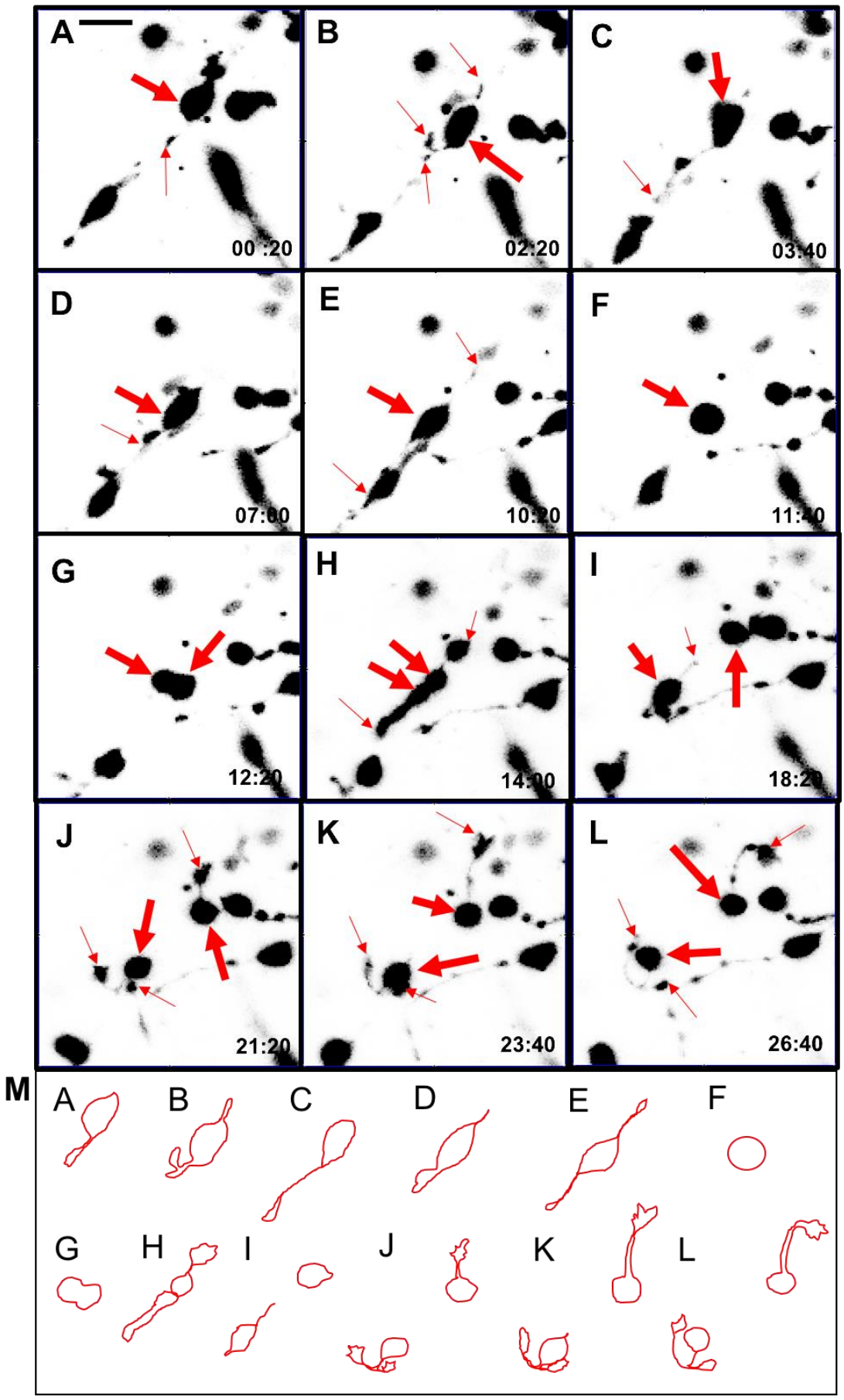

Figure 3-8 Characterization of the dividing granule cell precursor T4DC1

(next page)

Previous page:

Figure 3-8 Characterization of the dividing granule cell precursor T4DC1

A selection of time-frames from the time-lapse movie of T4DC1. Small red arrows point to processes that extend from the cell body. Thick red arrows point to the cell of interest and its two daughter cells after division. The panel **M**) shows a traced surface of each cell for visualisation.

A) At earliest observation the cell is extending one leading process. Whether it has a trailing process cannot be determined due to obstruction from another cell. **B**) Within 2 hours, the cell has migrated a small distance in a transverse direction and extends two small, thin processes. The leading process seems to bifurcate and a growth cone is visible at the tip of one of the processes. **C**) The cell continues to extend its leading process, which has become longer and thinner. **D**) The cell has migrated further, and extends a thicker and shorter process. **E**) Within 3 hours the cell once again shows two long, thin processes from both sides prior to **F**) the cell retracting all processes and rounding up for cell division. **G**) within an hour of division, the cell divides perpendicularly to the pial surface. **H**) Both daughter cells extend their own processes in the opposite directions. One daughter cell extends a process with a very broad growth cone, whereas the other daughter cell has a longer and much thicker process. **I**) The daughter cells separate from each other as each migrates in a different direction. **J-L**) One of the daughter cells seems to extend two processes in a T-shaped manner, resembling formation of parallel fibres. The other daughter cell extends a long process towards the pial surface with a large, very motile growth cone. At the end of the time-lapse, the cell seems to reverse its process slightly.

Scale bar = 20μm

3.2.3 Proliferative granule cell precursors can extend long and elaborate processes before division

Many dividing cells observed via this protocol underwent extensive morphological changes both before and after cell division. **Figure 3-9** shows the transitions of five example cells prior to division. The cells extended elaborate processes in multiple directions that are retracted prior to division, at which point all dividing precursors observed had a completely round morphology (see section 3.2.5). After division, the daughter cells extended processes usually within two hours after mitosis and generally migrated in opposite directions from each other (see section 3.2.8).

Each observed cell displayed a different sequence of morphological changes prior to division and extended varying number of processes into different directions (**Figures 3-2 to 3-8)**. For example, cell T1DC1 probably went through the most diverse morphological transitions seen during my project. The cell has extended and retracted up to 5 different processes at a time (**Fig 3-2 F**) and the processes continuously changed their shape, length and thickness. Other cells, for example cells observed in Tissue 2, have relatively lower number and motility of their processes.

The dividing granule cell precursors observed in this study had extended processes ranging from negligible length to 38.50μm in length. The number of processes extended at any one point ranged from 1 to 5. Some processes resembled leading processes with distinctive filopodia and lamellopodia at the growth cone, whereas others looked thin and 'axon-like'.

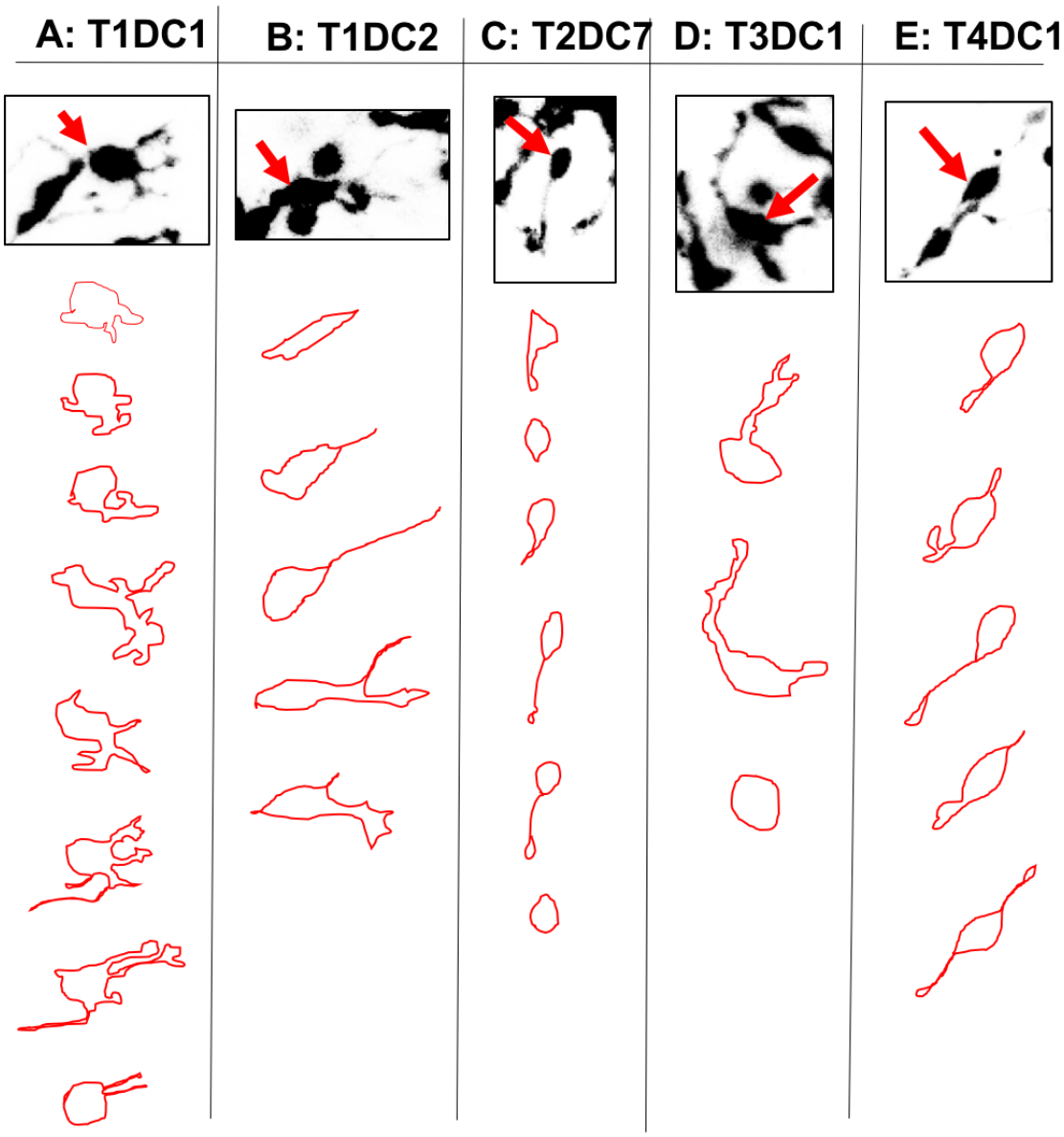

F

Cell	Max process length in µm	Max process number
T1DC1	36.50	5
T1DC2	30.15	2
T2DC7	23.56	1
T3DC1	30.96	2
T4DC1	38.50	2

Figure 3-9 Proliferative granule cell precursors can extend long and elaborate processes before division *(next page)*

Previous page:

Figure 3-9 Proliferative granule cell precursors can extend long and elaborate processes before division

A to E) A selection of 5 cells that showed interesting morphological transitions before division. Each cell is shown in a panel and its transitions are shown through the traced surfaces for clarity. **F**) The maximum length of the process of each cell, and the maximum number of processes extended by each cell at a time is summarised in the table.

A) Cell T1DC1 showed the most interesting morphological transitions of all imaged cells, having up to 5 extended processes at any one time. Additionally, the processes were very motile, changing their length, thickness and direction constantly.

B) Cell T2DC2 was a migratory cell and extended a long trailing process. The cell then extended another process, moving its cell body slightly in the same direction, before retracting both processes for division.

C) Cell T2DC7 is the only cell that could be seen migrating radially towards the inner EGL before division. It extended at first a short thick process, which it then retracted and followed with a long, thin process with a growth cone at the tip. The cell then migrated along the path of the processes and rounded up and divided within the inner EGL.

D) Cell T2DC1 was the only cell that could be seen extending a thick process towards the pial surface. It also briefly extended another short protrusion from the opposite side of its cell body, but retracted both processes before cell division.

E) Cell T4DC1 is also seen migrating tangentially a short distance and extending two long and thin processes from its cell body in opposite directions (one leading, one trailing).

3.2.4 Proliferative granule cell precursors can be highly motile and undergo tangential- and radial-like migration before division

A proportion (4/13) of granule cell precursors observed in the time-lapse movies underwent short migratory movements, sometimes changing direction, before retracting all processes and undergoing mitosis. The cell bodies of these migratory cells were spindle-shaped and elongated, as reported for tangentially migrating granule cells in other studies (e.g. Nakashima et al., 2015). The migratory movements were short and never exceeded around 20μm.

T1DC2 (**Fig 3-3**) exhibits clear migratory behaviour before it divides. The cell body is elongated as it migrates a short distance (A-P) (**Fig 3-3A**), before it briefly reverses the direction of its cell body movement, which is followed by rounding up and subsequent cell division. T4DC1 shows an even more pronounced migratory behaviour: long horizontal processes extended in both directions as during tangential migration and even further migration of its cell body. The cell then retracts its processes, rounds up, and divides.

Interestingly, one observed cell underwent a presumed cell division after displaying radial-like migration towards the Purkinje cell layer. The cell, T2DC7 (**Fig 3-6**), extends a long process (23.56μm) towards the ventral cerebellar tissue, followed by a radial migration of its cell body and a clear parallel division within the inner EGL. The cell appears to belong to a separate clone of GCPs to the other cells discussed within Tissue 2 (T2DC1-6). The cell is much less bright than other cells, but resembles in brightness other cells in its surroundings that also seem to divide within a similar time scale to T2DC7. One such cell can be seen in **Fig 3-6** (labelled with green arrows). However, they are not discussed further due to their low fluorescence and hence decreased suitability for morphological analysis.
Not all GCPs observed showed this same migratory behaviour of their cell bodies. In fact, the majority of observed GCPs maintained their cell bodies in a relatively stationary position, even if they expanded processes before division. Some cells showed only a very slight movement of their cell body (e.g. T1DC1) and therefore are not considered migratory.

3.2.5 Granule cell precursors retract their processes and round up their cell bodies prior to cell division

As **Figure 3-10** illustrates, each GC observed in this study retracted all of their processes and rounded up their cell bodies prior to cell division. The cells about to enter cytokinesis were therefore easily identifiable by their large and nearly perfectly round morphologies in the time-lapse movies. All cells with such round morphologies progressed to division. Similarly, no cell was seen dividing without having gone through this rounding-up process. It is possible that some cells leave behind very thin retraction fibres after retracting their processes, which could then be preferentially explored by the daughter cell after division. For example, cell T1DC1 can be seen rounding up (**Fig 3-2H**) but there are very thin fibres still visible extending from the cell body. They seem to disappear nearly altogether (**Fig 3-2I**), however if the brightness and contrast are manipulated on the original image, very faint processes can still be detected (**Fig3-10Aii**). The resolution power of the confocal microscope used however did not allow for a detailed analysis of these processes. **Fig 3-2L** shows that one of the daughter cells seems to extend its own processes from a similar location as the mother cell, suggesting that these retraction fibres might guide the cell division orientation and the migration of the daughter cell post division (Fink et al., 2011).

Next page:

Figures 3-10 Granule cell precursors retract their processes and round up their cell bodies prior to cell division

This figure contains a collection of examples of imaged GCPs at the time of their preparation for division, at a time point before two distinct daughter cells were visible. **A**) Shows the cell T1DC1 localisation in the tissue. **Ai**) shows an enlarged section of the picture to show the morphology of the cell clearly. **Aii**) shows the same cell as in Ai, but after manipulating the image by increasing brightness and contrast to show the possible remnants of the two processes previously extended from the cell body (red arrows). **Aiii**) shows the outline of the dividing cell and its positions within the tissue. **B-D** display other examples of rounding up of cells before division. All observed cells undergo this morphological transition at mitosis.

Cell	Image
Cell **T1DC1**	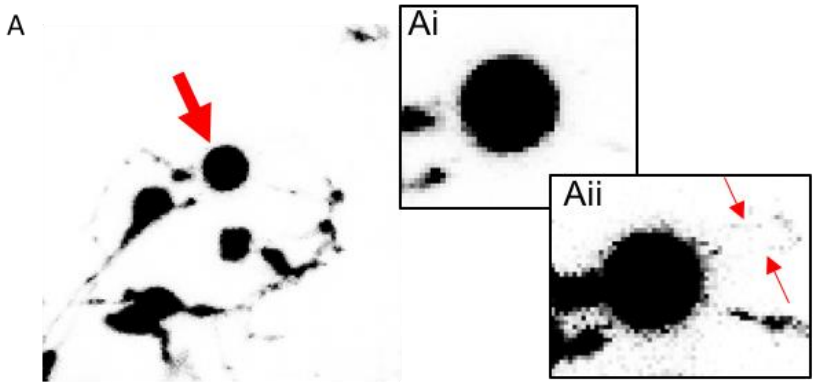
Cell **T1DC2**	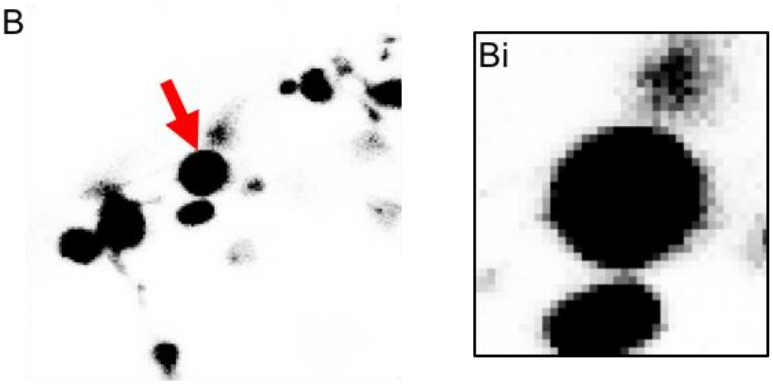
Cell **T2DC1** and **T2DC2**	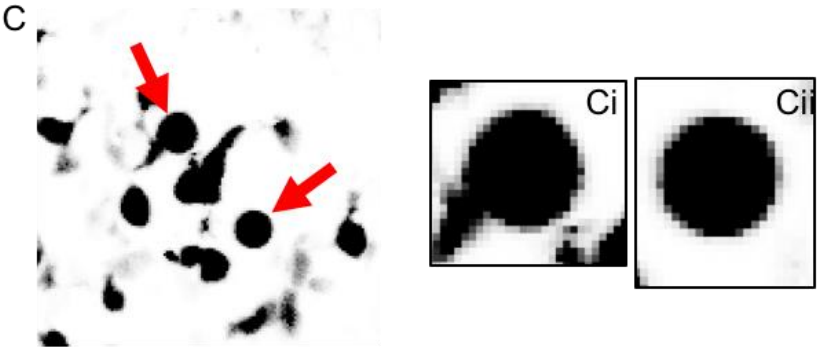
Cell **T2DC3** and **T2DC4**	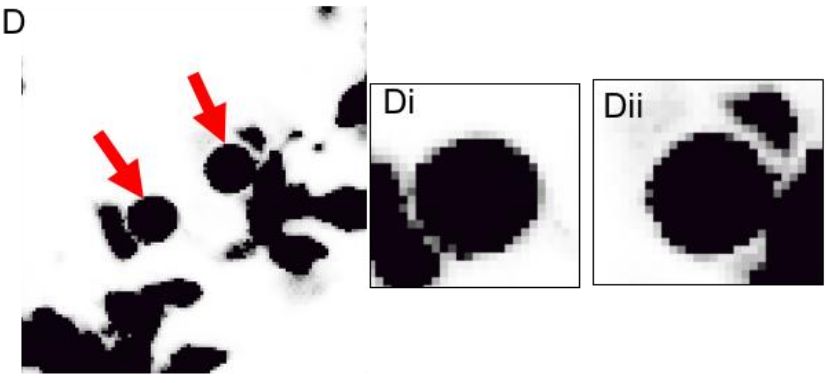

Figure 3-10 Granule cell precursors retract their processes and round up their cell bodies prior to cell division *(previous page)*

3.2.6 Granule cell precursors often divide in spatial proximity to other proliferative granule cell precursors

Possible coordinated divisions were observed during live imaging of GCP divisions. **Figure 3-11** groups all cells observed to be dividing next to or close to another dividing GCP. In total, 5 instances of such divisions were found and the cells were either touching or up to 30.45μm apart.

Cell T1DC2 found in Tissue 2 is one of three GCPs that divide within 3 hours of each other in spatial proximity. **In Fig 3-11A**, cell 1 divides first and as it divides it is in very close contact, presumably touching, cell 2. Cell 2 and cell 3 later divide at the same time, three hours after cell 1 completed its division. Slightly further away from cell 3, there are two other dividing GCPs that are not analysed in detail in this report due to their obstructed morphologies, however, they can be clearly seen dividing at similar times to cells 1-3. For illustration purposes, one of the cells, cell 4, is seen rounding up at the same time as cell 3 and divides 2 hours after (**Fig 3-11Aiii**). However, because it is at a relatively much longer distance (90.82μm) than all other cells, it was not considered proximal. Nevertheless, its presence and time of division suggest that all five cells from **Fig 3-11A** might be clonally related.

The cells found in Tissue 2 all seem to undergo synchronous divisions with their close neighbours, as the three pairs of cells (T2DC1 and T2DC2; T2DC3 and T2DC4; T2DC5 and T2DC6) all divide within 2 hours of each other. Cells T2DC5 and T2DC6 seem to be touching prior to division whereas T2DC1 and T2DC2 are 30.45μm apart and cells T2DC3 and T2DC4 are 21.08μm apart.

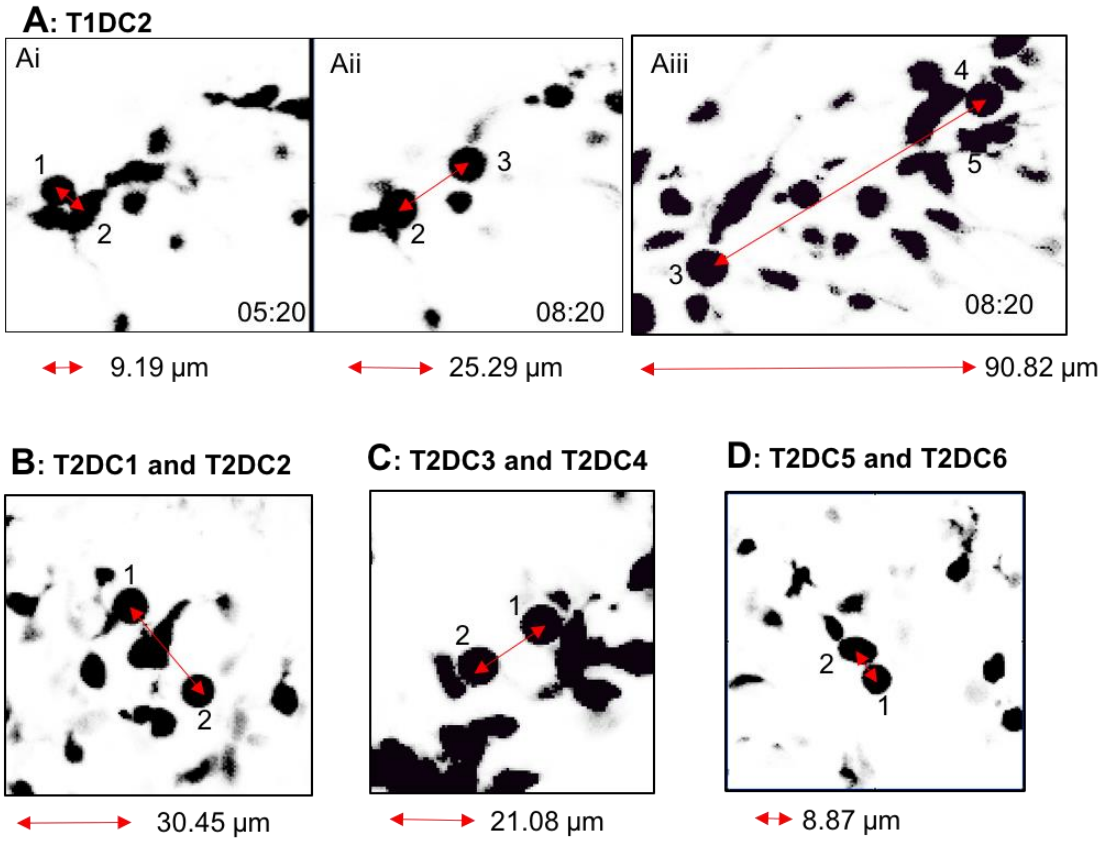

E

	Time of division			
Cell	Cell 1	Cell 2	Cell 3	Cell 4
T1DC2 +2 cells	05:20	08:20 (+03:00)	08:20 (+00.00)	10:20 (+02:00)
T2DC1 T2DC2	05:40	06:40 (+01:00)		
T2DC3 T2DC4	03:20	05:20 (+02:00)		
T2DC5 T2DC6	03:00	04:20 (+1.40)		

Figure 3-11 Granule cell precursors often divide in spatial proximity to or after touching other proliferative granule cell precursors *(next page)*

Previous page:

Figure 3-11 Granule cell precursors often divide in spatial proximity to or after touching other proliferative granule cell precursors

Granule cell precursors that divide often do so close to other dividing granule cell precursors. At least five such instances were observed. In **A,** cells 1, 2 and 3 divide sequentially within three hours of each other*. **Ai**) Firstly, cell 1 divides 9.19μm from cell 2. **Aii**) After 3 hours, cell 2 divides at the same time as cell 3, which is 25.29μm away. **Aiii**) Other cells are seen dividing in proximity to these three cells, such as cell 4 and 5 Cell 4 divides 2 hrs after cell 3. However, the distance between cell 3, and 4 and 5 is comparatively much greater (90.82μm) and therefore is not considered to be in close proximity. However, all those cells can potentially belong to the same GCP clone labelled at the rhombic lip.

In **B,** cells T2DC1 and T2DC2 divide within an hour of each other and they are located 30.45μm from each other. In **C,** cells T2DC3 and T2DC4 divide within two hours of each other and are located 21.08μm from each other. In **D,** cells T2DC5 and T2DC6 divide less than 2 hours from each other and are so close (8.87μm) that they are touching. **E**) A table that summarizes the time between divisions of the cells in the same location. The time in the movie at which the dividing cell was first seen as two separate cells was noted as the time of division.

* T1DC2 is one of the cells analyzed in detail in the report and corresponds to cell 2 in the figure. Cells 1,3,4 and 5 were seen dividing during the time-lapse movie but were not analysed in detail and hence do not have a separate name assigned to them.

3.2.7 Granule cell precursor divisions can be perpendicular or parallel to the pial surface

Granule cell precursors observed in the live-imaging movies divided in two characteristic ways: with their plane of division either parallel, or perpendicular to the pial surface. Cell divisions were considered parallel if the plane of division was between 0 and 45 degrees and perpendicular if the plane of division was between 45 and 90 degrees. Both types of divisions have been implicated in different types of modes of divisions, with parallel divisions correlated with differentiative divisions and perpendicular divisions corresponding to more proliferative divisions (Haldipur et al., 2015b). **Figure 3-12** shows four examples of each type of division and **Fig 3-12B** collects the type of division of each dividing cell seen in the movies. By counting the numbers of parallel and perpendicular divisions it has become clear that perpendicular divisions were more common. 64% of cells (9/14) have gone through a perpendicular division mode compared to 36% (5/14) of cells which divided parallel to the pial surface (**Fig 3-12C**).

Next page:

Figure 3-12 Granule cell precursor divisions can be perpendicular or parallel to the pial surface with a bias towards parallel division plane

Granule cell precursors undergo two types of divisions- parallel and perpendicular to the pial surface. Cell divisions were considered parallel if the plane of division was between 0 and 45 degrees. Cell divisions were considered perpendicular if the plane of division was between 45 and 90 degrees. Table **A** shows four examples of each type of division. The plane of division is depicted with a red line. The pial surface is shown with a purple dotted line. Table **B** shows all cells analysed and what plane of division was observed. Percentage of perpendicular and parallel divisions are shown in the pie chart in **C**. Parallel divisions are more frequent with 64% of observed cells undergoing parallel divisions compared to 36% of cells that undergo perpendicular divisions.

A

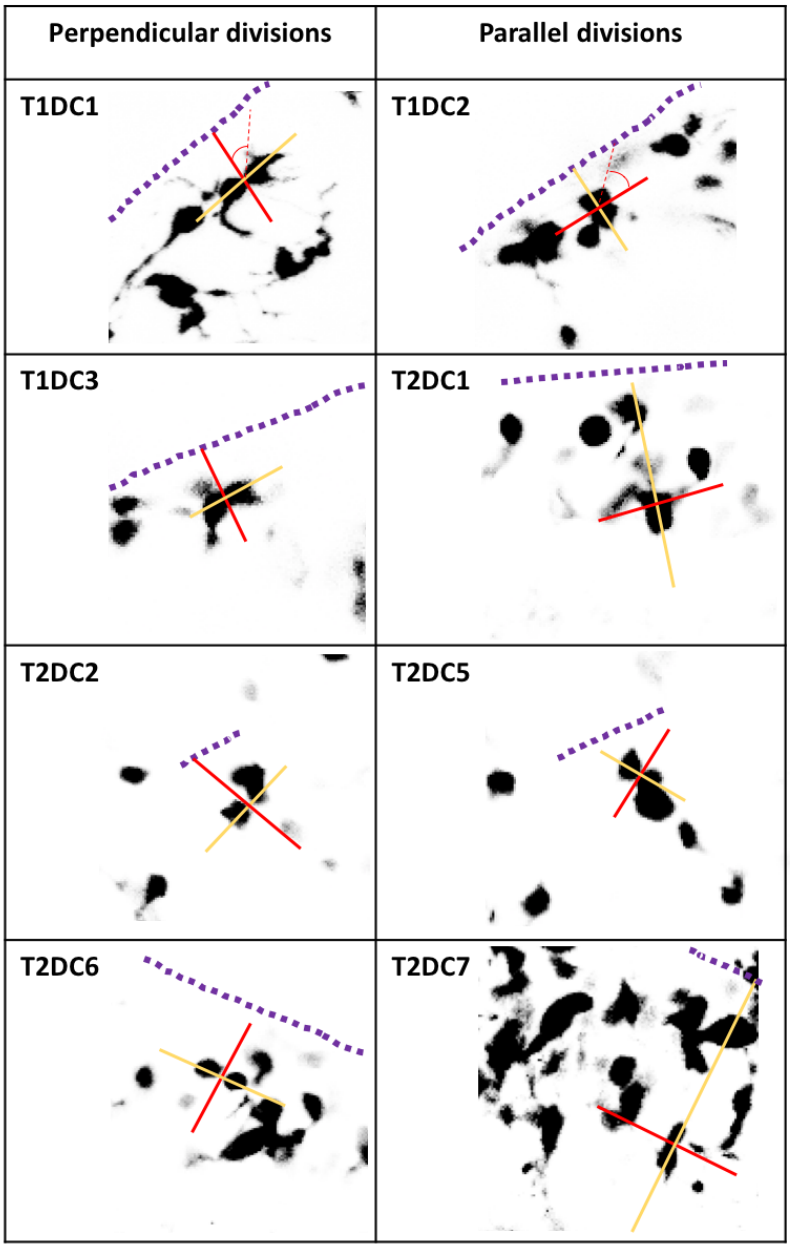

B

Cell	Division
T1DC1	Perp.
T1DC2	Parallel
T1DC3	Perp.
T1DC4	Perp.
T2DC1	Parallel
T2DC2	Perp.
T2DC3	Perp.
T2DC4	Perp.
T2DC5	Parallel
T2DC6	Perp.
T2DC7	Parallel
T2DC8	Perp.
T3DC1	Parallel
T4DC1	Perp.

C

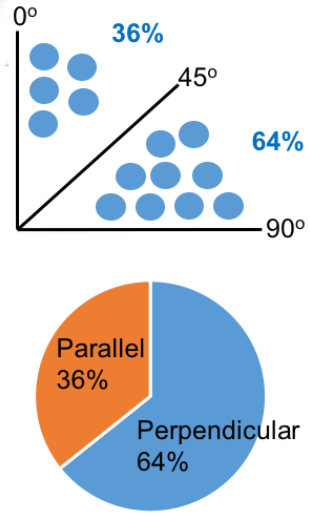

Figure 3-12 Granule cell precursor divisions can be perpendicular or parallel to the pial surface with a bias towards parallel division plane *(previous page)*

3.2.8 Daughter cells of granule cell precursors tend to migrate in opposite directions after division

In the majority of instances, it was possible to trace the behaviour of the daughter cells for a few hours following GCP division. As shown in **Figure 3-13**, after most divisions, daughter cells tended to orientate and move in opposite directions. Some daughter cells that that were traced for longer time periods seemed to migrate far away from each other. For example, after cell T3DC1 divided, the daughter cells migrated in opposite directions. One of the daughter cells migrated in a radial direction, towards the inner EGL, whereas the other one extended a leading process along the pial surface in an A-P direction before also turning radially (see **Fig 3-7** and **Fig 3-13**). For many other cells, the time-lapse finished before it was possible to see what happens to the daughter cells in the long term. However, most cells seem to share this characteristic of extending processes in opposite directions after division. For example, cell T1DC1 and T1DC3 and T4DC1 clearly exemplify this behaviour.

Nevertheless, not all GCPs divided and migrated in opposite directions. In fact, cell T1DC2 divides into two daughter cells, which both appear to undergo a slight radial migration, followed by tangential migration in a similar direction (see **Fig 3-3** and **Fig 3-13B**). Cell T2DC6 also produces two daughter cells that migrate radially in the same direction.

Cell	Just after division	At the end of time-lapse	Direction of leading process
T1DC1	Ai 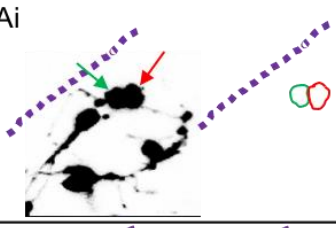	Aii 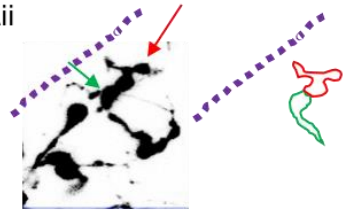	Aiii 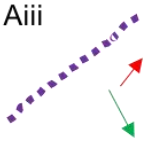
T1DC2	Bi 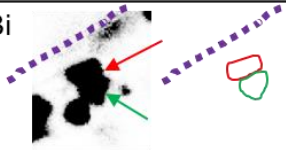	Bii 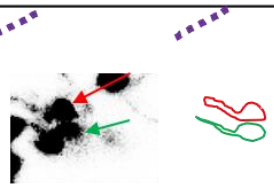	Biii 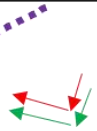
T1DC3	Ci 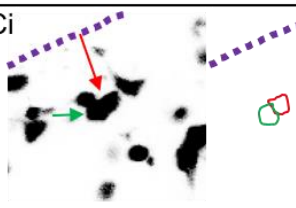	Cii 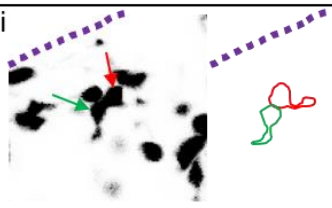	Ciii 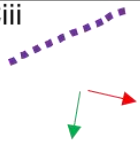
T2DC4	Di 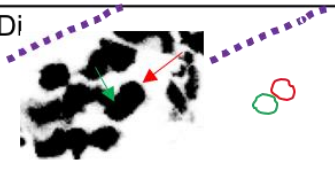	Dii 	Diii 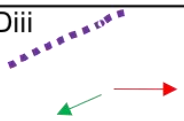
T3DC1	Ei 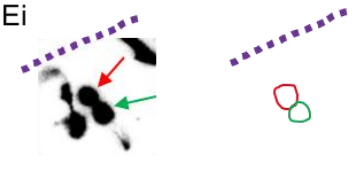	Eii 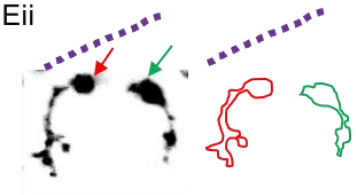	Eiii 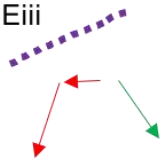
T4DC1	Fi 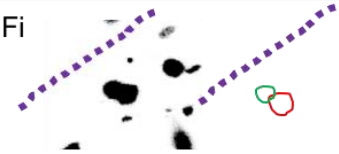	Fii 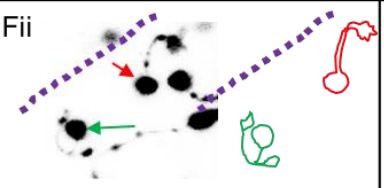	Fiii 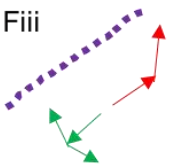

3-13 Daughter cells of granule cell precursors tend to migrate in opposite directions after division *(next page)*

Previous page:

3-13 Daughter cells of granule cell precursors tend to migrate in opposite directions after division

Images of daughter cells from dividing GCPs were collected at the end of their respective time-lapse to examine in which direction the daughter cell migrated or extended a process. Most daughter cells can be seen extending a process in the opposite directions. Cells T1DC3(**Cii**) and T2DC4 (**Dii**) both show extended processes extending from the cell body. Cells T3DC1 (**Eii**) and T4DC1 (**Fii**) have migrated away from each other and extend long and elaborate processes facing away from one another. T3DC1 daughter cells extend their process in the same general direction (radially) but it is difficult to predict how the cells would later migrate. Cell T4DC1 clearly shows that the daughter cells migrated far away from each other and one started to differentiate into a T-shaped cell, whereas the other has a long process with a pronounced growth cone. One cell, T1DC2 (**Bii**) generated two daughter cells which migrated in a similar general direction, first going through a short radial migration, followed by a tangential like extension of processes and migration.

3.3 Discussion

In this chapter, I have demonstrated that GCPs are able to extend elaborate processes and undergo short migratory movements before cell division, which preferentially happens perpendicular to the pial surface. I have shown that GCPs always retract their processes, and round up their cell bodies prior to cytokinesis. Additionally, I observed that the daughter cells of dividing GCPs generally migrate in opposite directions after division. Results suggest that clonally related GCPs (which are located in spatial proximity within the tissue) may display temporally synchronised divisions.

3.3.1 Technical limitations of the study

During my attempts at observing dividing GCPs in cerebellar tissue, it has become apparent that a very careful and strict protocol is required for successful experiments. I have performed a large number of time-lapse movies (>25 attempts), but only around 5 movies contained dividing GCPs. As I progressed, I became better at understanding the requirements of a successful experiment, however, it should be noted that imaging dividing GCPs *ex ovo* is technically challenging. During my project I tested different culture media and have found that the medium described in the methods section works best. Interestingly, when using neurobasal media I failed to observe any noticeable movement of the cells, and no divisions. Basal Medium Eagle allowed for much more interesting morphological transitions of cells, including long migratory movements of some, presumably differentiated granule cells, in the tissue. It is possible, however, that further optimisation and a different media formula could have improved longevity of proliferation.

Another major improvement to my protocol would involve installing an environmental chamber maintained at 37 degrees Celsius with constant gas flow to the tissue during imaging. Such protocol requirements seem essential when imaging live mammalian tissue as they increase the viability of the tissue. Chicken tissue has proven to be much more robust during handling and live imaging as

cells divided and migrated even at room temperature and in a sealed chamber with no gas exchange.

To avoid phototoxicity, I endeavoured not to overexpose the cells to the laser light and hence I minimised the exposure time of the tissue to the laser light, which resulted in poorer resolution of images. From the previous chapter, it is clear that the morphological changes that GCPs undergo are much more intricate than the images obtained in this part of the project. For example, the rounding up of cells I see in my movies may correspond to cell morphologies resembling those in Chapter 2 Fig 2-12, however such thin processes are difficult to see in the live-imaging data.

Another important consideration is that the cerebellar tissue used for imaging was sectioned in a sagittal orientation. GCPs normally differentiate and migrate in the medio-lateral axis (M-L) of the cerebellum. With a sagittal sectioning, I cut through the already formed parallel fibres of the postmitotic granule cells located in the IGL and the inner EGL, as well as block the normal migratory route of newly differentiated granule cells. I do observe some presumably newly differentiated GCs undergoing long transverse migrations through the anterior-posterior extent of the cerebellum in my tissue. However, this migration behaviour is forced upon the GC due to the M-L path being unavailable.

In many movies, it was difficult to observe GCPs morphological transitions completely unobstructed by other labelled cells, which resided nearby or migrated next to the cell of interest. This became an issue when trying to trace reliably some of the transitions of specific GCPs. For example, it is very difficult to trace the daughter cells of the cell T1DC2 because of other cells located next to it. For some cells it was necessary to very carefully go through every Z layer at each time-point to ascertain which process belongs to which cell, although sometimes this was not possible. For example, **Fig 3-3I** shows one of the daughter cells as a round cell with no processes, it is possible that a short process was indeed present, however if this is the case, it is obstructed by the surrounding cells. Some dividing cells were more difficult to analyse than others and hence to minimise confusion I decided to only analyse the cells whose morphologies were most clearly visible. This creates a

possibility that I have missed an important morphological transition or an interesting feature of GCPs. Ideally, a sparser electroporation could solve this problem. On the other hand, it reduces the probability of a labelled cell going through division during the time-lapse. Moreover, clones of a single GCP seem to reside close together in the tissue and hence cell-dense locations in a tissue might be unavoidable.

3.3.2 Proliferating granule cell precursors are morphologically diverse and undergo unexpected morphological transitions

Based on available literature regarding granule cell precursors, as summarised in Table 2-1, one could be excused for thinking that they are morphologically uniform, polyhydral, densely-packed population of cells that do not do much except divide symmetrically into new GCPs. The only time those cells extend a process, it would seem, is when they have made the decision to differentiate into a mature cell and start a descent into the inner EGL, and later into the IGL. However, in the previous chapter, as well as in this chapter, I present a rather different view of GCPs as highly motile, transformative cells that constantly explore their environment; as cells which can divide in all layers of the EGL, even after undergoing migratory movements normally considered a feature of differentiated granule cells.

Based on my time-lapse imaging movies, most cells that could be seen dividing had gone through interesting morphological transitions prior to division (**Fig 3-9**). GCPs not only extend elaborate and numerous processes in several directions, but are also capable of short migratory movements in tangential, as well as radial directions. These results represent a novel finding about the mitotic potential of GCPs during cerebellar development as neuronal migration is usually associated with postmitotic neurons only.

3.3.3 Proliferating GCPs do not have an identifiable attachment to the basal lamina and can divide deep within the EGL

As shown in the previous chapter, based on imaging of fixed tissue, GCPs can be seen dividing in all layers of the EGL. Even though in fixed tissue some GCPs can be seen attached to the pia with a short, thick process, few cell with such morphology co-label with PH3 antibody, suggesting that GCPs do not need an attachment to the pia for mitosis. However, one possibility to explain this observation is that GCPs only need a brief attachment to the basal membrane before they enter division, but they always retract the basal process before initiating mitosis. However, I found little evidence for this in my time-lapse imaging. Most GCPs that divided never extended a process that would attach them to the pial surface before or during division. GCPs that divided in the middle or inner EGL did not possess such a process at all, and those that divided closer to the outer EGL can be seen rounding up for division without going through a basal processes extension phase.

One exception to this rule was cell T3DC1 (**Fig 3-7**), which migrated towards the basal surface and can be seen touching the pial surface with a process before it divides. At this point, the cell somewhat resembles the cells seen in fixed tissue, with a thick process that connects them to the basal lamina. However, this was the only cell observed to behave this way and it cannot be ascertained that the cell movements were non-random and whether the cell received any signalling cues from the basal lamina. The cell touching the pial surface might simply be an outcome of an apparently random migratory and process extension behaviour seen in other GCPs.

Considering all the evidence gathered in this and the previous chapter, I conclude that GCPs can divide without an attachment to the basal lamina, in contrast with some previous reports (Hausmann and Sievers, 1985). Based on a simple PH3 stain often employed in the study of the cerebellum, and considering the pattern of distribution of proliferating cells, it would be unreasonable to expect all the cells dividing in the deeper layers of the EGL to have long basal processes, as cells with such morphologies have never been reported and I also did not find any evidence for their existence. Therefore, the question of why a certain population of GCPs

have an attachment to the basal lamina is still open to investigation. However, all the evidence suggests that the reason is not that GCPs require this attachment to remain in a proliferative state.

On the other hand, I have not investigated the possibility that GCPs that undergo terminal symmetric divisions, as indeed I suspect most of the cells in my preparation to be subject to, might not need a basal attachment. Yet, cells undergoing proliferative symmetric divisions might still require a basal attachment. This possibility could only be explored if I used a differentiation marker in my study to distinguish between division modes (Nakashima et al., 2015).

3.3.4 Clonally related GCPs reside in spatial proximity and seem to undergo synchronised cell divisions

Recent papers on GCPs suggested that clonally related GCPs might exit the cell cycle in a synchronised manner. A seminal paper on GCP proliferative dynamics combined genetic mosaic analysis and EdU-labelling to estimate that each GCP in the EGL generates a median of 250 GCs by an average of 8 divisions (Espinosa and Luo, 2008). Additionally, it was suggested that clonally related GCPs exit the cell cycle and differentiate at a similar time. The authors also suggested that GCPs progressively slow down their cell cycle during postnatal development, before increasing it for the final terminal divisions. Other studies have also suggested that neurogenesis is associated with the shortening of the cell cycle (Arai et al., 2011). However, a more recent study by Nakashima et al., 2015 did not observe such shortening of the cell cycle length between proliferative and neurogenic divisions. However, the authors note that the cell cycle lengths of sibling GCPs were significantly closer than non-sibling GCPs. Additionally, 50% of the observed GCP pairs tended to enter the mitotic phase in approximate synchronisation. The authors observed that paired divisions happened within 28±15 min of each other.

In this study, cells that were in close spatial proximity to each other were also observed to be dividing in apparent synchronisation. However, I can only make inferences about the clonal relationship between those cells through their spatial

proximity, as I have not followed them since birth. If the cells shown in **Fig 3-11** are indeed clonally related, presumably even sister cells, they show a slightly longer deviation in the time of division than the published results, of up to 2 hrs for cells T2DC1-6. On the other hand, when considering the cell T1DC2 and its dividing neighbours I cannot be sure which cell is more likely to be the sister cell. Cell 1 (**Fig 3-3Ai**) divides 3 hrs before T2DC2 yet it is spatially closer to T1DC2. Cell 3 (**Fig 3-3Aiii**) divides at the same time as T2DC2, yet it is slightly further away. Moreover, cell 4 divides 2 hrs after cell 3 and hence could be considered a sister cell if it was closer to cell 3. In conclusion, I cannot assign with certainty any clonal relationships between cells and cannot claim that any two cells are sister cells derived from a common GCP. From previously published studies on granule cell clones migration patterns (Ryder and Cepko, 1994) it can be inferred that GCPs, which most likely correspond to the 'deep polyhydral cells' are located close to one another in any portion of the EGL and only migrate further away after the attain their bipolar, transversally migrating morphologies. Therefore, it is likely that the cells located closest to each other in my movies are in fact sister cells and for my analysis here I treat them as such while being aware of the technical limitations of methods used.

3.3.5 Outstanding questions and future studies

Because parallel and perpendicular divisions are considered to result in different fates of the daughter cells (Haldipur et al., 2015), I attempted to correlate the type of division with the morphologies of the daughter cells in terms of their behaviour after division. However, it became apparent that I do not have enough information in my experimental set-up to make decisions on whether a cell was dividing symmetrically, asymmetrically or terminally. Most cells extended variable processes after mitosis, after both types of divisions. For example, T1DC2 resulted in two small, migratory cells that both migrated in a similar direction and extended leading processes. None of these cells looked classically like a GCP and if I had to make a judgement, I would consider their division as terminal symmetric. According to the literature, their parallel division would be more likely to be a neurogenic division.

Therefore, I decided to leave the question of whether parallel and perpendicular types of division result in different GC fates open for further experimentation, preferably at a time when a differentiation marker was available. Such a marker would work in a similar fashion to the doublecortin gene (Yang et al., 2015 and Nakashima et al., 2015). Unfortunately, I was not in possession of the construct or any similar one that would serve the same purpose. Using the doublecortin enhancer construct (Nakashima et al., 2015) or another differentiation marker would allow me to answer a number of interesting questions such as:

- What are the division modes I see in my movies? Do I see any symmetric proliferative divisions, or are they all symmetric terminal? Can I spot any asymmetric divisions in my set-up?
- What are the morphological changes that GCPs undergo before different types of division? For example, do GCPs that undergo proliferative divisions differ in their morphological transitions from GCPs that undergo terminal divisions?
- Are divisions in different layers of the EGL different? For examples, are proliferative divisions always localised to the outer EGL, and terminal divisions localised to the middle and inner layers?
- Do different division planes correspond to different fates of the daughter cells? For example, in a parallel division, does the basal cell go on to become a proliferating GCP whereas the more apical daughter cell differentiates as a neuron?

A further limitation of my approach was the inability to distinguish between different clones of GCPs labelled at the rhombic lip. The only indication of some GCPs belonging to a different clone was the differences in the levels of fluorescence that I could notice in some cells. This effect presumably resulted from the different regions on the genome into which Tol2 sequences happened to integrate. The less bright cells might have the coding sequence of the transposon or the GFP inserted in an area of more ‘closed’ chromatin, resulting in lower transcription rates.

If I could distinguish between cells belonging to different original clones, I would be able to answer questions such as:

- Do clonally related GCPs enter mitosis at similar time-points?
- Do clonally related GCPs switch from a symmetric proliferative to terminal symmetric division mode at the same time?
- How far from each other can clonally related GCPs be positioned within the cerebellum? Can GCPs migrate far away from each other in medio-lateral direction before differentiation?

One of the available tools I could use to distinguish between different clones is the 'Chickbow' tool set, which has been shown to work well in the chicken nervous system (Hadas et al., 2014) and in the chicken cerebellum (T Varela, personal communication). The technique is a powerful genetic tool for labelling cells with multiple colours by expressing a random combination of fluorescent genes. This technique is based on the Brainbow method (Livet et al., 2007) and can be modified to drive expression of plasmids in specific brain regions, such as the Math1 positive rhombic lip derivatives. To obtain stable and clone specific expression of the Chickbow, the Piggyback transposon system can be used. This system would be ideal to answer the above posed questions on clonally related GCPs.

Chapter 4: NeuroD1 expression and function in the development of rhombic lip derivatives

4.1 Background

In the previous two chapters I characterised the morphological transitions of chicken cerebellar granule cell precursors (CGPs) in fixed and live tissues. I observed morphological changes that GCPs undergo during development, but it was not possible to identify the point at which a specific GCP initiates terminal differentiation. Therefore, in this chapter, I characterise the expression pattern and function of NeuroD1 gene on the development of rhombic lip (RL) derivatives, including granule cells, in the chick cerebellum. NeuroD1 has previously been shown to be expressed in differentiating GCPs. I take advantage of a NeuroD1 conserved non-coding element recently identified in the Wingate group (Butts et al., 2014) as a potential differentiation marker of granule cells. I also use a full-length NeuroD1 construct to misexpress the gene at different stages of GCP development to further elucidate its function in chicken GCP development. Additionally, I observe the effect of misexpression of NeuroD1 on other RL derivatives.

4.1.1 NeuroD1 as a neuronal differentiation factor

During neural development, different types of neurons are generated in different parts of the developing nervous system, depending on a range of genetic factors that influence fate specification. Proteins that belong to the basic helix-loop-helix (bHLH) class of transcription factors play a central role in determination of neuronal lineages, both in the peripheral nervous system (PNS), as well as in central nervous system (CNS). These proteins are able to regulate cellular specification in a cascade manner, which means that the expression of one TF activates the expression of other TFs that direct cell specification further. Their regulation can be negative or positive and they exert their control via DNA binding and HLH protein dimerization domains. NeuroD1 is a prominent member of this

family of proteins, belonging to the same subfamily of proneural bHLH proteins as Atoh1 (Math1 in mouse), the *Ath* group.

NeuroD1 was first cloned using the yeast-two-hybrid system by two independent laboratories, and was also named *BETA2* due to its ability to transactivate Beta cells. NeuroD1 is widely expressed in the pancreatic endocrine cells and other endocrine cells throughout development so it has wide ranging roles in the developing organism. Here, I will concentrate on its role in the nervous system.

NeuroD1 has been isolated as a neurogenic differentiation factor from frog and mouse embryos. In Xenopus embryos, NeuroD1 ectopic expression converts non-neuronal cells, such as epidermal cells, into neurons (Lee et al., 1995). These results suggested that NeuroD1 regulates the formation of neurons from both neural precursors and can also induce neurogenesis in non-neural tissue. Numerous *in vitro* experiments confirmed the role of NeuroD1 in neurogenesis. For example, expressing NeuroD1 along with other neuronal differentiation genes converts mouse P19 carcinoma cells into differentiated neurons (Farah et al., 2000) and transient expression in F11 neuroblastoma cell line can induce neurite outgrowth (Cho and Tsai, 2004). More recently, NeuroD1 together with Pou3f2, Ascl1 and Myt1l, was successfully used to reprogram fetal and postnatal fibroblasts into neurons (Vierbuchen et al., 2010). Moreover, it was able to convert reactive glial cells and human astrocytes into functional neurons (Guo et al., 2014). Therefore, NeuroD1 is a highly potent factor for promotion of neuronal fate.

NeuroD1 is widely expressed throughout the vertebrate nervous system. In the mouse CNS, NeuroD1 is highly expressed in postmitotic cerebellar granule cells, neurons of the inferior colliculus, the hippocampus and limbic system. In the PNS, NeuroD1 expression is found in developing and mature sensory neurons. Much research has been performed on the function of NeuroD1 in the ear development where absence of NeuroD1 leads to severe reduction of vestibular and cochlear neurons. In the cerebral cortex, NeuroD1 is expressed highly in the ventricular zone, upregulated several fold in the subventricular zone, and downregulated in the cortical plate (Pataskar et al., 2016).

An important recent paper investigated in detail the genomic targets of NeuroD1 and the mechanisms through which it mediates neurogenesis (Pataskar et al., 2016). The authors show that NeuroD1 directly binds regulatory elements of neuronal genes that are developmentally silenced by epigenetic mechanisms. NeuroD1 is able to initiate events that confer transcriptional competence, including reprogramming of transcriptional landscape, conversion of heterochromatin to euchromatin and increased chromatin accessibility. These results suggest that NeuroD1 is a "pioneer factor": a protein that is able to recognise and bind its target sites even if they exist in closed chromatin. Additionally, NeuroD1 only needs to be transiently expressed for its effects to be maintained via epigenetic memory. Interestingly, the genes activated by NeuroD1 were not only those classically involved in neuronal differentiation, but also those implicated in epithelial to mesenchymal transition. This suggests that NeuroD1 is also important for neuronal migration, as suggested for vestibulocochlear neurons previously (Kim, 2013).

4.1.2 NeuroD1 role in granule cell development

In the cerebellum, NeuroD1 expression has been correlated with the differentiation of GCs. In the mouse cerebellum, NeuroD1 is strongly expressed both in the EGL and IGL. Expression starts around postnatal day 5 in mainly the postmitotic granule cells in the EGL and stably persists throughout adulthood in the IGL cells (Miyata et al., 1999; Cho and Tsai 2006). Expression of NeuroD1 has been detected in mitotically active cells (Lee et al., 2000), however NeuroD1 is most often considered to be a postmitotically expressed gene (Miyata et al., 1999, Cho and Tsai, 2006, Borghesani et al., 2002, Haldipur et al., 2015).

Regardless of its precise expression, NeuroD1 is necessary for normal granule cell development. A number of NeuroD1 KO mice have been generated to test NeuroD1 requirement in neural development (Miyata et al., 1999, Cho and Tsai, 2006, Schwab et al., 2000, Pan et al., 2009). Each mutant mouse shows a pronounced loss of cerebellar granule cells when NeuroD1 is removed prior to GC differentiation. Additionally, the mice show strong behavioural defects in motor functions and balance.

The first paper used NeuroD1-null mice with a transgenic rescue of the pancreatic NeuroD1 due to postnatal lethality of a full NeuroD1 knock-out phenotype (Miyata et al., 1999). The authors report that the size of the cerebellum is reduced by 40% mostly due to granule cell loss in the posterior lobules. The anterior lobules still contain some GCs in the IGL and the foliation pattern is discernible. Purkinje cells are disorganised posteriorly. The authors observed that apoptosis is a major reason for GC loss and conclude that NeuroD1 is required for the normal differentiation and maintenance of GCs in the cerebellum.

A more recent paper looked in more detail at the discrepancies between the posterior and anterior lobules in the NeuroD1-null mice. These mice were of a different genetic background and could survive postnatally (Cho and Tsai, 2006; Schwab et al., 2000). The authors find similar cerebellar defects to those described previously, but they additionally examined the expression pattern of NeuroD1. The expression of NeuroD1, and its direct target TrkC, commence earlier in the posterior cerebellum than in the anterior lobules. The preferential expression of NeuroD1 in the posterior cerebellum may explain the earlier start of cell apoptosis in the mutant and hence a greater loss of granule cell in those lobules.

Yet another paper examined a very specific knock-out of NeuroD1 in a conditional mouse mutant where NeuroD1 was removed only in Atoh1-expressing cells (Pan et al., 2009). The authors performed an even more detailed analysis of cerebellar defects in these mice and presented a previously unreported phenotype of Purkinje cells as well as GC. Purkinje cells in the anterior lobules of the mutant cerebella had inversely polarised dendrites or bifurcated dendritic trees, despite forming a nearly uniform monolayer. Additionally, the authors observed that Atoh1 expression persisted in NeuroD1 mutants, suggesting a negative feedback loop between NeuroD1 and Atoh1.

Overall, all available evidence strongly points to NeuroD1 as being indispensable in GC development, at least before the cells differentiate and move to their final positions in the IGL. After the cells are mature, NeuroD1 no longer seems necessary for their maintenance, as NeuroD1 KO at that stage does not lead to any gross morphological defects in the adult (Goebbels et al., 2005).

4.1.1.1 Expression of NeuroD1 in granule cells of the cerebellum

Due to some confusion in the literature about the expression pattern of NeuroD1, and specifically whether its expression is restricted to the differentiated GCs, I performed a survey of the literature to compare expression experiments performed for NeuroD1. Most papers suggest that NeuroD1 is expressed in differentiating GCs only, however there are some papers suggesting that NeuroD1 expression might be present in proliferating cells, as well as cells still expressing Atoh1. **Table 4-1** collects the examples of NeuroD1 expression experiments from the literature, noting the reference, the species and the method used for staining NeuroD1, along with a summary note for each example.

After reviewing all the evidence, for the purposes of my study, I assume that NeuroD1 is expressed in postmitotic, differentiating GCs, with the possibility that its expression might be present as GCPs make their final terminal divisions. This could explain the discrepancies seen in the literature, as papers that suggest that mitotic GCPs express NeuroD1 perform a BrdU staining 2 hours before sacrificing the animal (Lee et al., 2000). Therefore, it is possible that the co-labelled cells have just finished dividing and started differentiating within the 2 hours window. Alternatively, as seen in Haldipur (2015), there is a large population of cells within the middle EGL which co-express NeuroD1 and PCNA. Therefore, the exact point at which NeuroD1 is expressed in developing GC is not entirely resolved.

Reference	Species, stage	Staining method	Example picture	Summary
Miyata et al., 1990	Mouse, P0	*In situ* for NeuroD1 BrdU stain	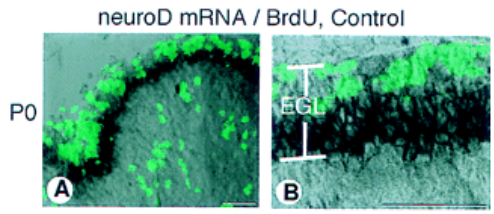	"NeuroD expression is not found in the outer EGL which consists of dividing GCP"
Lee et al., 2000	Mouse, X	*In situ* for NeuroD1 BrdU stain	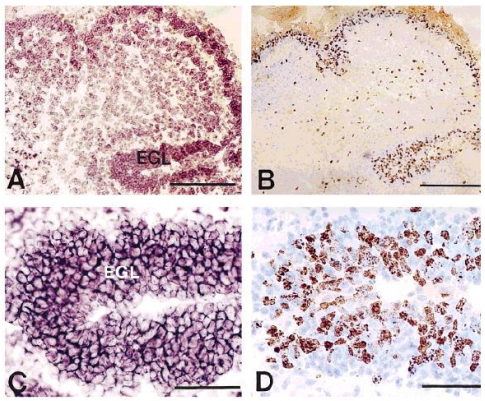	Authors suggest that proliferating (BrdU $^{+ve}$) GC can co-express NeuroD1. Animals were killed 2 hrs after BrdU injection.
Cho and Tsai, 2006	Mouse, E17.5, P1	Immuno for NeuroD1	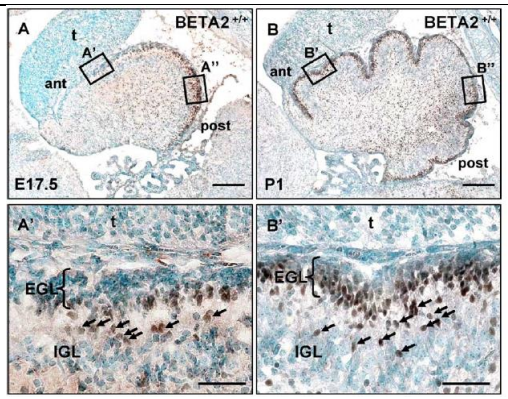	"Major immuno-reactivity was observed in the inner half of the EGL where postmitotic differentiatinf premigratory neuronal precursor cells are."
Pan et al., 2009	Mouse, P2, P11, P15	*In situ* for NeuroD1	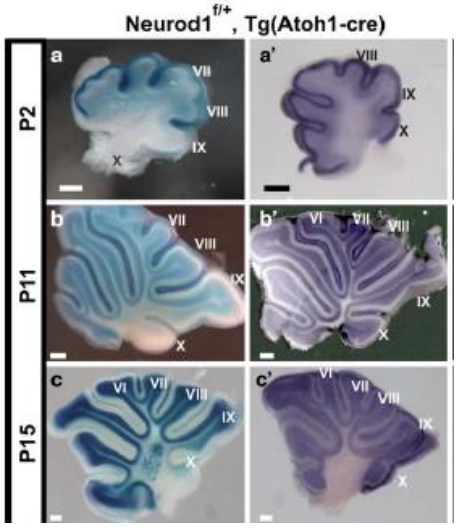	N/A

Table 4-1 Literature review of NeuroD1 expression studies

Reference	Species, stage	Staining method	Example picture	Summary
Klisch et al., 2011	Mouse, P0, P5	Immuno for NeuroD1, reporter for Atoh1	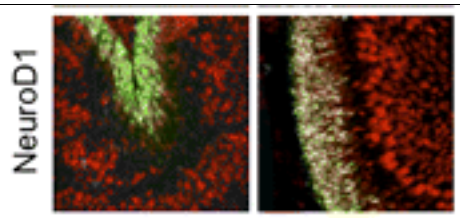	N/A
D'Amico et al., 2013	Xenopus laevis	*In situ* for NeuroD1, PCNA stain	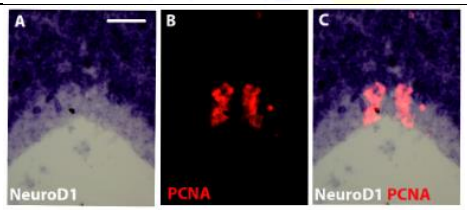	Expressed in differentiated granule cells
Borghesani et al., 2002	Mouse, P11	*In situ* for NeuroD1 and Atoh1	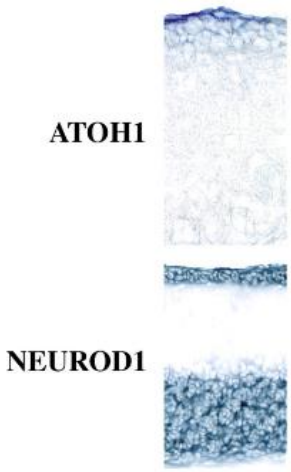	In this study the authors use NeuroD1 as marker of differentiation of GCPs
Schuller et al., 2006	Mouse, P0, P7, P15	*In situ* for NeuroD1	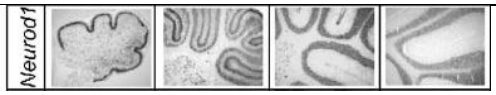	N/A
Volkmann et al., 2007	Zebrafish	*In situ*	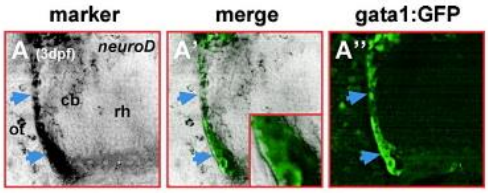	"expressed in differentiating migratory cerebellar granule cell precursors"
Haldipur, 2015	Mouse, P6	immuno	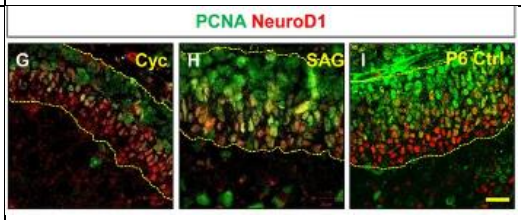	No mention of cell types labelled with NeuroD1, used as a differentiation marker

Table 4-1 Literature review of NeuroD1 expression studies

Allen Brain Atlas	Mouse E12.5, E13.5, E14.5, E15.5	*In situ*	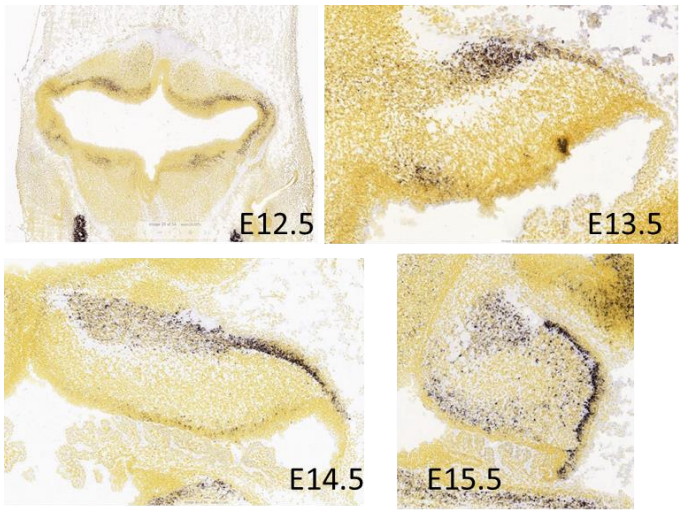

Table 4-1 Literature review of NeuroD1 expression studies

The table collects the studies where NeuroD1 expression was investigated in the cerebellum with various methods. The species, developmental stage and the staining method used are listed, as well as an example image. A summary column includes the conclusions about the expression profile presented in each reference. If the authors do not mention NeuroD1 expression in the EGL, it is indicated by N/A.

4.1.3 Identification of the NeuroD1 conserved non-coding element

Using the GENSAT (Gong et al., 2003) NeuroD1 BAC (RP24-151C22), which faithfully recapitulates NeuroD1 expression, Butts et al (2014) identified numerous candidate genomic regions for NeuroD1 expression. The most proximal conserved element is 183bp in length in mouse and was found to be conserved across osteicythyans (**Fig 4-1A**). Additionally, it resides within the large genomic regions previously shown to be capable of driving NeuroD1 expression in pancreatic and neuronal cell lines. The orthologous sequences of the mouse and Xenopus proximal element were cloned into reporter vectors upstream of the corresponding basal NeuroD1 promoter and GFP. Preliminary experiments suggested that the mouse CNE was capable of recapitulating endogenous NeuroD1 expression in the chick (**Fig 4-1C**) and this element is used in all my subsequent experiments.

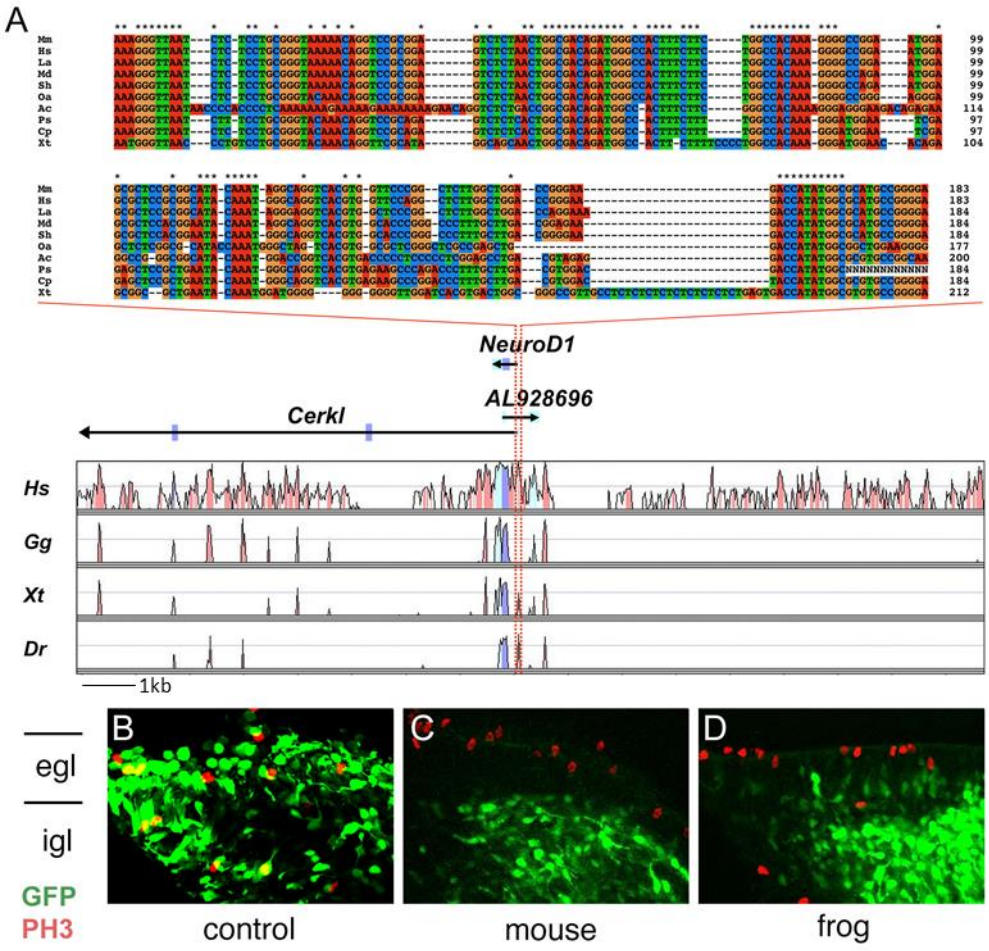

Figure 4-1 The NeuroD1 conserved non-coding element (NeuroD1-CNE)

A) Comparative genomic VISTA analysis of the region corresponding to GENSAT BAC RP24-151C22, with the mouse sequence as the base. Peaks correspond to regions of sequence homology (dark blue – exons; light blue – UTR; red – non-coding). An alignment of the conserved non-coding element investigated in this study from phylogenetically informative tetrapod species is shown above the VISTA plot**. B-D)** Confocal microscope images of sagittal sections of the E8 cerebellum stained for GFP (green) with PH3 (red) following electroporation with: **B**) a CAGGS-GFP control plasmid, **C**) the mouse conserved non-coding element (CNE) sequence upstream of the mouse basal promoter and **D**) the *Xenopus* CNE upstream of the *Xenopus* basal promoter.

Mus musculus, Mm; Homo sapiens, Hs; Loxodonta africana, La; Monodelphis domestica, Md; Sarcophilus harrisii, Sh; Ornithorhychus anatinus, Oa; Anolis carolinensis, Ac; Pelodiscus sinensis, Ps; Chrysemys picta bellii, Cp; Xenopus tropicalis, Xt; Gallus gallus, Gg; Danio rario, Dr. (*Figure modified from Butts et al., 2014*)

4.1.4 Aims of the study

In this part of the project I will explore the expression pattern of NeuroD1 during cerebellar development, particularly in cerebellar granule cells. I am especially interested in determining whether NeuroD1 expression is limited to postmitotic granule cells. I will use the conserved non-coding element of NeuroD1 to test its efficiency in reporting endogenous expression of NeuroD1. Further, I will explore the function of NeuroD1 in cerebellar development by misexpressing the gene at different stages of RL development.

4.2 Results

4.2.1 *NeuroD1* expression in the developing chick cerebellum

NeuroD1 endogenous expression in the developing chick cerebellum was analysed by *in-situ* hybridisation using full length sequence of NeuroD1 at E5, E6, E7, E8 and E12 embryos. The E12 embryos were sectioned sagitally and the tissue was additionally stained with anti-PH3 antibodies to see whether the expression of *NeuroD1* co-localises with proliferating cells. The results shown in **Figure 4-2A-H** show that *NeuroD1* is not expressed in the dorsal rhombomere 1 until E6 where it can be seen highly expressed in the nuclear transitory zone (NTZ) and faintly under the pial surface where either the EGL is forming, or the RL derivatives are still migrating towards the NTZ. There is also a faint expression in the ventricular zone but none at the RL. At E7 and E8 the *NeuroD1* expression increases in the EGL and at E8 the expression covers the entire surface of the cerebellum but seems to be downregulated from the forming cerebellar nuclei. **Figure 4-2 I-L** shows that at E12, a strong expression of *NeuroD1* is found in the inner layer of the EGL as it gradually increases from the outer to the inner EGL. Some PH3+ve cells are found within the *NeuroD1* expressing area (**Fig 4-2L**, arrows), suggesting that *NeuroD1* expressing cells can be proliferative.

4.2.2 NeuroD1-CNE recapitulates the endogenous expression of NeuroD1 in the developing chick cerebellum

To explore the pattern of expression of NeuroD1 at a cellular level, a conserved non-coding element of NeuroD1 has been cloned into an electroporation construct encoding a GFP protein (hereafter referred to as NeuroD1-CNE). The NeuroD1-CNE construct was electroporated into the RL of the chick embryo at E2 and E3-E5 and the pattern of fluorescence was analysed at E4, E5, E6, E7 and E8 to investigate whether NeuroD1-CNE recapitulates the endogenous expression of *NeuroD1*. The numbers of embryos in each condition are summarised in **Table 4-2**.

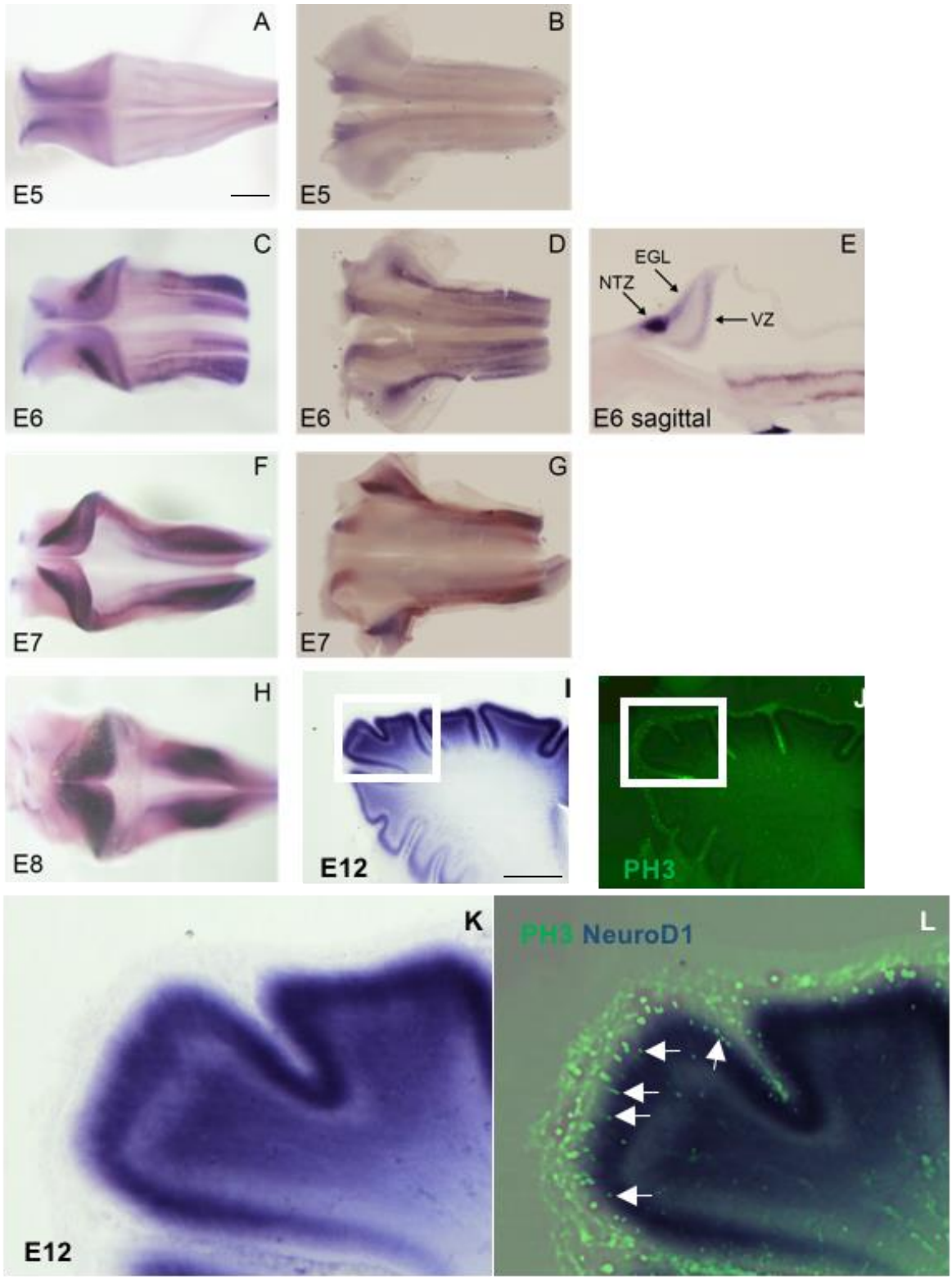

Figure 4-2 *In-situ* hybridisation for NeuroD1 in the chicken (*next page*)

Previous page:

Figure 4-2 *In-situ* hybridisation for *NeuroD1* in the chicken

In situ hybridisation for *NeuroD1* between E5 and E12 in the chicken embryos. **A-G)** Expression in wholemount embryos at E5-E8. Hindbrain shown in dorsal (A,C,F,H) or flat-mount (B,D,G) or sagittal section (E). Oriented rostral to left. Expression is seen in: ventral hindbrain stripes (A-E), nuclear transitory zone (C-G), external granule layer (C-H), cerebellar ventricular zone (E) and lower hindbrain populations (C-H). (*Experiment performed by Mary Green)*
I-L) Expression of *NeuroD1* in a sagittal section of E12 chicken cerebellum. Tissue was immunostained with anti-PH3 antibodies**. K)** A higher magnification of the tissue from I in the insert **L)** A merged magnified view from the insert in I and J to show co-labelling of cells (arrows). (*Experiment performed by Thomas Butts*)
Scale bar = 500μm

Embryos electroporated at:	***Embryos fixed at:***				
	E4	***E5***	***E6***	***E7***	***E8***
E2	6	6			
E3		5			
E4			11		4
E5				8	

Table 4-2 Numbers of embryos for experiment in Figures 4-3 and 4-4

Table collects the numbers of electroporated embryos with NeuroD1-CNE (and some with CAGGS-mCherry). Representative examples of embryos are shown in Figures 4-3 and 4-4

Firstly, the construct was electroporated into E2 embryos along with a ubiquitous expression vector CAGGS-mCherry to determine whether NeuroD1-CNE expression pattern was limited to cells of neuronal identity. **Figure 4-3** shows that, indeed, following an E2 electroporation, NeuroD1-CNE expression at E4 and E5 was absent from the roof plate cells derived from the boundary at the RL and only present in the neuronal cells migrating ventrally from the RL. In contrast, the control mCherry vector expression was found both in the roof plate cells (**Fig4-3Aii and Bii**, arrows) and in the RL neuronal derivatives. This suggests that NeuroD1-CNE is active only in cells fated to become neurons and not in other epithelial cells such as the non-neural roof plate epithelium.

Next, NeuroD1-CNE was electroporated into E3, E4 and E5 embryos to investigate the pattern of NeuroD1-CNE expression in the neuronal cells at different ages, from E5 to E8, comparing it with the previously described patterns of temporal specification of RL derivatives (Green et al., 2014, **Fig1-3**). Numbers of embryos used in each condition are summarised in **Table 4-2**. In **Figure 4-4**, the pattern of expression at E6, E7 and E8 corresponds to all neuronal derivatives found to be born from the RL from E4 to E6 i.e. cells in ventral rhombomere 1 (**Fig 4-4** red arrows), the nuclear transitory zone (**Fig 4-4** blue arrows) and on the pial surface of the cerebellum in the EGL (**Fig 4-4** green arrows). In some embryos, the expression of NeuroD1-CNE is also clearly visible in all of the described axonal projections of cells resulting from RL electroporations (some axonal projections result from electroporation of cell types other than Math1-expressing RL progenitors as reported in Green et al., 2014). The embryos at E8 in **Fig 4-4D** show the ipsilateral ascending (IA) axons and ventral ipsilateral descending (vID) axons from the ventral population of cells. Cells in the nuclear transitory zone show dorsal ipsilateral descending axons (dID) and axons of the fasciculus unicinatus (FU).

Overall, the results suggest that NeuroD1-CNE is expressed during the development of all neuronal derivatives born at the RL and its expression pattern corresponds to all cell populations born at the RL from E4 to E6, finishing in granule cell precursor generation at E6.

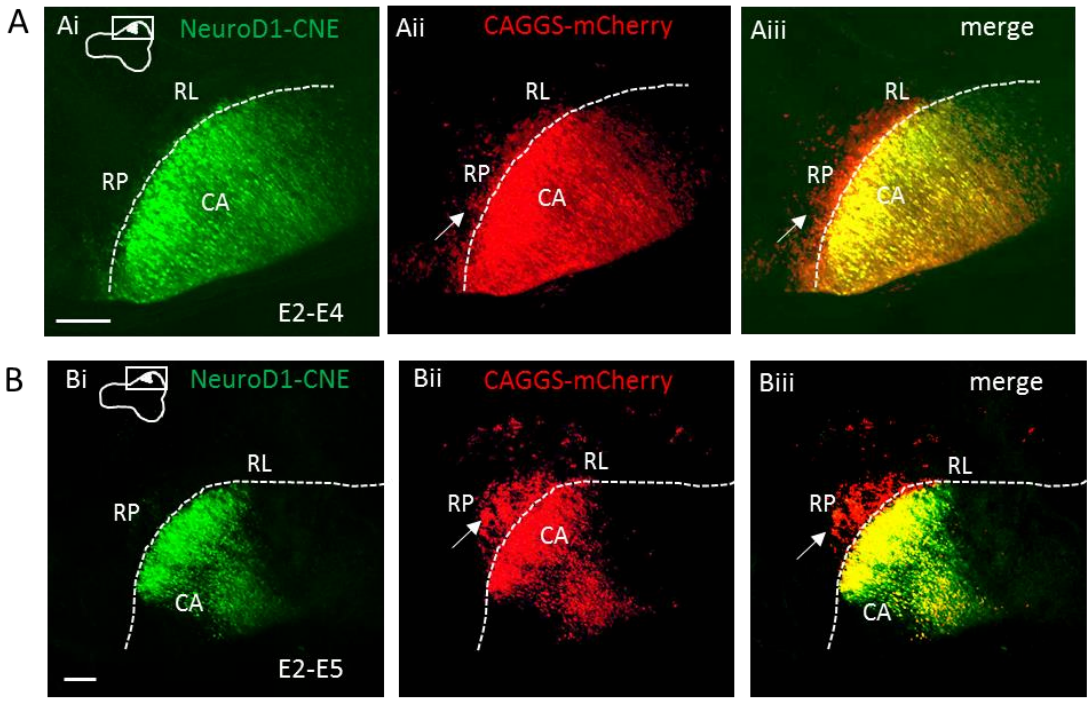

Figure 4-3 NeuroD1-CNE is expressed in rhombic lip neuronal derivatives but not the roof plate cells

Wholemount preparations of embryos electroporated with CAGGS-mCherry and NeuroD1-CNE at E2. **A** shows the embryo sacrificed at E4 (n=6), **B** shows an embryo sacrificed at E5(n=6). Panels **Ai and Bi** show the expression of NeuroD1-CNE, which can be seen only in the RL derivatives migrating away from the RL towards the ventral neural tube. **Aii and Bii** show a control electroporation of CAGGS-mCherry that labels all electroporated cells. Arrows show electroporated roof plate cells in red migrating away from the RL dorsally. **Aiii and Biii** show merged images which clearly show the separation between roof plate cells (red only) and neuronal RL derivatives (yellow cells). Scale bar = 200μm

***RP**: roof plate; **CA**: cerebellar anlagen; **RL**: rhombic lip*

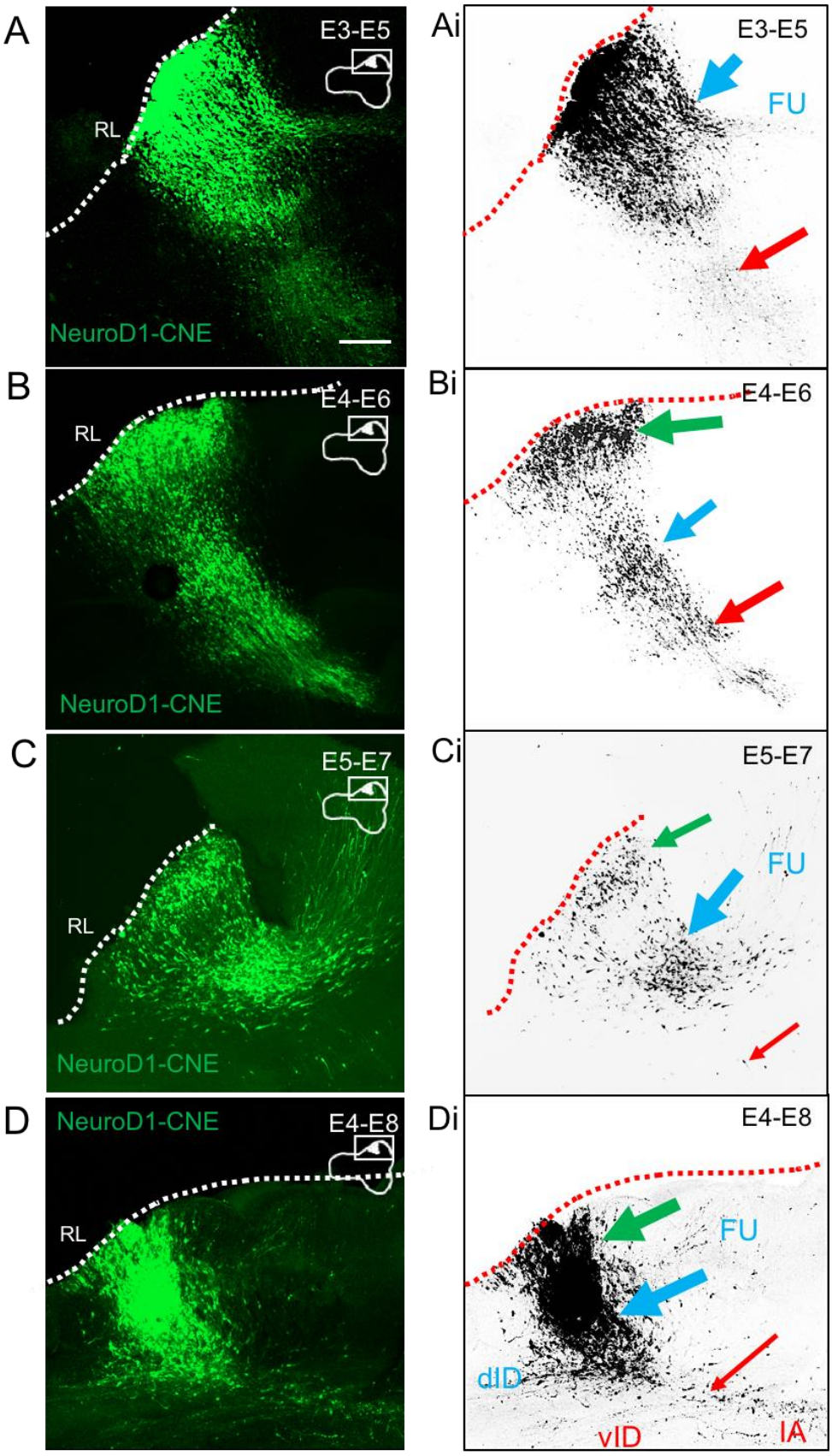

Figure 4-4 NeuroD1-CNE is expressed in all rhombic lip neuronal derivatives

(next page)

Previous page:

Figure 4-4 NeuroD1-CNE is expressed in all rhombic lip neuronal derivatives

Wholemount preparations of NeuroD1-CNE electroporated embryos at E3-E5 and fixed at E5-E8. The electroporations are shown alongside an inverse-colour image generated for easier visualisation of the different cellular populations. Days of electroporation and fixing are indicated for each embryo. The different neuronal populations are indicated with coloured arrows, size of which corresponds to the size of the population labelled. The white/red dotted line indicates the edge of the RL.

A) Embryo electroporated at E3 and fixed at E5 (n=5) shows labelling of extracerebellar neurons (red arrow) and cells migrating towards the NTZ (blue arrow). The EGL is not visible at this stage as GCPs have not started to be generated.

B) An E4 to E6 electroporation (n=11) reveals all RL populations i.e. cells in ventral rhombomere 1 (red arrows), the nuclear transitory zone (NTZ) (blue arrows) and on the pial surface of the cerebellum, the external granule layer (green arrows).

C) Electroporation at E5 to E7 (n=8) labels a small population of the ventral cells (red arrow) and mostly the NTZ (blue arrow) and EGL cells (green arrow).

D) The embryo fixed at E8 following and E4 electroporation (n=4) shows all three neuronal populations and also their axonal projections. Ipsilateral ascending (IA) axons and ventral ipsilateral descending (vID) axons from the ventral population of cells are observed. Additionally, cells in the NTZ show dorsal ipsilateral descending axons (dID) and axons of the fasciculus unicinatus (FU). Not all of these projections belong to Atoh1-positive RL derivatives but are also electroporated using this protocol.

Scale bar = 200μm

4.2.3 NeuroD1-CNE expression is lower at the rhombic lip and has variable expression in granule cell precursors

An important part of the project was determining if NeuroD1-CNE can discriminate between granule cell precursors and differentiated granule cells through its expression pattern. Therefore, the next step was to closely examine NeuroD1-CNE expression pattern in the last cohort of RL derivatives- the GCPs. To check whether NeuroD1-CNE is expressed in proliferating GCPs, a number of strategies were employed.

First, NeuroD1-CNE was electroporated into the RL at E5 or E6 and the tissue was stained with an anti-PH3 antibody at E8 to see whether there is any overlap of electroporated cells with the proliferation marker. Unfortunately, as already documented in Chapter 2 (Fig 2.2), electroporation of the RL has a negative effect on proliferation of electroporated cells. Therefore, as shown in **Figure 4-5,** even though co-expression of NeuroD1-CNE and PH3 was not observed, the results do not definitely mean that GCPs do not express NeuroD1-CNE, due to the technical issues with the electroporation protocol.

Secondly, it was important to distinguish between NeuroD1-CNE^{+ve} and NeuroD1-CNE^{-ve} cells in terms of their positions within the tissue and their morphologies in the forming EGL were GCP are located. If NeuroD1-CNE expression was absent from the outer EGL, then the construct is likely to recapitulate the endogenous *NeuroD1* expression pattern. To test this scenario, CAGGS-mCherry, which is expressed ubiquitously, was co-electroporated with the NeuroD1-CNE construct. As **Figure 4-6** shows, after electroporating both constructs at E4 and checking at E6 or E8 (numbers of embryos can be found in **Table 4-2**), NeuroD1-CNE^{-ve} , mCherry^{+ve} cells were observed at the pial surface of the cerebellum. The cells resembled potential GCPs, however, upon closer examination, the cells exhibited very unusual morphologies.

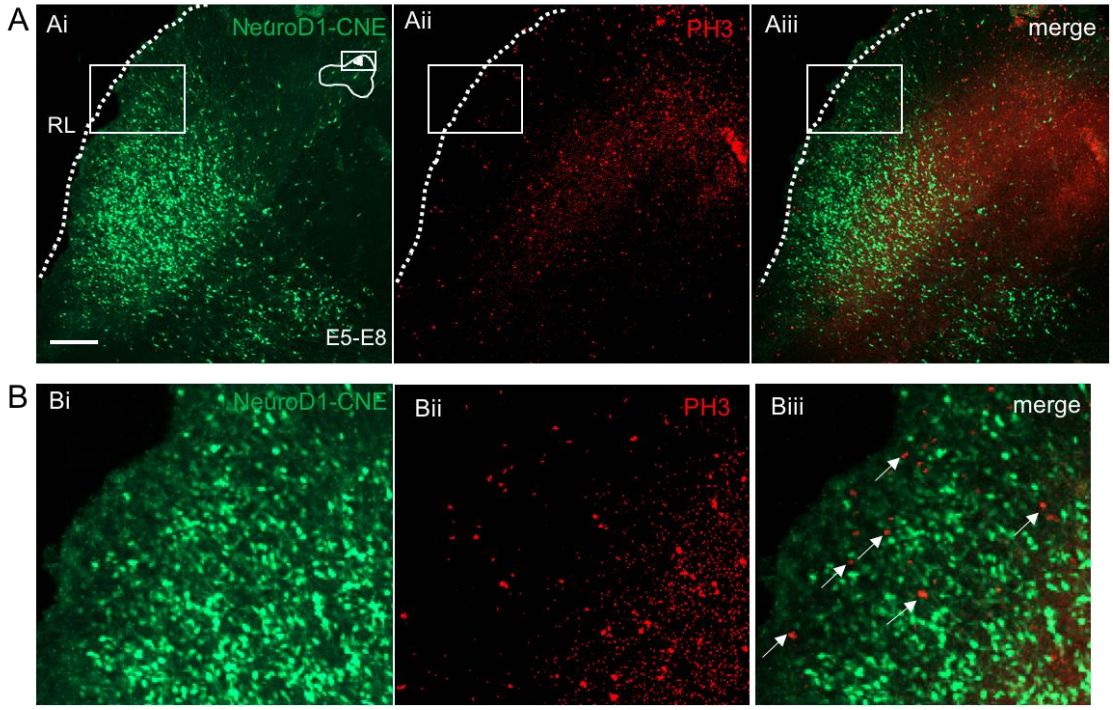

Figure 4-5 NeuroD1-CNE labelled cells do not co-express PH3

A) An example of an E8 wholemount of NeuroD1-CNE electroporated embryo at E5 immunostained for PH3 proliferation marker (n=5). There is no co-expression of NeuroD1-CNE and PH3 in the embryos analysed**. B)** A magnification from the insert in A showing no co-localisation of NeuroD1-CNE and PH3.

Scale bar = 200µm

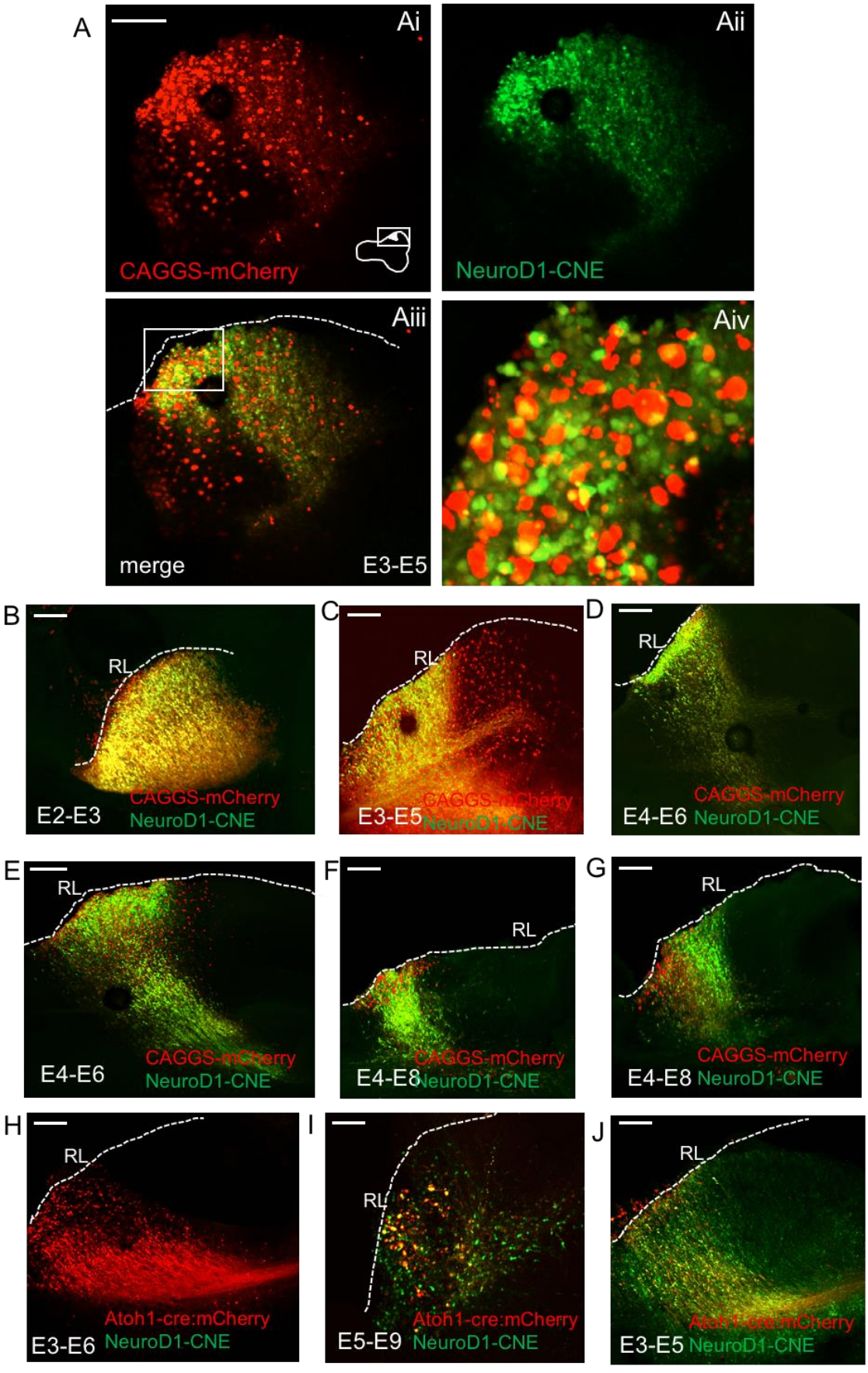

Figure 4-6 Electroporating mCherry-coding constructs results in abnormal cellular morphologies *(next page)*

Previous page:

Figure 4-6 Electroporating mCherry-coding constructs results in abnormal cellular morphologies

Wholemount preparations of embryos electroporated at various stages with NeuroD1-CNE and either CAGGS-mCherry or Atoh-cre:mCherry. Stage of electroporation and fixing is indicated on each image. **A)** An example of a typical embryo electroporated with CAGGS-mCherry at E3 and fixed at E5 (n=8). A population of very large, round and brightly fluorescent cells are visible on the pial surface of the embryo. Those cells do not co-express NeuroD1-CNE. **Aiv**) shows a magnified view of the cells found in **Aiii**. The cells have no processes and are unlikely to represent GCP population. **B-G**) Other examples of embryos electroporated at various stages and fixed from E3 to E8. Each embryo electroporated with CAGGS-mCherry shows an accumulation of the abnormal cells on the surface to a different extent. **H-J**) Similar but less severe phenotype is observed when Atoh1-cre and lox-stop-lox-mCherry constructs are used instead of CAGGS-mCherry, again regardless of the stage of electroporation or fixation, suggesting that the cells are not GCPs.

Scale bar = 200μm

Embryos electroporated at:	***Embryos fixed at:***				
	E3	***E5***	***E6***	***E8***	***E9***
E2	6				
E3		8	4		
E4			7	5	
E5					3

Table 4-3 Numbers of embryos for experiment in Figure 4-6

Table collects the numbers of electroporated embryos with NeuroD1-CNE and CAGGS-mCherry. Representative examples of embryos are shown in Figure 4-6.

The cells were larger than their NeuroD1-CNE^{+ve} neighbours, had an extremely high level of fluorescence and had no processes. Additional electroporations at earlier stages revealed that these cells are present long before GCPs are generated at the RL. For example, **Fig 4-6B** shows the presence of such cells already at E3, and they are also present in large numbers in embryos fixed at E5 (**Fig 4-6C**), before GCP are born.

Analogous experiments were performed with Atoh1-cre and stop-mCherry plasmids and similar results were obtained (**Fig 4-6 H-J**), albeit the cells were present in fewer numbers due to the cre-recombinase activity. Overall, the cells observed on the pial surface of the cerebellar anlagen that do not express NeuroD1-CNE cannot be granule cell precursors and possibly are a result of mCherry protein toxicity and invading macrophages, as observed in similar experiments in the past (Wingate and Hatten, 1999).

Using two different constructs encoding the mCherry protein resulted in abnormal cellular behaviours. Therefore, a CAGGS-TdTomato construct (hereafter referred to as TdTomato) was used instead as a control plasmid due to much higher brightness and therefore lower required concentration (Shaner et al., 2005). **Figure 4-7** shows that when TdTomato is used as a control plasmid, not all cells that express TdTomato express NeuroD1-CNE at the same intensity.

Specifically, there was a low level of NeuroD1-CNE expression in all electroporated cells (**Fig 4-7 Eiii**) and therefore its expression levels were normalised. Based on an assumption that there is no endogenous *NeuroD1* expression in the RL stem cells, the levels of NeuroD1-CNE expression were reduced digitally so that there was none observed in the RL cells. This resulted in two types of remaining cells: some expressing NeuroD1-CNE highly and some with lower levels of expression of NeuroD1-CNE. Overall, the results show that NeuroD1-CNE is expressed at different levels in different cells in the forming EGL.

Morphologically, the most brightly expressing NeuroD1-CNE $^{+ve}$ cells resemble migrating neurons with leading processes and are located away from the RL (**Fig 4-7E**, arrows). However, some of the cells were also round and resembling proliferating precursors and dividing cells. **Fig 4-8A** shows examples of NeuroD1-CNE^{+ve} cells close to the RL. Many cells located in this area are cell doublets, reminiscent of the dividing cells observed in the time-lapse movies in Chapter 3. Some cells show high levels of NeuroD1-CNE fluorescence, some show very low levels, and some presumptive daughter cells show different levels of NeuroD1-CNE fluorescence. Additionally, **Figure 4-8 B** shows an example of neighbouring cells expressing different levels of NeuroD1-CNE. These cells might represent daughter cells of a single precursor and suggest that NeuroD1-CNE may recapitulate the endogenous differences in *NeuroD1* expression levels between granule cells at different differentiation stages.

Figure 4-8C shows that the expression of the construct was also observed at the RL in sagittal section where most cells expressed NeuroD1-CNE at very low levels and only some expressed high levels of the construct. Additionally, expression of NeuroD1-CNE persisted until E11 (**Fig 4-8D**) where it could be observed differentially expressed in an established EGL. Some GCs in the EGL expressed much higher levels of the construct than others.

Taken together, these results show that NeuroD1-CNE expression, based on the fluorescence intensity of the construct, is variable and differs between cells. However, it is impossible to ascertain whether this change is due to the ability of the construct to reflect the endogenous differences in the expression levels of *NeuroD1*, or the effect is an artefact of the methodology employed (see discussion).

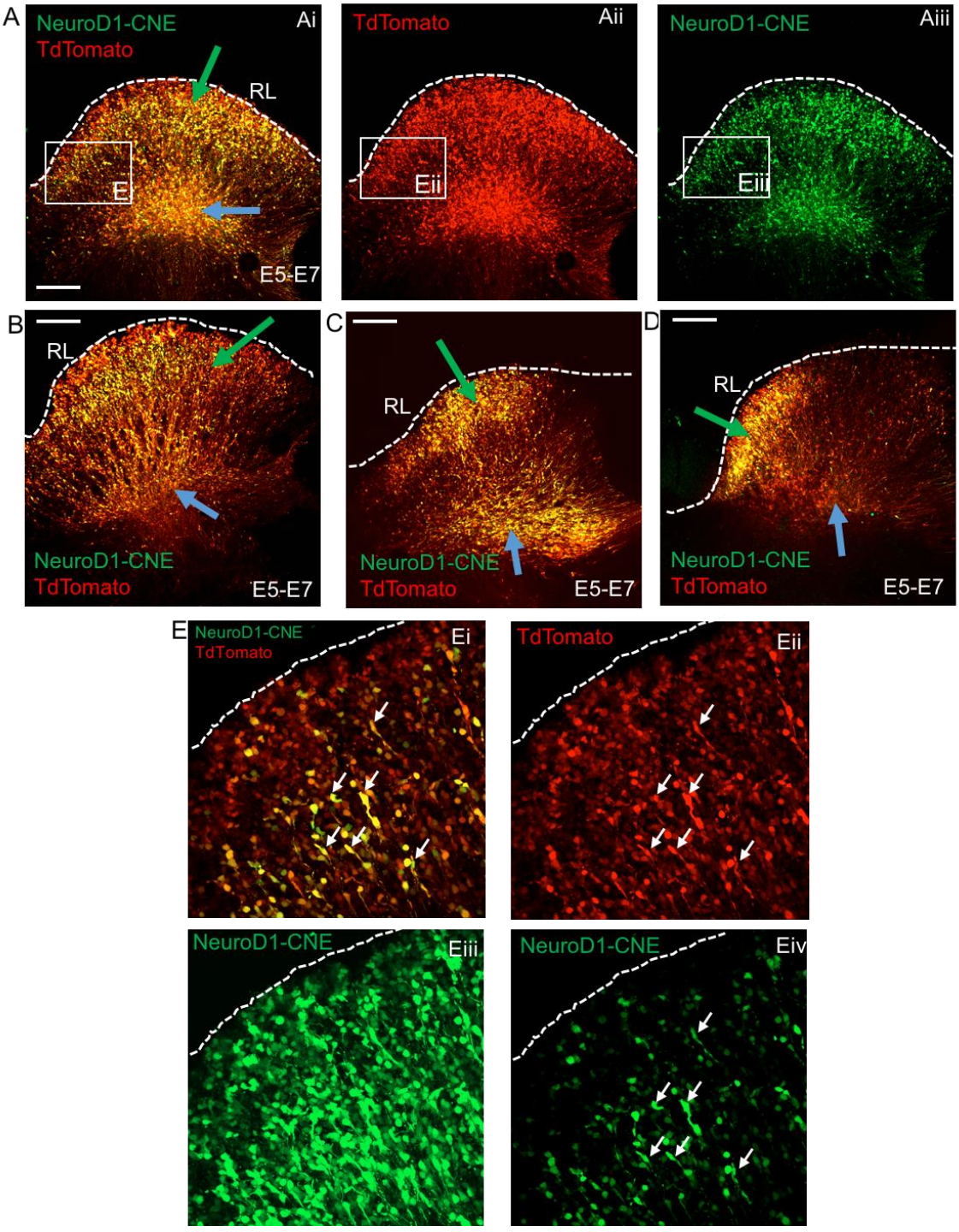

Figure 4-7: NeuroD1-CNE is expressed conditionally only in a subset of granule cell precursors and absent from most rhombic lip cells *(next page)*

Previous page:

Figure 4-7: NeuroD1-CNE is expressed conditionally only in a subset of granule cell precursors and absent from most rhombic lip cells

Wholemount preparations of embryos electroporated at E5 with NeuroD1-CNE and TdTomato control plasmid and sacrificed at E7 (n=8). **A)** When electroporated at E5, two populations of cells are clearly visible in the embryo at E7: cells in the the nuclear transitory zone (NTZ) (blue arrows) and on the pial surface of the cerebellum, the external granule layer (green arrows). **Aiii)** NeuroD1-CNE expression is found in both populations of cells. **B-D)** Other examples of embryos electroporated at E5 and sacrificed at E7. All show the two populations of cells. In all four examples (A-D) there is a clear population of Tdtomato positive cells at the RL with low levels of NeuroD1-CNE. **E)** A boxed area from A that shows in more detail the area close to the RL. **Eiii** shows that each electroporated cells has a low, non-conditional expression of NeuroD1-CNE. However, when this low expression is removed from the image, a pronounced loss of NeuroD1-CNE expressing cells can be observed at the RL and in some pial cells. **Eiv)** Strongly expressing NeuroD1-CNE cells are seen migrating away from the RL (arrows). These cells have a short leading process and are presumptive differentiated GCs.
Scale bar = 200μm

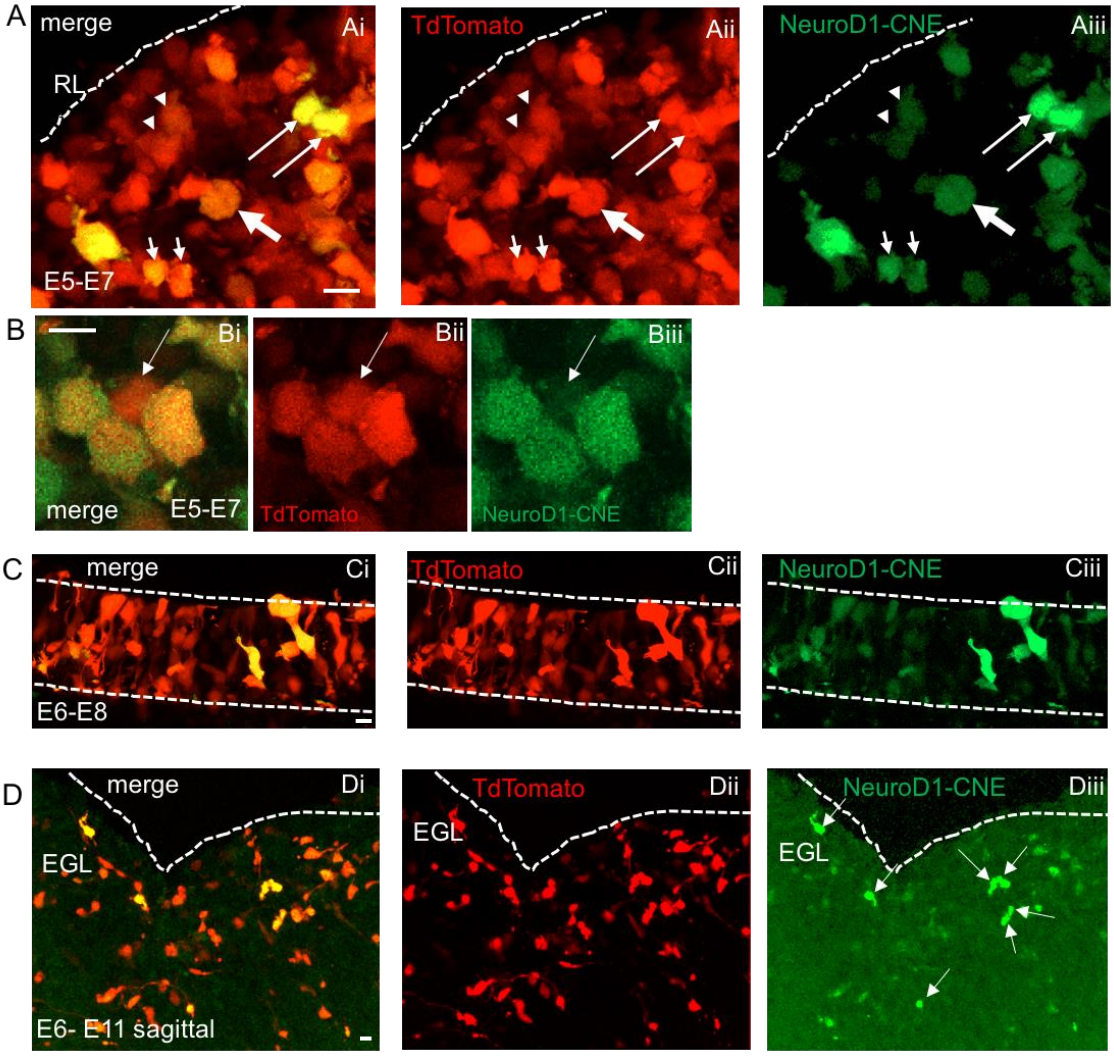

Figure 4-8 NeuroD1-CNE is expressed at different levels in subsets of granule cell precursors *(next page)*

Previous page:

Figure 4-8 NeuroD1-CNE is expressed at different levels in subsets of granule cell precursors

A) A magnification of cells found at the RL from E5-E7 embryos. A heterogeneous population of NeuroD1-CNE expressing cells are observed, with varying levels of fluorescence. Cells morphologically resemble dividing cells. Daughter cells can either be both highly expressing (long arrows), both lowly expressing (arrowheads), or of varying fluorescence levels (short arrows). Round cells about to divide can also express low levels of NeuroD1-CNE (thick arrow). Neighbouring the NeuroD1-CNE expressing cells are TdTomato expressing cells that do not express NeuroD1-CNE, which are presumptive GCPs undergoing rounds of proliferative divisions. **B)** Another example of the E5-E7 electroporated embryo showing four cells close together close to the RL. Three cells express NeuroD1-CNE and one of the cells does not (arrow). **C)** RL electroporated at E6 and sectioned sagitally at E8 shows near absence of NeuroD1-CNE expression in most of the RLprogenitor cells. Some cells express NeuroD1-CNE highly. The tissue pictured is the part of the RL that is normally removed during dissection and represents the neuroepithelial cells of the RL. **D)** At E11, the NeuroD1-CNE reporter construct is expressed highly in a subset of electroporated cells (white arrows) and very lowly in most of the electroporated cells still expressing TdTomato.

Scale bar = 10μm

4.2.4 NeuroD1-CNE is not expressed in the majority of PH3^{+ve} cells in the EGL of the E14 chick cerebellum

To examine the expression of NeuroD1-CNE in an established EGL without the technical issue of plasmid dilution, E14 chick cerebella were sectioned using a tissue chopper and electroporated *ex ovo* (Hanzel et al., 2015). Two approaches were used to establish whether NeuroD1-CNE is expressed in proliferating GCPs.

Firstly, as **Figure 4-9E** shows, NeuroD1-CNE was electroporated into the E14 cerebellar slices and the tissue was cultured for two days *in vitro* (div). After culture, the tissue was fixed and immunostained for PH3. As a control, separate cerebellar slices were electroporated with Atoh1-cre:stop-GFP and treated in the same way (**Fig 4-9A**). PH3^{+ve} electroporated cells were counted in both conditions. Results revealed that co-expression of Atoh1-cre:stop-GFP and PH3 was low (3%) (**Fig4-9C-D**), however, co-expression of NeuroD1-CNE and PH3 was near absent (0.005%) **(Fig4-9G-H)**. The two cells that did co-express NeuroD1-CNE and PH3 (**Fig4-9F**) looked more morphologically differentiated than the control PH3^{+ve} cells (**Fig4-9B**). Therefore, NeuroD1-CNE does not seem to be expressed in the majority of proliferating (PH3^{+ve}) cells of an established EGL.

Secondly, a control plasmid, along with NeuroD1-CNE were co-electroporated into E14 cerebellar slices to investigate whether NeuroD1-CNE is ubiquitously or conditionally expressed. **Figure 4-10** shows that both Atoh1-cre:stop-mCherry and CAGGS-mCherry were used as control plasmids. When using the Atoh1-cre:stop-mCherry combination, after 2 days in culture very few cells that do not co-express NeuroD1-CNE were observed (0.004%) (**Fig4-10A and C**). However, when using CAGGS-mCherry construct as a control, the number of NeuroD1-CNE^{-ve} cells increases to 10% of all electroporated cells (**Fig4-10B and D**). Therefore, there are cells electroporated in the slices that do not express NeuroD1-CNE and might represent proliferating, rather than differentiating, GCPs.

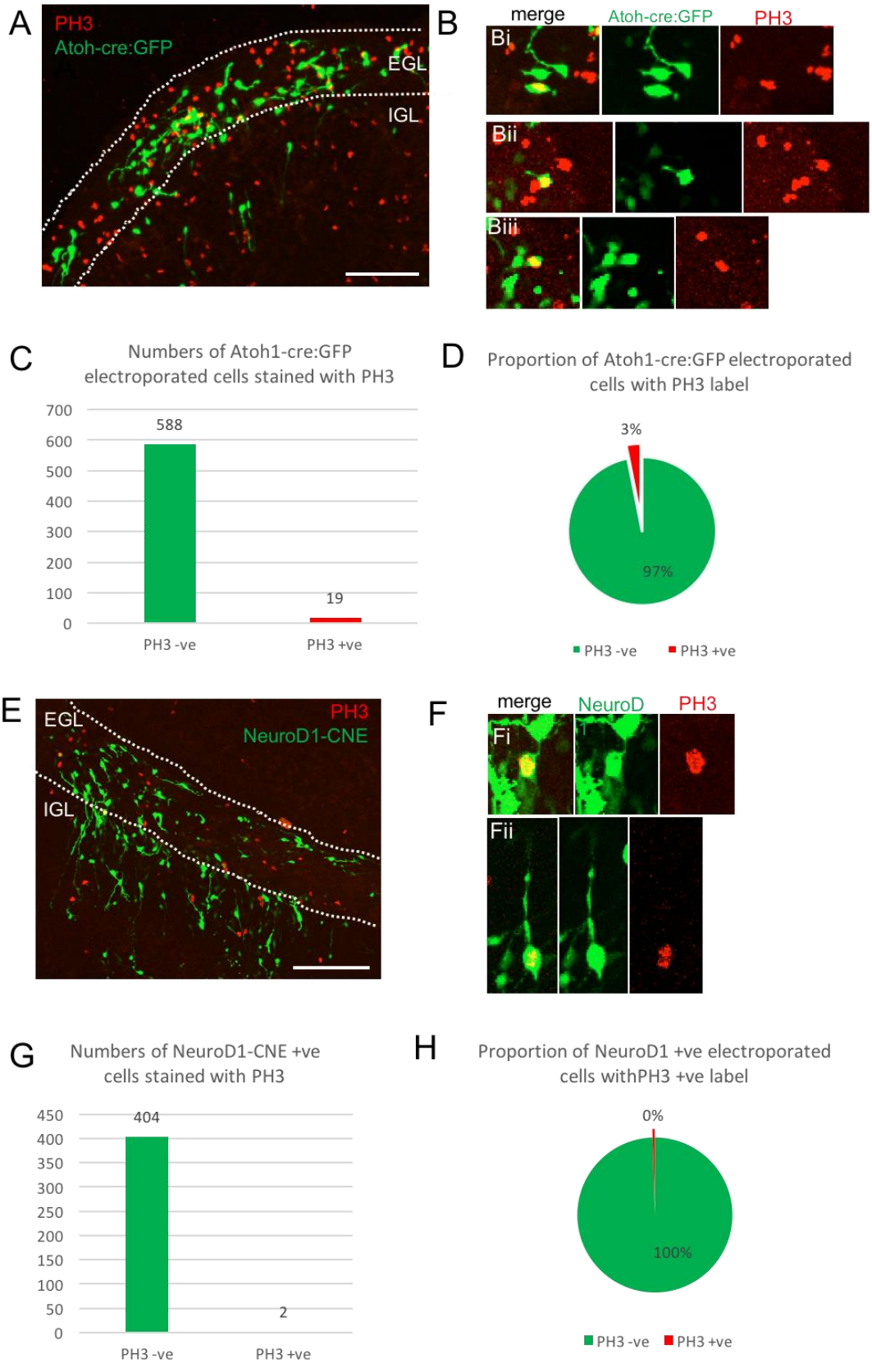

Figure 4-9 NeuroD1-CNE is rarely expressed in PH3 $^{+ve}$ cells in the chick EGL

(next page)

Previous page:

Figure 4-9 NeuroD1-CNE is rarely expressed in PH3^{+ve} cells in the chick EGL

E14 cerebellar slices (n=5) were electroporated with Atoh1-cre and lox-stop-lox-GFP plasmids, or with NeuroD1-CNE. Following two days in culture, the slices were stained for PH3. **A)** An example slice with Atoh1:GFP cells residing mostly in the EGL and some migrating towards the IGL. Some of the electroporated cells are labelled with PH3. **B)** Examples of the labelled cells and their co-localisation with the PH3 signal. **C)** The numbers of PH3^{+ve} and PH3^{-ve} cells expressing Atoh1:GFP. **D)** The proportion of the cells from C) in each category **E)** An example slice with NeuroD1-CNE^{+ve} cells. Very few cells co-label with PH3. **F)** Morphologies of two cells that were found to co-label with PH3. **G)** The numbers of PH3^{+ve} and PH3^{-ve} cells expressing NeuroD1-CNE. **H)** The proportion of the cells from G in each category.

Scale bar = 50μm

Next page:

Figure 4-10 NeuroD1-CNE is expressed in a subset of all electroporated cells in the chick EGL

E14 cerebellar slices were electroporated with Atoh1-cre and lox-stop-lox-mCherry plasmids (n=5) and NeuroD1-CNE, or with CAGGS-mCherry and NeuroD1-CNE (n=5). Following two days in culture, the slices were fixed and imaged. **A)** An example slice with Atoh1:mCherry and NeuroD1-CNE cells. Many cells can be seen co-expressing both plasmids. **B)** A higher magnification of an EGL. One NeuroD1-CNE $^{-ve}$ cell is found (thin arrow). NeuroD1 $^{+ve}$ Atoh1:mCherry $^{-ve}$ cells are seen (thick arrow).**C)** An example slice with CAGGS-mCherry and NeuroD1-CNE cells. **D)** A magnification of boxed area in C. Cells expressing CAGGS-mCherry only are visible (thin arrows). Cells expressing NeuroD1-CNE only are also present but in smaller quantities than A and B (thick arrow) **E)** The numbers of cells expressing the different combinations of plasmids when Atoh1:cre:mCherry and NeuroD1-CNE are co-electroporated. **F)** The numbers of cells expressing the different combinations of plasmids when CAGGS:mCherry and NeuroD1-CNE are co-electroporated.

Scale bar= 50μm

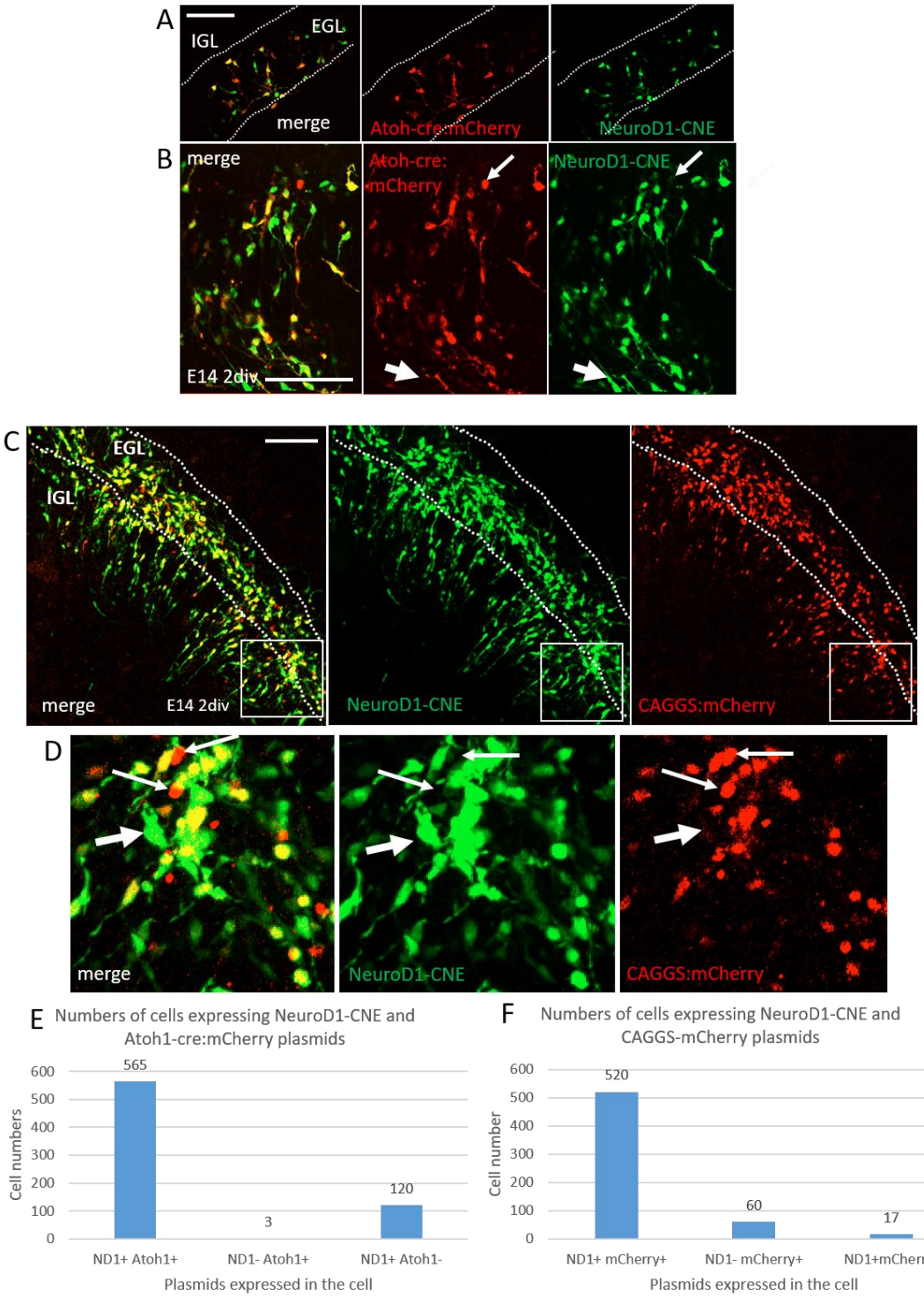

Figure 4-10 NeuroD1-CNE is expressed in a subset of all electroporated cells in the chick EGL *(previous page)*

The discrepancy between the two results may be explained by the relatively low expression of mCherry protein when driven by cre-recombinase recombination events. Consequently, I observe many NeuroD1-CNE^{+ve} cells that do not express mCherry when electroporated with Atoh1-cre:mCherry (17% of all electroporated cells) (**Fig 4-10A and C**). Overall, these results show that there are cells among all electroporated cells in the EGL that do not express NeuroD1-CNE. However, it is not possible to conclude whether they are proliferating GCPs from the above data.

4.2.5 NeuroD1-CNE is expressed in subset of cells in the mouse cerebellum

The expression of NeuroD1-CNE was also examined in developing mouse cerebellum. The construct was electroporated into the mouse cerebellum at P8, at a peak of GC proliferation in the EGL. Whole cerebella were electroporated, sectioned in coronal orientation using a vibratome and cultured for three div. As shown in **Figure 4-11A**, most electroporated granule cells have differentiated and migrated to the IGL by 3 div. However, as shown in **Figure 4-11B-C**, co-electroporation of NeuroD1-CNE with a ubiquitous TdTomato expression vector suggests that not all electroporated cells express the NeuroD1-CNE construct (**Fig 4-11 Bi**, **Ci**, thick arrows) and the cells that do not are located in the EGL and have a precursor-like morphology. NeuroD1-CNE construct is not expressed in any other cell type (based on morphology) and there is no co-expression of NeuroD1-CNE and calbindin, suggesting that the expression is not found in Purkinje cells. Admittedly, the numbers of mice for this experiment (n=2) are low and due to the long culture time (3 div) the potential numbers of GCPs are also low as most have differentiated. Therefore, it cannot be concluded that NeuroD1-CNE expression is restricted to differentiated granule cells based on these results.

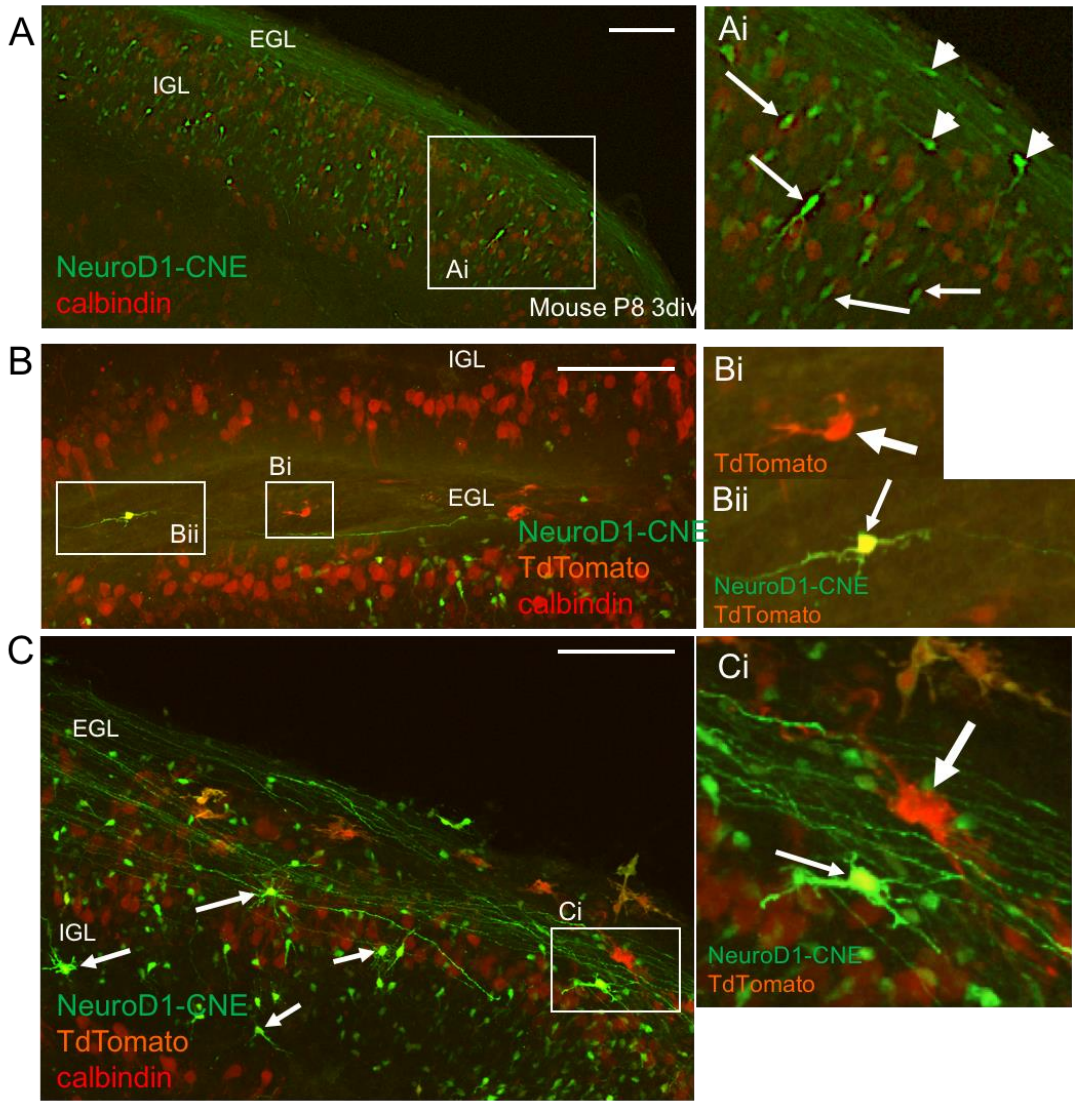

Figure 4-11 NeuroD1-CNE is expressed in granule cells in the mouse cerebellum

NeuroD1-CNE on its own, or along with TdTomato control plasmid was electroporated into whole mouse cerebella at P8 (n=3), which were sliced coronally and cultured for three days. **A**) Based on cellular morphologies, NeuroD1-CNE is only expressed in granule cells, and not any other cerebellar cells. Granule cells can be found within the EGL (arrowheads) and migrating towards, or located within the IGL (arrows). Calbindin labels Purkinje cells which never co-express NeuroD1-CNE **B-C**) When NeuroD1-CNE is co-expressed with CAGGS-TdTomato (n=2) and stained for calbindin, some cells in the EGL do not express NeuroD1-CNE and only express the control plasmid (Bi, Ci, thick arrows). These cells could potentially represent GCPs that have not started to differentiate, which morphologically differ from differentiating GCs (Bii, Ci, thin arrows)
Scale bar= 100µm. *EGL: External Germinal Layer; IGL: Internal Granular Layer*

4.2.6 NeuroD1 misexpression at the rhombic lip leads to premature differentiation and altered migration pattern of rhombic lip derivatives

After studying the expression of NeuroD1 in the developing cerebellum and establishing its expression in all neuronal derivatives at the RL, I decided to test whether misexpression of NeuroD1 would have any adverse effects on the development of RL derivatives. Therefore, the effect of misexpressing a full-length sequence of *NeuroD1* gene at different stages of cerebellum development was examined.

The construct used for the misexpression experiments contains a β-actin promoter in front of a full-length chick *NeuroD1* sequence. IRES sequence was inserted between the *NeuroD1* sequence and the sequence for Green Fluorescent Protein. Therefore, all electroporated cells should express both NeuroD1 and GFP proteins. The NeuroD1 overexpression construct will be referred to as NeuroD1-OE throughout.

At E5, the chicken RL gives rise to extracerebellar ventral neurons and the cerebellar nuclei neurons (Fig 1-3). In control (CAGGS-GFP) E5 electroporations (**Fig 4-12 A-C**) three populations of cells are observed in wholemount preparations at E7: cells in ventral rhombomere 1 (red arrows) cells in the nuclear transitory zone (NTZ) (blue arrows) and the external granule layer (green arrows). When NeuroD1-GFP is misexpressed at E5, the normal distribution of cells at E7 is disturbed. NeuroD1 misexpression results in the generation of cells that project long processes that span the cerebellar anlagen into the hindbrain. Cell bodies migrate along these processes but fail to reach the NTZ. Nucleogenesis is disturbed and no discernible NTZ is seen in the NeuroD1 misexpressing embryos. Projections of the fasciculus unicinatus are reduced or gone. A coronal section through the NeuroD1 misexpressing embryo (**Fig 4-12K**) reveals in more detail the cell bodies restricted dorsally and their axons spanning the cerebellum, as well as a population of cells with short processes migrating underneath that resemble the cells migrating from the NTZ in control embryos (**Fig 4-12J-K**, inserts). This suggests that some cells might be resistant to the effects of NeuroD1

misexpression, might not have been electroporated with the right dose of the construct, or might represent a RL population that NeuroD1 misexpression has no effect on. Overall, the results of electroporating at E5 suggest a premature differentiation of RL derivatives and their altered migration and abnormal behaviour.

When examined a day later, at E8, the number of cells stuck at the RL seems increased (**Fig 4-13A-C**). The chains of migrating cells are still present. When the NeuroD1 misexpressing embryos are stained for the proliferation marker, PH3, it is clear that a proliferative pool of cells persist at the RL (**Fig 4-13A-C**). However, a normal PH3 rich EGL does not form, as opposed to the neighbouring cerebellar tissue in which NeuroD1 has not been misexpressed. This suggests that either no GCPs are formed at the RL following NeuroD1 misexpression at E5, or that some GCs are formed but differentiate early and are non-proliferative.

When embryos were electroporated with NeuroD1 at E6, at the time GCPs are born, and fixed at E8 and immunostained for PH3, a considerable number of electroporated cells in the EGL co-expressed the proliferation marker (**Fig 4-13E**). Morphologically, the NeuroD1+ve cells resembled proliferating GCPs. Most were round and process-free (**Fig 4-13F**) whereas some had long, thick processes (**Fig 4-13G**), suggesting that NeuroD1 expression does not prevent proliferation in some GCPs.

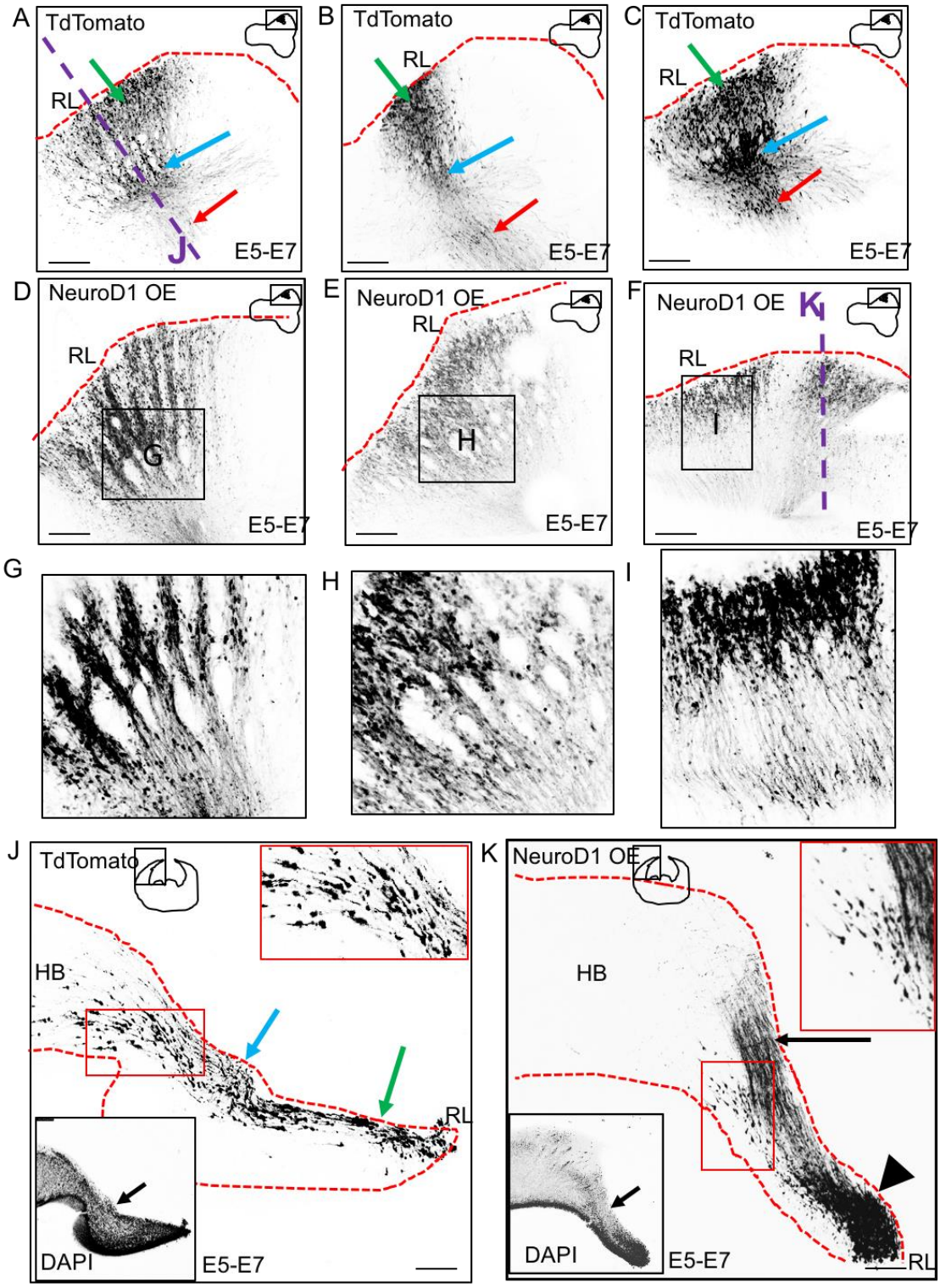

Figure 4-12 NeuroD1 misexpression at the rhombic lip at E5 results in migration defects of rhombic lip derivatives and disturbed NTZ nucleogenesis *(next page)*

Previous page:

Figure 4-12 NeuroD1 misexpression at the rhombic lip at E5 results in migration defects of rhombic lip derivatives and disturbed NTZ nucleogenesis

Wholemount preparations of control electroporations of TdTomato plasmid (A-C) and NeuroD1 OE and TdTomato plasmids (D-F) at E5. Embryos were sacrificed at E7. **A-C)** In the control electroporations (n=12), three populations of cells are clearly visible in the embryo at E7: cells in ventral rhombomere 1 (red arrows) cells in the nuclear transitory zone (NTZ) (blue arrows) and the external granule layer (green arrows). There is a clear separation between these cohorts of cells. The purple dotted line in A depicts a coronal cut through the embryo, shown in J. **D-F)** When NeuroD1 is misexpressed at E5 (n=7), there is a migration defects of cells from the RL as streams of cells with very long processes seem to form throughout the cerebellar anlagen**.** The cells also seem to be stuck at the dorsal side and normal NTZ nucleogenesis is disturbed. There are no clear projections of the fasciculus uncinatus that derive from Tbr $^{+ve}$ NTZ cells. The separation between the three cohorts of cells is not visible and it is not possible to deduce whether GCP production has started**.** The purple line in F depicts a coronal cut through the embryo, shown in K. **G-H)** Magnifications of images in D-F. Large 'holes' are formed between the streams of migrating cells. **J)** A coronal section through embryo from A shows the migrating cells from the RL. Blue arrow points to the forming NTZ with cell bodies and cells with relatively short processes migrating away (insert). The green arrow points to the GNPs generated from the RL. GCPs have very short processes and migrate in a subpial direction to form the EGL. Black arrow points to a DAPI staining of the NTZ. **K)** A coronal section through the embryo in F. The dorsally arrested cell bodies are clearly visible (arrowhead). Their axons span the cerebellar anlagen and reach the hindbrain (long black arrow). There is also a population of cells migrating below the axons with short processes, resembling the cells found in the control (insert). The short black arrow shows a low DAPI signal in the NTZ. Scale bar= 200µm

RL: rhombic lip; HB: hindbrain

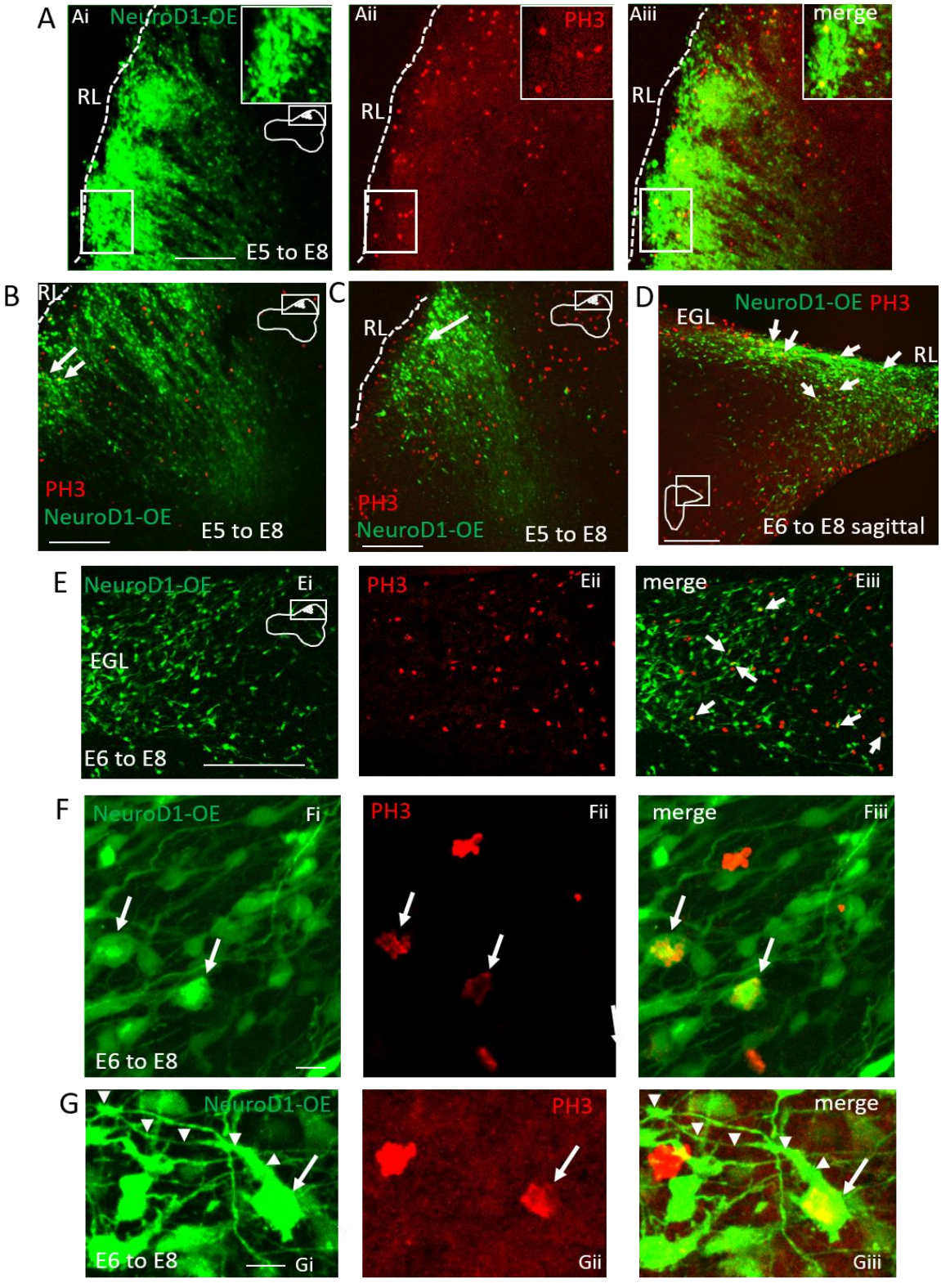

Figure 4-13 Effects on proliferation following misexpression of NeuroD1 at RL *(next page)*

Previous page:

Figure 4-13 Effects on proliferation following misexpression of NeuroD1 at RL

Wholemount or sagittal preparations of embryos electroporated at E5 or E6 with NeuroD1 OE construct. Embryos were sacrificed at E8 and stained for PH3. A, C and D) show three separate embryos that depict the continuation in migration defects of cells misexpressing NeuroD1 seen at E7 (Fig 4-12). Cells continue being 'stuck' close to the RL and streams of congested cells with long processes span the cerebellum from dorsal to ventral (n=6) **A)** Staining with PH3 reveals that there is a decreased area of proliferation in the EGL corresponding to the area of misexpression of NeuroD1. Some cells close to the RL do stain for the proliferation marker, PH3 (inserts). However, co-expression of NeuroD1 misexpressing cells with PH3 is rare and limited to the cells in proximity to the RL (7 cells). Embryo in **B)** shows only two cells co-expressing both markers and embryo in **C)** shows only one such cell.

D) After an E6 electroporation of NeuroD1, and fixing at E8, the cells form an EGL and many are seen expressing PH3 in the sagittal section at E8 (n=5). **E)** A wholemount view on the developing EGL electroporated at E6 and fixed at E8 stained for PH3. Arrows point to cells co-expressing NeuroD1 and PH3. **F)** Upon closer magnification, most dividing cells (arrows) have round morphologies and short or no processes.

G) Some cells staining for PH3 can have more elaborate morphologies, for example, extending a thick process (arrowheads) and a number of smaller processes from its cell body (arrow). Scale bar= 100μm (A-E), 10μm (F-G)

RL: rhombic lip; EGL: External Germinal Layer

4.2.7 NeuroD1 misexpression causes premature differentiation of granule cell precursors and reduced cerebellar foliation

From the above experiments, it seems clear that RL derivatives that misexpress NeuroD1 do not undergo their usual migration and differentiation behaviour. Although the EGL formation is supressed following an E5 NeuroD1 misexpression, as judged by PH3 staining and cellular morphologies, it is unclear what effect NeuroD1misexpression would have on GCPs directly. To examine the effects of NeuroD1 misexpression on the development of GCPs embryos were electroporated with NeuroD1 at E6, at the time of generation of GCPs.

When embryos were electroporated with NeuroD1 OE construct at E6 (along with a TdTomato construct for better visualisation of the electroporated cells) a distinct EGL was observed at E8. **Figure 4-14** shows sagittal and coronal sections through both control (**Fig4-14A-C,L**) and NeuroD1 misexpressing embryos (**Fig4-14D-K,M**). Results show that NeuroD1 misexpression does not prevent EGL formation, but causes premature differentiation of GCPs as many more cells are observed located in the IGL in the NeuroD1 misexpressing embryos. Additionally, the NeuroD1 misexpressing cells are morphologically more differentiated, as some already have developing dendrites (e.g. **Fig 4-14G,K**). A small number migrated close to the ventricular zone (e.g**. Fig 4-14M** arrows). In contrast, control cells mostly reside within the EGL, and by E8, the few that start to migrate towards the IGL only have a leading processes and none extend dendritic processes (**Fig 4-14A,B,L**). Misexpressing NeuroD1 also produces a population of RL derivatives that migrate in a sub-ventricular stream (**Fig 4-14C,H,J**) instead of following the pial migration route. These cells then seem to migrate towards the IGL from their ventricular location (**Fig 4-14C,H,I,J,**). Morphologically, they resemble differentiating GCs with long forming parallel-like fibres.

After establishing that GCPs differentiate earlier than normal following NeuroD1 misexpression, the longer-term fate of these cells were examined. NeuroD1 OE construct with TdTomato were electroporated into E6 cerebella and the embryos were sacrificed at E11, at the time when cerebellar foliation begins. The cerebella were sectioned sagitally and the positions of the electroporated cells was observed. **Figure 4-15A-B** shows that in control electroporations, a large number of electroporated cells were located in the EGL, which was a few cells thick. Many parallel fibres were also visible in the underlying cerebellar tissue, suggesting that at least a proportion of electroporated GCPs have fully differentiated. However, when NeuroD1 misexpressing cells were observed at E11, very few were located in the EGL (**Fig4-15C-D**). Rather, a dense bundle of parallel fibres was seen in the deep layers of the cerebellum. Interestingly, a substantial number of cells were located close to the RL (**Figure 4-15C,** red arrow), suggesting that some cells have differentiated soon after leaving the RL and remained at this location, as suggested by experiments looking at E8 effects. As **Figure 4-15E-G** shows, when the gross morphology of the NeuroD1 misexpressing cerebella is examined, a pronounced reduction in the size and foliation of the electroporated side is observed at the electroporated side.

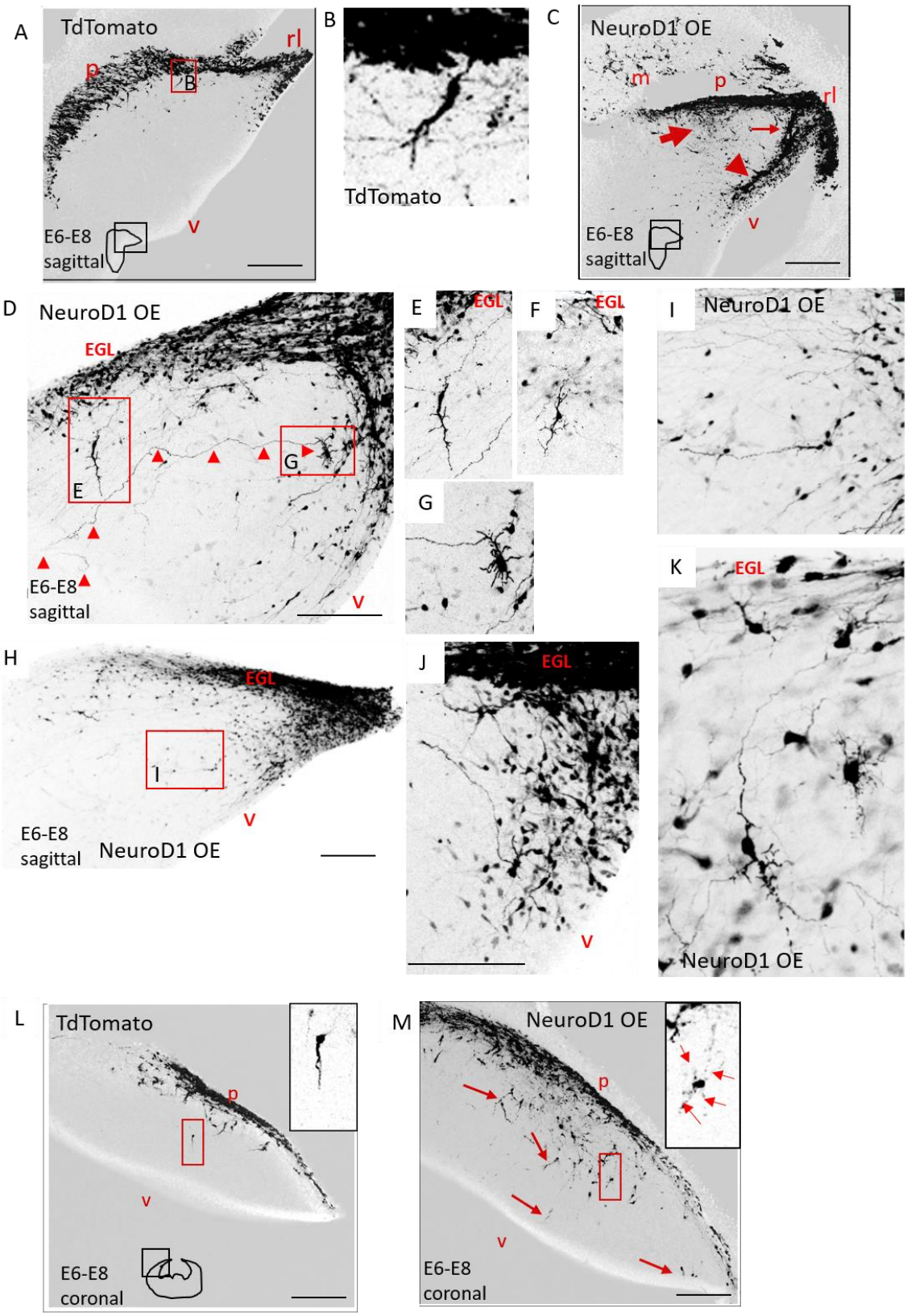

Figure 4-14 Misexpression of NeuroD1 in granule cells at the rhombic lip results in their enhanced differentiation *(next page)*

Figure 4-14 Misexpression of NeuroD1 in granule cells at the rhombic lip results in their enhanced differentiation

Sagittal and coronal sections of embryos electroporated with NeuroD1 OE plasmid and TdTomato plasmid, or NeuroD1-CNE and TdTomato control plasmids at E6. Embryos were sacrificed at E8 and cut into 150um sections. A-K show sagittal sections. L-M show coronal sections. A, B amd L show the control electroporation. All other pictures show electroporation with NeuroD1OE plasmid. **A)** In a sagittal section of control embryo a large number of GCPs are observed in the forming EGL. Very few GC are observed leaving the EGL to migrate towards the IGL, and the cells that do, have a single leading process and have not fully differentiated at this stage (n=10). **B**) A magnified view on the differentiating GC in the control embryo. It has a single leading process and only small additional processes**. C)**When NeuroD1 is misexpressed (n=5), GCPs still migrate to form an EGL, but many more are seen leaving the EGL early (thick arrow). Other phenotypes are also observed, such as a stream of cells leaving the RL to migrate towards the EGL, but instead changing direction towards the ventricular surface (thin arrow). Interestingly, cells from this stream seem to attempt to migrate back towards the EGL and resemble differentiating granule cells (arrowhead). Moreover, the cells seen in the pial membranes also have differentiated morphologies, instead of GCP-like morphology (labelled m). **D)** Another example of E6-E8 NeuroD1 misexpressing embryo. Note the highly differentiated GCs deep in the CB (boxes and **E and G**). Arrowheads point to a single parallel fibre developing from cell in G**. H-J**) Cells migrating from the ventricular side into the IGL. Many have long and thin, parallel fibre like processes. **K)** Examples of highly differentiated morphologies of NeuroD1 misexpressing cells radially migrating from an EGL. Note the large numbers of forming dendritic processes. **L)** A coronal section of a control embryo also shows a forming EGL at the pial surface and individual differentiating cells of the same morphology as in A (insert). **M)** In the NeuroD1 misexpression condition, the embryo has a forming EGL, but again, a much larger number of differentiating GCs can be seen in the IGL. The morphologies of these GCs are also much more differentiated with dendritic processes starting to form (insert). The differentiating cells also migrate much further towards the ventricular zone (arrows) compared to the control cells that keep close to the pial side Scale bar= 100µm. *p: pial side, v: ventricular side; rl: rhombic lip; m: meningeal membranes*

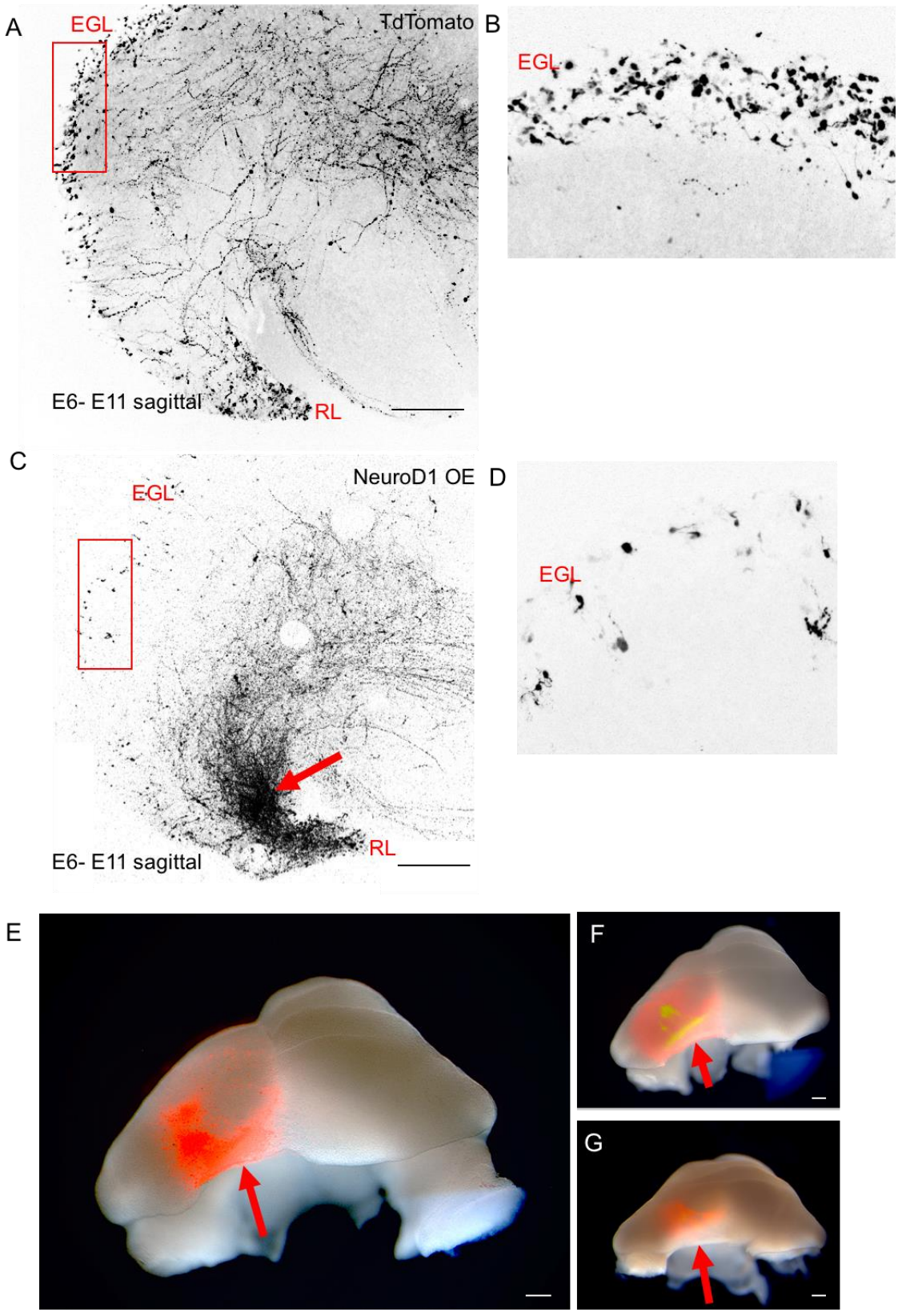

Figure 4-15 Granule cells leave the EGL prematurely following NeuroD1 misexpression, resulting in decreased cerebellar foliation *(next page)*

Previous page:

Figure 4-15 Granule cells leave the EGL prematurely following NeuroD1 misexpression, resulting in decreased cerebellar foliation

A) Following E6 electroporation control cells (expressing TdTomato) reside both in the EGL and the IGL, with a large proportion localised to the EGL Parallel fibres of differentiated GCs can be seen in the deeper layers of the cerebellum (n=10). **B)** A magnification of the control electroporation at the level of EGL. The EGL is many cell thick and electroporated cells are located in all layers **C)** NeuroD1 misexpression at E6 forces nearly all electroporated cells out of the EGL. Their parallel fibres are visible in the deeper layers of the cerebellum. There are many cells that reside close to the RL (red arrow) (n=12) **D)** Following NeuroD1 misexpression, the cells remaining in the EGL are sparse and some show abnormal morphologies**. E-G)** Three examples of whole E11 cerebella from embryos electroporated at E6 with NeuroD1 misexpression construct. The electroporated cells are in red and the site of electroporation is shown by the red arrows. Pronounced reduction in cerebellar foliation on the electroporated site is observed in all three cerebella.

Scale bar= 100μm

EGL: External Germinal Layer; RL: rhombic lip

4.2.8 NeuroD1 misexpression leads to inhibition of Atoh1 expression

Experiments performed so far aimed to establish the effect of NeuroD1 misexpression on early born GCPs and were performed by electroporating the RL at E6. The effects were analysed until E11. To examine the effects of NeuroD1 misexpression on the precursors located in the EGL directly, the NeuroD1-OE construct was electroporated into E14 cerebellar slices.

Because the latest time the cerebellum can be electroporated *in ovo* in the chick is E6, a time when granule cells are first generated at the RL, but no EGL has formed, an *ex ovo* electroporation protocol was used to target the cells in the EGL at a later developmental stage. The cerebella were removed from the chick embryos incubated until E14. The cerebella were then sectioned sagittaly using a tissue chopper and cerebellar slices were individually electroporated at the level of the EGL. This ensured that the effect of NeuroD1 misexpression is observed on EGL cells directly. Cerebella were electroporated either with a control CAGGS-GFP plasmid, or with NeuroD1 plasmid. As **Figure 4-16** shows, the cells misexpressing NeuroD1 were located in deeper layers of the cerebellum than the control cells, suggesting that their differentiation and migration is enhanced following NeuroD1 misexpression.

To explore the relationship between NeuroD1 and Atoh1, NeuroD1-OE was electroporated into the EGL of E14 cerebellar tissue along with Atoh1-cre and lox-stop-lox-mCherry constructs (**Fig 4-16**). Without NeuroD1 misexpression, this combination of constructs results in mCherry expression in the electroporated cells driven by the Atoh1 enhancer (Helms et al., 2001). However, when NeuroD1 is misexpressed at the same time, no red fluorescence is observed. This suggests that NeuroD1expression is silencing the expression of Atoh1 through its identified enhancer. Therefore, NeuroD1 acts rapidly to silence Atoh1 expression in the developing GCPs and hence enhance their differentiation.

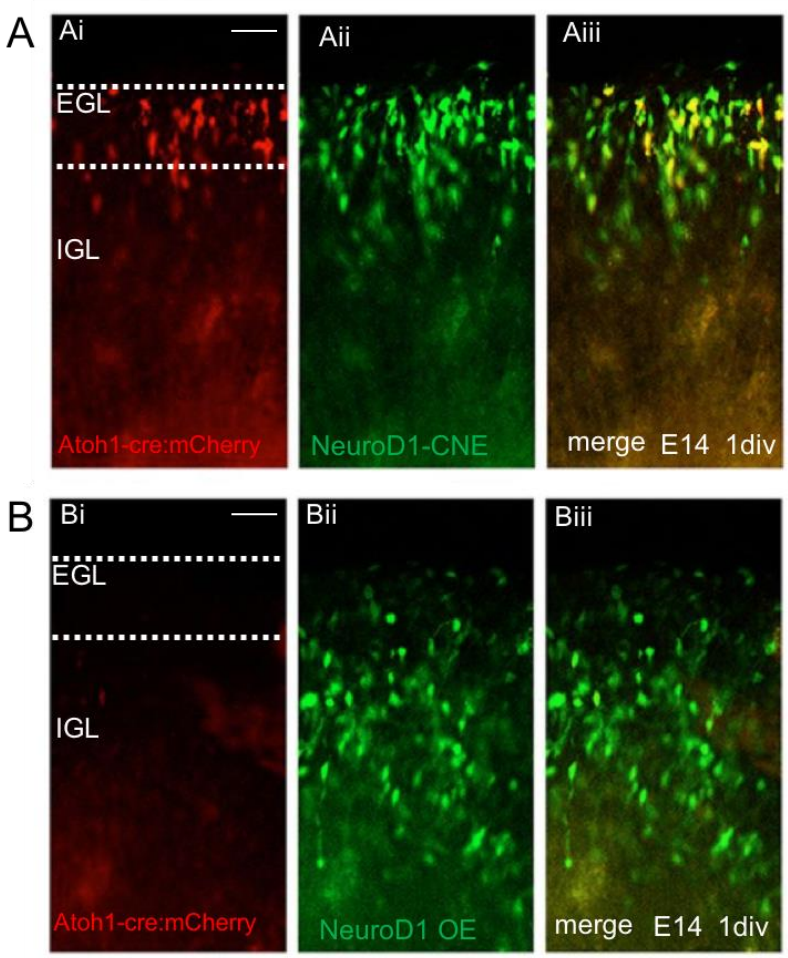

Figure 4-16: NeuroD1 misexpression in the EGL leads to enhanced granule cell differentiation and inhibition of Atoh1 expression.

E14 cerebellar slice electroporation of NeuroD1-CNE and Atoh1-cre:mCherry or NeuroD1 OE and Atoh1-cre:mCherry plasmids. Tissue was cultured for 24hrs.

A) In a control situation, NeuroD1-CNE expressing GC electroporated at E14 mostly reside in the EGL after one day of culture (Aii) and they retain the expression of perdurant mCherry (Ai), activated at the time of electroporation when the cells expressed endogenous Atoh1.

B) When NeuroD1 is misexpressed, the cells move away from the EGL after one day in culture and reside mostly within the IGL (Bii). The cells that misexpressed NeuroD1 do not express any mCherry driven by the Atoh1 enhancer as the expression of mCherry is inhibited in the cells by the presence of exogenous NeuroD1. Scale bar= 1*0µm

EGL: External Germinal Layer; IGL: Internal Granular Layer

4.3 Discussion

In this chapter I have explored the role of NeuroD1 in the development of RL derivatives, including cerebellar granule cells. NeuroD1 has been known to be expressed in differentiating granule cells of the cerebellum and has been used as a marker of postmitotic cells in numerous studies. Here, using *in situ* hybridisation and with a construct of NeuroD1 conserved non-coding element driving GFP expression, I show that in the chicken cerebellum NeuroD1 is expressed in a subset of proliferating granule cell precursors. However, co-expression of NeuroD1 and the proliferation marker PH3 is rare. I conclude that NeuroD1-CNE can potentially be used as a marker of a subset of differentiating GCPs. Additionally, I explore the effects of misexpression of NeuroD1 at the early developmental stages (E5-E8), as well as later developmental stages in a fully formed EGL (E14). At both times, misexpression of NeuroD1 has profound effects on the development of RL derivatives. Firstly, misexpression at the RL at E5 alters the migratory pathways of RL neuronal derivatives and causes premature differentiation. Nucleogenesis of cerebellar nuclei is affected, as the NTZ neurons become congested at the RL, their migration is hindered and therefore the cells do not form the NTZ. When misexpressed at the time of birth of GCPs, NeuroD1 leads to their premature differentiation and reduction in the size and foliation of the cerebellum. When misexpressed in an established EGL at E14 in cerebellar sices, NeuroD1 induces differentiation and radial migration of granule cells and downregulates Atoh1 expression. All these results taken together suggest an important role for NeuroD1 in the development of chick RL derivatives and broaden our understanding of the action of basic-HLH transcription factors in neuronal differentiation.

4.3.1 Limitations of the study

The biggest technical issue I encountered when performing experiments in this chapter was the realisation that electroporation as a technique seems to have an adverse effect on the development of electroporated cells. Specifically, electroporated cells had much lower levels of proliferation than neighbouring cells that had not been electroporated. This effect was seen when electroporating any combination of plasmids, including control plasmids. Because the main objective of

this project was to investigate the effect of NeuroD1 on proliferation of GCPs, and investigating the type of cells NeuroD1-CNE is expressed in, the fact that electroporation itself seems to hinder proliferation proved problematic when trying to analyse the results of the experiments. For example, Fig 2 in Butts et al., 2014 reports decreased area of proliferation at the site of electroporation of NeuroD1. Unfortunately, as subsequent experiments revealed, a similar result is observed when a control GFP plasmid is electroporated into the RL (see also Chapter 1), questioning the validity of such results. Throughout this project, this issue of electroporated cells being less proliferative obstructed my analysis of the effects of NeuroD1 and NeuroD1-CNE expression. This effect might be due to the physical damage resulting from electroporation that causes the cells to differentiate, through, for example, the effect on Atoh1 expression following electroporation (Broom et al., 2012). The effect was variable, however, as in some experiments, a reasonably large number of proliferating cells were observed (e.g. **Fig 4-13B**). Moreover, proliferation following electroporation at least partially recovers, as results in Chapter 2 and 3 suggest. When observing cells at E14 following an E5 electroporation, many stain for PH3 (Chapter 2). Therefore, at least a partial rescue of proliferation in GCPs is achieved during the development of the cerebellum. Nevertheless, when looking at the electroporated cells two or three days following electroporation, few seem to be proliferative in most experiments. Hence, the effect of NeuroD1 on proliferation has to be analysed in this context and the analysis of morphology and cell behaviour of electroporated cells can give a better indication of NeuroD1 effects on cellular development.

Another fact that complicates analysis is the variability in the copy number of the plasmid that individual cells uptake during electroporation. This is especially important when trying to deduce the differentiation state of GCPs based on the fluorescence levels of the reporter NeuroD1-CNE construct. Thus, the most brightly expressing TdTomato cells also tended to have most highly expressing NeuroD1-CNE signal. This suggested that the amount of plasmid electroporated into these cells were higher than the surrounding cells, hence they had higher levels of expression of both fluorophores. Cells with low levels of TdTomato expression also had low levels of NeuroD1-CNE expression. However, I cannot be confident that this is due to lower endogenous levels of *NeuroD1* in those cells.

Rather, TdTomato is a very bright fluorophore and might be visible still when NeuroD1-CNE (GFP positive) is dilute. Expressing the construct stably through genome integration would be a good way of minimising this issue.

4.3.2 NeuroD1-CNE partially recapitulates endogenous NeuroD1 expression

There is no published data on the expression of *NeuroD1* in the developing cerebellum prior to the establishment of the EGL. The only source of expression data of the gene can be found in the Allen Brain Atlas (**Table 4-1**), where it is observed that *NeuroD1* expression is present in the developing cerebellum at E12.5 at the time when GCPs are first generated. At E13.5 the expression is clearly visible in the NTZ and the cells migrating from the RL, which could include NTZ-directed neurons. At E14.5, the expression persists in the NTZ and is strong in the inner EGL and the cells migrating from the RL. At E15, the first IGL cells expressing NeuroD1 are observed, as well as a more ventricular population of cells. In the chicken, *in situ* hybridisation shows a very similar distribution of *NeuroD1* expression, with cells of the NTZ and EGL showing strong expression.

Based on the limited expression data of *NeuroD1* at these early developmental stages, the results obtained using the NeuroD1-CNE reporter suggest that it partially recapitulates the endogenous expression of the gene. The expression of NeuroD1-CNE is very high in all RL derivatives generated prior to GCPs (e.g. **Fig 4-4A**), and such high expression was not anticipated based on the available *in situ* data, which suggest that *NeuroD1* might be turned on in the early RL derivatives only as they arrive in the NTZ. However, the faint *in situ* expression of *NeuroD1* visible at E6 in the chick on the pial surface of the cerebellum, where NTZ-fated neurons are migrating, suggests that indeed *NeuroD1* might already be active in those migrating neurons, however at lower expression levels compared to those suggested by using the NeuroD1-CNE reporter. Therefore, it is possible that the reporter is expressed at higher levels than the endogenous *NeuroD1* gene.

4.3.3 NeuroD1-CNE is a potential differentiation marker for granule cell precursors

NeuroD1-CNE expression is very high in the last RL population (except UBCs) of cells born at the RL, the GCs. Most NeuroD1-CNE expressing cells born at the RL co-express a control plasmid, except, from E7 onwards, the cells closest to the RL and some pial cells that are presumably GCPs (**Fig 4-7**). A closer look at these cells reveal a large population of morphologically proliferating cells, as many of the cells exist in doublets that resemble cells that have just divided. Interestingly, some of these dividing cells express high levels of NeuroD1-CNE, some express low levels of NeuroD1-CNE, and some express no NeuroD1-CNE. Occasionally, doublet cells can be seen where one cell expresses a higher level of NeuroD1-CNE that the other cell. All these results taken together suggest that NeuroD1-CNE may be expressed at different levels depending on the stage of differentiation of GCPs. An intriguing idea that needs further investigation is whether high levels of NeuroD1-CNE in both daughter cells correspond to a terminal symmetric division of GCPs. Correspondingly, cells with no or low levels of NeuroD1-CNE might be proliferating GCPs. Further, cells with varying levels of NeuroD1-CNE could be undergoing asymmetric division with one daughter cell becoming a differentiated GC and the other undergoing further proliferative divisions. If NeuroD1-CNE indeed reported such differences in proliferative capacity of GCPs, it would be an excellent tool to study morphological changes and behaviour of GCPs at different stages of their development.

One slightly inconsistent result obtained during the project is the fact that in the early EGL (E8) morphologically proliferative cells can express NeuroD1-CNE, whereas NeuroD1-CNE expressing cells in cerebellar slices at E14 do not co-label with PH3. One possibility is that as the EGL develops, the differences between *NeuroD1*$^{-ve}$ and *NeuroD1*$^{+ve}$ cells become more pronounced and *NeuroD1* is expressed only in the differentiating, inner EGL cells. In contrast, in the early EGL the layers are not strictly defined and the production of new GCPs are less well orchestrated. Additionally, there might be other signals present in these early GCPs that allow them to proliferate even though *NeuroD1* is already present. As GCPs

migrate and become part of the EGL, they experience a changing environment and all these signals might be integrated to result in different outcomes for the cell.

To answer this question, one approach would be to clone the NeuroD1-CNE sequence into a Tol2 inducible construct so that its expression could be observed at later stages of EGL development, following integration into the genome. Unfortunately, in the performed experiments, due to dilution of the plasmid (past around E11), it is not possible to observe reliable expression levels of NeuroD1-CNE in an established EGL *in ovo* to assess and monitor its expression in different types of GCPs.

Therefore, NeuroD1-CNE presents potential as a differentiation marker of GCPs, but needs further investigation, especially to determine precisely at which stage of GCP differentiation it is expressed and whether the levels of expression correspond to specific developmental outcomes for the cell.

4.3.4 NeuroD1 promotes context dependent differentiation

The role of *NeuroD1* in GC development has been studied in some detail in the mouse model system. *NeuroD1* KO mice developed by different labs, with slightly different approaches (Miyata et al., 1999, Cho and Tsai, 2006, Schwab et al., 2000, Pan et al., 2009), all revealed the importance of *NeuroD1* in GC differentiation and the distinct loss of postmitotic GC following the loss of the *NeuroD1* gene. However, the effect of misexpressing the NeuroD1 protein prior to its endogenous expression time has not previously been attempted and the effects of *NeuroD1* loss on earlier RL derivatives have not been studied in detail in the mutant models. Overall, little data exists on the role of *NeuroD1* in the development of earlier RL derivatives such as the CN. In this chapter I reported the results of misexpressing the *NeuroD1* at different stages of RL neuron generation and show that regardless of the time of misexpression of *NeuroD1*, the corresponding cells born at the RL seem to differentiate prematurely following *NeuroD1* misexpression.

The strongest evidence for the ability of NeuroD1 to promote differentiation of RL derivatives is its effect on the developing GCPs. When *NeuroD1* was misexpressed at E6, at the time of GCP generation at the RL, GCPs migrated to form the EGL but a much larger number of differentiated GCs were identified in the forming IGL (**Fig 4-14**). Whilst in the control electroporation only a few cells were seen starting to migrate into the IGL at E8, the cells which overexpressed *NeuroD1* were present in the IGL in high numbers and had a more differentiated morphology. For instance, their dendritic processes were already forming and they had migrated deep into the IGL, some excessively close to the ventricular zone. Interestingly, the cells found within the pial meningeal membranes where GCPs are usually located after tangential migration also had very differentiated morphologies, suggesting that the GCPs can differentiate in abnormal locations. Therefore, misexpression of *NeuroD1* at the time of GCP generation result in earlier differentiation of these cells.

This finding is further strengthened by the results obtained by misexpressing *NeuroD1* in E6 embryos and observing their fate 5 days later, at E11. Whereas the control embryos have a cell-rich EGL with many electroporated cells residing and proliferating within the layer, the *NeuroD1* misexpressing cells are nearly all located within the IGL, with few remaining cells still seen within the EGL. The number of parallel fibres that can be seen extended in the slices of *NeuroD1* misexpressing embryos clearly exceeded the parallel fibres of E11 control embryos. Instead, most electroporated cells in control embryos still resided in the EGL and continue the proliferation stage. Gross morphology of the *NeuroD1* misexpressing cerebella clearly show the effect of the earlier differentiation of GCPs on the cerebellar size and foliation. Earlier differentiation of GCPs leads to reduced foliation pattern and smaller size of the cerebellum. Interestingly, at E11, there is no compensation from the unelectroporated GCP to correct this difference in EGL thickness and proliferation rate.

Moreover, misexpressing *NeuroD1* in the EGL in E14 cerebellar slices result in the electroporated cells migrating towards the deeper layers of the cerebellum, indicating their accelerated differentiation. Overall, performing *NeuroD1* misexpression experiments at two different time points of GCP development resulted in the same phenotype of accelerated differentiation of these cells.

The temporal context of misexpressing *NeuroD1* is important to consider. Even though *NeuroD1* expression has not been implicated in the development of the early RL derivatives, when *NeuroD1* is misexpressed at the RL at E5, at the time when the last few Lhx9^{+ve} neuronal cohort of cells are followed by generation of Lhx9^{-ve}/Tbr1^{-ve} and Tbr1^{+ve} neurons destined to become the CN neurons, the cells generated at the RL develop long processes that span the length of the cerebellar anlagen and project into the hindbrain. Most of the cells seem to accumulate at the dorsal side, instead of migrating towards their position in the NTZ.

Based on the cellular morphologies of the dorsally located cells alone, especially the lack of round cells with short processes that resemble GCPs, it is most likely that these are the early RL neurons that have started final stages of differentiation prematurely. The projections of the cells are extending over much longer distances than in the control situation and resemble the long axons of early born RL derivatives located in the hindbrain (Gilthorpe et al., 2002). Overall, the results suggest that misexpression of *NeuroD1* at E5 results in premature differentiation of early born RL derivatives.

4.3.5 NeuroD1 misexpression alters cell behaviour

NeuroD1 is a known differentiation factor so its effect on earlier differentiation is perhaps unsurprising. However, other unexpected cellular behaviours were observed after misexpressing *NeuroD1* at different stages. Firstly, following misexpression of *NeuroD1*, some granule cells migrate in an ectopic stream from the RL towards the ventricular side in large numbers, a situation never observed in control electroporations. In some embryos, the cells can be seen differentiating close to the ventricular zone and extending their parallel fibres outside of the molecular layer. Some cells that differentiate deep within the cerebellar anlagen extend parallel fibres that span the length of the cerebellum and are extended in opposite directions to the wild type parallel fibres. Additionally, some of the cells that migrate towards the ventricular side seem to later attempt to migrate towards the IGL, presumably to position themselves in their typical locations, with some success. However, many of the cells seem disorganised and go through differentiation at wrong locations.

Secondly, when misexpressed at E5, *NeuroD1* disturbs many cellular behaviours. For instance, the normal accumulation of cells in the NTZ is disturbed and no nucleogenesis is observed. The cells that normally reside in the NTZ (**Fig 4-12**, blue arrows) and send their axons in their respective directions (Green et al., 2014), now seem stuck at the more dorsal positions, closer to the RL. Interestingly, projections of the fasciculus uncinatus that develop from the Tbr^{+ve} NTZ cells are mostly eliminated. Additionally, the normal separation between the two cohorts of cells (NTZ and GCPs) seen in control embryos at E7 is not observed in the electroporated embryos.

It is difficult, therefore, to judge whether temporal transition between RL derivatives is maintained and the production of GCPs has started at their usual time, E6 (Wilson and Wingate, 2006). One possibility is that RL stem cells in which *NeuroD1* was misexpressed were forced to start differentiating themselves and could not produce GCPs, which are *NeuroD1*$^{-ve}$. Another possibility is that among the cells stuck at the dorsal side there are GCs. To investigate these possibilities, a marker specific for GCs would need to be used to label the cells. Unfortunately, most genes expressed in early GCPs are also expressed in CN neurons. One obvious marker, which is expressed in GCPs and not in preceding RL derivatives, is Atoh1 for which there is no easily available antibody. *In situ* hybridisation for Atoh1 is an option to try in the future to investigate generation of GCPs in *NeuroD1* misexpressing embryos. The fact that there is a limited proliferation of cells close to the RL (**Fig 4-13 A-C**) suggests that some proliferating GCPs might be present.

Nevertheless, a puzzling result was observed when staining the *NeuroD1* misexpressing cells with the PH3 proliferation marker. It was revealed that, contrary to expectations, *NeuroD1* misexpression is not sufficient to abrogate all proliferation in GCPs as some cells in the EGL still express PH3 at E8 following an E6 electroporation. Interestingly, a few cells are seen to express PH3 close to the RL following an E5 electroporation as well, suggesting that possibly the switch between NTZ cells and GCPs takes place following *NeuroD1* misexpression at E5. Because earlier RL derivatives are non-proliferative after they leave the RL, the $PH3^{+ve}$ cells can either represent RL progenitors or GCPs. Even if GCPs are formed in *NeuroD1* misexpressing embryos, their numbers would be small and they would

not form a typical highly proliferative EGL, as suggested by observing E5-E8 embryos that have a PH3 poor area where *NeuroD1* misexpressing cells are located.

It is important at this point to re-visit the results published in Butts et al., 2014 where the conclusions reached proved to be incomplete. In the paper, we suggest that misexpression of *NeuroD1* abolishes the formation of the EGL and that GC migrate straight into the IGL from the RL. However, the electroporation performed in that experiment (Fig 2F in Butts et al., 2014) was done at E4, two days before GCPs are born. Therefore, it is impossible to know whether GCs were affected by this manipulation. Based on the results from experiments that followed, presented in this thesis, it is more likely that GCPs were never formed following an E4 electroporation of NeuroD1. Rather, earlier RL derivatives were probably affected and their migration might have been disturbed, resulting in the deep localisation of cells at E7 and E8. However, these results would need to be clarified with molecular markers.

4.3.6 Outstanding questions and proposed further research

The results performed in this chapter raise a number of important questions about the role of *NeuroD1* in the development of RL derivatives and the usage of reporter constructs in assessing endogenous expression of genes.

Firstly, my results have shed some light on the role of *NeuroD1* in the development of RL derivatives and GCPs. However, important questions remain that were not fully answered in this project. Firstly, the endogenous expression of *NeuroD1* in all RL derivatives needs to be studied to understand the effect of *NeuroD1* manipulation on their development. At present it is unclear which populations are generated following NeuroD1 misexpression and whether the temporal sequence of RL neurons is preserved.

Secondly, the expression pattern of NeuroD1-CNE, although promising as a GCP differentiation reporter, needs further study. After cloning the reporter sequence into a Tol2 construct, it will be possible to tackle further outstanding question. For example, is NeuroD1-CNE expressed at different levels in different cells due to its ability to report on such variations in endogenous NeuroD1 levels, or the results obtained are due to plasmid dilution and variation in plasmid copy number following electroporation? Importantly, is endogenous *NeuroD1* expressed at a specific time in GCP differentiation? Is there a dosage effect, in that *NeuroD1* only activates terminal differentiation above a certain threshold? If so, will the NeuroD1-CNE reporter be powerful enough to discriminate between such threshold? Answering such question will permit the study of GCPs in unprecedented detail.

Chapter 5: General Discussion

In this thesis I have sought to further understand the development of granule cells of the cerebellum. I have concentrated my efforts on elucidating the morphological transitions of granule cell precursors in the developing chicken EGL both in fixed preparations and in live imaging studies. Additionally, I have explored the function of one transcription factor, NeuroD1, on the development of rhombic lip derivatives, especially granule cells. My results suggest that the mitotic and morphological transitions of GCPs in the EGL are more complex than previously reported. Moreover, I show that NeuroD1 is a potent differentiation factor that affects the development of all rhombic lip derivatives and leads to reduced granule cell proliferation, resulting in a smaller, unfoliated cerebellum.

5.1 Novel insights into granule cell precursors morphological transitions within the EGL

Current understanding of cerebellar granule cells morphological development is based on a number of key publications performed at the beginning of the last century and supplemented with additional studies in a number of species in 1960's to 1980's (Altman, 1972; Cajal, 1911; Quesada and Genis-Galvez, 1983; Rakic and Sidman, 1970). Those studies resulted in the established view on the sequence of morphological changes that granule cells undergo during development in the EGL. According to this view, GCPs proliferate in the outer EGL as round cells, potentially with a basal process. A postmitotic granule cell then extends two short process in a horizontal direction, parallel to the axis of the future folium. As the cell migrates tangentially in the inner EGL, the two processes extend and elongate, until the cell makes the switch from tangential to radial migration. The horizontal processes are then thought to transform into parallel fibres (Kumada et al., 2009). However, few studies have suggested that GCs can be mitotic while extending long processes or within the inner layers of the EGL and how such events could be explained in terms of linking proliferation, migration and differentiation of cells. Interestingly, even though some studies suggested that mitotic GCPs can extend processes or co-

express mitotic and neuronal differentiation genes (Wolf et al., 1997, Xenaki et al., 2011), this does not seem to be the established view in the field.

Results presented in this thesis offer evidence for a more complex view of GC development within the EGL and provides evidence for overturning some deep-rooted assumptions about their mitotic behaviour. Firstly, by labelling only a subset of granule cells in the chicken cerebellum it was possible to observe individual morphologies of GCs in the developing chicken EGL. A simple immunohistochemistry for the proliferation marker PH3 revealed an unexpected variety of morphological cell types labelled within the EGL. Granule cells in all layers of the EGL and possessing elaborate morphologies were labelled, strongly suggesting that traditionally postmitotic-looking GCs can in fact undergo mitosis. Secondly, live-imaging of cells in the developing EGL further strengthened the evidence for mitotic GCPs that can not only extend elaborate processes, but also migrate tangentially (and possibly radially within the EGL) before division. These results call for revisions to the current understanding of GCP biology and the role of the different morphologies they acquire within the EGL.

Taking these results into account, what exactly is the morphological sequence of events of GCPs in the EGL? Results obtained from both the fixed tissue and the live imaging suggest that some proliferating cells can extend long horizontal processes and undergo tangential migration. Additionally, all cells undergoing mitosis retract their long processes and round up prior to division. Therefore, one possibility is that as the cell migrates tangentially through the EGL, it continuously changes its shape from a migrating cell to a dividing cell and can undergo such changes repeatedly, until its final terminal division. From the current study, it is not possible to deduce what proportion of GCPs can undergo such elaborate changes. A relatively small number of $PH3^{+ve}$ cells were observed with very long processes in the inner EGL, suggesting that divisions of such morphologically differentiated cells are an exception, rather than a rule. Alternatively, cells start retracting their processes long before mitosis and therefore labelling cells with long processes is rare using anti-PH3 antibody. Using another proliferation marker would label a higher range of morphologies of GCPs.

Overall, I propose a model whereby the established sequence of morphological events in the EGL is largely correct, except for the fact that GCPs can revert to a less morphologically differentiated state throughout the EGL, until the point where such changes are no longer possible, following the final terminal division. I suggest that this decision is made by most cells in the middle EGL, before initiation of radial migration. Cells could make the decision of final division on an individual level, depending on the stochastic levels of various transcription factors and signalling molecules expressed in the cells or presence of a molecular switch might control the exit from the cell cycle (discussed in 5.3).

Moreover, the proportions of cells undergoing final terminal divisions is probably distributed throughout the EGL and only a small proportion of GCPs reach the highly differentiated morphologies seen in some cells in the inner EGL. It would be interesting to see how different morphologies of GCPs correlate with their division mode. For example, do GCPs with long horizontal processes only undergo terminal symmetric divisions, whereas the round outer EGL GCPs undergo symmetric proliferative divisions. Further, is there a certain morphological feature that predisposes GCPs to the relatively rare asymmetric divisions? A better culture system and longer live-imaging could potentially answer such questions in future studies.

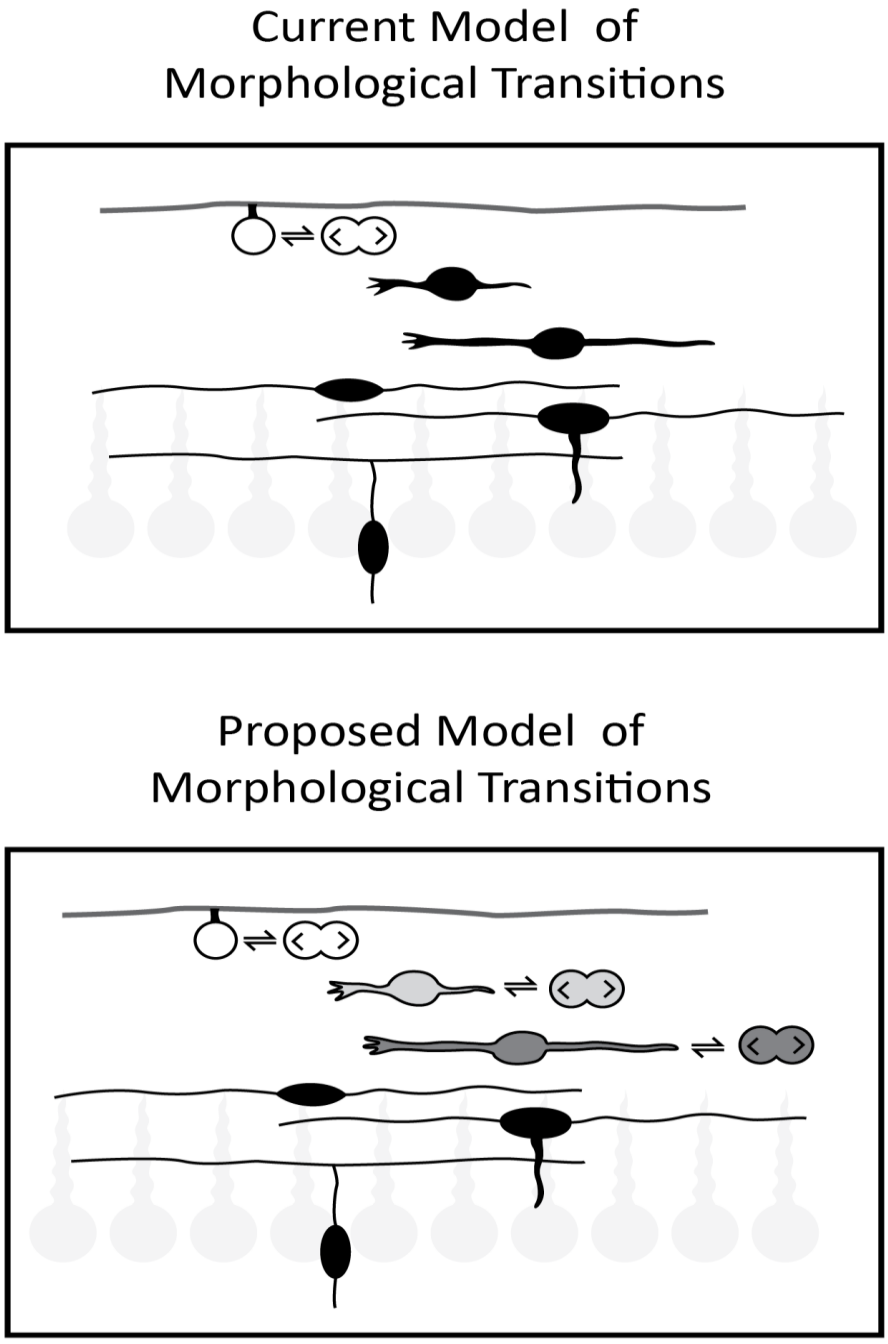

Figure 5-1 The proposed model of granule cell precursors morphological transitions in the EGL *(next page)*

Previous page:

Figure 5-1 The proposed model of granule cell precursors morphological transitions in the EGL

The current model of GCP morphological transitions postulates that mitotically active, polyhedral or round cells, with a basal attachment to the pial surface proliferate in the outer layer of the EGL. When the cell becomes postmitotic, it extends small horizontal processes and begins tangential migration. The processes continuously extend until the cell makes a switch to radial migration, at which point the horizontal processes are considered to be nascent parallel fibres.

Results from this work suggest that this model is incomplete. The proposed model retains and confirms the morphological features of GCs in the EGL, but suggest that cells previously considered postmitotic, can in fact be proliferative. Divisions of GCPs happen in all layers of the EGL and cells with long horizontal processes are able to revert back to mitosis by retracting all their processes and rounding up. In the picture, white shading represents a highly proliferative precursor, and black shading denotes a postmitotic cell. As cells migrate closer towards the inner EGL, the proliferative potential of the cells decreases, which means that the number of times the cell divides differs in the different layers, with many mitoses in the oEGL and few mitoses in the iEGL. A layer of Purkinje cells is shown in light grey.

5.2 The significance of granule cell precursor processes

One of the most important questions arising from the obtained results concerns the identity of the processes extended by GCPs at the different stages of their development, which include the basal process, the horizontal processes and the thin cytoneme-like processes. The basal process has been considered necessary for GCP proliferation. The current understanding implies that as GCPs start extending the two horizontal processes within the outer EGL, they represent leading and trailing processes of postmitotic neurons. These leading and trailing processes are then believed to transition into the parallel fibres, which are the axons of GCs. No study has ever suggested that GCPs can extend cytonemes.

My results have questioned the need for a basal process for GCP proliferation with the observations that GCPs can divide in the inner layer of the EGL and can migrate tangentially before dividing, without any apparent basal processes. What is therefore the role of the basal process of GCPs in the outer EGL? One possibility is that the signals from the basal lamina are required to maintain the Atoh1 expression in GCPs. Immunohistochemistry for Atoh1/Math1, revealed its expression to be limited to only the very outer EGL (Lewis et al., 2004, Xenaki et al., 2011). This suggests that only the cells in this layer, which have the possibility of retaining the short basal process, express Math1. Math1 expression has repeatedly been linked to mitotic activity of GCPs (Ayrault et al., 2010; Mulvaney and Dabdoub 2012; Zhao et al., 2008), however, cells expressing PCNA and Ki67 usually make up at least half of the EGL, suggesting that GCPs can stay proliferative even after cessation of Math1 expression. However, evidence against this conclusion comes from studies in mutant mice with perturbed organisation of the EGL where proliferation and Atoh1 expression is sustained outside of the oEGL (Zou et al., 1998). Therefore, the role of the basal process awaits further exploration.

Except for one report (Wolf et al., 1997) the possibility of proliferating GCPs extending processes has not been explored in any detail. Interestingly, Wolf et al (1997) obtained their results in cell culture and show a different morphological behaviour of GCPs to behaviour observed in this study. Namely, in Wolf et al.,

(1997), the processes extended from the cultured GCPs did not retract prior to cell division but maintained their length, thickness and orientation throughout cytokinesis. This result is in direct opposition to the results obtained in this study where in live-imaged cerebellar slices all dividing GCPs retracted their processes prior to cytokinesis. Data gathered from fixed tissue additionally show that cells in metaphase, anaphase and telophase never extend long and elaborate processes.

Many neuronal precursor cells extend processes during their proliferative activity but the role and fate of these processes differs in different progenitors. The best studied neuronal precursors include the PNS sympathetic neuroblasts, cerebral cortical radial glia and cortical basal progenitors, and the sub-ventricular zone (SVZ) neuronal progenitors. **Table 5-1** collects the similarities and differences between different precursor cells in different parts of the developing nervous system and compares them to GCPs.

During corticogenesis, radial glial cells have been studied extensively in the recent years. The current understanding is the neurons are born by asymmetric cell division of a polarised radial glial cell, which has an apical and a basal process that remains extended throughout cytokinesis. The neuronal daughter is a postmitotic cell that expresses neuronal markers such as Tuj1 and doublecortin. RGCs can also give rise to the transit amplifying precursors, which divide once and have no polarity before division. Newly discovered cortical basal progenitors retain their basal process during mitosis.

Similarly, the zebrafish retinal progenitors divide while retaining their basal processes, which is inherited by only one of the daughters or split between the daughter cells (Das et al., 2003).

In contrast, the SVZ neuronal progenitors that migrate within the rostral migratory stream into the olfactory bulb are capable of multiple divisions during migration, that are characterised by them retracting their processes prior to cytokinesis while also expressing a number of post-mitotic neuronal markers (Menezes et al., 1995, Coskun et al., 2007).

Even though this connection has not been proposed before, and even disputed (Wolf et al., 1997, Coskun et al., 2007) my results suggest that GCPs undergo very similar developmental behaviour to SVZ progenitors. They are not only able to proliferate during migration, but do so while expressing differentiation markers. Both precursors retract their processes prior to cytokinesis and extend them after division, presumably repeating this process multiple times. Additionally, clonally related SVZ precursors disperse during migration and are widely scattered in the olfactory bulb, in a similar fashion to clonally related GCs which reside at long distances from each other in the IGL (Espinosa and Luo, 2008), presumably subsequently to their migration away from each other after division, as shown though live imaging in this project. Overall, results suggest that GCPs are in many ways most similar to SVZ progenitors in their morphological differentiation sequence and might share common molecular mechanisms of de-differentiation.

5.3 Molecular explanation for granule cell precursor mitotic behaviour

An overriding principle of development is that neurons become permanently postmitotic once they initiate differentiation. Because neuronal migration follows neuronal birth in nearly all parts of the developing nervous system, a logical conclusion is that neurons are born from their proliferative progenitors, become postmitotic and start the differentiation processes which includes migration to their destination and integration within the forming neural circuits.

The first studies showing that this situation is not universal have explored the development of the SVZ progenitors, showing that they remain proliferative as they migrate in the RMS (Menezes et al., 1995; Pencea et al., 2001; Luskin and Coskun 2002; Coskun et al., 2007; Coskun and Luskin 2002). Other researchers have observed differentiating neurons in culture (expressing Tuj1 and bearing neurites) to undergo mitosis (DiCicco-Bloom et al., 1990; Memberg and Hall 1995).

Table 5-1 Comparison between different neuronal progenitors

Precursor type	Apico-basal polarity	Extends processes prior to division	Retracts processes prior to division	Migratory?	Expresses post-mitotic markers	Main division type	References
Cerebellar granule precursor	No	Yes	Yes	Yes, tangential migration	Yes, Tuj1, TAG1, DCX	SP, ST	This study, Xenaki et al, 2011
Subventricular zone progenitor in RMS	No	Yes	Yes	Yes, tangential migration	Yes	SP	Menezes et al. 1995; Pencea et al. 2001; Luskin and Coskun 2002; Coskun et al. 2007; Coskun and Luskin 2002
Apical progenitors (NEC, RGC)	Yes	Yes	No	No	No	AS	Götz and Huttner 2005 Miyata et al. 2015 Fietz and Huttner 2011
Cortical basal intermediate progenitors	No	No	No	No	No	ST, some SP	LaMonica et al. 2012 Nonaka-Kinoshita et al. 2013
Cortical basal radial glial cells	Some	Yes	No	No	No	ST	Nomura et al, 2016
Sympathetic neuroblasts (in culture)	N/A	Yes	No	NS	Yes	SP,ST	DiCicco-Bloom et al, 1990
Cortical GABA-ergic interneurons	Yes	Yes	No	No	No	AS,	Bandler et al, 2017

SP= symmetric proliferative division **ST**= symmetric terminal division **AS**= asymmetric division

However, following these early findings, surprisingly few researchers have continued the work of trying to explain how migration and proliferation can occur simultaneously in differentiating neurons This may be due to the fact that substantial amount of research into neuronal proliferation and differentiation is conducted in the developing cortex where neuronal migration has only been observed in postmitotic neurons

Granule cell precursors had always been known to be an exception to this developmental paradigm because they initiate a transit amplification stage after tangential migration from the rhombic lip. However, apart from a small number of reports to the contrary (Wolf et al., 1997), GCs are presumed postmitotic after extension of horizontal processes in the EGL. The only evidence suggesting that this might not be the case can be deduced from the existence of the middle EGL, where neuronal differentiation genes and mitotic markers are co-expressed (Xenaki et al., 2011). In this study, I provide evidence that GCPs divide whilst migrating tangentially in the middle and inner EGL and express known neuronal differentiation markers whilst mitotic. Because this is a relatively unexplored property of neuronal precursors anywhere in the developing nervous system, let alone in GCPs, identifying the possible molecular mechanisms for this behaviour will require additional research. Here, I present two possible mechanisms of GCP differentiation: a molecular switch hypothesis and accumulation of differentiation factors.

Because SVZ progenitors are the only other neuronal subtype to show similar behaviour to GCPs, parallel mechanisms might be at play to allow migratory cells to morphologically de-differentiate and revert to division. One suggested mechanism that explains the cellular behaviour of the SVZ progenitors involves the regulation of cell cycle regulatory proteins. Cyclin dependent kinase inhibitors (CKIs) are involved in the regulation of neurogenesis in many systems, by regulating timely withdrawal of progenitor cells from the cell cycle. Coskun and Luskin (2001) explored the role of the cell cycle inhibitor $p19^{INK4d}$ in the SVZ derived neuroblasts. They found a pronounced gradient of expression of $p19^{INK4d}$ in the RMS with increased numbers of immunoreactive cells closer to the olfactory bulb. This pattern was the opposite of BrdU labelled cells, which was highest close

to the SVZ. The authors proposed a model where $p19^{INK4d}$ is downregulated in the dividing RMS progenitors and re-expressed as the cell continues migration. This expression is regulated in a cyclical manner where a down regulation of $p19^{INK4d}$ is accompanied by morphological de-differentiation (Coskun et al., 2007). As cells migrate, they upregulate expression of $p19^{INK4d}$ and downregulate it again prior to mitosis. The same authors explored the role of BMP signalling in this system and found that proliferation and differentiation of SVZ derived cells are influenced by manipulated levels of BMP signalling, which might affect the expression of $p19^{INK4d}$ (Coskun et al., 2007).

Other implicated pathways and molecules in SVZ proliferation and differentiation include the Wnt pathway (Ikeda et al., 2010), axon guidance molecules (Jiao et al., 2008; Nguyen-Ba-Charvet et al., 2004; Saha et al., 2012) and many others (reviewed in Khodosevich et al., 2013).

Additionally, another CKI, $p27^{KIP1}$ has also been implicated in regulating proliferation and differentiation of SVZ migrating precursors (Li et al., 2009). Interestingly, differentiating granule cells in the inner EGL also express $p27^{KIP1}$ which can co-express with PCNA in the middle EGL. Miyazawa et al (2000) have found that p27 expression correlates with GC differentiation and plays a role in cessation of their proliferation, as part of a more complex mechanism. Unfortunately, $p19^{INK4d}$ expression has not been studied in cerebellum and no defects have been observed in the cerebellum of the mutant $p19^{INK4d}$ mouse (Behesti and Marino, 2009). However, numerous cell cycle proteins were found enriched in granule cell precursors, the role of many of which have not been studied in the cerebellum yet (Machold et al., 2011).

These results taken together suggest that CKIs or another cell cycle regulator might have a role in directing GCPs proliferation through cycling expression in the migrating GCPs in the middle EGL, analogous to the mechanism of cycling $p19^{INK4d}$ in the SVZ-derived neuroblasts. This kind of mechanisms would allow for the observed morphological differentiation and de-differentiation of GCPs.

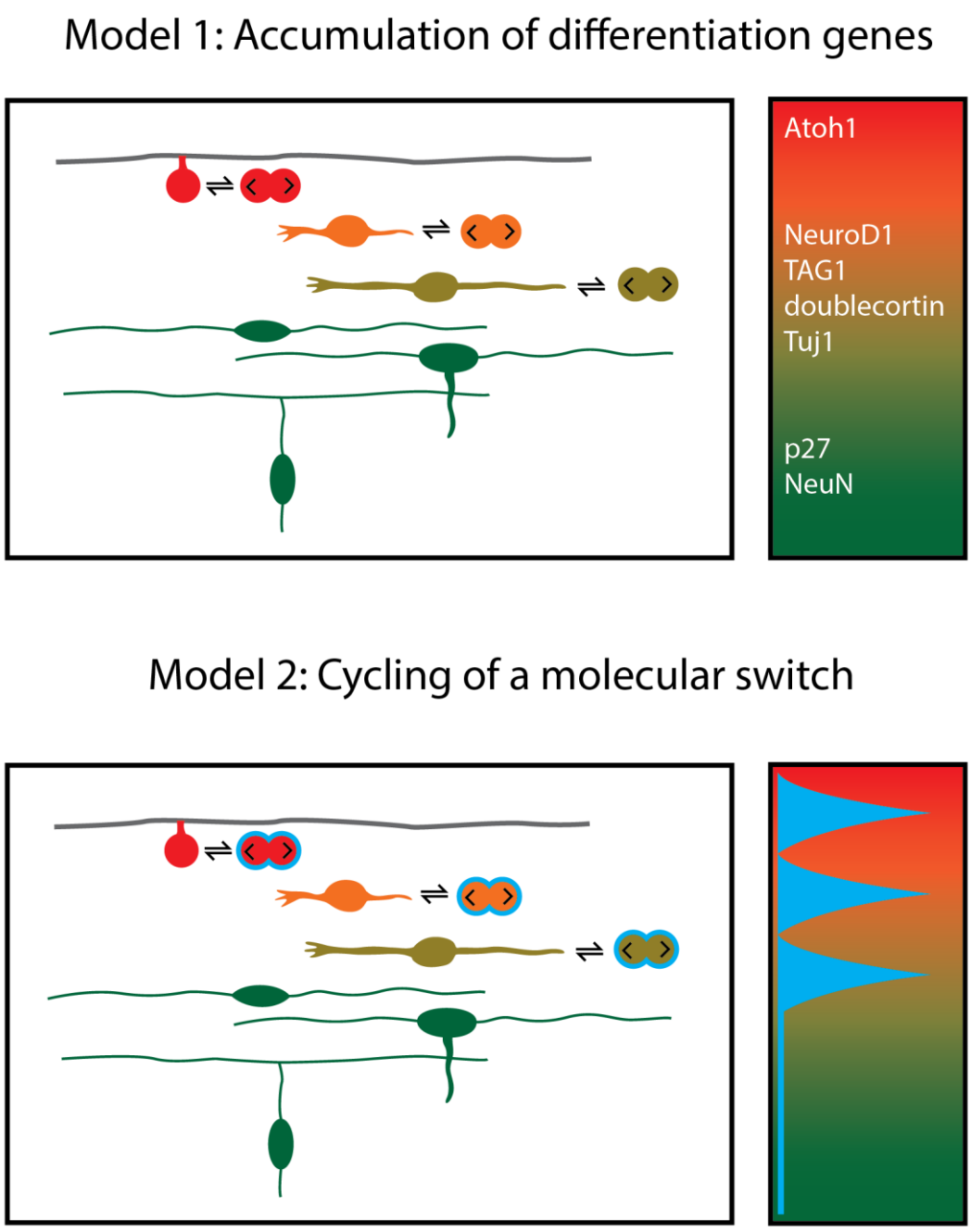

Figure 5-2 Possible models for differentiation of granule cell precursors

(next page)

Previous page:

Figure 5-2 Possible models for differentiation of granule cell precursors

As GCPs migrate away from the pial surface towards the inner EGL their gene expression profiles rapidly change. Atoh1 is downregulated, in part, by NeuroD1, which begins the differentiation process of GCPs. As the cells tangentially migrate within the inner EGL and begin to develop long parallel fibres they start expressing early axonal markers such as TAG1 and doublecortin and later new-born neuronal markers such as Tuj1 and NeuN. Differentiating granule cells also express cell cycle inhibitors such as p27. Throughout these differentiation stages GCPs are able to revert back to division by retracting their processes and undergoing mitosis.
One explanation for terminal differentiation of GCPs can be due to the accumulation of differentiation factors in the cell. As levels of various differentiation factors increase, the proliferative potential of GCPs decreases and in individual cells the stochastic levels dictate the time for final terminal division. Alternatively, an unidentified molecular switch might direct GCPs de-differentiation to allow them to revert back to mitosis, even though they are undergoing morphological differentiation processes such as migration and neurite extension. The levels of this molecular switch could fluctuate intrinsically and be independent of the extracellular environment. The withdrawal from the cell cycle would therefore coincide with morphological differentiation but not be governed by it.

Alternatively, the other model postulates that the accumulation of molecular changes turns a proliferating cell into a differentiated neuron. There are many different intrinsic and extrinsic signalling pathways and mechanisms involved in granule cell proliferation and differentiation in the EGL (Behesti and Marino 2009). One mechanism that is often used to explain differentiation of neuronal tissues is based on the interpretation of concentration gradients and induction of various genes at distinct threshold levels, including many feed-forward and feed-back loops that refine the genetic program. Therefore, not one gene is responsible for proliferation versus differentiation status of a cell, but the combined transcriptional landscape.

It is therefore impossible at this stage to elucidate the precise molecular mechanisms responsible for GCP proliferation and differentiation and the precise thresholds required for terminal differentiation. Results presented in this project complicate the matters even more by providing evidence for migratory and cycling behaviour of GCPs in the EGL, instead of the expected, cortex-like, postmitotic neuronal migratory behaviour. Available molecular studies of granule cell differentiation have not taken into account their ability to de-differentiate and should be re-evaluated in light of these recent findings. It might be useful to consider the implications from SVZ progenitor studies, which conclude that marker expression of SVZ progenitors represents a continuum of different cell types and various cell states (Mamber et al., 2013). It is possible that GCPs, even though they give rise to only one cell type, also represent a continuum of cell states, where transit amplifying progenitors give rise to differentiating intermediate GCP that can nonetheless de-differentiate and divide at least once.

Whether there is a single molecular switch that leads to terminal differentiation, or whether it is the accumulation of numerous molecular signals at the right levels in the cell, will need to be determined in future studies.

5.4 The role of NeuroD1 in cerebellar development

An important consideration following the second part of this project is where does NeuroD1 fit in the molecular landscape of GCP differentiation. Results collected in this project, as well as numerous previous studies, indicate that NeuroD1 is a potent differentiation factor. Recent studies have confirmed that NeuroD1 can be considered a pioneer factor in that it recognizes and binds its target sites even if they exist in closed chromatin (Pataskar et al., 2016). Neurogenic bHLH transcription factors have been shown to coordinate both neurogenesis and migration of neurons (Castro and Guillemot, 2011; Ge et al., 2006) and NeuroD1 has also been shown to regulate neuronal migration (Kim, 2013). Therefore, NeuroD1 is able to exert a complete neurogenic programme on the cells in which it is expressed. However, induction of target neuronal genes strongly depends on the levels of NeuroD1 and hence terminal differentiation would only occur at a certain threshold of NeuroD1 levels (Pataskar et al., 2016).

Interestingly, in the RMS, NeuroD1 expression has been observed with antibodies in some immature $BrdU^{+ve}$ cells, suggesting that its presence does not lead to immediate differentiation (Roybon et al., 2009). In contrast, Boutin et al (2010), have found by *in situ* hybridisation that only differentiating neurons in the olfactory bulb express NeuroD1, and its overexpression leads to induced terminal neuronal differentiation. Therefore, it seems that the expression of NeuroD1 is similarly unresolved in other systems, as it is in the cerebellum (see section 3.1.2.1).

Results from this project suggest that *NeuroD1* can be expressed in proliferating GCPs, but those neurons probably represent the later stages of GCP differentiation. Firstly, *NeuroD1* expression is not found in the outer EGL layer by *in situ* hybridisation. Secondly, *NeuroD1* misexpression leads to GCP premature differentiation. It would be interesting to be able to ascertain whether different levels of *NeuroD1* expression correspond to different fates of the dividing GCPs. Hypothetically, higher levels of *NeuroD1* expression should correspond to cells undergoing terminal symmetric divisions, whereas lower levels might lead to asymmetric divisions. Further, symmetrical proliferative might not be possible in

NeuroD1 expressing cells. However, these assumptions will need a more careful examination in long-term live imaging studies.

Results in this thesis support the long-held assumption that *NeuroD1* inhibits *Atoh1* expression in the GCPs. This correlation has been observed in numerous studies (especially Pan et al., 2009), but results in this thesis show for the first time that *NeuroD1* is a very potent inhibitor of *Atoh1* expression through one its most important enhancers (Helms et al., 2000). Therefore, a coordinated transition between the two bHLH TFs, Atoh1 and NeuroD1, is essential for normal cerebellar histogenesis and if the levels of either is manipulated, abnormal differentiation of granule cells is observed (Ben-Arie et al., 1997; Helms et al., 2001; Pan et al., 2009). In this study a particularly strong phenotype is observed in reduction of cerebellar size and foliation following *NeuroD1* misexpression in GCPs.

Chapter 6: Methods

6.1 Common solutions

ddH2O	Double distilled water (H2O), autoclaved
PBS	Phosphate buffered saline, autoclaved
PFA	4% paraformaldehyde in PBS
PBSTr	PBS with 1% Triton-X 100
Tris- HCl	Trizma base, minimum (Sigma) in ddH20 to desired pH with 2M HCl, autocalved
20xSSC (pH 4.5)	3M NaCl (BDH), 0.3M sodium citrate (Fisher Scientific); pH using 5M citric acid, autoclaved
5x MAB pH 7.5	500mM maleic acid (Sigma), 750MM NaCl (BDH); pH using 2M NaOH, autoclaved
MABT	1x MAB with 0.1% Tween-20 (Sigma)
Detergent mix:	1% IGEPAL CA-630 (Sigma), 1% SDS (Sigma), 0.5% deoxycholate (Fluka), 50mM Tris-HCL (pH 8), 1mM EDTA (Ambion), 150mM NaCl (BDH)
Whole mount hybridisation buffer:	50% formamide (Sigma), 5x SSC (pH4.5), 2% SDS (Sigma), 2% BBR in H2O
NTMT pH9.5	100mM NaCl (BDH), 100mM Tris-HCl (pH9.5), 50mM MgCl2 (BDH), 1% Tween-20 (Sigma); made up fresh
NTMT pH8	100mM NaCl (BDH), 100mM Tris-HCl (pH8), 50mM MgCl2 (BDH), 1% Tween-20 (Sigma); made up fresh
Tyrodes	137.0mM NaCl (BH), 2.7mM KCl (Sigma), 2.4mM CaCl2 (Sigma), 2.11 mM MgCl2.6H20 (BDH), 0.4mM NaH2PO4.2H2O (BDH), 5.6mM glucse (Sigma); autoclaved. For use added: 100U/ml penicillin, 100U/ml streptomycin, 0.3ug/ml Fungizone (Gibco)

Culture medium-chicken slices	Basal Medium Eagle, 0.5% (w/v) D-(+)-glucose, 1% B27 supplement, 2 mM L-Glutamine, 100 U/mL penicillin, 100 µg/mL streptomycin
Culture medium-mouse slices	48ml BME, 0.5ml 1x ITS, 0.5ml 45% glucose, 0.5ml Glutamine 0.5ml pen/strep
Culture medium-slice live imaging	Basal Medium Eagle, 0.5% (w/v) D-(+)-glucose, 1% B27 supplement, 2 mM L-Glutamine, 100 U/mL penicillin, 100 µg/mL streptomycin

6.2 Molecular techniques

6.2.1 Amplification of DNA constructs

DNA solutions were transformed into Subcloning Efficiency 5-alpha competent E.coli (NEB) according to manufacturer's instructions. Transforemed cells were plated out on appropriately selective LB agar (Sigma) plates and grow overnight at 37^{o}C. Individual colonies were picked to inoculate 150ml of appropriately selective LB (Sigma) and grown overnight at 37 ^{o}C, shaking at 213rpm. DNA for electroporation constructs was purified from cultures using QIAfilter plasmid maxi kit (Quiagen) or the NucleoBond Xtra maxiprep (Macherey-Nagel) according to the manufacturer's instructions.

6.2.2 Generation of NeuroD1-CNE

The full-length chick *NeuroD1* coding sequence was cloned into pGEMT-easy (Promega) by PCR (primers: forward – ATGACCAAGTCGTACAGCGAGA; reverse – TCACTCGTGGAAGATGGCGCTGA) from cDNA prepared from E12 cerebellum with TRIZOL (Invitrogen), and subcloned into the pCAGGS-IRES-GFP vector.

The genomic sequence of mouse covering the GENSAT BAC clone RP24-151C22 was used as the base sequence in a VISTA pairwise analysis with human, chick, *Xenopus tropicalis* and zebrafish. Conserved non-coding sequences were defined as those containing 70% sequence homology over a sliding window of 100bp. Using this data,

reporter constructs were constructed by building non-coding sequences directly upstream of GFP by PCR with long primers using proof reading Fusion polymerase (NEB) and cloned into pGEMT-Easy following A-addition. The mouse construct incorporates a conserved non-coding element upstream of the endogenous mouse basal NeuroD1 promoter and corresponds to the sequence from -401bp to +101bp relative to the longest 5'EST. The amphibian construct incorporates the *Xenopus tropicalis* conserved non-coding element upstream of the *Xenopus tropicalis* basal promoter, corresponding to the sequence from -372bp to +96bp relative to the longest 5'EST. As a control, we assembled a construct containing only the basal promoter from the mouse corresponding to the genomic sequence from -146bp to +101bp upstream of GFP. The Atoh1-cre plasmid (Kohl et al., 2012) was co-electroporated with pFlox-pA-mCherry (lox-stop-lox mCherry). All constructs were confirmed by sequencing.

6.3 Animals

6.3.1 Chicken embryos

All procedures on chicken embryos were performed with accordance to King's College London and UK Home Office animal care guidelines.
Fertilised wild type eggs (Henry Stewart, UK) were incubated at 38˚C for 3-14 days. For *in ovo* electroporations eggs were windowed using sharp scissors and closed with selotape after adding 1ml Tyrodes solution. Embryos were removed from windowed eggs using hooked forceps. From E7 heads of embryos were severed immediately upon removal from the egg and the bodies were discarded. E14 embryos were decapitated in the egg and their heads were removed into a Petri dish. The embryos were typically fixed overnight in 4% PFA and then stored in PBS with 0.02% NaN3 (sodium azide, Sigma).

6.3.2 Mouse embryos

All procedures on mouse embryos were performed with accordance to the Rockefeller University and US animal care guidelines. Embryos were used at P7-8.

6.4 *In ovo* chicken electroporation

Fertilised eggs were incubated at 38 °C for 4-6 days. The eggs were drained a day before use with a hypodermic needle; 3-4ml of egg white was removed. The eggs were then windowed using egg scissors and, depending on the age, the embryo was located and its position manipulated for ease of access. DNA constructs at 1-2ug/ul were mixed with trace amounts of fast green (Sigma) and injected into the fourth ventricle directly below the rhombic lip using a glass needle. Where two or more constructs were co-electroporated both were mixed in equal concentrations (unless otherwise stated), each at concentration of at 1-2ug/ul. The negative electrode was placed underneath the embryo at the level of rhombic lip and the positive electrode was placed on the embryo at the same level. The cerebellar rhombic lip was targeted this way. Three 50ms/10 V square waveform electrical pulses were passed between the electrodes so that DNA entered the right side of the neural tube. Eggs were then treated with the tyrodes solution (1ml) and sealed back using sticky tape. Eggs were incubated at 38 °C until the embryos were harvested at appropriate experimental age. The embryos were fixed overnight at 4 °C in 4%PFA.

6.4.1 List of electroporated constructs

Electroporation construct	**Reference**
pCAGGS-GFP	pCAGGS-eGFPm5 (Yaneza et al., 2002)
Math1-cre	Helms et al., 2000, Wingate lab, made by replacing LacZ with cre-recombinase
pT2K-CAGGS-EGFP	Kita et al., 2013
pCAGGS-T2TP	Kita et al., 2013
Lox-stop-lox-GFP	Morin et al., 2007
pCAAGS-RFP	Wingate lab
UAS-synaptophysin-GFP	Gift from Martin Mayer
UAS-PSD95-TdTomato	Gift from Martin Mayer
Geminin-GFP	Gift from David Solecki
Cdt1-RFP	Gift from David Solecki

KO2-GeminiMyrAG1	Gift from David Solecki
NeuroD1-CNE	Thomas Butts in the Wingate lab, Butts et al., 2014
NeuroD1	Thomas Butts in the Wingate lab, made using full-length NeuroD1 sequence, Butts et al., 2014
CAGGS-mCherry	Wingate lab
Lox-stop-lox-mCherry	Wingate lab
CAGGS-Tdtomato	Gift from Hatten lab
Math1-GAL4	Made in this study using Math1-cre and alpha-Tubulin-GAL4, a gift from Sarah Guthrie

6.5 *Ex vivo* chicken cerebellar electroporation and slice culture

6.5.1 Preparations and dissection of the cerebellum

Fertilised eggs were incubated at 38 ^{o}C for 14 days. Eggs were allowed to rest at room temperature for at least 1hr before being windowed with egg scissors. The chicken embryo was located in the egg and its neck was cut with sharp scissors, removing the head into a Petri dish containing ice cold PBS. The cerebellum was then dissected out using a preferred method. The dissected cerebellum was moved to a fresh Petri dish with ice cold HBSS.

6.5.2 Slicing of the cerebellum

The cerebellum was transferred to the sterile platform of a Tissue Chopper using a spatula or a 3ml Pasteur pipette with the tip cut away to widen the aperture. Excess liquid was removed using a pipette. The entire whole cerebellum was cut in the required orientation at 300 µm thickness using the tissue chopper set with a cutting speed at 50% of the maximum. Using a 3 ml Pasteur pipette, the sliced cerebellum was covered in ice cold HBSS. The slices were transferred in HBSS to a 60 mm petri dish containing ice cold fresh HBSS using a 3ml Pasteur pipette with cut tip. Under a dissecting microscope illuminated with a fiber optic light source, individual slices were separated using watchmaker forceps. Slices to be electroporated were identified based upon their tissue integrity and medio-lateral position.

6.5.1 Electroporation of slices

An electroporation chamber was constructed by fixing the anode of an electroporator to the base of a 60 mm petri dish with insulation tape. Approximately 1 ml of HBSS was added to cover the electrode. A 0.4 μm culture insert was placed on top of the electrode covered in HBSS. The culture insert was allowed to rest on the electrode and it was ensured that there is always contact between the insert and the electrode. Identified slices (up to five per culture insert) were transferred onto culture insert using 3 ml Pasteur pipette with the cut tip. The slices were separated and allowed to settle onto culture insert in a sagittal orientation. Using a pipette, excess HBSS was removed so that slices were no longer bathed in solution. Using a P10 pipette tip, DNA was pipetted (at a concentration of 1 μg/μL) diluted with 20% fast green over the surface of targeted region of a slice. 20% fast green ensures viscous DNA solution and prevents prohibitively wide dispersal of DNA. Approximately 5 μL DNA/fast green solution was added to each slice. The cathode was placed over desired targeted tissue, which was electroporated with 3 x 10 V, 10 ms duration pulses. Direct contact of the cathode with the tissue was avoided. Instead, the surface tension of the liquid was used to maintain conductance. DNA delivery and electroporation to multiple regions of EGL was repeated on each individual cerebellar slice as desired.

6.5.1 Slice culture

Upon completion of electroporation, culture insert was transferred to 30 mm petri dish. To each culture, 1 ml of pre-warmed culture medium was added underneath the culture insert such that the culture insert was in contact with the medium, but slices were not bathed in it. Cultures were incubated at 37 ^{0}C/6% CO_2 for up to 3 days. All of the culture medium was replaced every 24 hours with fresh pre-warmed medium. Following culture, fix slices on culture inserts for 1 hour at room temperature in 4% paraformaldehyde (or overnight at 4 ^{0}C) in a fresh 30 mm dish with no culture media.

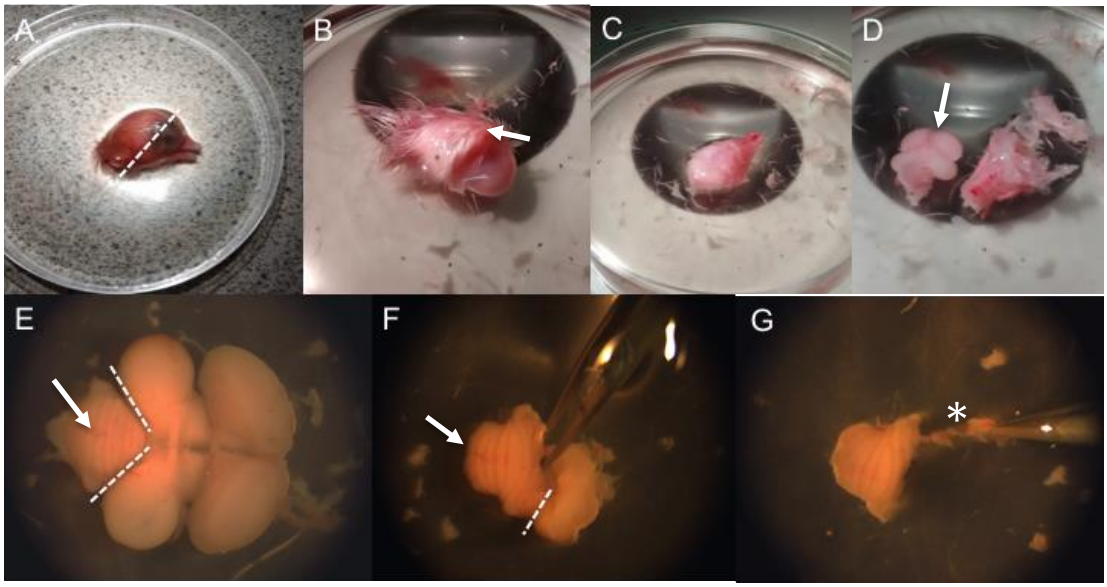

Figure 6-1 Dissection of the cerebellum from E14 chick embryos

A) Decapitate the chick in the egg and remove the head into a petri dish with ice cold PBS. Remove the lower jaw and the eyes by making incision behind the eyes and the pharynx (dashed line). **B)** Remove the skin from the surface of the skull (arrow). **C**) Remove the frontal and parietal bones and (**D**) remove the brain (arrow) from the mesenchyme and cartilage surrounding it. **E)** Under a dissecting microscope identify the location of the cerebellum at the posterior end of the brain (arrow). Cut between the midbrain and the hindbrain (dashed lines) to be left with the cerebellum and ventral hindbrain. **F)** Make incisions at the lateral junctions (peduncles) of the cerebellum (arrow) to separate the cerebellum from the hindbrain (dashed line). **G)** Remove the choroid plexus (asterisk) from the ventral side of the cerebellum until you are left with a whole intact cerebellum with the pia attached. Transfer the cerebellum into ice-cold HBSS before preparing slices with a tissue chopper.

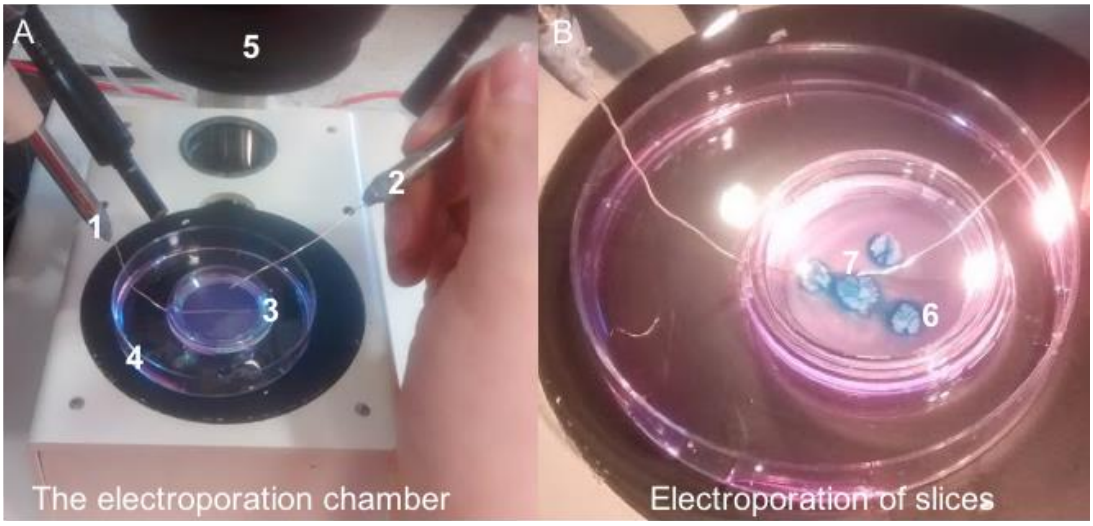

Figure 6-2 The electroporation chamber set up

A) A picture of the custom-made electroporation chamber. The chamber consists of an anode of an electroporator placed securely on the base of a 60 mm petri dish. Insulation tape can be used to secure the anode. The dish contains approximately 1 ml of HBSS to cover the electrode. The culture insert should rest on the electrode with constant contact between the insert and the electrode, maintaining the circuit but allowing spatial targeting of the cathode, which is manipulated by hand. **B)** A picture of slices being electroporated. Slices are covered with the DNA/fast green solution. The slices are electroporated as desired: electroporation can be targeted to one folium or multiple locations. After electroporation the insert is placed in a 30mm Petri dish with pre-warmed culture medium and cultured in the incubator. **1.** The anode **2.** The cathode **3.** Culture insert **4.** Petri dish with 1ml HBSS **5.** Dissecting microscope **6.** Individual slices from tissue chopper **7.** DNA solution with fast green dye.

6.6 *Ex vivo* mouse cerebellum electroporation and culture

Before starting, the DNA concentration and volume should be determined. To fill the electrode chamber at least 100ul of DNA is required. For 3-5 cerebella I made 300ul of DNA solution of 1.5-4.0ug/ul concentration. The DNA is diluted in complete HBSS with extra glucose (76mM glucose). 5x HBSS is used for these dilutions. Cerebella were dissected in complete HBSS with extra glucose, on ice. Cerebella for each condition were placed into separate 50ml tubes with complete HBSS with extra glucose. After dissections were completed all liquid was removed from the cerebella and the DNA solution was added on top. The cerebella were allowed to soak for 15-20min in the DNA solution. Afterwards, one cerebellum was placed in a petridish electrode chamber on ice and 100ul DNA solution was added on top to fill the chamber. The cerebellum was electroporated at 80V, 5 pulses, 50ms pulses and 500 ms intervals. Next, the cerebellum was removed and placed in ice-cold complete HBSS with extra glucose on ice to recover for ten minutes. The cerebellum was then imbedded in 3% agarose in complete HBSS with regular glucose (30mM). The cerebella were cut using a vibrotome into 250um slices and placed on inserts with 1.5ml pre-warmed slice medium underneath. The slices were incubated at 35^{o}C/5%CO2.

6.7 Time-lapse imaging of chicken cerebellar slices

Chicken embryos were electroporated with Tol2:GFP constructs at E4 and the embryos were incubated up to embryonic day 11 to 14. Cerebella were then dissected in cold HBSS and checked for fluorescence with an epifluorescent microscope. Cerebellum with appropriate levels of fluorescent cells was chopped using a tissue chopper into 250mm slices. Slices with best cellular morphologies were chosen and transferred using a plastic pipette into a pre-assembled coverslip with a glass ring attached with silicon grease to create vacuum in the Rose chamber. The chamber is constructed from two 25 mm2 coverslips, a silicon spacer, a metal planchet milled to accept a condenser lens. The whole assembly is held together by two metal clips attached to the sides. The chamber can be filled and drained using two 25G needles and a syringe. Excess liquid transferred with

the tissue was removed from the cover slip, making sure that the cerebellar slice lies flat on the cover slip. 500ul of collagen prepared to a neutral pH was then added on top of the slice in the glass ring, making sure that the slice remains close to the surface of the cover slip. The cover slip with the cerebellar slice was then incubated at 37^{o}C 5% CO_2 for 30 min to 1hr. After the collagen has set, another cover slip was placed on top of the ring and the rest of the rose chamber was assembled. 2ml of pre-warmed (37^{o}C 5%CO_2) culture medium was added to the sealed chamber and the preparation was immediately imaged using a confocal microscope overnight (12-16hrs) with 20min intervals between time points.

6.8 Histological techniques

6.8.1 Sectioning

6.8.1.1 Gelatine embedding and vibrotome sectioning

Fixed and washed embryos were placed in pre-warmed 20% gelatine (Fluka) in PBS at 65^{o}C for 1 hour. Embryos were transferred into fresh pre-warmed 20% gelatin in PBS in moulds and oriented appropriately before allowing gelatin to set by cooling the mould in an ice bath. Once set, gelatine blocks were cooled for further 30min at 4^{o}C and then removed from moulds and cut using a razor blade into blocks appropriate for sectioning. Blocks were fixed in 4% PFA overnight at 4^{o}C. Before sectioning, blocks were washed in PBS three times for 10mins, dried with a tissue and glued with superglue to the chick of a vibrotome (Leica VT1000S). The block was submerged in PBS and cut into 150um sections. Sections were mounted under a coverslip on Superfrost slides in Fluoroshield mounting medium with DAPI (Abcam).

6.8.1.2 Cryosectioning

E14 chicken cerebellum was fixed in 4% PFA overnight. The tissue was then washed in PBS 3 times for 15 min and then transferred into 10% sucrose (Sigma) in PBS for 30min until the tissue was perfused (sunk to the bottom). The tissue was then transferred to 20% sucrose solution until perfused and finally was transferred into 30% sucrose solution and allowed to perfuse overnight. The tissue was then transferred into OCT compounds (VWR) in moulds and placed on dry ice or liquid nitrogen to freeze. The tissue was then stored at -80˚C overnight. For

sectioning, the blocks were placed at -20˚C an hour before cutting to raise their temperature. The tissue was mounted on cryostat chucks using OCT compound and cut using a Zeiss Microm HM 560 cryostat at 50um thickness and transferred onto Superfrost Plus slides (VWR). The cut sections were allowed to air dry for two hours and were stored at -80˚C long term and -20˚C short term.

6.8.2 Wholemount RNA *in situ* hybridisation

The embryos were fixed in 4% PFA overnight at 4^{o}C. If the protocol was done on cultured cerebellar slices, they were left attached to the membrane throughout the protocol. The tissue was washed in PBSTw for 10min and dehydrated by washing 5 min each in 25%, 50%, 75% methanol in PBSTw. The tissue was then washed in 100% ethanol for 5 min and bleached in 1.8% H_2O_2 in methanol for 1 hr. The tissue was then washed twice in 100% methanol for 5min each time and rehydrated by washing for 5 min each in 75%, 50%, 25% methanol in PBSTw. The tissue was then washed 3 times for 5 min in PBSTw and transferred into a detergent mix, two times for 20min. Next, the tissue was fixed in 4%PFA for 20min and washed twice with PBSTw for 5min. Following the washes, pre-warmed hybridization buffer was added to the tissue for 1-4 hrs and incubation was performed at 70^{o}C. 1ug/ml DIG labelled probe was combined with fresh pre-warmed hybridization buffer and incubated at 70^{o}C for 10min. The buffer with the probe was then added to the tissue overnight at 70^{o}C. The next day, the tissue was washed in pre-warmed solution X at 70˚C twice for 5min and then again 2 times for 30min. Next, the tissue was washed five times for 5min in room temperature MABT and then again two times for 30min in room temperature MABT. The tissue was put in blocking solution for 1-2 hours. Next, the tissue was incubated overnight in blocking solution with alkaline phosphate conjugated anti-DIG antibody diluted 1:2000 at 4˚C. The following day the tissue was washed in MABT three times for 5 min, and again two time for 1 hr, and then overnight at 4^{o}C. The following day, the tissue was washed for 10min in pH9.5 NTMT. To develop blue signal, the tissue was bathed in 5ul/ml NBT/BCIP in pH 9.5 NTMT at RT in the dark. The staining solution was replaced every 4-5 hours. If staining has not happened that day, the tissue was stored in MABT overnight at 4 ^{o}C and staining was continued the following day. When staining was complete, the tissue was washed with MABT for

5 mins, and then washed with PBSTw two times for 5 mins. The tissue was fixed with 4%PFA overnight at 4 ^{o}C and stored in PBS with 0.02% NaN3.

The probes used in this project and conditions for making an antisense riboprobe are summarized below:

Gene	Restriction Enzyme	Transcribe with	Reference
Cath1	Not2	T3	Wilson and Wingate, 2006
NeuroD1	Sac1	T3	Thomas Butts

6.8.3 Immunohistochemistry

6.8.3.1 Whole-mount

This protocol refers to embryos sacrificed from E4 until E14 which were immunostained wholemount, without previous sectioning.
After obtaining the embryo from the egg, the embryo was dissected appropriately (usually the hindbrain was dissected completely at stages E4- E10, whole cerebellum was dissected at E11-E18). The embryo was fixed in 4% PFA for at least 2 hrs to overnight. For some antibodies, a short, 15 min, fixation was required. The tissue was then washed three times in PBS with 1% Triton 100x for 30 min each time. Embryos were then incubated for 1-3 hr at room temperature in block (PBS 1% Triton + 10% FCS +0.02% sodium azide). Afterwards, the embryos were incubated with the primary antibodies at the required concentration (see table in 6.8.3.3) for 1-3 nights on a gentle rotator at 4 degrees C. After incubation, the embryso were washed three times in PBS 1% Triton, 1 hr each time. Next, a combination of secondary antibodies (Alexa Fluor) was added to the tissue in block solution, for one night. The following day, the tissue was washed with PBS 1% Triton two times for 30 min. Afterwards, the tissue could be imaged or sectioned.

6.8.3.2 Frozen sections (cryosections)

Cryostat sections were defrosted for at least 30min at room temperature. The slides were then washed three times for 5 min in PBS. Slides were then covered in 500-800ul block (1% normal goat serum, 0.2% Triton in PBS) and incubated for 30min at RT. Primary antibody was diluted at an appropritate concentration in the blocking solution. After the blocking solution was removed from the slides, 150-200ul of the antibody solution was added onto the slide and covered with parafilm to prevent drying out. Incubation was performed overnight at 4^{o}C. The next day, primary antibody as washed off with PBS three times for 5 mins. Secondary antibody was diluted in block solution and put onto the slides for 2hrs at RT. The slides were then washed with PBS three time for 5mins and covered with a coverslip using Fluoroshield mounting medium with DAPI (Abcam).

6.8.3.3 List of antibodies used

Antigen	**Raised in**	**Company**	**Concentration**
calbindin	Rabbit	SWANT	1:2000
Phosphohistone H3	Rabbit	Cell signalling	1:150
GFP	Mouse	Abcam	1:1000
GFP	Rabbit	Life Technologies	1:1000
TAG1/Axonin1	Mouse	Hybridoma Bank 4D7/TAG1	1:100
Alexa Fluor 488, 568, 633	Mouse/ rabbit	Thermo Fisher Scientific	1:500

6.9 Imaging

Low magnification pictures of whole embryos and whole cerebella were captured using a Leica stereoscope fitted with a Q-imaging Retiga EXi camera. Embryos were photographed in PBS.

Hindbrains dissected in PBS were flat-mounted by cutting along the dorsal midline of the tissue and mounting the brains pial-side up on twinfrost glass slides. Tissue was mounted in 90% glycerol and silicon grease was used to support a coverslip on the tissue.

Fluorescent confocal images were taken with Zeiss LSM 800 microscope or Olympus FV 500. Z-stack projections were compiled using ImageJ. Z-stacks were taken at 1-20um intervals.

Live imaging was conducted using Nikon Eclipse EZ-C1 microscope using a 20x objective lens. Images were taken every 20mins for 12-28hrs. For analysis, variable z-stack projections were chosen from the whole z- stack, depending on the best combination to observe specific cell morphologies.

Bibliography

Alcántara, S., Ruiz, M., De Castro, F., Soriano, E., and Sotelo, C. (2000). Netrin 1 acts as an attractive or as a repulsive cue for distinct migrating neurons during the development of the cerebellar system. Development *127*, 1359–1372.

Alder, J., Cho, N.K., and Hatten, M.E. (1996). Embryonic precursor cells from the rhombic lip are specified to a cerebellar granule neuron identity. Neuron *17*, 389–399.

Alexandre, P., Reugels, A.M., Barker, D., Blanc, E., and Clarke, J.D.W. (2010). Neurons derive from the more apical daughter in asymmetric divisions in the zebrafish neural tube. Nat. Neurosci. *13*, 673–679.

Allen, G. (2006). Cerebellar contributions to autism spectrum disorders. Clin. Neurosci. Res. *6*, 195–207.

Altman, J. (1972). Postnatal development of the cerebellar cortex in the rat. I. The external germinal layer and the transitional molecular layer. J. Comp. Neurol. *145*, 353–397.

Anne, S.L., Govek, E.E., Ayrault, O., Kim, J.H., Zhu, X., Murphy, D.A., Van Aelst, L., Roussel, M.F., and Hatten, M.E. (2013). WNT3 inhibits cerebellar granule neuron progenitor proliferation and medulloblastoma formation via MAPK activation. PLoS One *8*.

Arai, Y., Pulvers, J.N., Haffner, C., Schilling, B., Nüsslein, I., Calegari, F., and Huttner, W.B. (2011). Neural stem and progenitor cells shorten S-phase on commitment to neuron production. Nat. Commun. *2*, 154.

Ayala, R., Shu, T., Tsai, L.-H., Humbert, S., Wu, C.L., Lanier, L.M., Gertler, F.B., Vidal, M., Etten, R.A. Van, Tsai, L.H., et al. (2007). Trekking across the brain: the journey of neuronal migration. Cell *128*, 29–43.

Ayrault, O., Zhao, H., Zindy, F., Qu, C., Sherr, C.J., and Roussel, M.F. (2010). Atoh1 Inhibits Neuronal Differentiation and Collaborates with Gli1 to Generate Medulloblastoma-Initiating Cells. Cancer Res. *70*, 5618–5627.

Bailey, F., and Miller, A. (1921). Textbook of Embryology (New York: William Wood and Co.).

Barthelery, N.J., and Manfredi, J.J. (2016). Cerebellum Development and Tumorigenesis: A p53-Centric Perspective. Trends Mol. Med. *22*, 404–413.

Behesti, H., and Marino, S. (2009). Cerebellar granule cells: Insights into proliferation, differentiation, and role in medulloblastoma pathogenesis. Int. J. Biochem. Cell Biol. *41*, 435–445.

Ben-Arie, N., Zoghbi, H.Y., Bellen, H.J., Armstrong, D.L., McCall, A.E., Gordadze, P.R., Guo, Q., and Matzuk, M.M. (1997). Math1 is essential for genesis of cerebellar granule neurons. Nature *390*, 169–172.

Bertrand, N., Castro, D.S., and Guillemot, F. (2002). Proneural genes and the specification of neural cell types. Nat. Rev. Neurosci. *3*, 517–530.

Bischoff, M., Gradilla, A.-C., Seijo, I., Andrés, G., Rodríguez-Navas, C., González-Méndez, L., and Guerrero, I. (2013). Cytonemes are required for the establishment of a normal Hedgehog morphogen gradient in Drosophila epithelia. Nat. Cell Biol. *15*, 1269–1281.

Blaess, S., Graus-Porta, D., Belvindrah, R., Radakovits, R., Pons, S., Littlewood-Evans, A., Senften, M., Guo, H., Li, Y., Miner, J.H., et al. (2004). 1-Integrins Are Critical for Cerebellar Granule Cell Precursor Proliferation. J. Neurosci. *24*, 3402–3412.

Boutin, C., Hardt, O., de Chevigny, A., Coré, N., Goebbels, S., Seidenfaden, R.,

Bosio, A., and Cremer, H. (2010). NeuroD1 induces terminal neuronal differentiation in olfactory neurogenesis. Proc. Natl. Acad. Sci. U. S. A. *107*, 1201–1206.

Broom, E.R., Gilthorpe, J.D., Butts, T., Campo-Paysaa, F., and Wingate, R.J.T. (2012). The roof plate boundary is a bi-directional organiser of dorsal neural tube and choroid plexus development. Development *139*, 4261–4270.

Buckner, R.L. (2013). The cerebellum and cognitive function: 25 years of insight from anatomy and neuroimaging. Neuron *80*.

Butts, T., Chaplin, N., and Wingate, R.J.T. (2011). Can clues from evolution unlock the molecular development of the cerebellum? Mol. Neurobiol. *43*, 67–76.

Butts, T., Green, M.J., and Wingate, R.J. (2014a). Development of the cerebellum: simple steps to make a "little brain." Development *141*.

Butts, T., Hanzel, M., and Wingate, R.J.T. (2014b). Transit amplification in the amniote cerebellum evolved via a heterochronic shift in NeuroD1 expression. Development *141*.

Cajal, S.R. (1911). Histologie du système nerveux de l'homme et des vertébrés. Vol. 2. Paris Maloine 891–942.

Carletti, B., and Rossi, F. (2008). Neurogenesis in the Cerebellum. Neurosci. *14*, 91–100.

Castro, D.S., and Guillemot, F. (2011). Old and new functions of proneural factors revealed by the genome-wide characterization of their transcriptional targets. Cell Cycle *10*, 4026–4031.

Chan, J.A., Balasubramanian, S., Witt, R.M., Nazemi, K.J., Choi, Y., Pazyra-Murphy, M.F., Walsh, C.O., Thompson, M., and Segal, R.A. (2009). Proteoglycan interactions with Sonic Hedgehog specify mitogenic responses. Nat. Neurosci. *12*, 409–417.

Cho, J.-H., and Tsai, M.-J. (2004). The role of BETA2/NeuroD1 in the development of the nervous system. Mol. Neurobiol. *30*, 35–47.

Cho, J.H., and Tsai, M.J. (2006). Preferential posterior cerebellum defect in BETA2/NeuroD1 knockout mice is the result of differential expression of BETA2/NeuroD1 along anterior-posterior axis. Dev. Biol. *290*, 125–138.

Compagnucci, C., Piemonte, F., Sferra, A., Piermarini, E., and Bertini, E. (2016). The cytoskeletal arrangements necessary to neurogenesis. Oncotarget *7*, 19414–19429.

Constantin, L., Constantin, M., and Wainwright, B.J. (2016). MicroRNA Biogenesis and Hedgehog-Patched Signaling Cooperate to Regulate an Important Developmental Transition in Granule Cell Development. Genetics *202*, 1105–1118.

Corrales, J.D. (2004). Spatial pattern of sonic hedgehog signaling through Gli genes during cerebellum development. Development *131*, 5581–5590.

Corrales, J.D., Blaess, S., Mahoney, E.M., and Joyner, A.L. (2006). The level of sonic hedgehog signaling regulates the complexity of cerebellar foliation. Development *133*, 1811–1821.

Coskun, V., and Luskin, M.B. (2001). The expression pattern of the cell cycle inhibitor p19(INK4d) by progenitor cells of the rat embryonic telencephalon and neonatal anterior subventricular zone. J. Neurosci. *21*, 3092–3103.

Coskun, V., and Luskin, M.B. (2002). Intrinsic and extrinsic regulation of the proliferation and differentiation of cells in the rodent rostral migratory stream. J. Neurosci. Res. *69*, 795–802.

Coskun, V., Falls, D.L., Lane, R., Czirok, A., and Luskin, M.B. (2007). Subventricular zone neuronal progenitors undergo multiple divisions and retract their processes prior to each cytokinesis. Eur. J. Neurosci. *26*, 593–604.

D'Arcangelo, G., G.Miao, G., Chen, S.-C., Scares, H.D., Morgan, J.I., and Curran, T. (1995). A protein related to extracellular matrix proteins deleted in the mouse mutant reeler. Nature *374*, 719–723.

Dahmane, N., and Ruiz i Altaba, A. (1999). Sonic hedgehog regulates the growth and patterning of the cerebellum. Development *126*, 3089–3100.

Das, R.M., and Storey, K.G. (2014). Apical Abscission Alters Cell Polarity and Dismantles the Primary Cilium During Neurogenesis. Science (80-.). *343*, 200–204.

Das, T., Payer, B., Cayouette, M., and Harris, W.A. (2003). In vivo time-lapse imaging of cell divisions during neurogenesis in the developing zebrafish retina. Neuron *37*, 597–609.

DiCicco-Bloom, E., Townes-Anderson, E., and Black, I.B. (1990). Neuroblast mitosis in dissociated culture: regulation and relationship to differentiation. J. Cell Biol. *110*.

Eddison, M., Toole, L., Bell, E., and Wingate, R.J.T. (2004). Segmental identity and cerebellar granule cell induction in rhombomere 1. BMC Biol. *2*, 14.

Elvers, M., Pfeiffer, J., Kaltschmidt, C., and Kaltschmidt, B. (2005). TGF-??2 neutralization inhibits proliferation and activates apoptosis of cerebellar granule cell precurors in the developing cerebellum. Mech. Dev. *122*, 587–602.

Englund, C., Kowalczyk, T., Daza, R.A.M., Dagan, A., Lau, C., Rose, M.F., and Hevner, R.F. (2006). Unipolar brush cells of the cerebellum are produced in the rhombic lip and migrate through developing white matter. J. Neurosci. *26*, 9184–9195.

Espinosa, J.S., and Luo, L. (2008). Timing Neurogenesis and Differentiation: Insights from Quantitative Clonal Analyses of Cerebellar Granule Cells. J. Neurosci. *28*.

Esteves de Lima, J., Bonnin, M.A., Bourgeois, A., Parisi, A., Le Grand, F., and Duprez, D. (2014). Specific pattern of cell cycle during limb fetal myogenesis. Dev. Biol. *392*, 308–323.

Farah, M.H., Olson, J.M., Sucic, H.B., Hume, R.I., Tapscott, S.J., and Turner, D.L. (2000). Generation of neurons by transient expression of neural bHLH proteins in mammalian cells. Development *127*, 693–702.

Fernandez, C., Tatard, V.M., Bertrand, N., and Dahmane, N. (2010). Differential modulation of sonic-hedgehog-induced cerebellar granule cell precursor proliferation by the IGF signaling network. Dev. Neurosci. *32*, 59–70.

Fietz, S.A., and Huttner, W.B. (2011). Cortical progenitor expansion, self-renewal and neurogenesis—a polarized perspective. Curr. Opin. Neurobiol. *21*, 23–35.

Fietz, S.A., Lachmann, R., Brandl, H., Kircher, M., Samusik, N., Schröder, R., Lakshmanaperumal, N., Henry, I., Vogt, J., Riehn, A., et al. (2012). Transcriptomes of germinal zones of human and mouse fetal neocortex suggest a role of extracellular matrix in progenitor self-renewal. Proc. Natl. Acad. Sci. U. S. A. *109*, 11836–11841.

Fink, J., Carpi, N., Betz, T., Bétard, A., Chebah, M., Azioune, A., Bornens, M., Sykes, C., Fetler, L., Cuvelier, D., et al. (2011). External forces control mitotic spindle positioning. Nat. Cell Biol. *13*, 771–778.

Fishell, G., and Hatten, M.E. (1991). Astrotactin provides a receptor system for CNS neuronal migration. Development *113*, 755–765.

Florio, M., Albert, M., Taverna, E., Namba, T., Brandl, H., Lewitus, E., Haffner, C., Sykes, A., Wong, F.K., Peters, J., et al. (2015). Human-specific gene ARHGAP11B promotes basal progenitor amplification and neocortex expansion. Science (80-.). *347*.

Fujita, S. (1967). Quantitative analysis of cell proliferation and

differentiation in the cortex of the postnatal mouse cerebellum. J. Cell Biol. *32*, 277–287.

Gao, W.Q., and Hatten, M.E. (1993). Neuronal differentiation rescued by implantation of Weaver granule cell precursors into wild-type cerebellar cortex. Science *260*, 367–369.

Ge, W., He, F., Kim, K.J., Blanchi, B., Coskun, V., Nguyen, L., Wu, X., Zhao, J., Heng, J.I.-T., Martinowich, K., et al. (2006). Coupling of cell migration with neurogenesis by proneural bHLH factors. Proc. Natl. Acad. Sci. *103*, 1319–1324.

Gilthorpe, J.D., Papantoniou, E.-K., Chédotal, A., Lumsden, A., and Wingate, R.J.T. (2002). The migration of cerebellar rhombic lip derivatives. Development *129*, 4719–4728.

Gleeson, J.G., Lin, P.T., Flanagan, L.A., and Walsh, C.A. (1999). Doublecortin is a microtubule-associated protein and is expressed widely by migrating neurons. Neuron *23*, 257–271.

Goebbels, S., Bode, U., Pieper, A., Funfschilling, U., Schwab, M.H., and Nave, K.A. (2005). Cre/loxP-mediated inactivation of the bHLH transcription factor gene NeuroD/Beta2. Genesis *42*, 247–252.

Gong, S., Zheng, C., Doughty, M.L., Losos, K., Didkovsky, N., Schambra, U.B., Nowak, N.J., Joyner, A., Leblanc, G., Hatten, M.E., et al. (2003). A gene expression atlas of the central nervous system based on bacterial artificial chromosomes. Nature *425*, 917–925.

Götz, M., and Huttner, W.B. (2005). The cell biology of neurogenesis. Nat. Rev. Mol. Cell Biol. *6*, 777–788.

Govek, E.E., Hatten, M.E., and Van Aelst, L. (2011). The role of Rho GTPase proteins in CNS neuronal migration. Dev. Neurobiol. *71*, 528–553.

Green, M.J., and Wingate, R.J. (2014a). Developmental origins of diversity in cerebellar output nuclei. Neural Dev. *9*, 1.

Green, M.J., and Wingate, R.J.T. (2014b). Developmental origins of diversity in cerebellar output nuclei. Neural Dev. *9*, 1.

Green, M.J., Myat, A.M., Emmenegger, B. a, Wechsler-Reya, R.J., Wilson, L.J., and Wingate, R.J.T. (2014). Independently specified Atoh1 domains define novel developmental compartments in rhombomere 1. Development *141*.

Guillemot, F. (2007) Spatial and temporal specification of neural fates by transcription factor codes. Development 134, 3771-3780

Guo, Z., Zhang, L., Wu, Z., Chen, Y., Wang, F., and Chen, G. (2014). In Vivo Direct Reprogramming of Reactive Glial Cells into Functional Neurons after Brain Injury and in an Alzheimer's Disease Model. Cell Stem Cell *14*, 188–202.

Hadas, Y., Etlin, A., Falk, H., Avraham, O., Kobiler, O., Panet, A., Lev-Tov, A., and Klar, A. (2014). A "tool box" for deciphering neuronal circuits in the developing chick spinal cord. Nucleic Acids Res. *42*, e148.

Hagan, N., and Zervas, M. (2012). Wnt1 expression temporally allocates upper rhombic lip progenitors and defines their terminal cell fate in the cerebellum. Mol. Cell. Neurosci. *49*, 217–229.

Hager, G., Dodt, H.-U., Zieglgänsberger, W., and Liesi, P. (1995). Novel forms of neuronal migration in the rat cerebellum. J. Neurosci. Res. *40*, 207–219.

Haldipur, P., Sivaprakasam, I., Periasamy, V., Govindan, S., and Mani, S. (2015a). Asymmetric cell division of granule neuron progenitors in the external granule layer of the mouse cerebellum. Biol. Open *4*.

Haldipur, P., Sivaprakasam, I., Periasamy, V., Govindan, S., and Mani, S. (2015b). Asymmetric cell division of granule neuron progenitors in the external granule layer of the mouse cerebellum. Biol. Open *4*, 865–872.

Hallonet, M.E., Teillet, M. a, and Le Douarin, N.M. (1990). A new approach to the development of the cerebellum provided by the quail-chick marker system. Development *108*, 19–31.

Hanaway, J. (1967). Formation and differentiation of the external granular layer of the chick cerebellum. J. Comp. Neurol. *131*, 1–13.

Hanzel, M., Wingate, R.J.T., and Butts, T. (2015). Ex vivo culture of chick cerebellar slices and spatially targeted electroporation of granule cell precursors. *2015*.

Hatten, M.E., and Roussel, M.F. (2011). Development and cancer of the cerebellum. Trends Neurosci. *34*, 134–142.

Hatten, M.E., Alder, J., Zimmerman, K., and Heintz, N. (1997). Genes involved in cerebellar cell specification and differentiation. Curr. Opin. Neurobiol. *7*, 40–47.

Hatton, B.A., Knoepfler, P.S., Kenney, A.M., Rowitch, D.H., de Alborán, I.M., Olson, J.M., and Eisenman, R.N. (2006). N-myc is an essential downstream effector of Shh signaling during both normal and neoplastic cerebellar growth. Cancer Res. *66*, 8655–8661.

Hausmann, B., and Sievers, J. (1985). Cerebellar external granule cells are attached to the basal lamina from the onset of migration up to the end of their proliferative activity. J. Comp. Neurol. *241*, 50–62.

Haydar, T.F., Ang, E., and Rakic, P. (2003). Mitotic spindle rotation and mode of cell division in the developing telencephalon. Proc. Natl. Acad. Sci. U. S. A. *100*, 2890–2895.

Helms, A.W., Abney, A.L., Ben-Arie, N., Zoghbi, H.Y., and Johnson, J.E. (2000). Autoregulation and multiple enhancers control Math1 expression in the developing nervous system. Development *127*, 1185–1196.

Helms, A.W., Gowan, K., Abney, A., Savage, T., and Johnson, J.E. (2001). Overexpression of MATH1 disrupts the coordination of neural differentiation in cerebellum development. Mol. Cell. Neurosci. *17*, 671–682.

Herculano-Houzel, S., Mota, B., Wong, P., and Kaas, J.H. (2010). Connectivity-driven white matter scaling and folding in primate cerebral cortex. Proc. Natl. Acad. Sci. *107*, 19008–19013.

Hoshino, M., Nakamura, S., Mori, K., Kawauchi, T., Terao, M., Nishimura, Y. V., Fukuda, A., Fuse, T., Matsuo, N., Sone, M., et al. (2005). Ptf1a, a bHLH Transcriptional Gene, Defines GABAergic Neuronal Fates in Cerebellum. Neuron *47*, 201–213.

Huang, C., Chan JC., Schuurmans C., Proneural bHLH Genes in Development and Disease, Current Topics in Developmental Biology, Volume 110, 2014, Pages 75-127,

Ikeda, M., Hirota, Y., Sakaguchi, M., Yamada, O., Kida, Y.S., Ogura, T., Otsuka, T., Okano, H., and Sawamoto, K. (2010). Expression and Proliferation-Promoting Role of Diversin in the Neuronally Committed Precursor Cells Migrating in the Adult Mouse Brain. Stem Cells *28*, 2017–2026.

Ito, M. (2006). Cerebellar circuitry as a neuronal machine. Prog. Neurobiol. *78*, 272–303.

Ito, M. (2008). Control of mental activities by internal models in the cerebellum. Nat. Rev. Neurosci. *9*, 304–313.

Jiao, J.-W., Feldheim, D.A., and Chen, D.F. (2008). Ephrins as negative regulators of adult neurogenesis in diverse regions of the central nervous system. Proc. Natl. Acad. Sci. U. S. A. *105*, 8778–8783.

Joyner, A.L., Liu, A., and Millet, S. (2000). Otx2, Gbx2 and Fgf8 interact to position and maintain a mid-hindbrain organizer. Curr. Opin. Cell Biol. *12*, 736–

741.

Katoh-Semba, R., Takeuchi, I.K., Semba, R., and Kato, K. (2000). Neurotrophin-3 controls proliferation of granular precursors as well as survival of mature granule neurons in the developing rat cerebellum. J. Neurochem. *74*, 1923–1930.

Kawaji, K., Umeshima, H., Eiraku, M., Hirano, T., and Kengaku, M. (2004). Dual phases of migration of cerebellar granule cells guided by axonal and dendritic leading processes. Mol. Cell. Neurosci. *25*, 228–240.

Kenney, A.M., Cole, M.D., and Rowitch, D.H. (2003). Nmyc upregulation by sonic hedgehog signaling promotes proliferation in developing cerebellar granule neuron precursors. Development *130*, 15–28.

Kerjan, G., Dolan, J., Haumaitre, C., Schneider-Maunoury, S., Fujisawa, H., Mitchell, K.J., and Chédotal, A. (2005). The transmembrane semaphorin Sema6A controls cerebellar granule cell migration. Nat. Neurosci. *8*, 1516–1524.

Khodosevich, K., Alfonso, J., and Monyer, H. (2013). Dynamic changes in the transcriptional profile of subventricular zone-derived postnatally born neuroblasts. Mech. Dev. *130*, 424–432.

Kim, W.-Y. (2013). NeuroD regulates neuronal migration. Mol. Cells *35*, 444–449.

Kita, Y., Kawakami, K., Takahashi, Y., and Murakami, F. (2013). Development of Cerebellar Neurons and Glias Revealed by in Utero Electroporation: Golgi-Like Labeling of Cerebellar Neurons and Glias. PLoS One *8*, e70091.

Klisch, T.J., Xi, Y., Flora, A., Wang, L., Li, W., and Zoghbi, H.Y. (2011). In vivo Atoh1 targetome reveals how a proneural transcription factor regulates cerebellar development. Proc. Natl. Acad. Sci. U. S. A. *108*, 3288–3293.

Knoepfler, P.S., Cheng, P.F., and Eisenman, R.N. (2002). N-myc is essential during neurogenesis for the rapid expansion of progenitor cell populations and the inhibition of neuronal differentiation. Genes Dev. *16*, 2699–2712.

Koirala, S., Jin, Z., Piao, X., and Corfas, G. (2009). GPR56-Regulated Granule Cell Adhesion Is Essential for Rostral Cerebellar Development. J. Neurosci. *29*, 7439–7449.

Komuro, H., and Rakic, P. (1995). Dynamics of granule cell migration: a confocal microscopic study in acute cerebellar slice preparations. J. Neurosci. *15*, 1110–1120.

Komuro, H., and Rakic, P. (1998). Distinct modes of neuronal migration in different domains of developing cerebellar cortex. J. Neurosci. *18*, 1478–1490.

Komuro, H., and Yacubova, E. Recent advances in cerebellar granule cell migration. Cell. Mol. Life Sci. C. *60*, 1084–1098.

Komuro, H., Yacubova, E., Yacubova, E., and Rakic, P. (2001a). Mode and tempo of tangential cell migration in the cerebellar external granular layer. J. Neurosci. *21*, 527–540.

Komuro, H., Yacubova, E., Yacubova, E., and Rakic, P. (2001b). Mode and Tempo of Tangential Cell Migration in the Cerebellar External Granular Layer. J. Neurosci. *21*.

Kornberg, T.B. (2014). Cytonemes and the dispersion of morphogens. Wiley Interdiscip. Rev. Dev. Biol. *3*, 445–463.

Kornberg, T.B. (2017). Distributing signaling proteins in space and time: the province of cytonemes. Curr. Opin. Genet. Dev. *45*, 22–27.

Kumada, T., Jiang, Y., Kawanami, A., Cameron, D.B., and Komuro, H. (2009). Autonomous turning of cerebellar granule cells in vitro by intrinsic programs. Dev. Biol. *326*, 237–249.

de la Torre-Ubieta, L., and Bonni, A. (2011). Transcriptional Regulation of Neuronal Polarity and Morphogenesis in the Mammalian Brain. Neuron *72*, 22–40.

Lai, H.C., Klisch, T.J., Roberts, R., Zoghbi, H.Y., and Johnson, J.E. (2011). In vivo neuronal subtype-specific targets of Atoh1 (Math1) in dorsal spinal cord. J. Neurosci. *31*, 10859–10871.

LaMonica, B.E., Lui, J.H., Wang, X., and Kriegstein, A.R. (2012). OSVZ progenitors in the human cortex: an updated perspective on neurodevelopmental disease. Curr. Opin. Neurobiol. *22*, 747–753.

Lancaster, M.A., and Knoblich, J.A. (2012). Spindle orientation in mammalian cerebral cortical development. Curr. Opin. Neurobiol. *22*, 737–746.

Larsell, O. (1948). The development and subdivisions of the cerebellum of birds. J. Comp. Neurol. *89*, 123–189.

Lee, J.E., and Gleeson, J.G. (2011). Cilia in the nervous system: linking cilia function and neurodevelopmental disorders. Curr. Opin. Neurol. *24*, 98–105.

Lee, H.Y., Angelastro, J.M., Kenney, A.M., Mason, C.A., and Greene, L.A. (2012). Reciprocal actions of ATF5 and Shh in proliferation of cerebellar granule neuron progenitor cells. Dev. Neurobiol. *72*, 789–804.

Lee, J.-K., Cho, J.-H., Hwang, W.-S., Lee, Y.-D., Reu, D.-S., and Suh-Kim, H. (2000a). Expression of neuroD/BETA2 in mitotic and postmitotic neuronal cells during the development of nervous system. Dev. Dyn. *217*, 361–367.

Lee, J.E., Hollenberg, S.M., Snider, L., Turner, D.L., Lipnick, N., and Weintraub, H. (1995). Conversion of Xenopus ectoderm into neurons by NeuroD, a basic helix-loop-helix protein. Science *268*, 836–844.

Lee, J.K., Cho, J.H., Hwang, W.S., Lee, Y.D., Reu, D.S., and Suh-Kim, H. (2000b). Expression of neuroD/BETA2 in mitotic and postmitotic neuronal cells during the development of nervous system. Dev. Dyn. *217*, 361–367.

Lee, M.K., Tuttle, J.B., Rebhun, L.I., Cleveland, D.W., and Frankfurter, A. (1990). The expression and posttranslational modification of a neuron-specific ?-tubulin isotype during chick embryogenesis. Cell Motil. Cytoskeleton *17*, 118–132.

Legué, E., Riedel, E., and Joyner, A.L. (2015). Clonal analysis reveals granule cell behaviors and compartmentalization that determine the folded morphology of the cerebellum. Development *142*, 1661–1671.

Legué, E., Gottshall, J.L., Jaumouillé, E., Roselló-Díez, A., Shi, W., Barraza, L.H., Washington, S., Grant, R.L., and Joyner, A.L. (2016). Differential timing of granule cell production during cerebellum development underlies generation of the foliation pattern. Neural Dev. *11*, 17.

Leto, K., Bartolini, A., and Rossi, F. (2010). The prospective white matter: an atypical neurogenic niche in the developing cerebellum. Arch. Ital. Biol. *148*, 137–146.

Leto, K., Arancillo, M., Becker, E.B.E., Buffo, A., Chiang, C., Ding, B., Dobyns, W.B., Dusart, I., Haldipur, P., Hatten, M.E., et al. (2015). Consensus Paper: Cerebellar Development. The Cerebellum 1–40.

Leung, C., Lingbeek, M., Shakhova, O., Liu, J., Tanger, E., Saremaslani, P., Van Lohuizen, M., and Marino, S. (2004). Bmi1 is essential for cerebellar development and is overexpressed in human medulloblastomas. Nature *428*, 337–341.

Lewis, P.M., Gritli-Linde, A., Smeyne, R., Kottmann, A., and McMahon, A.P. (2004). Sonic hedgehog signaling is required for expansion of granule neuron precursors and patterning of the mouse cerebellum. Dev. Biol. *270*, 393–410.

Li, P., Du, F., Yuelling, L.W., Lin, T., Muradimova, R.E., Tricarico, R., Wang, J., Enikolopov, G., Bellacosa, A., Wechsler-Reya, R.J., et al. (2013). A population of Nestin-expressing progenitors in the cerebellum exhibits increased tumorigenicity.

Nat. Neurosci. *16*, 1737–1744.

Li, X., Tang, X., Jablonska, B., Aguirre, A., Gallo, V., and Luskin, M.B. (2009). p27KIP1 Regulates Neurogenesis in the Rostral Migratory Stream and Olfactory Bulb of the Postnatal Mouse. J. Neurosci. *29*.

Lind, D., Franken, S., Kappler, J., Jankowski, J., and Schilling, K. (2005). Characterization of the neuronal marker NeuN as a multiply phosphorylated antigen with discrete subcellular localization. J. Neurosci. Res. *79*, 295–302.

Livet, J., Weissman, T.A., Kang, H., Draft, R.W., Lu, J., Bennis, R.A., Sanes, J.R., and Lichtman, J.W. (2007). Brainbow system. Nature *450*, 56–62.

Lorenzen, S.M., Duggan, A., Osipovich, A.B., Magnuson, M.A., and García-Añoveros, J. (2015). Insm1 promotes neurogenic proliferation in delaminated otic progenitors. Mech. Dev. *138*, 233–245.

Lui, J.H., Hansen, D.V., and Kriegstein, A.R. (2011). Development and Evolution of the Human Neocortex. Cell *146*, 18–36.

Luskin, M.B. (1993). Restricted proliferation and migration of postnatally generated neurons derived from the forebrain subventricular zone. Neuron *11*, 173–189.

Luskin, M.B., and Coskun, V. (2002). The progenitor cells of the embryonic telencephalon and the neonatal anterior subventricular zone differentially regulate their cell cycle. Chem. Senses *27*, 577–580.

Machold, R., and Fishell, G. (2005). Math1 is expressed in temporally discrete pools of cerebellar rhombic-lip neural progenitors. Neuron *48*, 17–24.

Machold, R., Klein, C., and Fishell, G. (2011). Genes expressed in Atoh1 neuronal lineages arising from the r1/isthmus rhombic lip. Gene Expr. Patterns *11*, 349–359.

Machold, R.P., Kittell, D.J., and Fishell, G.J. (2007). Antagonism between Notch and bone morphogenetic protein receptor signaling regulates neurogenesis in the cerebellar rhombic lip. Neural Dev. *2*, 5.

Mamber, C., Kozareva, D.A., Kamphuis, W., and Hol, E.M. (2013). Shades of gray: The delineation of marker expression within the adult rodent subventricular zone. Prog. Neurobiol. *111*, 1–16.

Manzini, M.C., Ward, M.S., Zhang, Q., Lieberman, M.D., and Mason, C.A. (2006). The Stop Signal Revised: Immature Cerebellar Granule Neurons in the External Germinal Layer Arrest Pontine Mossy Fiber Growth. J. Neurosci. *26*.

Marino, S., Hoogervoorst, D., Brandner, S., and Berns, A. (2003). Rb and p107 are required for normal cerebellar development and granule cell survival but not for Purkinje cell persistence. Development *130*, 3359–3368.

Martinez, S., and Alvarado-Mallart, R.-M. (1989). Rostral Cerebellum Originates from the Caudal Portion of the So-Called "Mesencephalic" Vesicle: A Study Using Chick/Quail Chimeras. Eur. J. Neurosci. *1*, 549–560.

McIntosh, R., Norris, J., Clarke, J.D., and Alexandre, P. (2017). Spatial distribution and characterization of non-apical progenitors in the zebrafish embryo central nervous system. Open Biol. *7*.

Méchali, M., and Lutzmann, M. (2008). The Cell Cycle: Now Live and in Color. Cell *132*, 341–343.

Memberg, S.P., and Hall, A.K. (1995). Dividing neuron precursors express neuron-specific tubulin. J. Neurobiol. *27*, 26–43.

Menezes, J.R.L., Smith, C.M., Nelson, K.C., and Luskin, M.B. (1995). The Division of Neuronal Progenitor Cells during Migration in the Neonatal Mammalian Forebrain. Mol. Cell. Neurosci. *6*, 496–508.

Meredith, A., and Johnson, J.E. (2000). Negative Autoregulation of Mash1

Expression in CNS Development. Dev. Biol. *222*, 336–346.

Miale, I.L., and Sidman, R.L. (1961). An autoradiographic analysis of histogenesis in the mouse cerebellum. Exp. Neurol. *4*, 277–296.

Migheli, A., Piva, R., Casolino, S., Atzori, C., Dlouhy, S.R., and Ghetti, B. (1999). A Cell Cycle Alteration Precedes Apoptosis of Granule Cell Precursors in the weaver Mouse Cerebellum. Am. J. Pathol. *155*, 365–373.

Millet, S., Campbell, K., Epstein, D.J., Losos, K., Harris, E., and Joyner, A.L. (1999). A role for Gbx2 in repression of Otx2 and positioning the mid/hindbrain organizer. Nature *401*, 161–164.

Mills, J., Niewmierzycka, A., Oloumi, A., Rico, B., St-Arnaud, R., Mackenzie, I.R., Mawji, N.M., Wilson, J., Reichardt, L.F., and Dedhar, S. (2006). Critical role of integrin-linked kinase in granule cell precursor proliferation and cerebellar development. J. Neurosci. *26*, 830–840.

Miyata, T., Maeda, T., and Lee, J.E. (1999). NeuroD is required for differentiation of the granule cells in the cerebellum and hippocampus. Genes Dev. *13*, 1647–1652.

Miyata, T., Okamoto, M., Shinoda, T., and Kawaguchi, A. (2015). Interkinetic nuclear migration generates and opposes ventricular-zone crowding: insight into tissue mechanics. Front. Cell. Neurosci. *8*, 473.

Miyazawa, K., Himi, T., Garcia, V., Yamagishi, H., Sato, S., and Ishizaki, Y. (2000a). A role for p27/Kip1 in the control of cerebellar granule cell precursor proliferation. J. Neurosci. *20*, 5756–5763.

Miyazawa, K., Himi, T., Garcia, V., Yamagishi, H., Sato, S., and Ishizaki, Y. (2000b). A Role for p27/Kip1 in the Control of Cerebellar Granule Cell Precursor Proliferation. J. Neurosci. *20*.

Momose, T., Tonegawa, + Akane, Takeuchi, J., Ogawa, H., Umesono, K., and Yasuda, K. (1999). Efficient targeting of gene expression in chick embryos by microelectroporation. Dev. Growth Differ. *41*, 335–344.

Morales, D., and Hatten, M.E. (2006). Molecular markers of neuronal progenitors in the embryonic cerebellar anlage. J. Neurosci. *26*, 12226–12236.

Mullen, R.J., Buck, C.R., and Smith, A.M. (1992). NeuN, a neuronal specific nuclear protein in vertebrates. Development *116*, 201–211.

Mulvaney, J., and Dabdoub, A. (2012a). Atoh1, an essential transcription factor in neurogenesis and intestinal and inner ear development: Function, regulation, and context dependency. JARO - J. Assoc. Res. Otolaryngol. *13*, 281–293.

Mulvaney, J., and Dabdoub, A. (2012b). Atoh1, an Essential Transcription Factor in Neurogenesis and Intestinal and Inner Ear Development: Function, Regulation, and Context Dependency. J. Assoc. Res. Otolaryngol. *13*, 281–293.

Murre, C., McCaw, P.S., Vaessin, H., Caudy, M., Jan, L.Y., Jan, Y.N., Cabrera, C. V, Buskin, J.N., Hauschka, S.D., and Lassar, A.B. (1989). Interactions between heterologous helix-loop-helix proteins generate complexes that bind specifically to a common DNA sequence. Cell *58*, 537–544.

Nagata, I., and Nakatsuji, N. (1994). Migration Behavior of Granule Cell Neurons in Cerebellar Cultures I. A PKH26 Labeling Study in Microexplant and Organotypic Cultures. Dev. Growth Differ. *36*, 19–27.

Nakamura, H., and Watanabe, Y. (2005). Isthmus organizer and regionalization of the mesencephalon and metencephalon. Int. J. Dev. Biol. *49*, 231–235.

Nakashima, K., Umeshima, H., and Kengaku, M. (2015). Cerebellar granule cells are predominantly generated by terminal symmetric divisions of granule cell precursors. Dev. Dyn. *244*, 748–758.

Namba, T., and Huttner, W.B. (2017). Neural progenitor cells and their role in the development and evolutionary expansion of the neocortex. Wiley Interdiscip. Rev. Dev. Biol. *6*, e256.

Nelson, B.R., Hodge, R.D., Bedogni, F., and Hevner, R.F. (2013). Dynamic Interactions between Intermediate Neurogenic Progenitors and Radial Glia in Embryonic Mouse Neocortex: Potential Role in Dll1-Notch Signaling. J. Neurosci. *33*, 9122–9139.

Nguyen-Ba-Charvet, K.T., Picard-Riera, N., Tessier-Lavigne, M., Baron-Van Evercooren, A., Sotelo, C., and Chédotal, A. (2004). Multiple Roles for Slits in the Control of Cell Migration in the Rostral Migratory Stream. J. Neurosci. *24*.

Noctor, S.C., Flint, A.C., Weissman, T.A., Dammerman, R.S., and Kriegstein, A.R. (2001). Neurons derived from radial glial cells establish radial units in neocortex. Nature *409*, 714–720.

Nomura, T., Ohtaka-Maruyama, C., Yamashita, W., Wakamatsu, Y., Murakami, Y., Calegari, F., Suzuki, K., Gotoh, H., and Ono, K. (2016). The evolution of basal progenitors in the developing non-mammalian brain. Development *143*, 66–74.

Nonaka-Kinoshita, M., Reillo, I., Artegiani, B., Martínez-Martínez, M.Á., Nelson, M., Borrell, V., Calegari, F., Artegiani, B., Lindemann, D., Calegari, F., et al. (2013). Regulation of cerebral cortex size and folding by expansion of basal progenitors. EMBO J. *32*, 1817–1828.

Pan, N., Jahan, I., Lee, J.E., and Fritzsch, B. (2009). Defects in the cerebella of conditional Neurod1 null mice correlate with effective Tg(Atoh1-cre) recombination and granule cell requirements for Neurod1 for differentiation. Cell Tissue Res. *337*, 407–428.

Paridaen, J.T.M.L., Huttner, W.B., Hatakeyama, J., Bessho, Y., Katoh, K., Ookawara, S., Fujioka, M., Guillemot, F., Kageyama, R., Sahara, S., et al. (2014). Neurogenesis during development of the vertebrate central nervous system. EMBO Rep. *15*, 351–364.

Park, J.Y., Hughes, L.J., Moon, U.Y., Park, R., Kim, S.-B., Tran, K., Lee, J.-S., Cho, S.-H., and Kim, S. (2016). The apical complex protein Pals1 is required to maintain cerebellar progenitor cells in a proliferative state. Development *143*.

Pataskar, A., Jung, J., Smialowski, P., Noack, F., Calegari, F., Straub, T., and Tiwari, V.K. (2016). NeuroD1 reprograms chromatin and transcription factor landscapes to induce the neuronal program. EMBO J. *35*, 24–45.

Pencea, V., Bingaman, K.D., Freedman, L.J., and Luskin, M.B. (2001). Neurogenesis in the Subventricular Zone and Rostral Migratory Stream of the Neonatal and Adult Primate Forebrain. Exp. Neurol. *172*, 1–16.

di Pietro, F., Echard, A., Morin, X., Tanaka, T., Glotzer, M., Kraut, R., Chia, W., Jan, L., Jan, Y., Knoblich, J., et al. (2016). Regulation of mitotic spindle orientation: an integrated view. EMBO Rep. *17*, 1106–1130.

Pilaz, L.-J., and Silver, D.L. (2014). Live imaging of mitosis in the developing mouse embryonic cortex. J. Vis. Exp. 1–10.

Pilaz, L.-J., McMahon, J.J., Miller, E.E., Lennox, A.L., Suzuki, A., Salmon, E., and Silver, D.L. (2016). Prolonged Mitosis of Neural Progenitors Alters Cell Fate in the Developing Brain. Neuron *89*, 83–99.

Ponti, G., Obernier, K., Guinto, C., Jose, L., Bonfanti, L., and Alvarez-Buylla, A. (2013). Cell cycle and lineage progression of neural progenitors in the ventricular-subventricular zones of adult mice. Proc. Natl. Acad. Sci. U. S. A. *110*, E1045-54.

Price, S.R. (2007). In Vivo Electroporation of Neurons. Cold Spring Harb. Protoc. *2007*, pdb.prot4788.

Quesada, A, and Genis-Galvez, J.M. (1983). Early development of the granule cell in the cerebellum of the chick embryo. J. Morphol. *178*, 323–334.

Rakic, P. (1971). Neuron-glia relationship during granule cell migration in developing cerebellar cortex. A Golgi and electonmicroscopic study in Macacus rhesus. J. Comp. Neurol. *141*, 283–312.

Rakic, P., and Sidman, R.L. (1970). Histogenesis of cortical layers in human cerebellum, particularly the lamina dissecans. J. Comp. Neurol. *139*, 473–500.

Renaud, J., Kerjan, G., Sumita, I., Zagar, Y., Georget, V., Kim, D., Fouquet, C., Suda, K., Sanbo, M., Suto, F., et al. (2008). Plexin-A2 and its ligand, Sema6A, control nucleus-centrosome coupling in migrating granule cells. Nat. Neurosci. *11*, 440–449.

Rivas, R.J., and Hatten, M.E. (1995). Motility and cytoskeletal organization of migrating cerebellar granule neurons. J. Neurosci. *15*, 981–989.

Rodríguez, F., Durán, E., Gómez, A., Ocaña, F.M., Álvarez, E., Jiménez-Moya, F., Broglio, C., and Salas, C. (2005). Cognitive and emotional functions of the teleost fish cerebellum. In Brain Research Bulletin, pp. 365–370.

Ross, S.E., Greenberg, M.E., and Stiles, C.D. (2003). Basic helix-loop-helix factors in cortical development. Neuron *39*, 13–25.

Rossman, I.T., Lin, L., Morgan, K.M., DiGiovine, M., Van Buskirk, E.K., Kamdar, S., Millonig, J.H., DiCicco-Bloom, E., Sur, M., Biffo, S., et al. (2014). Engrailed2 modulates cerebellar granule neuron precursor proliferation, differentiation and insulin-like growth factor 1 signaling during postnatal development. Mol. Autism *5*, 9.

Roussel, M.F., and Hatten, M.E. (2011). Cerebellum: Development and Medulloblastoma.

Roybon, L., Deierborg, T., Brundin, P., and Li, J.-Y. (2009). Involvement of Ngn2, Tbr and NeuroD proteins during postnatal olfactory bulb neurogenesis. Eur. J. Neurosci. *29*, 232–243.

Ryder, E.F., and Cepko, C.L. (1994). Migration patterns of clonally related granule cells and their progenitors in the developing chick cerebellum. Neuron *12*, 1011–1029.

Saha, B., Ypsilanti, A.R., Boutin, C., Cremer, H., and Chedotal, A. (2012). Plexin-B2 Regulates the Proliferation and Migration of Neuroblasts in the Postnatal and Adult Subventricular Zone. J. Neurosci. *32*, 16892–16905.

Sakaue-Sawano, A., Ohtawa, K., Hama, H., Kawano, M., Ogawa, M., and Miyawaki, A. (2008). Tracing the Silhouette of Individual Cells in S/G2/M Phases with Fluorescence.

Salero, E., and Hatten, M.E. (2007). Differentiation of ES cells into cerebellar neurons. Proc. Natl. Acad. Sci. U. S. A. *104*, 2997–3002.

Sanders, T.A., Llagostera, E., and Barna, M. (2013). Specialized filopodia direct long-range transport of SHH during vertebrate tissue patterning. Nature *497*, 628–632.

Sato, T., Araki, I., and Nakamura, H. (2001). Inductive signal and tissue responsiveness defining the tectum and the cerebellum. Development *128*, 2461–2469.

Schwab, M.H., Bartholomae, a, Heimrich, B., Feldmeyer, D., Druffel-Augustin, S., Goebbels, S., Naya, F.J., Zhao, S., Frotscher, M., Tsai, M.J., et al. (2000). Neuronal basic helix-loop-helix proteins (NEX and BETA2/Neuro D) regulate terminal granule cell differentiation in the hippocampus. J. Neurosci. *20*, 3714–3724.

Selvadurai, H.J., and Mason, J.O. (2012). Activation of Wnt/β-Catenin

Signalling Affects Differentiation of Cells Arising from the Cerebellar Ventricular Zone. PLoS One *7*, e42572.

Sgaier, S.K., Millet, S., Villanueva, M.P., Berenshteyn, F., Song, C., and Joyner, A.L. (2005). Morphogenetic and cellular movements that shape the mouse cerebellum; insights from genetic fate mapping. Neuron *45*, 27–40.

Singh, S., and Solecki, D.J. (2015). Polarity transitions during neurogenesis and germinal zone exit in the developing central nervous system. Front. Cell. Neurosci. *9*, 62.

Smeyne, R.J., and Goldowitz, D. (1989). Development and death of external granular layer cells in the weaver mouse cerebellum: a quantitative study. J. Neurosci. *9*, 1608–1620.

Smeyne, R., Chu, T., Lewin, A., Bian, F., Sanlioglu, S., S-Crisman, S., Kunsch, C., Lira, S.A., and Oberdick, J. (1995). Local Control of Granule Cell Generation by Cerebellar Purkinje Cells. Mol. Cell. Neurosci. *6*, 230–251.

Solecki, D.J., Liu, X., Tomoda, T., Fang, Y., and Hatten, M.E. (2001). Activated Notch2 signaling inhibits differentiation of cerebellar granule neuron precursors by maintaining proliferation. Neuron *31*, 557–568.

Solecki, D.J., Model, L., Gaetz, J., Kapoor, T.M., and Hatten, M.E. (2004). Par6alpha signaling controls glial-guided neuronal migration. Nat. Neurosci. *7*, 1195–1203.

Solecki, D.J., Trivedi, N., Govek, E.-E., Kerekes, R. a, Gleason, S.S., and Hatten, M.E. (2009). Myosin II motors and F-actin dynamics drive the coordinated movement of the centrosome and soma during CNS glial-guided neuronal migration. Neuron *63*, 63–80.

Sonmez, E., and Herrup, K. (1984). Role of staggerer gene in determining cell number in cerebellar cortex. II. Granule cell death and persistence of the external granule cell layer in young mouse chimeras. Brain Res. *314*, 271–283.

Sotelo, C. (2004). Cellular and genetic regulation of the development of the cerebellar system. Prog. Neurobiol. *72*, 295–339.

Stanganello, E., Hagemann, A.I.H., Mattes, B., Sinner, C., Meyen, D., Weber, S., Schug, A., Raz, E., and Scholpp, S. (2015). Filopodia-based Wnt transport during vertebrate tissue patterning. Nat. Commun. *6*, 5846.

Stoodley, C.J. (2012). The Cerebellum and Cognition: Evidence from Functional Imaging Studies. The Cerebellum *11*, 352–365.

Strick, P.L., Dum, R.P., and Fiez, J.A. (2009). Cerebellum and Nonmotor Function. Annu. Rev. Neurosci. *32*, 413–434.

Sudarov, A., and Joyner, A.L. (2007). Cerebellum morphogenesis: the foliation pattern is orchestrated by multi-cellular anchoring centers. Neural Dev. *2*, 26.

Swartz, M., Eberhart, J., Mastick, G.S., and Krull, C.E. (2001). Sparking New Frontiers: Using in Vivo Electroporation for Genetic Manipulations. Dev. Biol. *233*, 13–21.

Urbán, N., and Guillemot, F. (2014). Neurogenesis in the embryonic and adult brain: same regulators, different roles. Front. Cell. Neurosci. *8*, 396.

Valente, E.M., Rosti, R.O., Gibbs, E., and Gleeson, J.G. (2014). Primary cilia in neurodevelopmental disorders. Nat. Rev. Neurol. *10*, 27–36.

Vierbuchen, T., Ostermeier, A., Pang, Z.P., Kokubu, Y., Südhof, T.C., and Wernig, M. (2010). Direct conversion of fibroblasts to functional neurons by defined factors. Nature *463*, 1035–1041.

Wagner, M.J., Kim, T.H., Savall, J., Schnitzer, M.J., and Luo, L. (2017). Cerebellar granule cells encode the expectation of reward. Nature *544*, 96–100.

Wallace, V.A. (1999). Purkinje-cell-derived Sonic hedgehog regulates granule neuron precursor cell proliferation in the developing mouse cerebellum. Curr. Biol. *9*, 445–448.

Wang, V.Y., and Zoghbi, H.Y. (2001). Genetic regulation of cerebellar development. Nat. Rev. Neurosci. *2*, 484–491.

Wang, V.Y., Rose, M.F., and Zoghbi, H.Y. (2005). Math1 expression redefines the rhombic lip derivatives and reveals novel lineages within the brainstem and cerebellum. Neuron *48*, 31–43.

Wechsler-Reya, R.J., and Scott, M.P. (1999). Control of neuronal precursor proliferation in the cerebellum by Sonic Hedgehog. Neuron *22*, 103–114.

Wilkinson, G., Dennis, D., and Schuurmans, C. (2013). Proneural genes in neocortical development. Neuroscience *253*, 256–273.

Wilson, L.J., and Wingate, R.J.T. (2006). Temporal identity transition in the avian cerebellar rhombic lip. Dev. Biol. *297*, 508–521.

Wilson, L.J., Myat, A., Sharma, A., Maden, M., and Wingate, R.J. (2007). Retinoic acid is a potential dorsalising signal in the late embryonic chick hindbrain. BMC Dev. Biol. *7*, 138.

Wingate, R.J.T. (2001). The rhombic lip and early cerebellar development. Curr. Opin. Neurobiol. *11*, 82–88.

Wingate, R.J., and Hatten, M.E. (1999). The role of the rhombic lip in avian cerebellum development. Development *126*, 4395–4404.

Wolf, E., Wagner, J.P., Black, I.B., and DiCicco-Bloom, E. (1997). Cerebellar granule cells elaborate neurites before mitosis. Brain Res. Dev. Brain Res. *102*, 305–308.

Wullimann, M.F., Mueller, T., Distel, M., Babaryka, A., Grothe, B., and Köster, R.W. (2011). The long adventurous journey of rhombic lip cells in jawed vertebrates: a comparative developmental analysis. Front. Neuroanat. *5*, 27.

Xenaki, D., Martin, I.B., Yoshida, L., Ohyama, K., Gennarini, G., Grumet, M., Sakurai, T., and Furley, A.J.W. (2011). F3/contactin and TAG1 play antagonistic roles in the regulation of sonic hedgehog-induced cerebellar granule neuron progenitor proliferation. Development *138*, 519–529.

Yacubova, E., and Komuro, H. (2002a). Intrinsic Program for Migration of Cerebellar Granule CellsIn Vitro. J. Neurosci. *22*.

Yacubova, E., and Komuro, H. (2002b). Cellular and Molecular Mechanisms of Cerebellar Granule Cell Migration. Cell Biochem. Biophys. *37*, 213–234.

Yaguchi, Y., Yu, T., Ahmed, M.U., Berry, M., Mason, I., and Basson, M.A. (2009). Fibroblast growth factor (FGF) gene expression in the developing cerebellum suggests multiple roles for FGF signaling during cerebellar morphogenesis and development. Dev. Dyn. *238*, 2058–2072.

Yang, R., Wang, M., Wang, J., Huang, X., Yang, R., and Gao, W.Q. (2015). Cell division mode change mediates the regulation of cerebellar granule neurogenesis controlled by the sonic hedgehog signaling. Stem Cell Reports *5*, 816–828.

Ye, P., Xing, Y., Dai, Z., and D'Ercole, A.J. (1996). In vivo actions of insulin-like growth factor-I (IGF-I) on cerebellum development in transgenic mice: Evidence that IGF-I increases proliferation of granule cell progenitors. Dev. Brain Res. *95*, 44–54.

Zanin, J.P., Abercrombie, E., Friedman, W.J., Chen, Y., Choi, Y., Tolias, K., Bikoff, J., Hong, E., Greenberg, M., Segal, R., et al. (2016). Proneurotrophin-3 promotes cell cycle withdrawal of developing cerebellar granule cell progenitors via the p75 neurotrophin receptor. Elife *5*, 162–172.

Zhang, L., and Goldman, J.E. (1996). Generation of cerebellar interneurons

from dividing progenitors in white matter. Neuron *16*, 47–54.

Zhao, H., Ayrault, O., Zindy, F., Kim, J.H., and Roussel, M.F. (2008a). Post-transcriptional down-regulation of Atoh1/Math1 by bone morphogenic proteins suppresses medulloblastoma development. Genes Dev. *22*, 722–727.

Zhao, H., Ayrault, O., Zindy, F., Kim, J.-H., and Roussel, M.F. (2008b). Post-transcriptional down-regulation of Atoh1/Math1 by bone morphogenic proteins suppresses medulloblastoma development. Genes Dev. *22*, 722–727.

Zielke, N., and Edgar, B.A. (2015). FUCCI sensors: Powerful new tools for analysis of cell proliferation. Wiley Interdiscip. Rev. Dev. Biol. *4*, 469–487.

Zigova, T., Betarbet, R., Soteres, B.J., Brock, S., Bakay, R.A.E., and Luskin, M.B. (1996). A Comparison of the Patterns of Migration and the Destinations of Homotopically Transplanted Neonatal Subventricular Zone Cells and Heterotopically Transplanted Telencephalic Ventricular Zone Cells. Dev. Biol. *173*, 459–474.

Zou, Y.R., Kottmann, A.H., Kuroda, M., Taniuchi, I., and Littman, D.R. (1998). Function of the chemokine receptor CXCR4 in haematopoiesis and in cerebellar development. Nature *393*, 595–599.

Video Article

Ex Vivo Culture of Chick Cerebellar Slices and Spatially Targeted Electroporation of Granule Cell Precursors

Michalina Hanzel[1], Richard J.T. Wingate[1], Thomas Butts[2]

[1]MRC Centre of Developmental Neurobiology, King's College London

[2]School of Biological and Chemical Sciences, Queen Mary, University of London

Correspondence to: Thomas Butts at thomas.butts@qmul.ac.uk

URL: https://www.jove.com/video/53421
DOI: doi:10.3791/53421

Keywords: Developmental Biology, Issue 106, cerebellum, development, chick, external granule layer, slice culture, granule cells, Purkinje cells, electroporation.

Date Published: 12/14/2015

Citation: Hanzel, M., Wingate, R.J., Butts, T. *Ex Vivo* Culture of Chick Cerebellar Slices and Spatially Targeted Electroporation of Granule Cell Precursors. *J. Vis. Exp.* (106), e53421, doi:10.3791/53421 (2015).

Abstract

The cerebellar external granule layer (EGL) is the site of the largest transit amplification in the developing brain, and an excellent model for studying neuronal proliferation and differentiation. In addition, evolutionary modifications of its proliferative capability have been responsible for the dramatic expansion of cerebellar size in the amniotes, making the cerebellum an excellent model for evo-devo studies of the vertebrate brain. The constituent cells of the EGL, cerebellar granule progenitors, also represent a significant cell of origin for medulloblastoma, the most prevalent paediatric neuronal tumour. Following transit amplification, granule precursors migrate radially into the internal granular layer of the cerebellum where they represent the largest neuronal population in the mature mammalian brain. In chick, the peak of EGL proliferation occurs towards the end of the second week of gestation. In order to target genetic modification to this layer at the peak of proliferation, we have developed a method for genetic manipulation through *ex vivo* electroporation of cerebellum slices from embryonic Day 14 chick embryos. This method recapitulates several important aspects of *in vivo* granule neuron development and will be useful in generating a thorough understanding of cerebellar granule cell proliferation and differentiation, and thus of cerebellum development, evolution and disease.

Video Link

The video component of this article can be found at https://www.jove.com/video/53421/

Introduction

The cerebellum sits at the anterior end of the hindbrain and is responsible for the integration of sensory and motor processing in the mature brain as well as regulating higher cognitive processes[1]. In mammals and birds, it possesses an elaborate morphology and is heavily foliated, a product of extensive transit amplification of progenitors during development that produces over half of the neurons in the adult brain. The cerebellum has been a subject of study for neurobiologists for centuries and in the molecular era has likewise received significant attention. This relates not only to its inherently interesting biology, but also to the fact that it is heavily implicated in human disease including developmental genetic disorders such as autism spectrum disorders[2] and most prominently the cerebellar cancer, medulloblastoma[3], which is the most prevalent paediatric brain tumour. Importantly, it is an excellent model system within which to study fate allocation and neurogenesis during brain development[4]. In recent years, it has also been established as a model system for the comparative study of brain development, owing to the huge diversity of cerebellar forms seen across the vertebrate phylogeny[5-10].

The cerebellum develops from the dorsal half of rhombomere 1 in the hindbrain[11] and developmentally is comprised of two primary progenitor populations, the rhombic lip and the ventricular zone. The rhombic lip extends around the dorsal region of the neuroepithelium of the hindbrain at the border with the roof plate. It is the birthplace of the glutamatergic excitatory neurons of the cerebellum[12-14]. The ventricular zone gives rise to the inhibitory GABAergic cerebellar neurons, most prominently the large Purkinje neurons[14,15]. Later in development (from about embryonic day 13.5 in mouse; e6 in chick[16]), glutamatergic progenitors migrate tangentially from the rhombic lip and form a pial layer of progenitors: a secondary progenitor zone called the external granule layer (EGL). It is this layer that undergoes the extensive transit amplification that leads to the huge numbers of granule neurons found in the mature brain.

Proliferation in the EGL has long been linked to the sub-pial location that results from tangential migration from the rhombic lip[17], with the switch to cell cycle exit and neuronal differentiation of progenitors being associated with their exit from the outer EGL layer into the middle EGL[18]. Extensive tangential migration of post-mitotic granule cells in medial-lateral axis occurs in the middle and inner EGL[19], before final radial migration into the inner granule layer of the mature cerebellar cortex. Migration of cells from the rhombic lip over the cerebellar surface is dependent upon CXCL12 signalling from the pia[20-22] and granule cells express the CXCL12 receptor CXCR4. Their tangential migration is thus reminiscent of that of neocortical tangentially migrating inhibitory interneuron populations[23-25]. Intriguingly, electron microscopic studies[17] have suggested that EGL cells with a proliferative morphology maintain pial contact, linking cell behaviour with proliferative capability in a manner

reminiscent of the basal progenitors of the mammalian cortex[26]. This is reflected in the aforementioned stratification of the EGL into three sublayers that are defined by distinct extracellular environments and where granule precursors have distinct gene expression signatures[18].

Proliferation of progenitors in the oEGL occurs with a normal distribution of clone sizes such that when progenitors are individually genetically labelled at the end of embryonic development in the mouse, they give rise to a median average of 250-500 postmitotic granule neurons[27,28]. Proliferation is dependent upon mitogenic SHH signalling from underlying Purkinje neurons[29-32]. The ability to respond to SHH has been shown to be entirely dependent upon cell autonomous expression of the transcription factor *Atoh1*, both *in vitro*[33] and *in vivo*[34,35]. Likewise, cell cycle exit and differentiation has been shown to be dependent upon the expression of the downstream transcription factor *NeuroD1*[36], which is likely a direct repressor of *Atoh1*[37].

Despite this progress, and considerable advancement in deciphering the cell biological basis of cell cycle exit[38-42], the fundamental molecular mechanism(s) that underlie the decision to exit the cell cycle and to transition from a progenitor to a differentiating neuron, and the associated postmitotic tangential migration in the inner EGL as well as the later switch to radial migration, remain incompletely understood. This is to a large extent because of the experimental intractability of the EGL: it is late developing, and difficult to target genetically since many of the same neurogenic molecules are also crucial earlier in the life of granule precursors at the rhombic lip. To overcome this issue, numerous authors have developed *in vivo* and *ex vivo* electroporation as a method to target the postnatal cerebellum in rodents[43-48]. Here, we pioneer the use of *ex vivo* electroporation in chick to study the EGL, which represents considerable advantages in terms of cost and convenience. Our method of electroporation and *ex vivo* slice culture of chick cerebellar tissue uses tissue dissected from embryonic Day 14 chicks at the peak of EGL proliferation. This method allows genetic targeting of the EGL independently of the rhombic lip and will set the stage for genetic dissection of the transition from granule progenitor to postmitotic granule neuron in the cerebellum.

Protocol

Note: All experiments were performed with accordance to King's College London, UK and the UK Home Office animal care guidelines.

1. Dissection of e14 Cerebellum

1. Incubate brown fertilised hens' eggs at 38 °C to embryonic Day 14.
2. Using egg scissors decapitate chick embryo *in ovo* and remove head to a Petri dish containing ice cold PBS (**Figure 1A**).
3. Using standard forceps, make incisions behind each eye all the way through the tissue, removing the eyes and upper jaw. Make a second incision all the way through the pharynx removing the lower jaw (**Figure 1B**).
4. Using standard forceps, remove all skin from surface of skull by peeling it away (**Figure 1C**) and remove frontal and parietal bones, revealing brain.
5. From a ventral aspect, remove pharyngeal cartilage and auxiliary mesenchyme.
6. From a dorsal aspect, carefully remove mesenchyme dorsal to the hindbrain taking care not to damage pia, and separate entire brain (**Figure 1D**).
7. Make incision all the way through the tissue between midbrain and hindbrain and separate hindbrain including cerebellum (**Figure 1E**).
8. By making incisions all the way through the tissue at both lateral junctions of cerebellum and alar plate of the hindbrain, remove entire cerebellum, taking care to maintain the integrity of the pia throughout dissection (**Figure 1F**). Remove the forming choroid plexus (**Figure 1G**).
9. Move the dissected cerebellum into ice cold HBSS.

2. Slice Culture of e14 Cerebellum

1. Transfer the whole cerebellum to the sterile platform of a Tissue Chopper using a spatula or a 3 ml Pasteur pipette with the tip cut away to widen the aperture. Remove excess liquid using a pipette.
2. Cut entire whole cerebellum in the required orientation at 300 µm thickness using the tissue chopper set with a cutting speed at 50% of the maximum. Tissue integrity is most easily preserved in sagittal section; however, orientation is also an important consideration for cell analysis (Purkinje cell dendrites are sagittally aligned, while granule cell axons run transversely, perpendicular to the plane of Purkinje cell dendrites).
3. Using a 3 ml Pasteur pipette, cover the sliced cerebellum in ice cold HBSS.
4. Transfer the slices in HBSS to a 60 mm Petri dish containing ice cold fresh HBSS using a 3 ml Pasteur pipette with cut tip.
5. Under a dissecting microscope illuminated with a fiber optic light source, ensure separation of individual slices using watchmaker forceps. Identify slices to be electroporated, based upon their tissue integrity and medio-lateral position.
   Note: Each dissection from embryo through to slice incubation in culture medium takes around 10-20 min depending upon experience. Perform dissections one at a time to ensure that cerebella spend minimum amount of time between decapitation and *ex vivo* culture.

3. Electroporation of Slices

1. Construct an electroporation chamber by fixing the anode of an electroporator to the base of a 60 mm Petri dish with insulation tape. Add approximately 1 ml of HBSS to cover the electrode.
2. Place a 0.4 µm culture insert on top of the electrode covered in HBSS. Allow the culture insert to rest on the electrode making sure there is always contact between the insert and the electrode.
   Note: In this setup, the culture insert with the slices will rest upon the surface of the solution, maintaining the circuit but allowing spatial targeting of the cathode.
3. Transfer identified slices (up to five per culture insert) onto culture insert using 3 ml Pasteur pipette with the cut tip. Separate and allow to settle onto culture insert in a sagittal orientation.
4. Using a pipette, remove excess HBSS so that slices are no longer bathed in solution.

5. Using a P10 pipette tip, pipette DNA (at a concentration of 1 µg/µl) diluted with 20% fast green over the surface of targeted region of a slice. 20% fast green ensures viscous DNA solution and prevents prohibitively wide dispersal of DNA. Add approximately 5 µl DNA/fast green solution to each slice (**Figure 2B**).
6. Place the cathode over desired targeted tissue and electroporate with 3 x 10 V, 10 msec duration pulses. Avoid direct contact of the cathode with the tissue. Instead, take advantage of surface tension of the liquid to maintain conductance (place the cathode as close to the tissue as possible without actually touching the tissue).
7. Repeat DNA delivery and electroporation to multiple regions of EGL on each individual cerebellar slice as desired.
8. Upon completion of electroporation, transfer culture insert to 30 mm Petri dish.
9. To each culture, add 1 ml of pre-warmed culture medium (Basal Medium Eagle, 0.5% (w/v) D-(+)-glucose, 1% B27 supplement, 2 mM L-Glutamine, 100 U/ml penicillin, 100 µg/ml streptomycin) underneath the culture insert such that the culture insert is in contact with medium, but slices are not bathed in it.
10. Incubate cultures at 37 °C/6% CO_2 for up to 3 days. Replace all of the culture medium every 24 hr with fresh pre-warmed medium.
11. Following culture, fix slices on culture inserts for 1 hr in 4% paraformaldehyde (or O/N at 4 °C) in a fresh 30 mm dish with no culture media.

4. Imaging of Cerebellar Slices

1. Following fixation, wash slices 3 times for 5 min in PBS.
2. Using a razor blade, dissect each electroporated and cultured cerebellar slice from the culture insert by cutting around the slice and removing the slice and the region of insert it is adhered to. Do not attempt to remove slice from the culture insert surface.
3. Mount slices in approximately 1 ml of mounting medium containing DAPI (if desired) under a coverslip taking care not to introduce bubbles, and image using laser-scanning confocal microscopy.
   Note: Imaging parameters can be varied according to the constructs electroporated, and at the discretion of the individual user.

Representative Results

This section illustrates examples of results that can be obtained using slice electroporation and culture of cerebellum from embryonic Day 14 chick. The dissection of the cerebellum is illustrated in **Figure 1** and the electroporation chamber set up is shown in **Figure 2**. We show that it is possible to electroporate and successfully culture cerebellar slices, which retain their structure and cellular morphologies *in vitro* (**Figure 3A**). Targeted electroporation to individual folia is easily achieved (**Figure 3B**). We successfully electroporate a number of different plasmids into the EGL cells and show that it is possible i) to label cells with reporter constructs to observe their behaviour (**Figure 3C**), ii) to test possible genomic regions for functionality in cerebellar cells (**Figure 3D**), and iii) to manipulate genetically the cells in the EGL by misexpressing proteins of interest (**Figure 3E**). Additionally, pharmacological manipulations on electroporated slices are possible (results not shown). After culturing it is possible to perform additional tissue analysis such as immunohistochemistry or proliferation assays (**Figure 3F**). We perform tissue health analysis by calbindin and PH3 immunostaining and show that tissue integrity is maintained for at least 3 div after culture (**Figure 4**). These results demonstrate that the EGL is now an accessible and easily manipulated structure that can be fully examined and genetically altered in the chick model system.

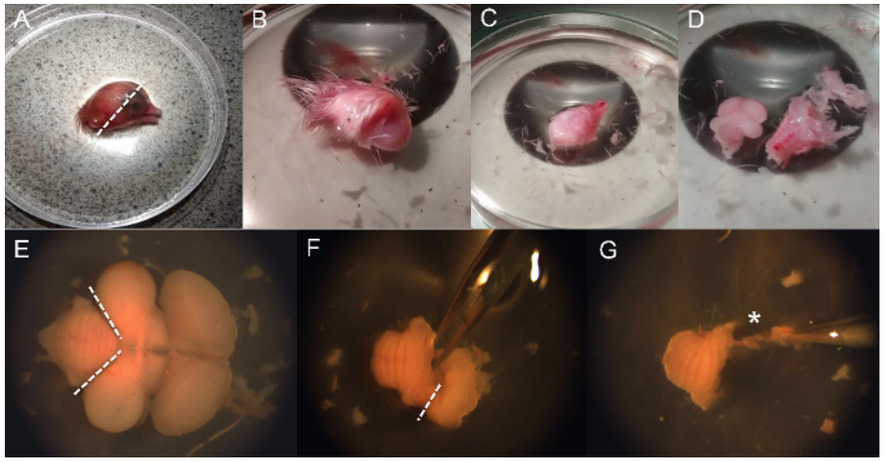

Figure 1. Dissection of the cerebellum from E14 chick embryos. (**A**) Decapitate the chick in the egg and remove the head into a petri dish with ice cold PBS. Remove the lower jaw and the eyes by making incision behind the eyes and the pharynx (dashed line). (**B**) Remove the skin from the surface of the skull. (**C**) Remove the frontal and parietal bones and (**D**) remove the brain from the mesenchyme and cartilage surrounding it. (**E**) Under a dissecting microscope identify the location of the cerebellum at the posterior end of the brain. Cut between the midbrain and the hindbrain (dashed lines) to be left with the cerebellum and ventral hindbrain. (**F**) Make incisions at the lateral junctions (peduncles) of the cerebellum to separate the cerebellum from the hindbrain (dashed line). (**G**) Remove the choroid plexus (asterisk) from the ventral side of the cerebellum until you are left with a whole intact cerebellum with the pia attached. Transfer the cerebellum into ice-cold HBSS before preparing slices with a tissue chopper. Please click here to view a larger version of this figure.

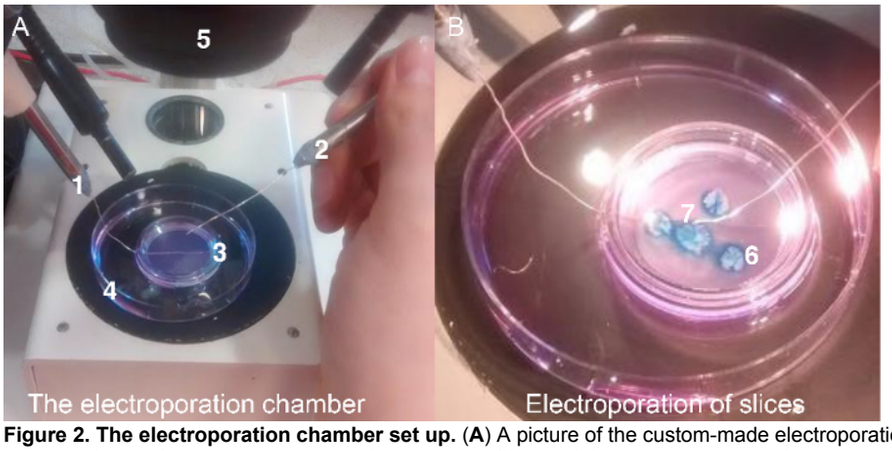

Figure 2. The electroporation chamber set up. (**A**) A picture of the custom-made electroporation chamber. The chamber consists of an anode of an electroporator placed securely on the base of a 60 mm Petri dish. The dish contains approximately 1 ml of HBSS to cover the electrode. The culture insert should rest on the electrode with constant contact between the insert and the electrode, maintaining the circuit but allowing spatial targeting of the cathode, which is manipulated by hand. (**B**) A picture of slices being electroporated. Slices are covered with the DNA/fast green solution. The slices are electroporated as desired: electroporation can be targeted to one folium or multiple locations. After electroporation the insert is placed in a 30 mm Petri dish with pre-warmed culture medium and cultured in the incubator. 1. The anode 2. The cathode 3. Culture insert 4. Petri dish with 1 ml HBSS 5. Dissecting microscope 6. Individual slices from tissue chopper 7. DNA solution with fast green dye. Please click here to view a larger version of this figure.

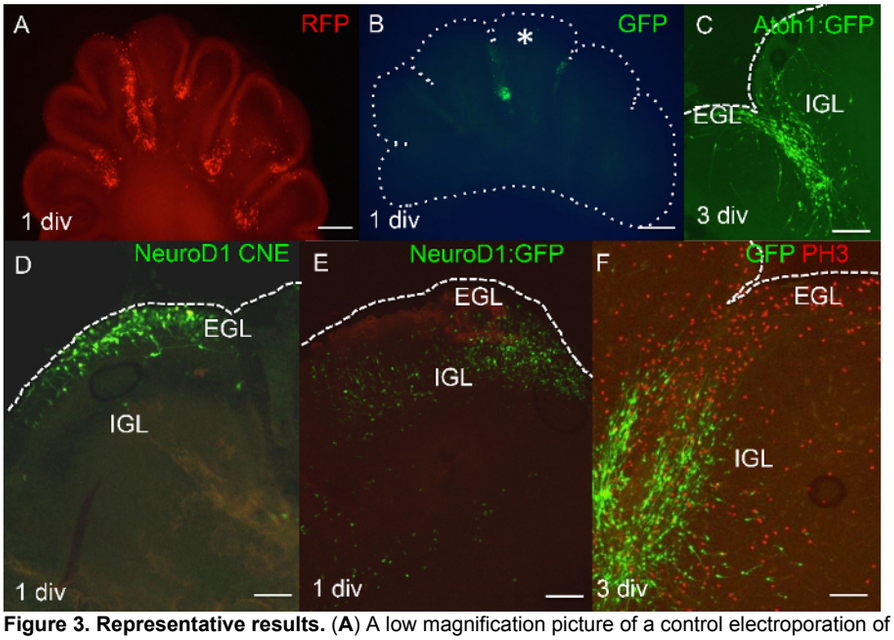

Figure 3. Representative results. (**A**) A low magnification picture of a control electroporation of an RFP encoding plasmid into the EGL at multiple locations. The tissue retains its structure and electroporated cells are clearly visible in a thick subpial layer of the cerebellum. (**B**) An example of a targeted electroporation with a control GFP plasmid. The targeted folium is indicated by an asterisk. Scale bar A-B = 500 µm. (**C**) An example where a construct encoding GFP driven by an Atoh1 enhancer has been electroporated into the EGL. The expression of *Atoh1* defines granule cell precursors within the EGL. Various cell morphologies are clearly visible at 3 div and cell behaviour can be monitored. (**D**) An example of labelling following the electroporation of a construct containing a putative conserved non-coding element (CNE) of the NeuroD1 gene driving GFP. The CNE reports activity in the cells expected based on endogenous NeuroD1 expression suggesting an active role of this CNE in development. NeuroD1 expression correlates with the initiation of granule cell differentiation. (**E**) An example where the tissue can be genetically manipulated by misexpression of NeuroD1 protein and a change in granule cell behaviour can be observed. (**F**) An example where the electroporated tissue (control GFP plasmid) can be fixed and stained for markers of proliferating cells, such as phosphohistone H3 (PH3). Scale bar C-F = 50 µm Please click here to view a larger version of this figure.

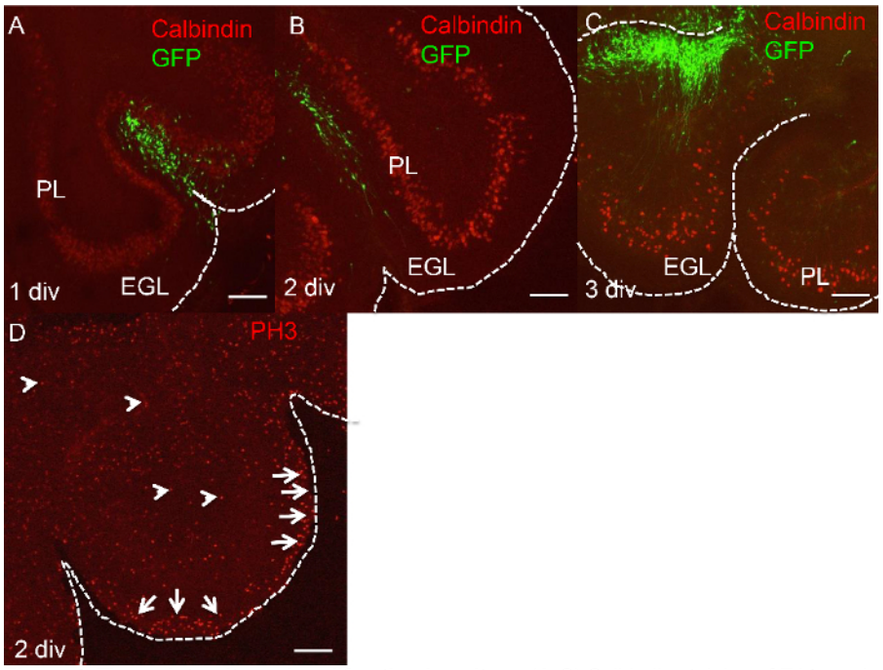

Figure 4. Tissue integrity and proliferation in culture. (**A**-**C**) Calbindin staining of E14 cerebellar tissue electroporated with a control GFP plasmid at 1-3 days *in vitro* (div). Calbindin staining shows that tissue integrity is maintained in culture for at least 3 div. The Purkinje cell layer does not form a monolayer at this stage in chick development but it is clearly seen forming a layer underneath the EGL where granule cells (green) are located. (**D**) Phosphohistone H3 (PH3) staining on cerebellar tissue cultured for 2 div. PH3 staining is visible in the EGL (arrows) but also in other cerebellar regions (arrowheads). This staining is representative of all stages in culture examined (1-3 div). Scale bar A-D = 50µm
Please click here to view a larger version of this figure.

Discussion

The protocol reported here describes a method for dissecting, electroporating and culturing slices of embryonic Day 14 cerebellum from the chick. This protocol enables targeting of electroporation to small focal regions of the EGL, including isolated targeting of individual cerebellar lobes. It enables genetic analysis and imaging at a high resolution and convenience, and at a low cost compared to established techniques in rodents[43-47]. Such analysis is not currently possible *in vivo* due to the extended developmental time period, the paucity of EGL-specific genetic targeting possibilities in mouse, and the commonality of molecular mechanisms between the rhombic lip and the EGL, which means that alterations that may affect EGL biology frequently cannot be analysed since they affect rhombic lip neurogenesis and abrogate EGL formation[49]. Our system thus represents a major advance in terms of targeting genetic modification to the EGL specifically, and we anticipate it will be applicable to other species beyond the chick that maybe of comparative interest, such as non-model mammals and reptiles.

In performing the slice culture electroporation technique, a number of technical considerations are paramount. Firstly, the robustness of slices to survive in culture without on the one hand undergoing extensive cell death or on the other losing structural integrity limits the thickness of slice to 300 µm in our hands. A second important consideration is the viscosity of the DNA solution, which ensures electroporation of DNA at concentrations that are high enough to induce visible or relevant levels of genetic modification. In *in ovo* electroporation of DNA solutions injected into the early embryonic hindbrain, concentrations of fast green dye of approximately 1% are typical. However, in our protocol, we typically use concentrations of fast green of 20%. This ensures a sufficiently viscous DNA solution to prevent dispersal of the DNA following pipetting but before electroporation, but a sufficiently dilute one to mediate efficient electrical conduction.

In addition to these technical considerations, we observed that proliferative behavior that we observe *ex vivo* does not precisely match that predicted from *in vivo* studies probably due to pial integrity being disrupted by the tissue preparation. Under such conditions, when a GFP expression construct is electroporated, a large proportion of electroporated cells appear to have left the cell cycle after just one day of culture as judged by PH3 staining (**Figure 3F**). This does not correlate with expected EGL proliferative behavior, where proliferation of clones in both mouse and chick extends over a large time period[27]. The implication that the pia modulates proliferation is supported by the observation that when we electroporate a reporter construct with a *NeuroD1* regulatory element driving expression of GFP all electroporated cells express GFP after one day in culture (**Figure 3D**). *In vivo*, this construct mirrors endogenous *NeuroD1* expression in marking cells of the inner EGL that are post-mitotic[36,37], while full length NeuroD1 is sufficient to drive cell differentiation (**Figure 3E**). This suggests that under certain conditions, the proliferative capability of cells may not be maintained as it is in the outer EGL at equivalent stages *in vivo*. PH3 staining does however suggest that there is a lot of proliferation in culture, often localized to the EGL area (**Figure 4D**). Extensive proliferation outside the EGL indicates possibly enhanced gliogenesis or proliferation of Pax2 GABAergic precursors in white matter. The implication is that interpretation of any experimental procedure will have to take the into account the above proliferative behaviour, the fact that Purkinje cells do not form a monolayer until E18 in chick and that normal development may be compromised after slice preparation (*e.g.,* due to lack of interaction with climbing fibres *etc.*)

Despite these limitations, our protocol represents a significant step forward in relation to studying many aspects of granule cell biology. The crucial advantage of enabling spatially and temporally specific labeling of the EGL as distinct from the rhombic lip will facilitate multiple examinations of the both the cell biology of granule progenitors and the genetic regulation underpinning it in a manner that is not possible at

present *in vivo*. Our technique in chick will complement existing *ex vivo* culture and electroporation protocols in rodents[43-48] and carries the considerable advantages in cost and convenience that are associated with chick. Additionally, it represents a significant advance over existing techniques of culturing granule progenitors[39]. While it will complement rather than replace the latter, our protocol will open up the control of granule neuron differentiation to a wide variety of pharmaceutical treatments and to the diversity of cell autonomous genetic manipulations that are possible in the chick. It provides a foundation for examining granule cell biology in unprecedented detail.

Disclosures

The authors have nothing to disclose.

Acknowledgements

The method presented in this article arose from work funded by the BBSRC BB/I021507/1 (TB, RJTW) and an MRC doctoral studentship (MH).

References

1. Schmahmann, J. D. The role of the cerebellum in cognition and emotion: personal reflections since 1982 on the dysmetria of thought hypothesis, and its historical evolution from theory to therapy. *Neuropsychology Review.* **20**, 236-260 (2010).
2. Becker, E. B., & Stoodley, C. J. Autism spectrum disorder and the cerebellum. *International Review of Neurobiology.* **113**, 1-34 (2013).
3. Hatten, M. E., & Roussel, M. F. Development and cancer of the cerebellum. *Trends in Neurosciences.* **34**, 134-142 (2011).
4. Butts, T., Green, M. J., & Wingate, R. J. Development of the cerebellum: simple steps to make a 'little brain'. *Development.* **141**, 4031-4041 (2014).
5. Rodriguez-Moldes, I. *et al.* Development of the cerebellar body in sharks: spatiotemporal relations of Pax6 expression, cell proliferation and differentiation. *Neuroscience Letters.* **432**, 105-110 (2008).
6. Kaslin, J. *et al.* Stem cells in the adult zebrafish cerebellum: initiation and maintenance of a novel stem cell niche. *The Journal of Neuroscience : the Official Journal of the Society for Neuroscience.* **29**, 6142-6153 (2009).
7. Chaplin, N., Tendeng, C., & Wingate, R. J. Absence of an external germinal layer in zebrafish and shark reveals a distinct, anamniote ground plan of cerebellum development. *The Journal of Neuroscience : the Official Journal of the Society for Neuroscience.* **30**, 3048-3057 (2010).
8. Kani, S. *et al.* Proneural gene-linked neurogenesis in zebrafish cerebellum. *Developmental Biology.* **343**, 1-17 (2010).
9. Butts, T., Modrell, M. S., Baker, C. V., & Wingate, R. J. The evolution of the vertebrate cerebellum: absence of a proliferative external granule layer in a non-teleost ray-finned fish. *Evolution & Development.* **16**, 92-100 (2014).
10. Corrales, J. D., Blaess, S., Mahoney, E. M., & Joyner, A. L. The level of sonic hedgehog signaling regulates the complexity of cerebellar foliation. *Development.* **133**, 1811-1821 (2006).
11. Wingate, R. J., & Hatten, M. E. The role of the rhombic lip in avian cerebellum development. *Development.* **126**, 4395-4404 (1999).
12. Machold, R., & Fishell, G. Math1 is expressed in temporally discrete pools of cerebellar rhombic-lip neural progenitors. *Neuron.* **48**, 17-24 (2005).
13. Wang, V. Y., Rose, M. F., & Zoghbi, H. Y. Math1 expression redefines the rhombic lip derivatives and reveals novel lineages within the brainstem and cerebellum. *Neuron.* **48**, 31-43 (2005).
14. Yamada, M. *et al.* Specification of spatial identities of cerebellar neuron progenitors by ptf1a and atoh1 for proper production of GABAergic and glutamatergic neurons. *The Journal of Neuroscience : the Official Journal of the Society for Neuroscience.* **34**, 4786-4800 (2014).
15. Hoshino, M. *et al.* Ptf1a, a bHLH transcriptional gene, defines GABAergic neuronal fates in cerebellum. *Neuron.* **47**, 201-213 (2005).
16. Wilson, L. J., & Wingate, R. J. Temporal identity transition in the avian cerebellar rhombic lip. *Developmental Biology.* **297**, 508-521 (2006).
17. Hausmann, B., & Sievers, J. Cerebellar external granule cells are attached to the basal lamina from the onset of migration up to the end of their proliferative activity. *The Journal of Comparative Neurology.* **241**, 50-62 (1985).
18. Xenaki, D. *et al.* F3/contactin and TAG1 play antagonistic roles in the regulation of sonic hedgehog-induced cerebellar granule neuron progenitor proliferation. *Development.* **138**, 519-529 (2011).
19. Komuro, H., Yacubova, E., Yacubova, E., & Rakic, P. Mode and tempo of tangential cell migration in the cerebellar external granular layer. *The Journal of Neuroscience : the Official Journal of the Society for Neuroscience.* **21**, 527-540 (2001).
20. Klein, R. S. *et al.* SDF-1 alpha induces chemotaxis and enhances Sonic hedgehog-induced proliferation of cerebellar granule cells. *Development.* **128**, 1971-1981 (2001).
21. Zhu, Y. *et al.* Role of the chemokine SDF-1 as the meningeal attractant for embryonic cerebellar neurons. *Nature Neuroscience.* **5**, 719-720 (2002).
22. Hagihara, K. *et al.* Shp2 acts downstream of SDF-1alpha/CXCR4 in guiding granule cell migration during cerebellar development. *Developmental Biology.* **334**, 276-284 (2009).
23. Borrell, V., & Marin, O. Meninges control tangential migration of hem-derived Cajal-Retzius cells via CXCL12/CXCR4 signaling. *Nature Neuroscience.* **9**, 1284-1293 (2006).
24. Paredes, M. F., Li, G., Berger, O., Baraban, S. C., & Pleasure, S. J. Stromal-derived factor-1 (CXCL12) regulates laminar position of Cajal-Retzius cells in normal and dysplastic brains. *The Journal of Neuroscience : the Official Journal of the Society for Neuroscience.* **26**, 9404-9412 (2006).
25. Lopez-Bendito, G. *et al.* Chemokine signaling controls intracortical migration and final distribution of GABAergic interneurons. *The Journal of neuroscience : the official journal of the Society for Neuroscience.* **28**, 1613-1624 (2008).
26. Florio, M., & Huttner, W. B. Neural progenitors, neurogenesis and the evolution of the neocortex. *Development.* **141**, 2182-2194 (2014).
27. Espinosa, J. S., & Luo, L. Timing neurogenesis and differentiation: insights from quantitative clonal analyses of cerebellar granule cells. *The Journal of Neuroscience : the Official Journal of the Society for Neuroscience.* **28**, 2301-2312 (2008).
28. Legue, E., Riedel, E., & Joyner, A. L. Clonal analysis reveals granule cell behaviors and compartmentalization that determine the folded morphology of the cerebellum. *Development.* **142**, 1661-1671 (2015).

29. Dahmane, N., & Ruiz i Altaba, A. Sonic hedgehog regulates the growth and patterning of the cerebellum. *Development.* **126**, 3089-3100 (1999).
30. Wallace, V. A. Purkinje-cell-derived Sonic hedgehog regulates granule neuron precursor cell proliferation in the developing mouse cerebellum. *Current Biology : CB.* **9**, 445-448 (1999).
31. Wechsler-Reya, R. J., & Scott, M. P. Control of neuronal precursor proliferation in the cerebellum by Sonic Hedgehog. *Neuron.* **22**, 103-114 (1999).
32. Lewis, P. M., Gritli-Linde, A., Smeyne, R., Kottmann, A., & McMahon, A. P. Sonic hedgehog signaling is required for expansion of granule neuron precursors and patterning of the mouse cerebellum. *Developmental Biology.* **270**, 393-410 (2004).
33. Zhao, H., Ayrault, O., Zindy, F., Kim, J. H., & Roussel, M. F. Post-transcriptional down-regulation of Atoh1/Math1 by bone morphogenic proteins suppresses medulloblastoma development. *Genes & Development.* **22**, 722-727 (2008).
34. Flora, A., Klisch, T. J., Schuster, G., & Zoghbi, H. Y. Deletion of Atoh1 disrupts Sonic Hedgehog signaling in the developing cerebellum and prevents medulloblastoma. *Science.* **326**, 1424-1427 (2009).
35. Klisch, T. J. *et al. In vivo* Atoh1 targetome reveals how a proneural transcription factor regulates cerebellar development. *Proceedings of the National Academy of Sciences of the United States of America.* **108**, 3288-3293 (2011).
36. Miyata, T., Maeda, T., & Lee, J. E. NeuroD is required for differentiation of the granule cells in the cerebellum and hippocampus. *Genes & Development.* **13**, 1647-1652 (1999).
37. Butts, T., Hanzel, M., & Wingate, R. J. Transit amplification in the amniote cerebellum evolved via a heterochronic shift in NeuroD1 expression. *Development.* **141**, 2791-2795 (2014).
38. Rios, I., Alvarez-Rodriguez, R., Marti, E., & Pons, S. Bmp2 antagonizes sonic hedgehog-mediated proliferation of cerebellar granule neurones through Smad5 signalling. *Development.* **131**, 3159-3168 (2004).
39. Anne, S. L. *et al.* WNT3 inhibits cerebellar granule neuron progenitor proliferation and medulloblastoma formation via MAPK activation. *PloS One.* **8**, e81769 (2013).
40. Chedotal, A. Should I stay or should I go? Becoming a granule cell. *Trends in Neurosciences.* **33**, 163-172 (2010).
41. Penas, C. *et al.* Casein Kinase 1delta Is an APC/C(Cdh1) Substrate that Regulates Cerebellar Granule Cell Neurogenesis. *Cell Reports.* **11**, 249-260 (2015).
42. Penas, C. *et al.* GSK3 inhibitors stabilize Wee1 and reduce cerebellar granule cell progenitor proliferation. *Cell Cycle.* **14**, 417-424 (2015).
43. Yang, Z. J. *et al.* Novel strategy to study gene expression and function in developing cerebellar granule cells. *Journal of Neuroscience Methods.* **132**, 149-160 (2004).
44. Jia, Y., Zhou, J., Tai, Y., & Wang, Y. TRPC channels promote cerebellar granule neuron survival. *Nature Neuroscience.* **10**, 559-567 (2007).
45. Umeshima, H., Hirano, T., & Kengaku, M. Microtubule-based nuclear movement occurs independently of centrosome positioning in migrating neurons. *Proceedings of the National Academy of Sciences of the United States of America.* **104**, 16182-16187 (2007).
46. Famulski, J. K. *et al.* Siah regulation of Pard3A controls neuronal cell adhesion during germinal zone exit. *Science.* **330**, 1834-1838 (2010).
47. Puram, S. V. *et al.* A CaMKIIbeta signaling pathway at the centrosome regulates dendrite patterning in the brain. *Nature Neuroscience.* **14**, 973-983 (2011).
48. Holubowska, A., Mukherjee, C., Vadhvani, M., & Stegmuller, J. Genetic manipulation of cerebellar granule neurons in vitro and *in vivo* to study neuronal morphology and migration. *J Vis Exp.* (2014).
49. Ben-Arie, N. *et al.* Math1 is essential for genesis of cerebellar granule neurons. *Nature.* **390**, 169-172 (1997).

© 2014. Published by The Company of Biologists Ltd | Development (2014) 141, 2791-2795 doi:10.1242/dev.101758

RESEARCH REPORT

Transit amplification in the amniote cerebellum evolved via a heterochronic shift in *NeuroD1* expression

Thomas Butts, Michalina Hanzel and Richard J. T. Wingate*

ABSTRACT

The cerebellum has evolved elaborate foliation in the amniote lineage as a consequence of extensive *Atoh1*-mediated transit amplification in an external germinal layer (EGL) comprising granule cell precursors. To explore the evolutionary origin of this layer, we have examined the molecular geography of cerebellar development throughout the life cycle of *Xenopus laevis*. At metamorphic stages *Xenopus* displays a superficial granule cell layer that is not proliferative and expresses both *Atoh1* and *NeuroD1*, a marker of postmitotic cerebellar granule cells. Premature misexpression of *NeuroD1* in chick partially recapitulates the amphibian condition by suppressing transit amplification. However, unlike in the amphibian, granule cells fail to enter the EGL. Furthermore, misexpression of *NeuroD1* once the EGL is established both triggers radial migration and downregulates *Atoh1*. These results show that the evolution of transit amplification in the EGL required adaptation of *NeuroD1*, both in the timing of its expression and in its regulatory function, with respect to *Atoh1*.

KEY WORDS: Cerebellum, Evolution, Atoh1, *Xenopus*, Chick

INTRODUCTION

Transit amplification is a widespread strategy in neural development that allows the fine-tuning of cell numbers in specific neuronal populations. It is mediated by transient, fate-committed progenitor cells that are spatially and molecularly distinct from precursors in the ventricular layer of the neural tube. Increasing evidence suggests that such cells can be defined by a basal cellular attachment to the pial membrane (Hansen et al., 2010) and respond to distinct mitogenic signals (Klein et al., 2005).

The impact of transit amplification on the evolution of brain structures is most clearly seen in the highly foliated, laminar structure of the mammalian cortex and cerebellum. In the cortex, variation in basal progenitor number in the subventricular zone (SVZ) is a significant determinant of cortex gyrification (Lui et al., 2011; Stahl et al., 2013). The tempo and magnitude of SVZ amplification are also likely to be responsible for variation in the relative proportions of interneuron types and their layering between mammals and between the cortical areas of a given mammal (Fietz and Huttner, 2011; Borrell and Reillo, 2012). The situation is far simpler in the cerebellum where (in both birds and mammals) a single, transit amplifying population of granule cell precursors with a distinct pial attachment (Hausmann and Sievers, 1985) forms a transient external germinal layer (EGL). Proliferation in the EGL is regulated by the morphogen Sonic hedgehog (Shh), for which underlying Purkinje cells are a prominent local source (Dahmane and Ruiz-i-Altaba, 1999; Wallace, 1999; Wechsler-Reya and Scott, 1999; Lewis et al., 2004). Elegant genetic titration experiments have shown that Shh can precisely regulate the degree of cerebellar foliation (Corrales et al., 2006).

Despite these insights, relatively little is known about the emergence of transit amplification as a developmental strategy. In the cerebellum, there is a dramatic disjunction between developmental strategies used in birds and mammals with that in actinopterygian fish and chondrichthyes, which lack an EGL defined as a distinct basal progenitor population covering the pial surface and expressing the bHLH transcription factor *Atonal1* (*Atoh1*) (Rodriguez-Moldes et al., 2008; Kaslin et al., 2009; Chaplin et al., 2010; Butts et al., 2014). Intriguing studies by Amos Gona in the 1970s suggest that amphibians represent an evolutionarily intermediate condition. For at least part of its development, the frog displays an amniote-like EGL that is apparently non-proliferative (Gona, 1972). We investigated Gona's model in *Xenopus laevis* using modern, molecular tools and find that there is a remarkable shift from anamniote to amniote developmental mechanisms of granule cell development within a single species at metamorphosis. Furthermore, we propose that lack of proliferation in the otherwise amniote-like, postmetamorphic frog EGL is enforced by the precocious expression of another bHLH protein, NeuroD1, which in amniotes marks postmitotic granule cells. We have recapitulated this non-proliferative condition experimentally in the early chick cerebellum through the premature misexpression of *NeuroD1*. Moreover, once the EGL has formed, and in contrast to the situation in the frog, *NeuroD1* misexpression in the chick downregulates *Atoh1* and drives the radial migration of granule cells. Thus, the relative timing of *NeuroD1* expression and a change in its function with respect to *Atoh1* represent a previously unidentified regulatory mechanism for amniote cerebellum growth, providing an explanation for the origin of the proliferative EGL.

RESULTS AND DISCUSSION

Different stages of the *Xenopus* life cycle exhibit different modes of cerebellar development

In amniotes, granule cell precursors migrate into the EGL as the last-born population generated from a thin strip of *Atoh1*-positive neuroepithelial precursors bordering the fourth ventricle roof plate: the rhombic lip (Gilthorpe et al., 2002; Machold and Fishell, 2005). To determine how granule cells are generated in amphibians we compared the expression of *Atoh1* (in *X. laevis*) with that of genes that characterise the rhombic lip lineage across most vertebrates: *Barhl1* [a direct downstream target of *Atoh1* (Chellappa et al., 2008)], *Lhx9* [expressed in non-granule cells, early-born rhombic lip derivatives (Rose et al., 2009)], *Zic1* [expressed in both granule cell precursors and postmitotic neurons (Aruga et al., 1998)] and *NeuroD1* [expressed in postmitotic granule neurons (Miyata et al., 1999)]. At tadpole stages (stage 48), *Atoh1* expression is confined to the rhombic lip (Fig. 1A), which is distinguished by a high density of cells in M phase of mitosis, as shown by staining for

MRC Centre for Developmental Neurobiology, King's College London, 4th Floor New Hunt's House, London SE1 1UKL, UK.

*Author for correspondence (richard.wingate@kcl.ac.uk)

Received 29 July 2013; Accepted 15 May 2014

Development (2014) 141, 2791-2795 doi:10.1242/dev.101758

phosphohistone H3 (PH3; Fig. 1B). Within the cerebellum, *Atoh1* and PH3 are coextensive and confined to the rhombic lip (Fig. 1C), while sagittal sectioning reveals that the superficial layer of the cerebellum contains no proliferative cells (PCNA; Fig. 1D). In a lateral view of the mid/hindbrain region, *Barhl1*-positive rhombic lip derivatives can be seen across the dorsoventral surface of the cerebellum (Fig. 1E) and rostral hindbrain. Extra-cerebellar *Lhx9*-positive cells in ventral hindbrain (Fig. 1F) are spatially segregated from *NeuroD1*-positive postmitotic granule cells in cerebellum (Fig. 1G). At this stage of development, *Atoh1* is confined to the rhombic lip and there is no evidence of an *Atoh1*-positive EGL (Fig. 1H).

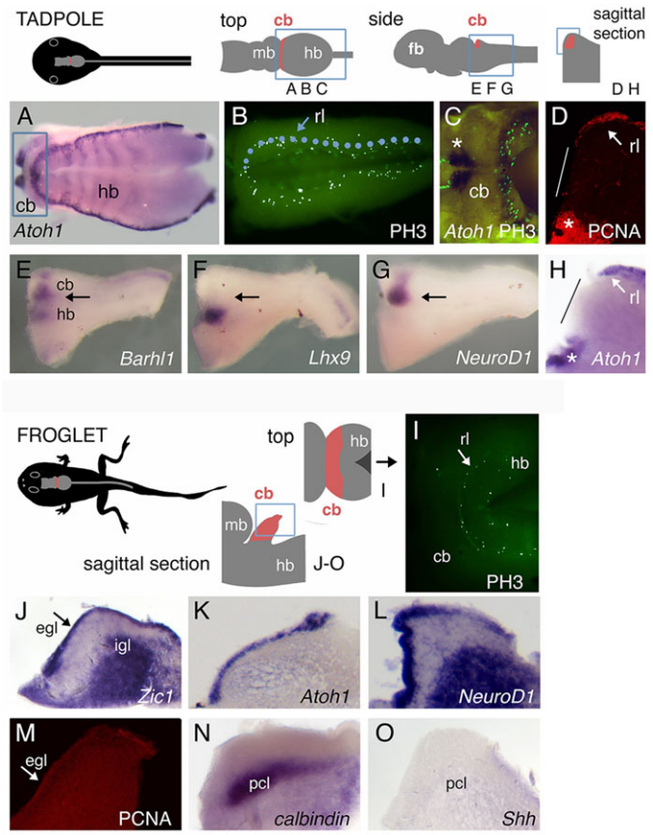

Fig. 1. *Xenopus* displays a non-proliferative EGL at metamorphosis. Schematic drawings of tadpole (stage 48: A-H) and froglet (stage 58: I-O) stages of development are shown with corresponding brain profiles [cerebellum (cb) in red] and location of whole-mount and section views (blue boxes). (A) *Atoh1* expression in whole-mount hindbrain (hb) and cerebellum. (B) Mitotic cells in the rhombic lip (rl; blue dotted line) in an equivalent embryo stained for PH3. (C) Cerebellum of embryo in A (boxed region) counterstained for PH3. The anterior extra-cerebellar *Atoh1*-postive regions (asterisk, also in D,H) correspond to the primordium of isthmic nuclei. (D) In sagittal section, PCNA staining shows that the cerebellum anlage (white line) is devoid of superficial proliferative neurons. (E) *Barhl1* is expressed in cerebellum (arrow) and hindbrain. (F) *Lhx9* is expressed in hindbrain only. (G) *NeuroD1* is expressed in cerebellum (arrow). (H) In sagittal section, *Atoh1* is not expressed on the surface of the cerebellum anlage (black line). (I) In the froglet, mitotic cells in the cerebellum are still confined to the rhombic lip. (J) *Zic1*, a marker of granule neurons at all stages of development, is expressed in both an internal granule cell layer (igl) and an external germinal layer (egl, arrow). (K) *Atoh1* is also expressed in the EGL. (L) *NeuroD1* is expressed in both layers. (M) PCNA staining in sagittal section confirms that the EGL is non-proliferative. (N) *Calbindin* is expressed in the Purkinje cell layer (pcl). (O) Purkinje cells do not express *Shh*. mb, midbrain; fb, forebrain.

After metamorphosis and the breakthrough of the arms (from stage 58), proliferation remains restricted to the rhombic lip and, as in the tadpole, there is no superficial germinal layer within the cerebellum (Fig. 1I). However, *in situ* hybridisation for *Zic1* reveals not only a large internal granule cell layer (IGL), but also labels a distinct, superficial, *Zic1*-positive cell layer (Fig. 1J), which disappears by the completion of metamorphosis (data not shown). The resemblance of this transient layer to the amniote EGL is confirmed by the specific expression of *Atoh1* (Fig. 1K). However, *NeuroD1*, which is a marker of postmitotic granule cells (Fig. 1L), is co-expressed in the EGL with both *Zic1* and *Atoh1*. Lack of proliferation within the EGL (Fig. 1M) corresponds with a Purkinje cell layer that expresses *calbindin* (Fig. 1N) but not *Shh* (Fig. 1O). The *Xenopus* EGL is thus a hybrid of progenitor and postmitotic characteristics: a pial *Atoh1*-positive transient population that nevertheless expresses *NeuroD1* and is non-proliferative, which lies adjacent to an *Shh*-negative Purkinje cell layer.

Although the presence of an EGL in anamniotes has been debated in recent years (Wullimann et al., 2011), there is little evidence for its manifestation in the cerebellum of sharks (Rodriguez-Moldes et al., 2008; Chaplin et al., 2010), basal ray-finned fish (Butts et al., 2014) and early or adult zebrafish (Kaslin et al., 2009, 2013; Chaplin et al., 2010; Kani et al., 2010). We conclude that a transit amplifying precursor layer is also absent in the frog. However, at metamorphic stages, *Xenopus* displays a transient, superficial layer of non-proliferative yet *Atoh1*-positive granule cells. Lack of proliferation in this EGL analogue might explain why the amphibian cerebellum is one of the simplest and proportionately smallest in the vertebrate radiation (Nieuwenhuys et al., 1998). These observations also suggest that an external granule cell layer might serve a function that is independent of proliferation and that, furthermore, this function is not required in either the tadpole or in the EGL-less (Rodriguez-Moldes et al., 2008; Kaslin et al., 2009, 2013; Chaplin et al., 2010; Kani et al., 2010; Butts et al., 2014) anamniote cerebellum.

What, then, is the purpose of a non-proliferative EGL in metamorphic *Xenopus*? One possibility is that an amniote-like EGL may provide a means of establishing a uniform layer of late-born granule cells prior to inward radial migration into a pre-existing, definitive cerebellar neuronal scaffold. Evidence for such a scaffold comes from experiments showing that an EGL can form even when depleted of granule cells (Eddison et al., 2004). By contrast, anamniotes are characterised by a CNS that is subject to continuous growth and remodelling (Otteson and Hitchcock, 2003), negating the need for transient developmental scaffolds. We speculate that if this cytoarchitectonic role represents the ancestral condition for the EGL then transit amplification would necessarily represent a secondary evolutionary adaptation.

NeuroD1 overexpression prevents granule cell proliferation

The coincidence of a lack of transit amplification and the premature expression of *NeuroD1* in the *Xenopus* EGL prompted us to test whether *NeuroD1* is sufficient to suppress proliferation in amniotes. We misexpressed *NeuroD1* in the chick cerebellar rhombic lip at E4 and analysed the cerebellum at E8. A view of the surface of the cerebellum reveals *NeuroD1*-overexpressing GFP-positive cells coincident with regions of reduced PH3 label (Fig. 2A-C), suggesting that ectopic NeuroD1 suppresses proliferation. When viewed in parasagittal section, control GFP electroporations produce a densely labelled superficial EGL (Fig. 2D), with half of the labelled granule lineage cells residing in the EGL. By contrast, cells expressing *NeuroD1:GFP* (Fig. 2E) show a highly significant asymmetric bias in location towards the IGL ($P<0.001$). This is also reflected in PH3

Development (2014) 141, 2791-2795 doi:10.1242/dev.101758

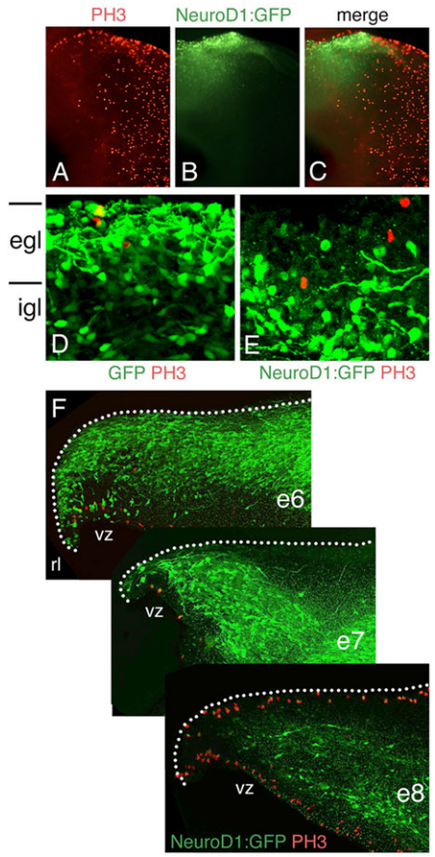

Fig. 2. *NeuroD1* expression at E4 abrogates proliferation and alters migration paths of granule cell precursors in chick. GFP:IRES:*NeuroD1* (or GFP-only control) was electroporated into the chick cerebellar rhombic lip at E4 and the cerebellum analysed at E6-8. (A) Surface view of the EGL in a whole-mount E8 cerebellum anlagen expressing GFP:IRES:*NeuroD1* and stained for PH3 (red). (B) GFP signal (green). (C) Merged PH3 and GFP images. (D) PH3 (red)-labelled section through a control GFP-electroporated cerebellum at E8. Yellow cells are proliferating granule precursors in the EGL. (E) GFP:IRES:*NeuroD1* expression drives cells from the EGL and none is co-stained for PH3. (F) Timecourse of migration of GFP:IRES:*NeuroD1*-expressing cells from the rhombic lip at E6, E7 and E8 in sagittal section counterstained for PH3 (red).

staining at E8: in GFP controls, 179 cells across 17 cerebella were co-labelled with PH3, whereas none that overexpressed *NeuroD1* was co-labelled ($P<0.001$). This suggests that *NeuroD1* expression is sufficient to terminate proliferation and suppress EGL formation by driving postmitotic granule cells into an internal layer.

We followed the timecourse at E6, E7 and E8 of rhombic lip migration following *NeuroD1* misexpression at E4 (Fig. 2F). Prior to granule cell precursor specification at E6 (Wilson and Wingate, 2006), migrating cells follow their normal subpial migration route. However, at E7 and E8, *NeuroD1*-expressing cells avoid the EGL and follow a deep migration path, presumably severing contact with the basal lamina. At no point are labelled cells seen superficially, indicating that the normal phases of accumulation within the EGL and radial migration are bypassed. This suggests that *NeuroD1* expression in granule cells has different consequences for migratory behaviour in amniote and *Xenopus* cerebellum that are manifest at the point of granule cell specification.

Together with the expression data from *Xenopus*, these observations suggest that *NeuroD1* expression suppresses proliferation and that *Atoh1* expression is not sufficient to drive transit amplification. By contrast, *Atoh1* misexpression within the mouse EGL binds *NeuroD1*-positive postmitotic granule cells to this subpial layer (Helms et al., 2001), replicating to some extent the situation within the metamorphic *Xenopus* EGL. This raises the possibility that *Atoh1* acts primarily as a determinant of cellular basal/pial attachment. Thus, although *Atoh1* expression is a necessary prerequisite for transit amplification (Flora et al., 2009), possibly by determining basal attachment (Hausmann and Sievers, 1985), whether amplification occurs is determined by the timing of the onset of *NeuroD1* expression.

Evolutionary heterochrony of *NeuroD1* expression and modification of *NeuroD1* function in amniotes

Given that differences in *NeuroD1* expression correlate with the regulation of proliferative activity and granule cell laminar distribution within the cerebellum of different species, we examined the regulatory basis of *NeuroD1* expression across tetrapods and the interaction between *NeuroD1* and *Atoh1*. Using a comparative genomic analysis of human, mouse, chick, frog and zebrafish, we identified a conserved non-coding element (CNE) upstream of the *NeuroD1* basal promoter that is 183 bp in length in mouse and conserved across osteichthyeans. We tested whether this element could reproduce species-specific *NeuroD1* expression patterns in chick. Whereas a control electroporation of GFP at the rhombic lip labels equal numbers of cells within the EGL and IGL (Fig. 3A), the orthologous proximal elements from both mouse (Fig. 3B) and frog (Fig. 3C) drive GFP expression predominantly within the IGL (Fig. 3D), when combined with the endogenous basal promoter, mirroring the endogenous expression of chick *NeuroD1*. Although it is possible that autoregulation is playing a role, we suggest that this conserved element is interchangeable between tetrapod groups. It might thus be expected to recapitulate an anamniote *NeuroD1* expression pattern if expressed in the metamorphic frog, although this remains to be tested. Which upstream factors act through this element (plausibly via epigenetic modifications) to co-ordinate the differential timing of expression of *NeuroD1* in is an important open question.

To ascertain whether the function of *NeuroD1* with respect to *Atoh1* expression has also been modified during amniote evolution, we misexpressed *NeuroD1* in the EGL of cerebellar slices prepared from E14 chick. Whereas an *Atoh1* enhancer construct robustly tags EGL cells that go on to express the *NeuroD1* reporter at 24 h *in vitro* (Fig. 3E), when *NeuroD1* is misexpressed the expression of the *Atoh1* reporter is absent (Fig. 3F). Thus, in contrast to the situation in *Xenopus*, in which both bHLH transcription factors are co-expressed in the EGL, *NeuroD1* in chick both cell-autonomously downregulates *Atoh1* expression and triggers inward radial migration.

In conclusion, whatever the extrinsic factors regulating *NeuroD1* through its functionally conserved enhancer, our study identifies that the interplay of *Atoh1* and *NeuroD1* expression establishes a temporal window for EGL proliferation that might represent a novel mechanism of growth regulation in the cerebellum. In terms of the evolution of cerebellum development, our results infer that granule progenitor transit amplification emerged through a heterochronic shift of expression of *NeuroD1* and a modification of its regulatory function with respect to *Atoh1* in an ancestral amniote.

MATERIALS AND METHODS

Electroporation of DNA constructs

The full-length chick *NeuroD1* coding sequence was cloned into pGEM-T Easy (Promega) by PCR (primers: forward, 5′-ATGACCAAGTCGTACA-GCGAGA-3′; reverse, 5′-TCACTCGTGGAAGATGGCGCTGA-3′) from cDNA prepared from E12 cerebellum with TRIzol (Invitrogen), and

Development (2014) 141, 2791-2795 doi:10.1242/dev.101758

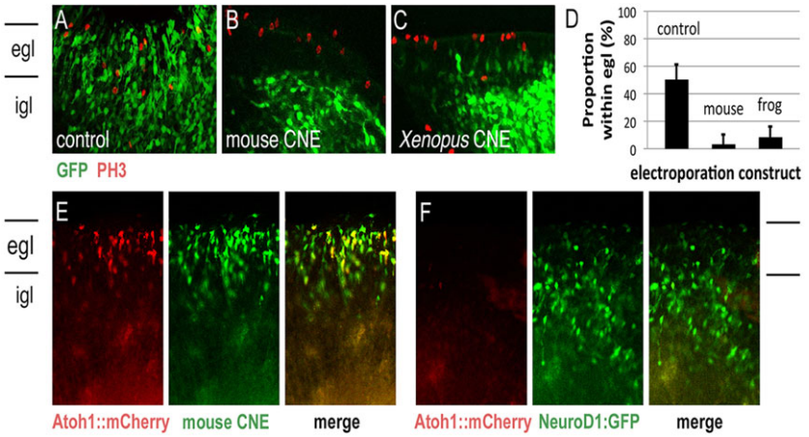

Fig. 3. *NeuroD1* regulation is conserved across tetrapods, but its activity is modified in the amniote lineage. Confocal microscopy images of sagittal sections of E8 chick cerebellum stained for GFP (green) and PH3 (red) following electroporation with: (A) a control plasmid encoding GFP, (B) the CNE upstream of the mouse basal *NeuroD1* promoter and (C) the CNE upstream of the *Xenopus* basal *NeuroD1* promoter. (D) Percentage of GFP-labelled cells in the EGL following electroporation of control (n=15), mouse (n=20) and *Xenopus* (n=12) CNE constructs. The difference between the control and either the mouse or *Xenopus* construct is highly significant (P<0.0001). Expression of the basal promoter of mouse alone is unable to drive the expression of GFP (data not shown). (E) *Atoh1* reporter driving the expression of mCherry (red), co-expressed at E14 with *NeuroD1* (mouse CNE) GFP reporter (green) labels granule cells in the EGL. After 24 h in culture, a large proportion of cells expressing *NeuroD1* retain perdurant mCherry (red), indicating that they had previously activated *Atoh1*. Most have yet to leave the EGL. (F) By contrast, when *NeuroD1* is co-expressed with the *Atoh1* reporter, no mCherry (red) can be detected and the majority of cells have exited the EGL, indicating that *NeuroD1* suppresses the activity of the *Atoh1* enhancer.

subcloned into the pCAβ-IRESeGFPm5 vector (http://www.ncbi.nlm.nih.gov/pubmed/19602272).

The genomic sequence of mouse covering the GENSAT BAC clone RP24-151C22 was used as the base sequence in a VISTA pairwise analysis with human, chick, *Xenopus tropicalis* and zebrafish. Conserved non-coding sequences were defined as those exhibiting at least 70% sequence homology over a sliding window of 100 bp. Using these data, reporter constructs were constructed by building non-coding sequences directly upstream of *GFP* by PCR with long primers using proof reading Fusion polymerase (NEB) and cloning into pGEM-T Easy following A-addition. The mouse construct incorporates a conserved non-coding element upstream of the endogenous mouse basal *NeuroD1* promoter and corresponds to the sequence from −401 bp to +101 bp relative to the longest 5′EST. The amphibian construct incorporates the *X. tropicalis* conserved non-coding element upstream of the *X. tropicalis* basal promoter, corresponding to the sequence from −372 bp to +96 bp relative to the longest 5′EST. As a control, we assembled a construct containing only the basal promoter from the mouse corresponding to the genomic sequence from −146 bp to +101 bp upstream of *GFP*. The Atoh1-Cre plasmid (Kohl et al., 2012) was co-electroporated with pFlox-pA-mCherry (lox-stop-lox mCherry). All constructs were confirmed by sequencing.

Constructs were expressed in fertilised brown chicken eggs (Henry Stewart) incubated at 38°C to embryonic day (E) 4. Briefly, embryos in windowed eggs were injected with DNA constructs into the fourth ventricle and an electric pulse (3×10 V/10 ms) passed through the dorsal neural tube, targeted to the rhombic lip. Eggs were sealed with tape and reincubated until E6, E7 or E8 before fixation in 4% paraformaldehyde. E14 electroporation was carried out on 300 µm slices of chick cerebellum using a modified *in vitro* protocol. Slices were cultured for 24 h at 37°C in 5% CO_2 (Green et al., 2014). Experiments involving live chick embryos were performed in accordance with UK Home Office regulatory standards.

In situ hybridisation and immunofluorescence

X. laevis probes were T/A-cloned using standard PCR from mixed larval cDNA kindly provided by Esther Bell (King's College London) into pGEM-T Easy. RNA *in situ* hybridisation was carried out on dissected whole brains or hindbrains according to standard protocols (Myat et al., 1996) using riboprobes generated for *Xenopus Atoh1*, *Barhl1*, *Zic1*, *Shh*, *calbindin* and *NeuroD1*. Immunohistochemistry was carried out using a standard protocol with rabbit anti-phosphohistone H3 (Cell Signaling Technology, 9701L; 1:100), anti-PCNA (AbCam, ab18197; 1:500) or mouse anti-GFP (Life Technologies, a6455; 1:500) and appropriate Alexa Fluor secondary antibodies (Life Technologies). Hindbrains were embedded in 20% gelatin and vibratome sectioned at 50 µm. Whole-mount *Xenopus* hindbrains were photographed on a Zeiss Stemi SV6 microscope equipped with an Olympus DP camera. Sections were photographed on a Leica MZFLIII microscope and QCapture camera. Confocal images were captured using a Nikon Eclipse 80i microscope with EZ-C1 3.70 software. Images were compiled and cell quantifications made in ImageJ (v10.2) and Adobe Photoshop (v5.5). Statistical significance was calculated using Student's *t*-test.

Competing interests

The authors declare no competing financial interests.

Author contributions

T.B. and R.J.T.W. designed the study. T.B. and M.H. performed experiments. T.B., M.H. and R.J.T.W. wrote the manuscript.

Funding

This work was supported by a Biotechnology and Biological Sciences Research Council (BBSRC) project grant [BB/F020570/1] to R.J.T.W.

References

Aruga, J., Minowa, O., Yaginuma, H., Kuno, J., Nagai, T., Noda, T. and Mikoshiba, K. (1998). Mouse Zic1 is involved in cerebellar development. *J. Neurosci.* **18**, 284-293.

Borrell, V. and Reillo, I. (2012). Emerging roles of neural stem cells in cerebral cortex development and evolution. *Dev. Neurobiol.* **72**, 955-971.

Butts, T., Modrell, M. S., Baker, C. V. H. and Wingate, R. J. T. (2014). The evolution of the vertebrate cerebellum: absence of a proliferative external granule layer in a non-teleost ray-finned fish. *Evol. Dev.* **16**, 92-100.

Chaplin, N., Tendeng, C. and Wingate, R. J. T. (2010). Absence of an external germinal layer in zebrafish and shark reveals a distinct, anamniote ground plan of cerebellum development. *J. Neurosci.* **30**, 3048-3057.

Chellappa, R., Li, S., Pauley, S., Jahan, I., Jin, K. and Xiang, M. (2008). Barhl1 regulatory sequences required for cell-specific gene expression and autoregulation in the inner ear and central nervous system. *Mol. Cell. Biol.* **28**, 1905-1914.

Corrales, J. D., Blaess, S., Mahoney, E. M. and Joyner, A. L. (2006). The level of sonic hedgehog signaling regulates the complexity of cerebellar foliation. *Development* **133**, 1811-1821.

Dahmane, N. and Ruiz-i-Altaba, A. (1999). Sonic hedgehog regulates the growth and patterning of the cerebellum. *Development* **126**, 3089-3100.

Eddison, M., Toole, L., Bell, E. and Wingate, R. J. T. (2004). Segmental identity and cerebellar granule cell induction in rhombomere 1. *BMC Biol.* **2**, 14.

Fietz, S. A. and Huttner, W. B. (2011). Cortical progenitor expansion, self-renewal and neurogenesis-a polarized perspective. *Curr. Opin. Neurobiol.* **21**, 23-35.
Flora, A., Klisch, T. J., Schuster, G. and Zoghbi, H. Y. (2009). Deletion of Atoh1 disrupts Sonic Hedgehog signaling in the developing cerebellum and prevents medulloblastoma. *Science* **326**, 1424-1427.
Gilthorpe, J. D., Papantoniou, E. K., Chedotal, A., Lumsden, A. and Wingate, R. J. (2002). The migration of cerebellar rhombic lip derivatives. *Development* **129**, 4719-4728.
Gona, A. G. (1972). Morphogenesis of the cerebellum of the frog tadpole during spontaneous metamorphosis. *J. Comp. Neurol.* **146**, 133-142.
Green, M. J., Myat, A. M., Emmenegger, B. A., Wechsler-Reya, R. J., Wilson, L. J. and Wingate, R. J. T. (2014). Independently specified Atoh1 domains define novel developmental compartments in rhombomere 1. *Development* **141**, 389-398.
Hansen, D. V., Lui, J. H., Parker, P. R. and Kriegstein, A. R. (2010). Neurogenic radial glia in the outer subventricular zone of human neocortex. *Nature* **464**, 554-561.
Hausmann, B. and Sievers, J. (1985). Cerebellar external granule cells are attached to the basal lamina from the onset of migration up to the end of their proliferative activity. *J. Comp. Neurol.* **241**, 50-62.
Helms, A. W., Gowan, K., Abney, A., Savage, T. and Johnson, J. E. (2001). Overexpression of MATH1 disrupts the coordination of neural differentiation in cerebellum development. *Mol. Cell. Neurosci.* **17**, 671-682.
Kani, S., Bae, Y.-K., Shimizu, T., Tanabe, K., Satou, C., Parsons, M. J., Scott, E., Higashijima, S.-i. and Hibi, M. (2010). Proneural gene-linked neurogenesis in zebrafish cerebellum. *Dev. Biol.* **343**, 1-17.
Kaslin, J., Ganz, J., Geffarth, M., Grandel, H., Hans, S. and Brand, M. (2009). Stem cells in the adult zebrafish cerebellum: initiation and maintenance of a novel stem cell niche. *J. Neurosci.* **29**, 6142-6153.
Kaslin, J., Kroehne, V., Benato, F., Argenton, F. and Brand, M. (2013). Development and specification of cerebellar stem and progenitor cells in zebrafish: from embryo to adult. *Neural Dev.* **8**, 9.
Klein, C., Butt, S. J. B., Machold, R. P., Johnson, J. E. and Fishell, G. (2005). Cerebellum- and forebrain-derived stem cells possess intrinsic regional character. *Development* **132**, 4497-4508.
Kohl, A., Hadas, Y., Klar, A. and Sela-Donenfeld, D. (2012). Axonal patterns and targets of dA1 interneurons in the chick hindbrain. *J. Neurosci.* **32**, 5757-5771.
Lewis, P. M., Gritli-Linde, A., Smeyne, R., Kottmann, A. and McMahon, A. P. (2004). Sonic hedgehog signaling is required for expansion of granule neuron precursors and patterning of the mouse cerebellum. *Dev. Biol.* **270**, 393-410.
Lui, J. H., Hansen, D. V. and Kriegstein, A. R. (2011). Development and evolution of the human neocortex. *Cell* **146**, 18-36.
Machold, R. and Fishell, G. (2005). Math1 is expressed in temporally discrete pools of cerebellar rhombic-lip neural progenitors. *Neuron* **48**, 17-24.
Miyata, T., Maeda, T. and Lee, J. E. (1999). NeuroD is required for differentiation of the granule cells in the cerebellum and hippocampus. *Genes Dev.* **13**, 1647-1652.
Myat, A., Henrique, D., Ish-Horowicz, D. and Lewis, J. (1996). A chick homologue of Serrate and its relationship with Notch and Delta homologues during central neurogenesis. *Dev. Biol.* **174**, 233-247.
Nieuwenhuys, R., ten Donkelaar, H. J. and Nicholson, C. (1998). *The Central Nervous System of Vertebrates*. Berlin: Springer-Verlag.
Otteson, D. C. and Hitchcock, P. F. (2003). Stem cells in the teleost retina: persistent neurogenesis and injury-induced regeneration. *Vision Res.* **43**, 927-936.
Rodríguez-Moldes, I., Ferreiro-Galve, S., Carrera, I., Sueiro, C., Candal, E., Mazan, S. and Anadón, R. (2008). Development of the cerebellar body in sharks: spatiotemporal relations of Pax6 expression, cell proliferation and differentiation. *Neurosci. Lett.* **432**, 105-110.
Rose, M. F., Ren, J., Ahmad, K. A., Chao, H.-T., Klisch, T. J., Flora, A., Greer, J. J. and Zoghbi, H. Y. (2009). Math1 is essential for the development of hindbrain neurons critical for perinatal breathing. *Neuron* **64**, 341-354.
Stahl, R., Walcher, T., De Juan Romero, C., Pilz, G. A., Cappello, S., Irmler, M., Sanz-Aquela, J. M., Beckers, J., Blum, R., Borrell, V. et al. (2013). Trnp1 regulates expansion and folding of the Mammalian cerebral cortex by control of radial glial fate. *Cell* **153**, 535-549.
Wallace, V. A. (1999). Purkinje-cell-derived Sonic hedgehog regulates granule neuron precursor cell proliferation in the developing mouse cerebellum. *Curr. Biol.* **9**, 445-448.
Wechsler-Reya, R. J. and Scott, M. P. (1999). Control of neuronal precursor proliferation in the cerebellum by Sonic Hedgehog. *Neuron* **22**, 103-114.
Wilson, L. J. and Wingate, R. J. (2006). Temporal identity transition in the avian cerebellar rhombic lip. *Dev. Biol.* **297**, 508-521.
Wullimann, M. F., Mueller, T., Distel, M., Babaryka, A., Grothe, B. and Köster, R. W. (2011). The long adventurous journey of rhombic lip cells in jawed vertebrates: a comparative developmental analysis. *Front. Neuroanat.* **5**, 27.